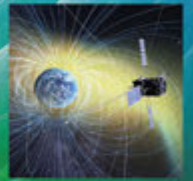
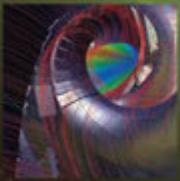


The 25th International Toki Conference

Creating the Future:
— Innovative Science of Plasma and Fusion —

3rd - 6th November, 2015, Ceratopia Toki, Toki, Gifu, Japan



Book of Abstracts

25th International Toki Conference (ITC-25)

Creating the Future
– Innovative Science of Plasma and Fusion –

Book of Abstracts

3rd – 6th November, 2015
Ceratopia Toki, Toki-city, Gifu, JAPAN

Scope

The International Toki Conference is a topical meeting dedicated to a specific subject related to plasma and fusion science. The series began in 1989 with the founding of the National Institute for Fusion Science and has been held on an annual basis ever since. The last 10 years have seen great advances in the plasma and fusion sciences based on progress in basic physics and technology. These developments related to plasma and fusion sciences also accelerate innovative applications of plasmas in industrial, biomedical, agricultural, and other fields. With this background, we are planning the 25th International Toki Conference to explore new aspects in creating the future through the innovative sciences of plasma and fusion.

Topics

Helical Plasma Research

Tokamak and ITER Related Research

Innovative Applications of Plasmas

- Industrial/Chemical/Medical and Agricultural Applications -

Basic Plasma Science - Laboratory and Space Plasmas -

Fusion Technology Research

Theory and Simulation Research

Laser Plasma Sciences

Plasma Wall Interaction Research

Other Fields of Sciences

General Contact Address

National Institute for Fusion Science

322-6 Oroshi-cho, Toki 509-5292, Japan

E-mail:itc25@nifs.ac.jp

The 25th International Toki Conference is organized by National Institute for Fusion Science (NIFS), and is supported by SOKENDAI (The Graduate University for Advanced Studies), National Institutes of Natural Sciences (NINS) and YU-KWAI (Fusion Science Association).

International Advisory Committee

Y. Takeiri (Japan, Chair)	H. Azechi (Japan)	A. Ando (Japan)
N. Ohno (Japan)	Y. Ogawa (Japan)	Y. Nakashima (Japan)
K. Hanada (Japan)	A. Fukuyama (Japan)	T. Mizuuchi (Japan)
M. Mori (Japan)	M. Wada (Japan)	O. Kaneko (Japan)
T. Morisaki (Japan)	M. Osakabe (Japan)	R. Horiuchi (Japan)
A. Sagara (Japan)	S. Imagawa (Japan)	T. Mutoh (Japan)
T. Mito (Japan)	T. Muroga (Japan)	S. Ishiguro (Japan)
K. Nishimura (Japan)	H. Sugama (Japan)	S. Sakakibara (Japan)
T. Klinger (Germany)	M. Zarnstroff (USA)	M. Kwon (Korea)
V. Antoni (Italy)		

International Program Committee

M. Ichimura (Japan, Chair)	S. Kubo (Japan, Vice-Chair)	T. Mutoh (Japan)
H. Laqua (Germany)	V. Antoni (Italy)	M. Ono (USA)
J. Noterdaeme (Germany)	M. Nagatsu (Japan)	Y. Sakawa (Japan)
S. Murakami (Japan)	A. Hatayama (Japan)	H. Idei (Japan)
M. Inomoto (Japan)	Y. Nakamura (Japan)	H. Sugama (Japan)
I. Murakami (Japan)	Y. Suzuki (Japan)	J. Miyazawa (Japan)
K. Tsumori (Japan)	S. Ohdachi (Japan)	T. Nagasaka (Japan)
K. Nagaoka (Japan)	T. Ii (Japan)	

Local Organizing Committee (LOC)

T. Mutoh (Chair)	K. Nagaoka (Scientific Secretary)	S. Kubo
T. Shimozuma	M. Osakabe	Y. Nakamura
K. Tsumori	S. Ohdachi	K. Saito
T. Seki	Y. Yoshimura	H. Igami
H. Kasahara	K. Ikeda	H. Nakano
H. Takahashi	M. Kisaki	R. Seki
S. Kamio	A. Ito	S. Takada
T. Ii	T. Kobayashi	H. Noto
M. Nakata	R. Makino	T. Kato
S. Sugie		

Contents

Program

			<u>Page</u>
Tuesday	3rd November	-----	6
Wednesday	4th November	-----	7
Thursday	5th November	-----	8
Friday	6th November	-----	9
Poster			
Session 1	3rd November	-----	10
Session 2	4th November	-----	17

Abstracts of Papers

			<u>Page</u>
Plenary / Invited / Oral presentations			
Tuesday	3rd November	-----	23
Wednesday	4th November	-----	31
Thursday	5th November	-----	43
Friday	6th November	-----	49
Poster presentations			
Session 1	3rd November	-----	57
Session 2	4th November	-----	175

Program

Tuesday, 3rd November, 2015

Time	No	Presenter	Title	Page
9:00 - 9:20			Registration	
9:20 - 9:25			Opening and Welcome Addresses	
9:50 - 10:10			Group Photo	
10:10 - 10:55			Plenary 1 session (M. Ichimura)	
10:10	PL - 1	N.J. Fisch	Pushing Particles with Waves: Current Drive and Alpha Channeling	23
10:55 - 11:15			Coffee Break	
11:15 - 12:15			Invited 1 session (M. Ichimura)	
11:15	I - 1	M. Osakabe	Current status of the LHD project and its prospect for deuterium experiment	24
11:45	I - 2	K. Itoh	Non-equilibrium and Extreme State of Plasmas	25
12:15 - 14:15			Lunch	
14:15 - 16:15			Poster Session 1 P1-1 ~ P1-118	57
16:15 - 16:35			Coffee Break	
16:35 - 18:15			Invited 2 / Oral 1 session (M. Osakabe)	
16:35	I - 3	M. Shiratani	Plasma assisted enhancement of agricultural yield	26
17:05	I - 4	K. Kitano	Innovative medical technology in plasma disinfection of human body with low-temperature atmospheric-pressure plasmas ~ the reduced-pH method and the plasma-treated water (PTW) ~	27
17:35	O - 1	H. Saitoh	Recent status of the PAX and APEX projects toward the formation of electron-positron plasma	28
17:55	O - 2	M. Sato	An Application of Fusion Oriented Neutrons for Transmutations of Long Life Fission Products	29

Wednesday, 4th November, 2015

Time	No	Presenter	Title	Page
9:00 - 10:15				
Plenary 2 / Invited 3 session (N.J. Fisch)				
9:00	PL - 2	M. Ono	Spherical Tokamaks and Fusion Energy Development Path	31
9:45	I - 5	H. Meyer	Research towards operation with tolerable ELMs on European Tokamaks	32
10:15 - 10:35 Coffee Break				
10:35 - 12:05				
Invited 4 session (A. Sagara)				
10:35	I - 6	H. Tamura	Design status of structural components of helical fusion reactor FFHR-d1	33
11:05	I - 7	M. Sakamoto	Hydrogen recycling in the divertor simulation plasma on GAMMA 10/PDX	34
11:35	I - 8	Y. Ueda	Interactions of tungsten plasma facing material with edge plasma	35
12:05 - 13:35 Lunch				
13:35 - 14:45				
Invited 5 / Oral 2 session (C.Z. Cheng)				
13:35	I - 9	B. Unterberg	Research on Plasma Wall Interaction Facilities for Fusion Reactors	36
14:05	O - 3	Y. Ueki	Velocity profile measurement of lead-lithium duct flow by ultrasonic Doppler velocimetry	37
14:25	O - 4	A. Kimura	Impacts of Material Innovation on Advanced Blanket Design	38
14:45 - 15:05 Coffee Break				
15:05 - 15:35				
Invited 6 / Oral 3 session (B. Unterberg)				
15:05	I - 10	A. Kasugai	Progress of Linear IFMIF Prototype Accelerator in Rokkasho	39
15:35	O - 5	H. Shishido	Discussion on the effect of NaF on physical properties of Flinabe in comparison to Flibe from molecular dynamics simulations	40
15:55	O - 6	H. Etoh	Experimental and numerical study of H- production in DC H- source of medical cyclotron	41
16:15 - 18:15				
Poster Session 2 P2-1 ~ P2-89				
				175

Thursday, 5th November, 2015

Time	No	Presenter	Title	Page
9:00 - 10:15				
Plenary 3 / Invited 7 session (H.P. Laqua)				
9:00	PL - 3	J-M. Noterdaeme	Innovations that make the Ion Cyclotron Range of Frequency Power suitable for Fusion Reactors	43
9:45	I - 11	S. Murakami	Predictions of Plasma Performance and Fusion Reactions in the Deuterium Experiment Plasma of LHD	44
10:15 - 10:35 Coffee Break				
10:35 - 12:25				
Invited 8 / Oral 4 session (H. Meyer)				
10:35	I - 12	G. Serianni	The full-size source and injector prototypes for ITER neutral beams	45
11:05	I - 13	K. Ikeda	Recent Studies of Hydrogen Negative Ion Source and Beam Production for NBI in Large Helical Device	46
11:35	I - 14	N.C. Luhman, Jr.	Advances in 2-D Millimeter-Wave Plasma Imaging of Magnetic Fusion Plasmas	47
12:05	O - 7	B.D. Blackwell	Recent results from the H-1 heliac on MHD activity, fluctuations and RF propagation	48
12:25 - 13:25 Lunch				
13:25 - 17:30 Social Program / Excursion				
18:30 - 20:30 Banquet				

Friday, 6th November, 2015

Time	No	Presenter	Title	Page
9:00 - 9:15				
Plenary 4 / Invited 9 session (B.D. Blackwell)				
9:00	PL - 4	H.P. Laqua	Commissioning and First Plasma Operation at the Wendelstein7-X Stellarator	49
9:45	I - 15	M. Nunami	Progress of Gyrokinetic Turbulence Simulation in Helical Plasmas	50
10:15 - 10:35 coffee break				
10:35 - 12:25				
Invited 10 / Oral 5 session (N.C. Luhmann, Jr.)				
10:35	I - 16	C.Z. Cheng	Kinetic physics of magnetic reconnection in collisionless plasmas	51
11:05	I - 17	Y. Miyoshi	Geospace Exploration Mission: ERG	52
11:35	I - 18	T. Minea	Magnetized plasma modelling: common approach interesting for fusion and processing plasmas	53
12:05	O - 8	N. Sato	Self-Organization and Heating by Inward Diffusion in Magnetospheric Plasmas	54
12:25 - 13:55 Lunch				
13:55 - 14:55				
Invited 11 session (J.-M. Noterdaeme)				
13:55	I - 19	K. Nishiyama	Development and Initial Cruise Operation of the Hayabusa2 Ion Engine System	55
14:25	I - 20	M. Tendler	The origin and the impact of stochasticity resulting from edge localized perturbations	56
14:55 - 15:25				
Summary				
		T. Mutoh	Summary of ITC-25	
15:25 - 15:40 Closing				

Poster Session 1

No	Presenter	Title	Page
P1 - 1	T. Kanzaki	Change in Reynolds stress induced by end-plate biasing in a cylindrical laboratory plasma	57
P1 - 2	Y. Miwa	How to Identify Ion Temperature Gradient Mode in Cylindrical Plasma	58
P1 - 3	T. Tarumi	Observation of radial scale length of fluctuations in PANTA	59
P1 - 4	F. Kin	Reconstruction of Cross-Sectional Structure of Reynolds Stress in End-Plate Biasing Experiment in PANTA	60
P1 - 5	R. Minato	Evaluation of flow velocity with a frequency comb Doppler Backscattering in PANTA	61
P1 - 6	H. Takahashi	Helium volumetric recombining plasma formation for energetic ion injection in a radio-frequency plasma device DT-ALPHA	62
P1 - 7	S. Tsubota	Development of linear plasma device for proof of principle of energetic ion injection	63
P1 - 8	T. Onda	Observation of Plasma Dynamics in TPD-sheet IV	64
P1 - 9	Y. Kaminou	Experimental and Numerical Studies of Hall Effect on Merging Formation Process of a Field-Reversed Configuration	65
P1 - 10	T. Ushiki	Generation of Energetic Electrons during Spherical Tokamak Merging in UTST	66
P1 - 11	M.C.C. Lacdan	Characterization of an atmospheric pressure plasma by a Gerdien condenser	67
P1 - 12	S. Nakanobo	Supersonic Gas Injection for High Density Operation and Associated Development of 140 GHz Interferometer in RELAX RFP	68
P1 - 13	M. Nishiura	Evidence of increased ion temperature by slow wave heating in RT-1	69
P1 - 14	Y. Kawazura	Anisotropy in tail component of H α in RT-1	70
P1 - 15	Y. Nakatsuka	Studies on power dependence of plasma production and ion heating by a single helical antenna for a simple thruster	71
P1 - 16	R. Yanai	Characteristics of Magnetic Fluctuations during Magnetic Reconnection in Counter-helicity Spheromak Merging Experiment	72
P1 - 17	N. Pathak	Role of Kinetic Alfvén Wave in Energy Transportation in Magnetopause	73

No	Presenter	Title	Page
P1 - 18	H. Kawazome	Numerical study of spectral line shapes in high-density He plasmas	74
P1 - 19	J. Kohagura	Doppler reflectometer system for measuring plasma rotation velocity in GAMMA 10	75
P1 - 20	C.L.S. Mahinay	Co-extraction of Low Energy Ar ⁺ and C ₂ H ₂ ⁻ Ions for Space Charge Effect Mitigation and Increased Beam Intensity	76
P1 - 21	C.J.M. Dela Cruz	Synthesis of hydrogenated amorphous carbon nitride using DC graphite hollow cathode discharge	77
P1 - 22	T. Fukuyama	Study on operating principle of Cockcroft-Walton circuit to produce plasmas using high-voltage discharge	78
P1 - 23	M.-J. Lee	Nonthermal and geometric effects on the dual-mode surface waves in a Lorentzian dusty plasma slab	79
P1 - 24	S. Kogoshi	High density plasma sustainment in microwave plasma source with slot antennas	80
P1 - 25	J.P.N. Gonda	Formation of Diamond-like Carbon (DLC) on Silicon using Low Energy Ion Beam Deposition	81
P1 - 26	M. Toida	Parallel electric fields in nonlinear magnetosonic waves in a multi-ion-species plasma	82
P1 - 27		(Withdrawal)	83
P1 - 28	M. Kondo	Design study on double layer type interface structure for heat exchanger of Fusion DEMO blanket	84
P1 - 29	D. Kato	Thermal quench of ion-beam induced luminescence of Er ₂ O ₃	85
P1 - 30	J. Yagi	Hydrogen solubility in molten salt FLiNaK mixed with nano-Ti powder	86
P1 - 31	T. Tanaka	Fabrication and characterization of MOD ceramic coatings on coolant duct materials	87
P1 - 32	S. Takayama	Investigation of the selective heating of the metal powder with hydrogen in the molten salts using by microwave	88
P1 - 33	D. Isshiki	Performance evaluation of a three-surface-multi-layered channel with a reinforced metal layer	89
P1 - 34	Y. Hishinuma	Adhesion strength of Er ₂ O ₃ /buffer stacked MOCVD coating for advanced breeding blanket	90
P1 - 35	T. Goto	Proposal of the maintenance method of breeder blankets of LHD-type helical fusion reactor FFHR	91
P1 - 36	M. Tanaka	Observations of gas stream from fusion test device for the design of exhaust detritiation system	92

No	Presenter	Title	Page
P1 - 37	Y. Aoki	Development of Soft-X Ray Computed Tomography Diagnostic System for MHD Dynamics Study in RELAX RFP	93
P1 - 38	M. Hamabe	Studies on the effect of radio frequency field in a cusp-type charge separation device for direct energy conversion	94
P1 - 39	T. Katsura	Studies on the axial position of the decelerator in traveling wave direct energy converter	95
P1 - 40	T. Watanabe	Improvement of charge separation by increase of magnets in a PM-CuspDEC simulator	96
P1 - 41	H. Noto	Development of high strength W/V/Au/ODS-Cu joint using HIP process	97
P1 - 42	T. Yamada	Development of Oxide Dispersion Strengthened-Copper Using MA-HIP Method	98
P1 - 43	M.M. Alam	Real-Time Display System of the Equilibrium Reconstruction for Long Time Discharge in QUEST	99
P1 - 44	H. Braune	W7-X ECRH plant - Control System Design Features	100
P1 - 45	Min Thu San	Experimental Study on W-Band Oversized Surface Wave Oscillator Driven by Weakly Relativistic Electron Beam	101
P1 - 46	Y. Annaka	Experimental Study on Slow Cyclotron Interaction under Anomalous Doppler Effect in W-band Backward Wave Oscillator	102
P1 - 47	S. Geng	Depth of Influence on the Plasma by Beam Extraction in a Negative Hydrogen Ion Source for NBI	103
P1 - 48	R. Makino	Power and polarization monitor developed for ECRH and ECCD on LHD	104
P1 - 49		(Withdrawal)	105
P1 - 50	E. Wakai	Absorption Behavior of Nitrogen in Nitrogen Hot Trap	106
P1 - 51	E. Wakai	Materials Test Plan and Design Summary in PIE Facility of IFMIF	107
P1 - 52	R. Ichimiya	Installation and commissioning of components for IFMIF/EVEDA Prototype Accelerator	108
P1 - 53	R. Nishikiori	Evaluation of dark current profile for prediction of voltage holding capability on multi-aperture multi-grid accelerator for ITER	109
P1 - 54	T. Wada	Variation in secondary electron collection and energy recovery concerning electrode angle in a high energy ion penetration scheme	110
P1 - 55	K. Tsumori	Numerical Design on New Steering Grid of Negative Ion Source for NBI	111

No	Presenter	Title	Page
P1 - 56	T. Tanaka	Fabrication and property investigation of metal hydride blocks for neutron shielding in a fusion reactor	112
P1 - 57	H. Muta	Improvement of weight density and thermal conductivity of hydride neutron shielding material using metal coated powder	113
P1 - 58	H. Watanabe	Environmental Effects on V-4Cr-4Ti Alloy during Irradiation	114
P1 - 59	Y. Hamaji	ACT2: a high heat flux test facility using electron beam for fusion application	115
P1 - 60	J. Miyazawa	Conceptual design of the new liquid metal divertor VOLD-X	116
P1 - 61	Y. Tanaka	Experimental simulations for detached plasma with Super-X divertor using a liner divertor simulator TPD-Sheet IV	117
P1 - 62	K. Ogawa	Effects of gamma-ray irradiation on electronic and non-electronic equipment of the Large Helical Device	118
P1 - 63	M. Kondo	Desorption of non-metal impurities from Pb and Pb-Li alloy	119
P1 - 64	M. Kondo	Conceptual design of temporally storage area in hot cell for fusion DEMO reactor	120
P1 - 65	H. Fu	Effect of HIP temperature and cooling rate on the microstructure and hardness of dissimilar-metal joints between ODS-RAFM steels and JLF-1 steel	121
P1 - 66	X. Ji	Investigation on the Magnetic Field Distortion by Ferromagnetism of the Blanket for the Helical Fusion Reactor	122
P1 - 67	S. Imagawa	Feasibility study of react-and-wind method for helical coils wound from cable-in-conduit conductors	123
P1 - 68	L. Aparicio	Evaluation of Shear Strength in Soldered and Mechanical Lap joints of High-Temperature Superconducting tapes Intended for a Remountable Magnet	124
P1 - 69	N. Yanagi	NITA Coil —Innovation for Enlarging the Blanket Space in the Helical Fusion Reactor	125
P1 - 70	T. Obana	Summary of conductor and joint test results of JT-60SA CS and EF coils using NIFS test facility	126
P1 - 71	M.M. Islam	Effect of Laval Nozzle in the GAMMA 10 SMBI Experiments	127
P1 - 72	A. Kamitani	Speedup of shielding current analysis in high-temperature superconducting film: implementation of H-matrix method	128

No	Presenter	Title	Page
P1 - 73	S. Koike	Fuelling effect by axial injection of torus plasma into ST plasma	129
P1 - 74	R. Ikeda	Progress in development of TE31,11 mode gyrotron for ITER EC system	130
P1 - 75	Y. Sasaki	Characteristics of a Large diameter RF negative hydrogen ion source	131
P1 - 76	N. Ikemoto	Temperature dependence of tritium enrichment by electrolysis with solid polymer electrolyte	132
P1 - 77	H. Date	Study of tritium release behavior from soil particle	133
P1 - 78	K. Furuichi	Evaluation of tritium sorption rate in soil packed bed by numerical analysis	134
P1 - 79	T. Sugiyama	Effects of gas-liquid ratios on separative performance of dual-temperature water hydrogen chemical exchange column	135
P1 - 80	Y. Morita	Preparation of hydrophobic platinum catalyst with porous silica supports for water hydrogen chemical exchange	136
P1 - 81	N. Akata	A new pretreatment technique for environmental tritium analysis with microwave heating method	137
P1 - 82	N. Ashikawa	Tritium decontamination from carbon deposited layer by baking	138
P1 - 83	T. Muroga	Microstructural and Microchemical Evolution of V-4Cr-4Ti under Heavy Ion Irradiation	139
P1 - 84	H. Funaba	Transport properties of high-beta plasmas in the inward shifted configurations on LHD	140
P1 - 85	K. Nagaoka	Heat Transport Characteristics of High Temperature Discharges in LHD - Dependence on Hydrogen/Helium Ratio -	141
P1 - 86	P. Vincenzi	Analysis of LHD NBI-plasma interaction with upgraded FIT3D module of TASK3D-a analysis transport suite	142
P1 - 87	H. Nakano	Design study for high spatial resolution of beam emission spectroscopy viewing from 6-O port on large helical device	143
P1 - 88	B.J. Peterson	Preliminary design of an imaging bolometer for W7X	144
P1 - 89	K. Mukai	Development of in-situ calibration system for foil detector of infrared imaging video bolometer in Large Helical Device	145
P1 - 90	R. Sano	Improvement of 3D radiation imaging using Euclidean distance from model phantom in LHD	146
P1 - 91	A. Tani	Design and evaluation of broad-band high pass filter using metal perforated plates with circular holes	147

No	Presenter	Title	Page
P1 - 92	K. Nagasaki	Development of Electron Bernstein Emission Diagnostic for Heliotron J and LHD	148
P1 - 93	H. Tsuchiya	Validation of the Digital Correlation ECE measurement technique using low frequency fluctuation in LHD	149
P1 - 94	Y. Goto	Development of OXB mode conversion window searching method using inverse emission process in the LHD	150
P1 - 95	Y. Shimooka	Magnetic flux surface measurements on TOKASTAR-2	151
P1 - 96	A. Shimizu	The development of 2D potential profile measurement with heavy ion beam probe on the Large Helical Device	152
P1 - 97	M. Irie	X-Y-t Edge Plasma Reconstruction with Digital Imaging Technique	153
P1 - 98	H. Zhang	Estimation of total carbon radiation at each ionization stage of C2+ to C5+ ions in Large Helical Device	154
P1 - 99	T. Sakito	Measurement of tokamak plasma with the external helical field using a high-speed camera in TOKASTAR-2	155
P1 - 100	Y. Nagayama	Observation of Electron Density Fluctuations by Using the O-mode Microwave Imaging Reflectometry (O-MIR) in LHD	156
P1 - 101	H. Igami	Examination of efficient electron Bernstein wave heating and measurement scenario with ray-tracing and full-wave calculations in LHD	157
P1 - 102	Y. Yoshimura	Improvement in flexibility of ECCD by use of upgraded ECH antenna system on LHD	158
P1 - 103	T. li Tsujimura	Optimization of ECH injection polarization in real-time polarization scan experiments	159
P1 - 104	H. Takahashi	Ion heating by ECRH through the equipartition process in the LHD	160
P1 - 105	S. Kamio	Experimental Evaluation of Fast-ion Velocity Distribution Produced by Neutral Beam with Si-FNA in LHD	161
P1 - 106	T. Tokuzawa	Developments of millimeter-wave interferometer for electron density measurements with beam extraction in the negative ion source	162
P1 - 107	H. Yamaguchi	Simulation study of NBI beam ion distributions in the presence of magnetic islands in helical plasmas	163
P1 - 108	S. Okamura	Optimization of helical coil structure for the improved magnetic configuration of LHD	164

No	Presenter	Title	Page
P1 - 109	T. Ido	Spatial structures of energetic-particle driven geodesic acoustic mode in the LHD	165
P1 - 110	Y. Takemura	Slowing down mechanism of instability leading to minor collapse in LHD	166
P1 - 111	X.D. Du	Stabilization of Helically Trapped Energetic Ions driven Resistive Interchange Mode by High Power Injection of Electron Cyclotron Resonance Heating	167
P1 - 112	N. Nakada	Development of fast-neutron directional detector for fusion neutron profile monitor at LHD	168
P1 - 113	M. Shoji	Observation of termination process of long pulse plasma discharges using stereoscopic fast framing cameras in the Large Helical Device	169
P1 - 114	A. Sanpei	Identification of helical structure of visible light in Low-A RFP with concave lens array	170
P1 - 115	T. Nishitani	Radiation field estimation for the diagnostic and control components by Monte Carlo neutronics calculations with LHD 3-dimensional modeling	171
P1 - 116	S. Maeta	Integrated heat transport simulation of the helium-hydrogen plasma of LHD by TASK3D	172
P1 - 117	J. Tachibana	Full-orbit simulation of fast α -particle in heliac configurations	173
P1 - 118	M. Isobe	Recent progress of fast-ion loss detector project in magnetic confinement fusion devices in Japan, Korea and China	174

Poster Session 2

No	Presenter	Title	Page
P2 - 1	U. Jenica Rozette	Silicon Nitride Film Deposition on Glass Substrates via Plasma Sputter-Type Negative Ion Source	175
P2 - 2	S.J. Park	Anti-fog on PMMA by Nitrogen-Argon Atmospheric Plasma Jet Treatment	176
P2 - 3	M. Wada	Ion species separated atmospheric pressure plasma source	177
P2 - 4	G. Tang	Degradation of acetic acid in water using gas-liquid plasma with SPG membrane	178
P2 - 5	S.M. Palardonio	Fourier Transform Infrared Spectroscopy of Plasma Polymerized Polyaniline	179
P2 - 6	Y. Okuno	Effect of electrode shapes and the working gases on production amount of hydroxyl radicals in atmospheric-pressure plasma jets	180
P2 - 7	H. Nabuchi	Effects of a magnetic Laval nozzle to the thrust performance on an MPD thruster	181
P2 - 8	D. Adachi	Design of electron supplier in a new concept of neutron generator for BNCT	182
P2 - 9	T. Matsui	Beam ion confinement in a new concept of neutron generator for BNCT	183
P2 - 10	A.M. Gouda	Formation Mechanism of Periodic Nano-Grating Structure by Surface Plasma Wave	184
P2 - 11	S. Ikuno	Krylov Subspace Method with Communication Avoiding Technique for Linear System Obtained from Electromagnetic Analysis	185
P2 - 12	K. Terashima	Magnetic property analysis for spherical shell magnetic substance using Monte Carlo simulation	186
P2 - 13	S. Fujiwara	Dissipative particle dynamics simulation of self-assembly in bolaamphiphilic solution	187
P2 - 14	H. Matsuura	Improvement of divertor probe array for heat flux measurement of Heliotron J divertor leg plasma	188
P2 - 15	M.S. Islam	Study of Heat and Particle flux in the case of Gas Injection in the D-module of GAMMA 10/PDX	189
P2 - 16	K. Ichimura	Study of the axial plasma confinement for high particle flux operations in GAMMA 10/PDX	190
P2 - 17	H. Bi	A study on hydrogen transport in liquid lithium under steady state plasma bombardment	191
P2 - 18	Y. Hayashi	Characterization of detached recombining plasma in Pilot-PSI	192

No	Presenter	Title	Page
P2 - 19	S. Saito	Erosion of bubble formed tungsten materials	193
P2 - 20	Y. Xu	Hydrogen gas-driven permeation through F82H steel coated with vacuum plasma sprayed tungsten	194
P2 - 21	Y. Torikai	Tritium accumulation on carbon deposition layer and its decontamination by glow discharge	195
P2 - 22	K. Katayama	Measurement of tritium sorbed in tungsten deposition layer by imaging plate technique	196
P2 - 23	H. Nakamura	Tungsten-surfaces-structure Dependence of Sputtering Yield for Noble Gas	197
P2 - 24	G. Motojima	Color measurements of the first wall toward the systematic evaluation of the thickness distribution of deposition layer in LHD	198
P2 - 25	T. Futakuchi	Linear stability analysis of Alfvén eigenmodes with arbitrary velocity distribution in tokamak plasmas	199
P2 - 26	T. Nicolas	Bifurcation of the interchange mode growth rate and rotation frequency due to the perpendicular heat conductivity in stellarator plasmas	200
P2 - 27	B. Huang	Comparison of bootstrap current calculation in helical plasmas among different types of approximations in drift-kinetic equation	201
P2 - 28	Y. Ohno	Chaos of nonlinear ion acoustic waves with vorticity	202
P2 - 29	G. Purohit	Electron impact ionization cross sections of the fusion plasma hydrocarbon gas: methane	203
P2 - 30	T. Pianpanit	Kinetic dynamics simulation of the detached plasma	204
P2 - 31	H. Sugama	Local approximation of the drift kinetic equation	205
P2 - 32	Y. Kawamoto	Modification of neutron emission spectra and its effect on determination of fuel ion ratio n_d/n_t in beam injected DT plasma	206
P2 - 33	H. Matsuura	A verification scenario of knock-on tail formation due to nuclear elastic scattering using γ -ray-generating ${}^6\text{Li}+\text{D}$ reaction in deuterium plasmas	207
P2 - 34	Y. Fujita	Transmission Mode Analysis in Polarizer Miter Bend	208
P2 - 35	S.A. Khan	Kinetic full wave analysis of electron cyclotron wave mode conversion in tokamak plasmas	209
P2 - 36	S. Maeyama	Benchmark of electromagnetic gyrokinetic codes in high performance fusion plasma	210
P2 - 37	T.-H. Watanabe	Moment extracted formulation for describing kinetic Alfvén waves	211
P2 - 38	D. Sharma	Equilibrium reconstruction of plasma discharges in the Aditya tokamak	212

No	Presenter	Title	Page
P2 - 39	M. Yanagi	Two dimensional hybrid simulation of a translated field-reversed configuration	213
P2 - 40	K. Matsuzaki	Influences of Hall effect on MHD behavior of two axially colliding FRCs	214
P2 - 41	R. Sekiguchi	Flux supply by Neutral Beam Injection into Field-Reversed Configuration plasma with resistive decay	215
P2 - 42	M. Homma	Estimations of Beam-Beam Fusion Reaction Rates in the Deuterium Experiment Plasma on LHD	216
P2 - 43	H. Wang	Simulations of Energetic Particle Driven Geodesic Acoustic Mode in 3-dimensional LHD equilibrium	217
P2 - 44	S. Toda	Advances in applying the gyrokinetic heat diffusivity model to transport simulations for helical plasmas	218
P2 - 45	R. Seki	Development of TASK3D/WM module for evaluation the ICRF wave propagation and absorption in LHD	219
P2 - 46	S. Mochizuki	Analysis of High Energy Electron Tail and Its Effect on the H- Production in the Linac4 H- Source	220
P2 - 47	I. Goto	Effect of Coulomb Collision on the Negative Ion Extraction Mechanism in Negative Ion Sources	221
P2 - 48	Y. Idomura	Saturation mechanism of ion temperature gradient driven trapped electron mode turbulence	222
P2 - 49	T. Takahashi	Kinetic equilibrium of a non-adiabatic trap	223
P2 - 50	M. Hata	Kinetic behavior of electron magnetohydrodynamic structures	224
P2 - 51	A. Takayama	Simulation study on helium in the vicinity of tungsten grain boundary	225
P2 - 52	K. Ichiguchi	Three-dimensional numerical analysis of shear flow effects on MHD stability in LHD plasmas	226
P2 - 53	R. Ueda	Pressure anisotropy analyses based on MHD equilibrium calculations and magnetic diagnostics in LHD	227
P2 - 54	S. Satake	Benchmark of multi-ion-species collision operator for delta f Monte-Carlo neoclassical simulation	228
P2 - 55	S. Usami	Improvement of a Multi-Hierarchy Simulation Model for Magnetic Reconnection Studies	229
P2 - 56	S. Sugiyama	Neutron incident angle and energy distribution to vacuum vessel in beam-injected LHD deuterium plasmas	230
P2 - 57	T. Haruki	Particle-in-cell simulations of a kink instability in a pinched current filament	231
P2 - 58	R. Tatsumi	Basic Comparison of the Numerical Method to Solve Fluid Equations for SOL/Divetror Plasmas	232

No	Presenter	Title	Page
P2 - 59	T. Ogawa	Multi-scale simulation of magnetic reconnection using particle-in-cell with magnetohydrodynamics on adaptively refined mesh	233
P2 - 60	N. Tsujine	Three dimensional magnetic reconnection of stressed X-point collapse	234
P2 - 61	Y. Nagamine	Simulation study on resistive instabilities in a small aspect ratio reversed field pinch	235
P2 - 62	T. Takayama	Large-scale simulation of contactless crack detection in HTS films: application of H-matrix method to fast matrix-vector multiplication	236
P2 - 63	A. Saitoh	Performance Improvement of Extended Boundary Node Method for Solving Elliptic Boundary Value Problems	237
P2 - 64	Y. Ohi	Stability analysis on node arrangement in Meshless Time-Domain Method	238
P2 - 65	H. Miura	Structure transition in forced magnetohydrodynamic turbulence with uniform background magnetic field	239
P2 - 66	M. Sato	Extension of integrated transport analysis suite, TASK3D-a, to be capable for analysis of fast ion particles and plasma flows in LHD	240
P2 - 67	Y. Shimizu	Validation of Tungsten Transport Model in JT-60U Plasmas	241
P2 - 68	H. Hasegawa	Study of Plasma Coherent Structure Transport Dynamics with Particle-in-Cell Simulation	242
P2 - 69	Y. Tamura	Intuitive interface for visualizing numerical data using gesture recognition	243
P2 - 70	H. Ohtani	Applications of the virtual-reality technology to Plasma Physics and Fusion Plasmas	244
P2 - 71	M. Yoshikawa	Direct observation of electron heating by electron Landau damping of Alfvén ion cyclotron waves with Thomson scattering system in the tandem mirror GAMMA 10/PDX	245
P2 - 72	T. Yamamoto	New Proposal on Development of Machine Protection Function in Conventional Control System Using Information Technologies	246
P2 - 73	H. Kiyonaga	Studies of AM He Atomic Magnetometer for Application in Fusion Plasmas	247
P2 - 74	R. Rajpal	Digital Signal Processing on FPGA for Plasma Diagnostics	248
P2 - 75	J.-H. Lee	Progress of KSTAR Thomson Scattering Diagnostic System in 2015	249

No	Presenter	Title	Page
P2 - 76		(Withdrawal)	250
P2 - 77	S. Purohit	Behavior of non-thermal electrons during ECR pre-ionization at Aditya tokamak	251
P2 - 78	J.-Y. Kim	Fast ion loss associated with RMP in KSTAR	252
P2 - 79	D. Seo	The temperature calibration for IR camera of the IRVB system including periscope system for KSTAR	253
P2 - 80	M. Tanaka	The effect of thermal history on microstructure of Er ₂ O ₃ coating layer prepared by MOCVD process	254
P2 - 81	M. Ishikawa	Development of the In-vessel Components of ITER Microfission Chamber System for Fusion Power Measurements in ITER	255
P2 - 82	M. Ichikawa	Clarification of arcing mechanism on filament-driven high-current arc discharge in Cs-seeded negative ion source	256
P2 - 83	H. Nuga	Fokker-Planck Simulation for Runaway Electron Generation in ITER Disruptions	257
P2 - 84	M. Uchida	Effect of UHR location on non-inductive formation of overdense spherical tokamak by electron Bernstein wave heating and current drive on LATE	258
P2 - 85	H. Kudoh	Inter-strand conductance measurement of ITER TF coil under epoxy impregnation	259
P2 - 86	T. Maruyama	Preliminary thermal analysis for ITER Lower Port #02 Integration Engineering in JADA	260
P2 - 87	O. Watanabe	Reduction Rate of MHD potential energy by toroidal plasma current drive at tokamak plasma formation with stationary direct current of central solenoidal coil	261
P2 - 88	T. Wakatsuki	Investigation of pressure profile controllability during plasma current ramp-up with reduced magnetic flux consumption in JT-60SA	262
P2 - 89	F. Wang	The effects of current density profiles on core toroidal rotation in EAST plasmas	263

Tuesday, 3rd November, 2015

PL-1

Pushing Particles with Waves: Current Drive and α Channeling

N. J. Fisch

*Princeton Plasma Physics Laboratory
Princeton University, Princeton, NJ 08543, USA*

It can be advantageous to push particles with waves in tokamaks, relying on wave-particle resonances to accomplish specific goals.

Waves that damp on electrons or ions in toroidal fusion devices can drive currents if the waves are launched with toroidal asymmetry. These currents are called non-inductive, since they operate in the absence of an electric field with curl. Driving non-inductive toroidal current enables steady state operation of tokamaks. The lower hybrid wave and the electron cyclotron wave have been demonstrated to drive significant currents. Non-inductive current also stabilizes deleterious tearing modes. To the extent that waves carry momentum, they may also cause toroidal rotation.

Waves can also be used to broker the energy transfer between energetic α particles and the background plasma. The energetic byproducts of DT fusion reactions, the 3.5 MeV α particles, tend to slow down on electrons, but that could take up to hundreds of milliseconds for typical tokamak reactor densities. Before that happens, the energy in these α particles can destabilize on collisionless timescales toroidal Alfvén modes and other waves, in a way deleterious to energy confinement. However, it has been speculated that this energy might be instead be channeled instead into useful energy, that heats fuel ions or drives current.

This effect would be catalyzed by waves that diffuse α particles, but in such a way that the diffusion in energy of the α particles is fundamentally coupled to diffusion in space. If these diffusion paths in energy-position space point from high energy in the center to low energy on the periphery, then α particles will be cooled while forced to the periphery, while the amplified wave can heat ions or drive current. This process or paradigm for extracting alpha particle energy collisionlessly has been called α channeling. Realized to its full potential, the α -channeling effect would divert most of the α particle power to rf power.

It is likely that it will take more than one wave to realize the full potential of this effect. Yet how waves might work in concert to realize this potential remains to a large extent an open question for research. While the α -channeling effect is speculative, the upside potential for economical fusion is immense. We are now entering an age of advanced fusion devices, where α particles may be produced in abundance. Yet concerns regarding the economic uncertainties of fusion energy remain. It thus becomes particularly urgent to explore now the advantageous possibilities in tokamak fusion when rf waves play a dominant role.

Current status of the LHD project and its prospect for deuterium experiment

^{a,b}M. Osakabe, ^{a,b}M. Yokoyama, ^cK. Nagasaki, ^{a,b}R. Sakamoto, ^{a,d}K. Y. Watanabe, ^{a,b}K. Nagaoka, ^{a,b}H. Takahashi, ^eS. Murakami, ^dT. Fujita, ^fY. Ohya, ^{a,b}S. Sakakibara, ^{a,b}M. Isobe, ^aT. Akiyama, ^{a,g}T. Morisaki, and LHD experiment group

^a National Institute for Fusion Science, 322-6 Oroshi-cho, Toki 509-5292, Japan

^b SOKENDAI (Grad. Univeristy for Advanced Studies), 322-6 Oroshi-cho, Toki 509-5292, Japan

^c Kyoto University, Gokasho, Uji 611-0011, Japan

^d Nagoya University, Furo-cho, Nagoya 464-8603, Japan

^e Kyoto University, Nishikyoku-ku, Kyoto 615-8540, Japan

^f Shizuoka University, Suruga-ku, Shizuoka 422-8529, Japan

^g Nagoya University, Furo-cho, Nagoya 464-8602, Japan

Achievement of reactor relevant plasma condition in Helical type magnetic configurations and exploration in related plasma physics and fusion technologies are the aim of Large Helical Device (LHD) project. Following achievements are major goals of the LHD project; achievements of (1) high temperature plasmas exceeding 10[keV] at electron density of $2 \times 10^{19} [\text{m}^{-3}]$, (2) high density plasmas exceeding $4 \times 10^{20} [\text{m}^{-3}]$ with electron temperature of 1.3[keV], (3) high beta plasmas exceeding 5[%] at 1[T], and (4) long pulse plasma operation exceeding 1 [hour] with 3[MW] input heating power. Among them, the achievement of high temperature, especially ion temperature, is the primary important. In the recent experiments on LHD, we have achieved ion-temperature of 8.1[keV] at $1 \times 10^{19} [\text{m}^{-3}]$ by the optimization of wall conditioning using long pulse discharge by Ion Cyclotron Heating (ICH). The electron temperature of 10keV at $1.6 \times 10^{19} [\text{m}^{-3}]$ was also achieved by the optimization of Electron Cyclotron Heating (ECH).

For further improvement in plasma performance, a project of deuterium experiments are planned on the Large Helical Device (LHD). The objectives of the experiment are (1) to realize high-performance plasmas by confinement improvement in helical plasmas, (2) to study the isotope effects on plasma confinement in toroidal plasma devices and (3) to demonstrate the confinement capability of energetic ions in helical systems. In the presentation, current status of LHD and its prospects for Deuterium experiments will be discussed.

Non-equilibrium and Extreme State of Plasmas

Kimitaka Itoh^{1,2}

¹*National Institute for Fusion Science, Toki, 509-5202, Japan*

²*Research Center for Plasma Turbulence, Kyushu University, Kasuga, 816-8580, Japan*

Research of plasmas is basic to the modern science, civilization and industry, and will be the origin of future progress of mankind. In particular, the study of the extremely-nonequilibrium plasmas has the impact in advancing the central issue of modern physics and has possibility to accelerate the scientific innovation.

Non-equilibrium properties of plasmas are characterized by, e.g., the spatial inhomogeneity, deviation from equi-partition, selective excitation of fluctuation, cross-scale interaction of fluctuations, interferences of dynamics with different time scales (violation of scale-separation for time and space), and others. In order to illuminate the elementary processes, we explain three prototypical examples. One is the problem of the physics of H-mode, in which the cross-scale interaction plays the essential role [1]. The second is the cross-ferroic turbulence, in which multiple structure formation mechanisms in scalar and vector fields take place [2]. The third is the physics of abrupt onset of large-scale deformation, which will solve the mystery of trigger problems [3,4].

Creating the Future: This is the time to develop the research to unify the physics progresses that have been established in the past for various types of plasmas.

This work is partly supported by a grant-in-aid for scientific research of JSPS, Japan (15H02155, 23244113) and by the collaboration programs of NIFS and of the RIAM of Kyushu University.

[1] S.-I. Itoh and K. Itoh: Nucl. Fusion **54** (2014) 114017

[2] S.-I. Itoh, et al.: “Cross-Ferroic Plasma Turbulence“, Meeting of Phys. Soc. Jpn. (September 2015) 17aCN-10

[3] S.-I. Itoh, et al.: Plasma Phys. Control. Fusion **40** (1998) 879

[4] A. Bhattacharjee: Lecture Notes in Physics 614: Turbulence and Magnetic Fields in Astrophysics (ed. E. Falgarone and T. Passot, Springer 2003) 351

Plasma assisted enhancement of agricultural yield

Masaharu Shiratani and Kazunori Koga

*Graduate School of Information Science and Electrical Engineering, Kyushu University
744 Motoooka, Nishi-ku, Fukuoka, 819-0395, Japan*

The sharp growth in food demand is mainly the result of world population growth to over 9 billion by 2050 [1]. There are three main categories of improvement methods of the agricultural productivity and output: irrigation, fertilization, and crop protection. Atmospheric pressure nonthermal plasmas can contribute such improvements in the three categories by various ways such as sterilization, fertilization, water treatment and purification, soil treatment, seed treatment, storage improvement, insecticide, pre-harvest treatments, post-harvest treatments, because they provide radicals, ions, electrons, light, as well as electric field without appreciable thermal damage to plants, crops, and fruits. Improvement of agricultural productivity has been tried by gas fumigation, seed treatments using radiations, UV light, laser, electric field, and magnetic field. It is important to clarify advantages and disadvantages of plasma treatments over other methods. One important advantage of plasma treatments is the fact that highly reactive and short lifetime species of high density can be provided by plasmas. Highly reactive species are more effective than stable chemicals and have much less residual harmful effects due to their short lifetime.

As one of such approaches using plasmas, we have shown that atmospheric pressure plasma irradiation to seeds can induce cell proliferation and continuous growth enhancement of several plants for weeks after their germination [2-6]. The main results are summarized as follows. 1) Air, O₂, and NO (10%)+N₂ plasma irradiation enhance their growth, whereas N₂, He and Ar plasma irradiation do not. 2) 3 min irradiation of air plasma with 40-90% humidity leads to more than 2.3 times faster growth for several weeks. 3) Even for a long storage duration of 30 days, seeds with air plasma irradiation still keep growth enhancement ability. 4) OH and O are key species to growth enhancement based on growth enhancement experiments together with optical emission spectra of plasmas and radical detection using ESR. 5) The growth enhancement is attributed not to an increase in each cell volume but to an increase in the number of cells. 6) The growth enhancement is attributed not to DNA mutation but to modification of DNA expressions induced by plasma irradiation.

Plasma physics contributes to agricultural applications of plasmas in various ways. We will give some issues of agricultural applications of plasmas related with plasma physics.

Work supported by JSPS.

- [1] The environmental food crisis, UNEP, ISBN: 978-82-7701-054-0.
- [2] S. Kitazaki, et al., Proc. IEEE TENCON (2010) p.1960.
- [3] N. Hayashi, et al., Jpn. J. Appl. Phys. **50** (2011) 08JF04.
- [4] S. Kitazaki, et al., Jpn. J. Appl. Phys. **51** (2012) 01AE01.
- [5] S. Kitazaki, et al., Curr. App. Phys. **14** (2014) S149.
- [6] T. Sarinont, et al., J. Phys.: Conf. Series **1** (2014) 015078.

Innovative medical technology in plasma disinfection of human body with low-temperature atmospheric-pressure plasmas ~ the reduced-pH method and the plasma-treated water (PTW) ~

K. Kitano^{1,4}, S. Ikawa², Y. Nakashima², A. Tani³, T. Yokoyama¹, T. Ohshima^{4,1}

¹Graduate School of Engineering, Osaka University, Suita, 565-0871, Japan,

²Technology Research Institute of Osaka Prefecture, Izumi, 594-1157, Japan

³Graduate School of Science, Osaka University, Toyonaka, 560-0043, Japan

⁴School of Dental Medicine, Tsurumi University, Yokohama, 230-8501, Japan

Considering wet conditions of human tissues, plasma process in liquid is an essential concept. Various kinds of chemical species in liquid induced by gas plasma can be used for some desirable medical treatment. For disinfecting human body in dental and surgical applications by low-temperature atmospheric-pressure plasmas, the inactivation of bacteria in body fluid is essential. The reduced-pH method was developed that strong bactericidal activity can be achieved if the solution is sufficiently acidic [1]. Induced $\text{HOO}\cdot$ into solution was confirmed to key active species, where $\text{O}_2^-\cdot$ in liquid is known to be changed into $\text{HOO}\cdot$, which has much stronger bactericidal activity, with acid dissociation equilibrium (pK_a 4.8). Infected models of human extracted tooth were effectively sterilized only at low pH condition [2].

In addition to direct and remote plasma exposures, the plasma-treated water (PTW) was confirmed to be effective with the reduced-pH method. Attenuation rate of PTW bactericidal activity were in accordance with Arrhenius equation both in liquid and solid states (Fig. 1). From the experimental results of ESR (Electron Spin Resonance) measurement of $\text{O}_2^-\cdot$ in liquid [3] against PTW with spin trapping method, half-lives of PTW were also in accordance with the Arrhenius equation (Fig.1). Half-lives of PTW activities at deep freezer temperature ($-80\text{ }^\circ\text{C}$) and body temperature ($+37\text{ }^\circ\text{C}$) are respectively calculated to 7 centuries and 3.9 seconds from the Arrhenius equation. This indicates that PTW can be cryopreserved in freezer and toxicity to human body seems to be low. Key species can be preserved in liquid under cool condition to bring high concentration PTW as integrated value. Based on cryopreservation concept, sequential production apparatus of high concentration PTW was developed with 1 meter glass tube and cooling system. The bactericidal activity of the PTW is extremely high that undiluted PTW corresponded 22 log reduction (i.e. 10^{-22}) of spore cell (*B. subtilis*). This corresponds to 65% H_2O_2 . PTW is ideal disinfectant solution for safety and strong disinfection. Recently, many types of PTW, containing plasma activated medium, are reported. But the active controls of pH and temperature have been still omitted. We believe that more physicochemical study must be required for further scientific discussions of plasma medicine.

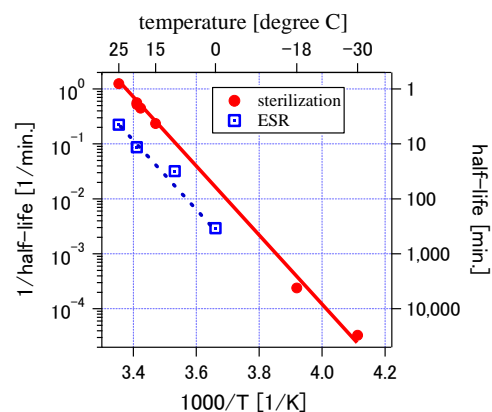


Fig. 1: Arrhenius plots for bactericidal activity and ESR measurement of PTW.

[1] S. Ikawa, K. Kitano, S. Hamaguchi, Plasma Process. Polym., 7, 33 (2010).

[2] E. Usui, T. Ohshima, H. Yamazaki, S. Ikawa, K. Kitano, N. Maeda, Y. Momoi, The Japanese Journal of Conservative Dentistry Vol.58, No.2, 101-108 (2015).

[3] A. Tani, Y. Ono, S. Fukui, S. Ikawa, K. Kitano, Appl. Phys. Lett., 100, 254103 (2012).

Recent status of the PAX and APEX projects toward the formation of electron-positron plasma

U. Hergenbahn^a, H. Niemann^{ab}, N. Paschowski^a, T. Sunn Pedersen^{ab}, H. Saitoh^{af}, J. Stanja^a,
E. V. Stenson^a, M. R. Stoneking^{ac}, C. Hugenschmidt^d, C. Piochacz^d, S. Vohburger^d,
L. Schweikhard^b, J. R. Danielson^e, and C. M. Surko^e

^a *Max-Planck-Institute for Plasma Physics, Greifswald and Garching, Germany*

^b *Ernst-Moritz-Arndt-Universität Greifswald, Greifswald, Germany*

^c *Lawrence University, Appleton, Wisconsin, USA*

^d *Technische Universität München, Garching, Germany*

^e *University of California, San Diego, USA*

^f *The University of Tokyo, Kashiwa, Japan*

haruhiko.saitoh@ipp.mpg.de

Electron-positron plasmas are predicted to exhibit unique properties as a result of the equal masses of the two particle species [1]. Motivated by recent successful confinement of pure electron non-neutral plasmas in toroidal geometries [2,3], we aim to create the first magnetically-confined electron-positron plasma in stellarator and dipole traps [4] operated at the NEPOMUC facility [5], the world's strongest positron source ($\sim 10^9$ moderated positrons per second). In order to realize confinement of positrons and electrons as plasma, we have started two experimental projects in parallel. One is the PAX (Positron Accumulation eXperiment), which aims to accumulate on the order of 10^{11} positrons using a buffer-gas trap and a multicell type linear trap [6]. On the way of constructing such a trap system, electron confinement experiments have been conducted with a Penning-Malmberg trap in a high-field (5 T) magnet. More than 1 hour of confinement and observation of collective mode for $\sim 10^9$ electrons have been realized. Based on these results, we will design a new accumulator with large electrostatic potential wells and rotating wall fields.

The second project is APEX (A Positron Electron eXperiment), focusing on efficient injection and confinement of positrons and electrons in toroidal geometries. In APEX, we started positron injection experiments using a prototype dipole field trap generated by a permanent neodymium magnet. In the first experimental campaign at NEPOMUC in 2015, we achieved efficient (40%) injection of the remoderated 5 eV positron beam into the dipole field. Injection was realized using static electric fields applied by ExB plates located outside the confinement region. We also measured the parallel and perpendicular positron beam energies, which are important parameters for further optimization of the injection efficiency. In the near future, we will construct a levitated dipole trap which can simultaneously confine positrons and electrons in closed field lines. Design studies on the trap configurations and the levitation system are ongoing.

- [1] P. Helander, *Phys. Rev. Lett.* **113** (2014) 135003.
- [2] P. W. Brenner and T. S. Pedersen, *Phys. Plasmas* **19** (2012), 050701.
- [3] Z. Yoshida *et al.*, *Phys. Rev. Lett.* **104** (2010) 235004.
- [4] T. Sunn Pedersen *et al.*, *New J. Physics* **14** (2012) 035010.
- [5] C. Hugenschmidt *et al.*, *New J. Physics* **14** (2012) 055027.
- [6] J. R. Danielson, T. R. Weber, C.M. Surko, *Phys. Plasmas* **13** (2006), 123502.

An Application of Fusion Oriented Neutrons for Transmutations of Long Life Fission Products

Motoyasu Sato, Norimasa Yamamoto, Atsuo Iiyoshi
Yoshihiko Hirooka, Takashi Muto,

An application of D-T fusion neutrons is proposed for the transmutation processing of Long Life Fission Products (LLFP).

Our simulations have revealed that the LLFP with a half lifetimes of million years can be transmuted to the isotopes or other atoms with shorter life time of 5~20 years under one year of continuous irradiations of 14.1MeV neutrons at the rate of $10^{19}/s$.

The mirror confinement devices are the candidates of the neutron production system. The ion of high energy tail will serve for more effective productions than the ordinary fusion reactors using thermally equilibrium ions to produce the large amount of neutrons of $10^{19}/s$.

Tsukuba University reported an estimation for which a neutron of $1 \times 10^{14}/s$ is provided at magnetic field strength 2T powered by the 20keVx30A NBI on Gamma-10. Neutrons of $5 \times 10^{18}/s$ may be possible by upgrading to 10T and NBI input to 8 times. Slow wave of ICRH is the other candidate.

Our basic study performs underlying research and development about the implementation of neutron source characterized by the monochromatic energy spectrum and uniform distributed radiation pattern. As an alternative to ADS device, that uses a high energy accelerator, our study suggests to new academic views and development to an application of fusion technology to solve a nuclear processing problem on a large scale.

This study is proceeded by the support of ImPACT research program by Japanese government, # 2015-PM08-05-01.

Wednesday, 4th November, 2015

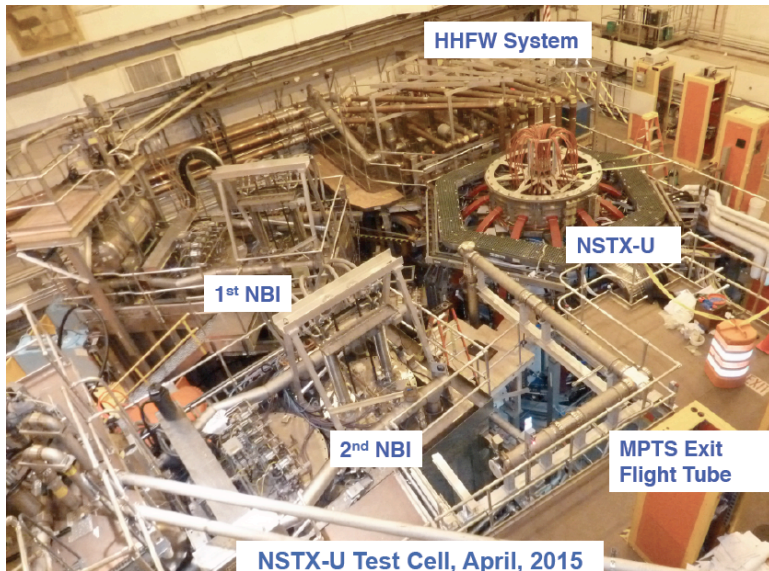
PL-2

Spherical Tokamaks and Fusion Energy Development Path*

M. Ono

Plasma Physics Laboratory, Princeton University, Princeton, New Jersey 08543, USA

The spherical torus or spherical tokamak (ST) is a member of the tokamak family with its aspect ratio ($A = R_0/a$) reduced to A near 1.5, well below the normal tokamak operating range of A equal to 2.5 or greater. As the aspect ratio is reduced, the ideal tokamak beta (ratio of plasma to magnetic pressure) stability limit increases rapidly, approximately as $1/A$ achieving $\sim 40\%$ toroidal beta (β_T). The plasma current I_p it can sustain for a given edge safety factor q_{95} also increases rapidly with I_p approaching I_{TF} . Because of the above, as well as the natural plasma elongation which makes its plasma shape appear spherical, the ST configuration can yield exceptionally high tokamak performance in a compact geometry. Due to its compactness and high performance, in addition to the longer term goal of an attractive fusion energy power source, the ST configuration has various near term applications, including a compact Fusion Nuclear Science Facility (FNSF) with relatively low fusion neutron power. A compact ST-based FNSF has the promise of achieving the high neutron fluence needed for reactor component testing with relatively modest tritium consumption. At the same time, the unique operating regimes of STs can contribute to several important issues in the physics of burning tokamak plasmas to optimize the performance of ITER. Since the start of the two mega-ampere class ST facilities in 2000, the National Spherical Torus Experiment (NSTX) in the US and Mega Ampere Spherical Tokamak (MAST) in the UK, active ST research has been conducted worldwide. More than sixteen ST research facilities operating during this period have achieved remarkable advances in all areas of fusion research, including fundamental fusion energy science as well as technological innovation [1]. These results suggest exciting future prospects for ST research in both the near and longer term. Recently, a series of upgrades are being implemented in the ST facilities including NSTX, MAST, and GLOBUS-M (RF) where the toroidal magnetic fields are increased from $\sim 0.5T$ to $\sim 1T$. The first plasma of NSTX-U is planned in August 2015. The talk will summarize the key physics results from worldwide ST experiments, and describe ST community plans to provide the database for FNSF design while improving predictive capabilities for ITER and beyond. The initial results from the newly commissioned NSTX-U will be also presented.



*This work supported by DoE Contract No. DE-AC02-09CH11466

[1] M. Ono and R. Kaita "Recent progress on spherical torus research," *Physics of Plasmas* 22, 040501 (2015).

Research towards operation with tolerable ELMs on European Tokamaks

H Meyer¹

¹CCFE, Culham Science Centre, Abingdon, OX14 3DB, UK

The high confinement scenarios currently foreseen for ITER/DEMO are unlikely to be compatible with the heat flux factor, $\eta_{\text{ELM}} = E_{\text{ELM}} / (A_w \tau_{\text{ELM}}^{1/2})$, for the divertor target (E_{ELM} : energy of the ELM to the divertor, A_w : wetted area and τ_{ELM} : ELM duration) or the ELM energy losses due to the naturally occurring type-I ELMs. Two routes are open for mitigating the effect of the ELMs: active ELM control, or the development of natural small or no ELM scenarios. The coordinated research on the European tokamaks AUG, JET, MAST and TCV aims at advancing the understanding in both areas.

With resonant magnetic perturbations a reduction of η_{ELM} by a factor of 2-4 by has been demonstrated at low pedestal top collisionality $\nu^* \leq 0.4$ on AUG and MAST. This reduction is observed for a magnetic perturbation which is most strongly amplified by the H-mode barrier edge pressure gradient and that is significantly off field alignment. ELM mitigation is accompanied with a strong density pump-out leading to a 15%-30% reduction in stored energy. On MAST the lost density could be replenished by pellets whilst still maintaining the ELM mitigation. At high collisionality type-I ELMs have been suppressed on AUG and JET with negligible loss in confinement and are replaced by smaller, more frequent ELMs symptomatic of type II-ELMs. Increasing the heating to lower the collisionality in these regimes lead to a reappearance of the type-I ELMs on both devices as also observed in plasmas with naturally occurring type-II ELMs.

ELM pacing with vertical kicks has been demonstrated on AUG, TCV and most recently on JET. The JET results show that a minimum kick amplitude depending on the pedestal temperature is needed. The data are consistent with an increased edge current caused by the movement. The trigger potential is only limited by the achievable edge current and the distance from the stability boundary, which allows triggering of an ELM quite close to a preceding ELM.

The pellet pacing efficiency, seen to be greatly diminished by the lack of C in all-metal devices, can be restored by seeding of N to levels that also increase the confinement. The potential of triggering an ELM after the previous ELM on AUG is scenario dependent and independent of pellet mass and velocity. This is in contrast to JET results where 20Hz-30Hz pellet pacing is achieved reliably with sufficiently large mini-fuelling pellets in clean plasmas and ELMs can be triggered immediately after the previous ELM as well as shortly after the L-H transition.

N seeding can also lead to smaller type-I ELMs. Various small or no ELM regimes (type-II, type-III, type-IV, grassy ELMs, QH-mode) have been demonstrated in medium sized tokamaks. However, the operation with an all-metal wall has largely closed the access window for regimes relying on low recycling such as the QH-mode. Type-II like ELMs have been accessed close to the ITER baseline scenario on AUG and by magnetic perturbations at high recycling. In both cases recycling at the high field side seems to be important. Type-III ELMs are encountered at high density and high power with 5%-10% confinement loss. This research shows that apart from the pedestal region also the conditions in the SOL are important for the ELM characteristics. Our focus is on physics understanding, since an ITER/DEMO like high recycling SOL together with low pedestal ν^* can't be achieved in today's devices.

Design status of structural components of helical fusion reactor FFHR-d1

H. Tamura, T. Goto, N. Yanagi, J. Miyazawa, T. Tanaka, S. Masuzaki, R. Sakamoto, A. Sagara, S. Ito^a, H. Hashizume^a, and the FFHR Design Group

National Institute for Fusion Science, 322-6 Oroshi-cho, Toki 509-5292, Japan

^a*Tohoku University, 6-6-01-2 Aramaki-Aza-Aoba, Aoba-ku, Sendai 980-8579, Japan*

The FFHR-d1 is a conceptual design of the LHD-type fusion reactor being developed at NIFS. Several design optimizations for FFHR-d1 have been conducted under a multipath strategy [1]. The base model has major and minor radii of 15.6 m and ~3.9 m, respectively. The superconducting magnet system consists of one pair of helical coils and two sets of vertical field coils. The magnetic field of the confinement center is 4.7 T. Since the FFHR-d1 is a fusion power plant, a blanket system and a divertor system is composed in the device. In the LHD-type configuration, the space between the plasma boundary and the helical coil is limited. Therefore, the structural design started from a radial build design of components, especially at the inboard of the torus. The support structure has to be rigid enough so that a constant geometric position of the components. On the other hand, large apertures are required for a maintenance work of in-vessel components. A shape of the support structure was carefully chosen and the analytic results showed that the stress level was in the permissible limit.

The divertor heat flux in the FFHR-d1 is anticipated to have a high peak of >10 MW/m². The neutron load on the divertor can be reduced by setting it behind a blanket to prevent direct neutron irradiation of the divertor region [2]. Developing this concept, a novel divertor structure was introduced in which the coil-support structure was modified to create a region receiving relatively low amounts of radiation. Using this proposed design would increase the lifetime of the divertor components. In addition, the divertor could be accessed from either the upper or lower sides of the device, simplifying maintenance [3]. Another idea to solve the divertor high heat flux together with easy maintenance and low radioactive wastes has been proposed using liquid metal flow [4]. This new divertor system can remove more than 20 MW/m² heat flux and more than 90% of the magnetic field lines directed toward the divertor region can be corrected. The novel divertor structure also matches this liquid divertor system for ease of maintenance. The feasibility study of a construction and maintenance for a blanket component with a helical shape has been conducted [5]. In this study, the blanket is simply sliced by the plane with a constant toroidal angle. Using large aperture of the support structure, these toroidally-sliced modules can be extracted by a simple movement with radial and vertical directions.

An innovative winding method was developed by connecting high-temperature superconducting conductors [6]. Winding feasibility investigations using an additive manufacturing (3D printing) were conducted and it was found that the conductor which has one helical pitch length could be inserted into the coil casing without deformation. Furthermore, a new idea for enlarging the blanket space by installing additional helical coils is also being considered [7] and to be integrated into the design.

- [1] A. Sagara, et al., *Fusion Engineering and Design* **89** (2014) 2114.
- [2] T. Tanaka, et al., *Fusion Engineering and Design* **89** (2014) 1939.
- [3] H. Tamura, et al., *Fusion Engineering and Design*, in press.
- [4] J. Miyazawa, et al., in this conference.
- [5] T. Goto, et al., in this conference.
- [6] N. Yanagi, et al., *Nucl. Fusion* **55** (2015) 053021.
- [7] N. Yanagi, et al., in this conference.

Hydrogen recycling in the divertor simulation plasma on GAMMA 10/PDX

M. Sakamoto, A. Terakado, K. Nojiri, K. Oki^a, N. Ezumi, Y. Nakashima,
K. Ichimura, K. Shimizu, M. Fukumoto^b, D. Kato^c, H. Sakaue^c, M. Yoshikawa,
J. Kohagura, T. Imai, M. Ichimura

Plasma Research Center, University of Tsukuba, 1-1-1 Tennodai, Tsukuba, Ibaraki 305-8577, Japan
^a *Graduate School of Electrical and Electronic Engineering, Chiba University, 1-33 Yayoicho, Inage-ku,
Chiba, 263-8522, Japan*

^b *Japan Atomic Energy Agency, 801-1, Mukoyama, Naka 311-0193, Japan*

^c *National Institute for Fusion Science, 322-6 Oroshi-cho, Toki 509-5292, Japan*

In the tandem mirror GAMMA 10/PDX, a new project has been promoted to study the boundary plasma and plasma surface interaction (PSI). The divertor simulation experimental module (D-module) has been installed in the end region of the mirror device to make best use of a linear plasma device with plasma confinement. The features of GAMMA 10/PDX for the boundary plasma and PSI studies are the following: (1) high ion temperature of the plasma exposed to the D-module (i.e. a few hundreds eV), (2) high magnetic field (0.15 ~ 1.5 T), (3) large plasma size (0.1 ~ 0.3 m), (4) low background pressure in the vacuum vessel and (5) high controllability of the plasma exposure since plasma heating systems of ECH, ICH and NBI are equipped. Noted that ion energy of the plasma is distributed, meaning that condition of PSI is equivalent to that of the torus plasma from a viewpoint of hydrogen recycling. We have studied hydrogen recycling with high temperature target and plasma detachment due to molecular activated recombination (MAR) using the D-module. Moreover, an electrically excited state of hydrogen atoms reflected on the tungsten target has been studied.

The D-module consists of a rectangular box (0.5 m square and 0.7 m in length) with an inlet aperture (0.2 m in diameter) at the front panel and a V-shaped target system inside the box. Tungsten target plates with the thickness of 0.2 mm are attached on a V-shaped base made of Cu. The target size is 0.3 m in width and 0.35 m in length. The length between the front edge of the target and the inlet of the D-module is about 0.3 m. The open-angle of the V-shaped base can remotely be changed from 15 degrees to 80 degrees. The sheath electric heaters are attached on the backside of the Cu base to control the target plate temperature (T_{target}) up to 573 K. Besides, additional hydrogen gas can be supplied near the inlet of the D-module. Measurements with Langmuir probe, spectroscopy, fast camera, ASDEX gauge and so on have been done for the plasma characterization. Moreover, another tungsten target plate with the diameter of 100 mm has been used to study the hydrogen recycling instead of the D-module.

When the additional hydrogen gas was supplied into the D-module, the electron density on the target (0.175 m from the corner of the target) increased up to $2 \times 10^{17} \text{ m}^{-3}$ at $\sim 0.4 \text{ Pa}$ of the internal pressure of the D-module and then it decreased to $\sim 0.6 \times 10^{17} \text{ m}^{-3}$, and the electron temperature decreased from 34 eV to $\sim 3 \text{ eV}$, suggesting the detachment occurred near the corner of the V-shaped target. The dependence of the H_{α} and H_{β} line intensities on the neutral pressure suggests that molecular activated recombination (MAR) occurred near the corner of the V-shaped target. When the T_{target} was increased upto 573 K shot by shot in another experiment, it is found that the intensities of balmer lines inside the V-shaped target and the electron density increased with increase in T_{target} , indicating that the recycling was enhanced due to increase in the target temperature.

Interactions of tungsten plasma facing material with edge plasma

Y. Ueda, K. Ibano, H. T. Lee

Graduate School of Engineering, Osaka University, 2-1 Yamadaoka, Suita, Osaka 565-0871, Japan

Tungsten is a leading candidate for plasma facing materials for ITER and DEMO. Because it has various preferable natures such as high thermal conductivity, high melting point, and low sputtering erosion by fuel ions. However, there still remain several issues such as evaluation of lifetime and impacts on plasma performance under complicated heat and particle exposure conditions, which include transient heat (ELMs and disruption) and mixed plasma (DT, He, edge cooling gas). In addition, fuel particles behavior is still under investigation such as fuel particle recycling which affects edge plasma control, T retention and permeation which affect system design, safety and T economy in fusion reactors. In reactor conditions, heavy neutron irradiation makes these more complicated since it deteriorate mechanical properties and increase retention.

In this presentation, recent research results and issues towards ITER and DEMO on tungsten plasma facing materials are reviewed especially on fuel retention and pulse heat loading effects.

On fuel retention, a large database as function of fluence [1] ($\leq 10^{26} \text{ m}^{-2}$), temperature (300-800 K), microstructure [3] and displacement damage [4] now exists from controlled laboratory experiments. Therefore, within the above parameter range hydrogen retention behavior is qualitatively well understood. However, quantitative understanding of the microscopic nature of the trap sites (e.g. concentration, energies, etc) still requires further work. Translating the laboratory findings to tritium inventory in fusion machines remains challenging due to several unique and complicated conditions such as the effect of high flux irradiations ($\leq 10^{25} \text{ m}^{-2}\text{s}^{-1}$), transient temperature excursions by ELMs, and evolution of radiation damage under complicated temporal and spatial temperature conditions. The development of radiation damage resistant advanced W-materials often require processing that increase retention and such conflicting requirements must be balanced.

On pulsed heat response, the most important issues remained are high cycle pulsed heat loading effects on tungsten. It is known that unmitigated ELMs would cause frequent surface melting, which is unacceptable in terms of enhanced erosion and plasma contamination. But even under pulsed heat less than that of the melting threshold could cause surface cracking and local melting. Acceptable ELM pulse energy for tungsten is still unknown, but this information is very important for development of ELM control in DEMO. Synergistic effects of pulsed heat and particle loadings (especially He) make conditions more complicated. Comprehensive database and appropriate modeling are necessary. In addition, melt layer behavior due to unmitigated disruption heat loading also should be known well. This closely relates to lifetime evaluation and requirement of disruption suppression. One of the key physics is vapor shielding effects but they require more works.

- [1] Z. Tian et al, Journal of Nuclear Materials 399 (2010) 101–107
- [2] V.K. Alimov et al., Journal of Nuclear Materials 438 (2013) S959–S962
- [3] A. Manhard, Deuterium inventory in tungsten after plasma exposure: a microstructural survey, Ph.D Thesis, University of Augsburg, 2011
- [4] M.H.J. ‘t Hoen et al., Nuclear Fusion 52 023008 (2012)

Research on Plasma Wall Interaction Facilities for Fusion Reactors

B. Unterberg

Institut für Energie- und Klimaforschung – Plasmaphysik, Forschungszentrum Jülich, D-52425 Jülich, Germany

Plasma-wall interactions (PWI) will decisively determine the availability and thus the economy of a fusion reactor because of their impact on the lifetime of the first wall (erosion and deposition) and on safety (tritium retention and dust production).

In view of plasma-wall interactions in future fusion devices such as ITER and a demonstration reactor, new challenges have to be met: extended operational regimes with respect to particle and heat flux densities onto plasma facing components, both steady-state and transient, the use of toxic first wall materials (Be in ITER), the presence of Tritium, the impact of neutron irradiation onto first wall materials and synergistic effects of the above mentioned operational conditions in fusion reactors.

Important PWI issues are related to short time scales of physical processes and can be investigated in devices with short pulse length such as power exhaust, erosion behavior and the subsequent transport of eroded wall material into the plasma edge. However, major PWI issues become significant on long time scales because they are related to long fluencies: The build-up of deposited layers and their stability, the evolution of surface morphology of plasma facing components, the accumulation of dust, the build-up of fuel inventory in plasma facing components, fatigue effects associated with a large number of transients and – last but not least – the accumulation of neutron damage with its impact on PWI processes.

To characterize plasma surface interactions under these conditions, dedicated plasma surface interaction facilities such as linear plasma devices can be used, which allow for detailed investigations not possible in magnetic confinement devices. Such experiments are complementary to studies in toroidal confinement devices.

In this contribution, we will exemplarily show important contributions from linear plasma devices for the understanding of PWI processes and introduce the Jülich Linear plasma Experiment (JULE-PSI), the construction of which is currently starting and which will be capable to investigate PWI processes with neutron irradiated material samples inside a Hot Cell.

Velocity profile measurement of lead-lithium duct flow by ultrasonic Doppler velocimetry

Y. Ueki, J. Yagi^a, Y. Noguchi, T. Tanaka^a, T. Yokomine^b, M. Hirabayashi^c,
K. Ara^c, T. Kunugi^b, A. Sagara^a

Osaka University, 2-1 Yamadaoka, Suita, Osaka 565-0871, Japan

^a *National Institute for Fusion Science, 322-6 Oroshi-cho, Toki 509-5292, Japan*

^b *Kyoto University, Kyoto-Daigaku Katsura, Nishikyo-ku, Kyoto, 615-8540, Japan*

^c *Japan Atomic Energy Agency, 4002 Narita, Oarai, Ibaraki, 311-1393, Japan*

ueki@mech.eng.osaka-u.ac.jp

The lead-lithium eutectic alloy is a promising liquid breeder. Lead-lithium flows need to be quantitatively evaluated, especially in the presence of a strong magnetic field, for better understanding its thermofluid in fusion blankets and sophisticating blanket designs. However, any velocity profile measurement techniques were not proposed before our research and development demonstrated that ultrasonic Doppler velocimetry (UDV) is able to measure the lead-lithium flow under a certain condition that an ambient oxygen concentration is enough low [1-2]. Sagara et al. of NIFS have constructed a new lead-lithium loop named as the Oroshhi-2 loop (See Fig. 1 [3]). In the present study, it is going to be reported that a velocity profile of a lead-lithium flow in the Oroshhi-2 loop is measured by means of UDV. A circular pipe is employed as our test-section (See Fig. 2), which is mounted on the Oroshhi-2 loop. The velocity profile is measured at the point where the flow is fully developed, and thus the measurement result is evaluated in comparison with a theoretical predication. As well as the velocity profile, pressures of the lead-lithium are measured with high-temperature pressure sensors. Based on them, UDV measurement characteristics and accuracy are quantitatively evaluated.

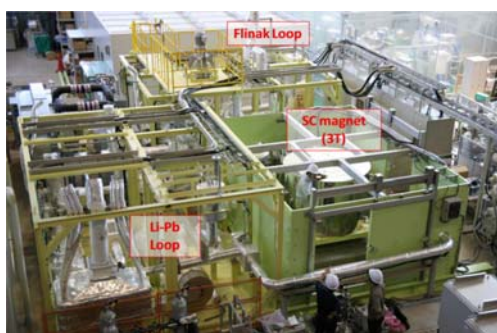


Fig. 1. Photograph of Oroshhi-2 loop [3].

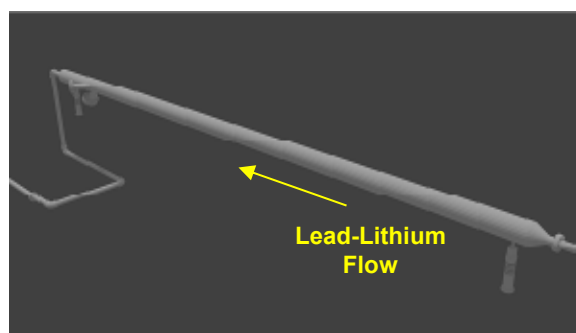


Fig. 2. Schematic drawing of test-section.

[1] Y. Ueki, et al., *Fusion Engineering and Design*, **89** (2014) 77-81.

[2] Y. Ueki, et al., *Fusion Sci. Technol.* **60** (2011) 506-LMX510.

[3] A. Sagara, et al., presented at 21st TOFE, Nov. 10th, 2014 Anaheim, USA.

Impacts of Material Innovation on Advanced Blanket Design

A. Kimura, H.I. Je, Y.S. Ha, D. Chen, W. Han,
K. Yabuuchi, T. Okuda^a, S. Ohnuki^b, S. Ukai^b, S. Ohtsuka^c,
P. Dou^d, S.H. Noh^e, A. Hasegawa^f

Institute of Advanced Energy, Kyoto University, Gokasho, Uji, Kyoto, Japan

^a *KOBELCO Research Institute, Kobe, Japan*

^b *Hokkaido University, Sapporo, Japan*

^c *Japan Atomic Energy Agency, Oarai, Ibaraki, Japan*

^d *Chonghong University Chonghong, China*

^e *Korea Atomic Energy Research Institute, Daejeon, Korea*

^f *Dept. of Engineering, Tohoku University, Sendai, Japan*

kimura@iae.kyoto-u.ac.jp

Materials development is essential for realization of fusion DEMO reactor and beyond. High performance materials R&D has been conducted for the last several decades, and there have been made some remarkable technology innovations of fusion blanket structural material including first wall material. In this work, current status of blanket structural materials R&D is summarized and the impacts of some material innovations on blanket design are introduced for each blanket system.

Among the candidate blanket structural materials, oxide dispersion strengthened (ODS) steels are considered to be promising for advanced blanket systems with high thermal efficiency, because the ODS steels have high-strength at elevated temperatures and good resistance to corrosion and irradiation degradation. The operation temperature can be elevated up to 700°C. Corrosion resistance was considerably improved by a dispersion of nano-sized oxide particles, which also resulted in suppression of irradiation-induced loss of tensile elongation, namely irradiation embrittlement.

In comparison to 9Cr martensitic steels, both the advantages and critical issues exist for the ODS steels, which will be discussed for each blanket system based on the surveillance test results on corrosion, long-term aging and irradiation experiments of the steels.

Finally, the R&D issues of structural materials towards advanced DEMO blankets are presented.

Progress of Linear IFMIF Prototype Accelerator in Rokkasho

A. Kasugai ^{A)}, J-M Ayala ^{B)}, B. Bolzon ^{D)}, P. Cara ^{C)}, N. Chauvin, S. Chel ^{D)}, E. Fagotti ^{E)}, D. Gex ^{C)}, R. Gobin ^{D)},
F. Harrault ^{D)}, R. Heidinger ^{C)}, R. Ichimiya ^{A)}, J. Knaster ^{B)}, K. Kondo ^{A)}, A. Marqueta ^{B)}, J. Molla ^{F)}, Ohira ^{A)},
Y. Okumura ^{B)}, M. Perez ^{B)}, G. Phillips ^{C)}, A. Pisent ^{E)}, G. Pruneri ^{B)}, K. Sakamoto ^{A)}, F. Scantamburlo ^{B)}, F. Senee ^{D)},
K. Shinto ^{A)}, M. Sugimoto ^{A)}, H. Takahashi ^{A)} and M. Valette ^{D)}

A) Japan Atomic Energy Agency (JAEA), Rokkasho Fusion Institute, Rokkasho, Aomori, Japan

B) IFMIF/EVEDA Project Team, Rokkasho, Aomori, Japan

C) F4E, Fusion for Energy, BFD Department, Garching, Germany

D) Commissariat à l'Énergie Atomique et aux Energies Alternatives (CEA/Saclay), France

E) Istituto Nazionale di Fisica Nucleare, Laboratori Nazionali di Legnaro (INFN-LNL), Italy

F) Centro de Investigaciones Energéticas, Medioambientales y Tecnológicas (CIEMAT), Spain

Under the framework of Broader Approach (BA) agreement between Japan and EU in the field of fusion energy research, the Engineering Validation and Engineering Design Activities (EVEDA) phase of the International Fusion Materials Irradiation Facility (IFMIF), in force since 2007, is validating the key technologies for IFMIF construction on schedule and cost. Whereas the Engineering Design Activities were successfully accomplished within the allocated time, as well as most of the validation activities related with the Target and Test facilities, the Accelerator Facility is being validated with the Linear IFMIF Prototype Accelerator (LIPAc). LIPAc is demonstrating the feasibility of the low energy section of an IFMIF deuteron accelerator up to 9 MeV with a beam current of 125 mA in CW at International Fusion Research Energy Center (IFERC) of Japan Atomic Energy Agency (JAEA) in Rokkasho, Japan. The deuterium ion beam injector developed in CEA Saclay was delivered in Rokkasho in 2014, and is under commissioning. At this stage, a 100keV/120mA/CW hydrogen ion beam and 100keV/90mA/CW deuteron ion beam have been produced with a low beam emittance of 0.21π mm-mrad (rms, normalized) and mass fractions above 90%. Delivery of RFQ components, consisting of RFQ accelerator developed by INFN in Italy and RF power supplies developed by CIEMAT in Spain is under way, followed by the installation of RF power supplies scheduled for this year as well. After the commissioning of the injector, RFQ, MEBT, D-Plate, HEBT, beam dump and SRF linac will be installed and tested in step-by-step approach.

Discussion on the effects of NaF on physical properties of Flinabe in comparison to Flibe from molecular dynamics simulations

H. Shishido, N. Yusa, H. Hashizume, Y. Ishii^a, N. Ohtori^b

*Department of Quantum Science and Energy Engineering, Graduate School of Engineering,
Tohoku University, Sendai, Japan*

^a Graduate School of Science and Technology, Niigata University, Niigata, Japan

^b Department of Chemistry, Faculty of Science, Niigata University, Niigata, Japan

hshishi@karma.qse.tohoku.ac.jp

Molten salt Flibe, which is a binary mixture of LiF and BeF₂, has been proposed as a candidate for a self-cooled liquid fusion blanket system [1], because of its such excellent characteristics as chemical stability, low vapor pressure, and much lower magnetohydrodynamic effects than those of liquid metals. Meanwhile, Flibe suffers from inefficiency in removing heat from the first wall due to the fact that it has high melting point and high Prandtl number. Another salt Flinabe, a ternary mixture of LiF, BeF₂ and NaF, has attracted attention recently [2] because it has lower melting point than Flibe. Whereas physical properties are necessary to discuss the applicability of Flinabe to a blanket system, experiment at high temperature involves technical difficulty because of high corrosiveness, and toxicity of beryllium. Furthermore, Flinabe is a ternary mixture consisting of three compounds, which implies that finding a suitable composition of Flinabe experimentally would require many resources.

A polarizable ion model has been developed to simulate the physicochemical characteristics of molten salts by molecular dynamics (MD) simulations [3]. Several studies have parameterized the interaction potentials for many molten salts based on first-principles simulations and indicated that molecular dynamics simulations with the polarizable ion model are quite useful to predict the physical properties of molten salts. Encouraged by these studies, our previous study [4] simulated density and viscosity of Flibe and Flinabe with the pair-potential parameterized by ref [5]. Results revealed that Flinabe shows lower viscosity than that of Flibe even when they contain almost the same BeF₂. However, the maximum discrepancy between the calculated viscosities and the experimental data was about 18 %. These results led us to consider that it is necessary to improve the potential parameters in order to predict the properties accurately.

This study aims to reconstruct the pair-potential parameters of Flibe and Flinabe, and evaluate the effects of NaF on the physical properties. Firstly, the force and the dipole on each ion are analyzed by first-principles simulations based on density functional theory. Then, the interaction potentials are fitted to results from first-principles calculation. This study has obtained the parameters fitted well, rather than the earlier study [5]. Then, the physical properties (density, viscosity, and thermal conductivity) are evaluated with the potential parameters obtained above and compared with the experimental data. Finally, the influence of NaF on the properties of the salts will be discussed.

[1] A. Sagara et al., *Fusion Sci. Technol.* **47** (2005) 524.

[2] A. Sagara et al., *Fusion Eng. Des.* **89** (2014) 2114.

[3] P. A. Madden and M. Wilson, *Chem. Soc. Rev.* **25** (1996) 339.

[4] H. Shishido et al., *Fusion Sci. Technol.*, in press.

[5] R. J. Heaton et al., *J. Phys. Chem. B* **110** (2006) 11454.

Experimental and numerical study of H^- production in DC H^- source of medical cyclotron

H. Etoh^a, M. Onai^b, Y. Aoki^a, H. Mitsubori^a, Y. Arakawa^a, J. Sakuraba^a, T. Kato^a, T. Mitsumoto^a, S. Yajima^a, T. Shibata^c, A. Hatayama^b, and Y. Okumura^d

^a Sumitomo Heavy Industries, Ltd., Tokyo, Japan

^b Graduate School of Science and Technology, Keio University, Kanagawa, Japan

^c High Energy Accelerator Research Organization (KEK), Ibaraki, Japan

^d Fusion Research and Development Directorate, Japan Atomic Energy Agency, Aomori, Japan

Negative hydrogen ion (H^-) beam is widely used for medical proton cyclotrons whose applications are cancer therapy and diagnostics, such as boron neutron capture therapy (BNCT) and the radioisotope production for PET and SPECT. These applications require high intensity beam extracted from cyclotron to shorten the irradiation time for BNCT and increase the production rate of medical radioisotope.

A high current DC H^- source has been developed for improving the cyclotron's beam intensity [1, 2]. The source is a multi-cusp DC arc-discharge source and H^- ions are produced by the volume production mechanism. The addition of Caesium (Cs) into this type of source is known to increase the production rate of H^- on the surface of the plasma electrode. Cs-free and Cs-seeded operations have been tested on our source. 10 mA of H^- beam current has been obtained stably in the Cs-free operation, and H^- current has reached 22 mA in the Cs-seeded operation.

In addition to these encouraging results, the relationship between the H^- production and the design/operating parameters (such as magnetic field configuration, arc-discharge power, and so on) is now being studied experimentally, in order to enhance the H^- current. Moreover, a systematic numerical study of electron energy distribution function (EEDF) in the source plasma is also now underway by KEIO-MARC simulation code [3]. The resultant H^- production in the source is analyzed by the zero dimensional (0D) rate equation for H^- ion. Initial results show a reasonable agreement with the experimental results. For example, the simulation by KEIO-MARC code reproduces the magnetic filter effects, i.e., the large reduction of the electron temperature across the magnetic filter field. Figure 1 shows the results of EEDF at each distance from the plasma electrode. For further enhancement of the H^- beam current, more detailed comparison between the experiment and the modeling is now underway.

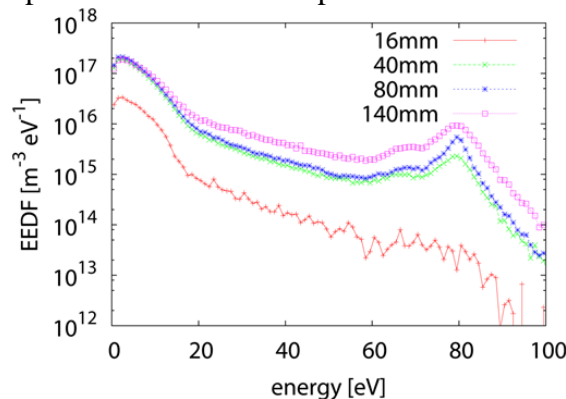


Figure 1. EEDF at each distance from the plasma electrode

- [1] H. Etoh *et al.*, *Rev. Sci. Instrum.* **85**, 02B107 (2014).
- [2] H. Etoh *et al.*, *AIP Conference Proceedings*, **1655**, 030014 (2015).
- [3] T. Shibata *et al.*, *J. Appl. Phys.* **114**, 143301 (2013).

Thursday, 5th November, 2015

PL-3

Innovations that make the Use of Ion Cyclotron Power suitable for Fusion Reactors

J.-M. Noterdaeme^{1,2}, V. V. Bobkov¹, H. Fuenfgelder¹, R. D'Inca¹, R. Ochoukov¹, J. Jacquot¹, I. Stepanov², W. Zhang¹, H. Faugel¹, K. Cromb  ^{2,3}, R. Ragona^{2,3}, A. Messiaen³, D. Van Eester³, A. A. Tuccillo⁴, O. Tudisco⁴, G. Rocchi⁴, Q. Yang⁵, D. Milanesio⁶, R. Maggiora⁶, L. Colas⁷, S. Heuraux⁸, E. Faudot⁸, J. Moritz⁸, A. Silva⁹, the ASDEX Upgrade¹ and EUROfusion MST1* Teams

¹ Max-Planck-Institut f ur Plasmaphysik, Boltzmannstr. 2, D-85748 Garching, Germany

² Ghent University, Applied Physics Department, B-9000 Gent, Belgium

³ LPP-ERM/KMS, B-1000 Brussels, Belgium

⁴ ENEA, Frascati, Italy

⁵ ASIPP, Institute of Plasma Physics, Chinese Academy of Sciences, Hefei, China

⁶ Politecnico de Torino, Torino, Italy

⁷ CEA, IRFM, F-13108 Saint-Paul-Lez-Durance, France

⁸ IJL UMR 7198 CNRS-Universit  de Lorraine, BP70239, F-54506 Vandoeuvre, France

⁹ Instituto de Plasmas e Fus o Nuclear, IST, 1049-001 Lisboa, Portugal

The coupling of power in the Ion Cyclotron Range of Frequency, to the plasma, has been one of the first heating methods used in fusion research, and is, in principle, also one of the most promising. Over the years, it has encountered challenges, which have put its future use into question. These can be classified into two broad range of categories: the *sensitivity to the plasma edge density profile* with the corresponding difficulty to couple the power to the plasma and *enhanced plasma-antenna interaction* with, among others, the resulting impurity production.

Following a short historical overview, we concentrate on the systematic approach taken and recent results obtained at the Max-Planck-Institut f ur Plasmaphysik in cooperation with other institutes, to tackle step by step those challenges, leading to solutions applicable to fusion reactors.

In the category *sensitivity to the plasma edge density profile*, the first serious problem encountered followed the appearance of the H-mode and the resulting strong ELMs. The use of 3-dB couplers isolated the generators from the antenna. More recently, tailoring the density profiles with local gas puffing was shown experimentally to increase the coupling. A systematic study confirmed that the coupling can be properly calculated if the local density profile is known. The combination of a theoretical approach to model the local density profile and local measurements at the antenna, which will soon be available, is expected to develop into a predictive capability to calculate and optimize the coupling. We will be able to rely on those tools for the design of a new antenna concept for DEMO (360  toroidally distributed, travelling wave type antenna), which is by itself already less sensitive to the edge density profile and has a better coupling.

In the category *enhanced plasma-antenna interaction*, a persistent enhanced impurity production was exacerbated in the all-metal ASDEX Upgrade when the antenna limiters were also coated with W. The hypothesis that this enhanced interaction is due to RF sheaths – possibly a consequence of undesirable induced current – has, up to now, not been invalidated. New 3-strap antennas in ASDEX Upgrade, designed to lower these RF sheaths by cancelling the undesirable induced currents, have shown experimentally to indeed reduce the impurity production. Theoretical approaches to model in detail the development of the sheaths are being developed and will be checked against measurements on ASDEX Upgrade and on IShTAR, a dedicated test stand. Here too, the combination of theory and experiments is expected to lead to a better understanding of the sheath production mechanism, and to a solidly grounded approach to design antennas with reduced sheaths. The new antenna concept for DEMO conceptually avoids, with its 360  symmetry, undesired induced currents and possibly prevents the occurrence of sheaths. The optimization of the DEMO antenna concept will benefit from a better understanding of sheath production and the availability of benchmarked tools.

* <http://www.euro-fusionscipub.org/mst1>

Predictions of Plasma Performance and Fusion Reactions in the Deuterium Experiment Plasma of LHD

S. Murakami, H. Yamaguchi, M. Homma, S. Maeta, A. Sakai, A. Fukuyama, K. Nagaoka, H. Takahashi, H. Nakano, M. Osakabe, M. Yokoyama, K. Tanaka, K. Ida, M. Yoshinuma, M. Isobe, H. Tomita, K. Ogawa, LHD Experiment Group

Department of Nuclear Engineering, Kyoto Univ., Nishikyo, Kyoto, JAPAN

^aNational Institute for Fusion Science, Toki, JAPAN

^bDepartment of Quantum Engineering, Nagoya Univ., Nagoya, JAPAN

The deuterium experiment project from 2017 is planned in LHD, where the deuterium NBI heating beams with the power more than 30MW is injected into the deuterium plasma. Main objects of this project are to make clear the isotope effect on the heat and particle transport in the helical plasma and to study energetic particle confinement in a helical magnetic configuration measuring triton burn-up neutrons.

We have developed an integrated transport simulation code, TASK3D[1], and applied to the high ion temperature plasma of LHD[2, 3]. The particle and heat transport equations are solved and compared with LHD experimental results. Heat and particle transports are assumed to be the sum of the neoclassical transport and the turbulent transport. We obtain relatively good agreements between the simulated and experimental radial profiles of the density and temperature in the steady state plasma of LHD[2, 3]. Also, to study the kinetic behavior of the energetic particle in a helical magnetic configuration, we have developed GNET[4] code, in which the drift kinetic equation of energetic particles is solved in five-dimensional phase space. GNET code is improved to evaluate the D-D and D-T fusion reaction between the energetic and thermal ions.

In this paper, we study the deuterium experiment plasma of LHD by TASK3D and GNET. We solve the heat and particle transport of the deuterium plasma assuming the improvement of the turbulent transport from that of the hydrogen plasma due to the isotope effect. We consider a simple and H-He experiment based turbulent transport models. The radial profile of densities and temperatures of the deuterium experiment plasma are evaluated. Next we study the production and confinement of Tritons (1.01MeV) by GNET code. We show characteristic distributions of Tritons in the real and velocity spaces. We also evaluate D-T fusion reaction rates and Triton burn-up neutron signals of the diagnostic system using the obtained triton distributions.

References

- [1] M. Sato et al., Plasma Fusion Res. **3**, S1063 (2008).
- [2] S. Murakami et al., Plasma Phys. Control. Fusion **57**, 054009 (2015).
- [3] A. Sakai et al., Plasma Fusion Res. **10**, 3403048 (2015).
- [4] S. Murakami et al., NUCLEAR FUSION **46**, S425 (2006).

The full-size source and injector prototypes for ITER neutral beams

G. Serianni, P. Agostinetti, V. Antoni, D. Aprile, C. Baltador, M. Cavenago^a, G. Chitarin, N. Marconato, D. Marcuzzi, E. Sartori, P. Sonato, V. Toigo, P. Veltri, P. Zaccaria

*Consorzio RFX (CNR, ENEA, INFN, UNIPD, Acciaierie Venete SpA), Corso Stati Uniti 4 – 35127
Padova, Italy*

^a INFN-LNL, viale dell'Università n. 2, 35020 Legnaro, Italy

Two Neutral Beam Injectors (NBI) will provide a substantial fraction of the heating power necessary to ignite thermonuclear fusion reactions in ITER. The development of the NBI system at unprecedented parameters (40 A of negative ion current accelerated up to 1 MV) requires a strong demonstration activity, which was endorsed by ITER to optimise the crucial components and systems. A test facility, PRIMA (Padova Research on ITER Megavolt Accelerator), is presently in the final phase of construction at Consorzio RFX (Padova, Italy) in the CNR research area and will house two experiments, named SPIDER and MITICA. A full-size negative ion source, SPIDER (Source for the Production of Ions of Deuterium Extracted from Rf plasma), will be operated in the facility to demonstrate the creation and extraction of a D^-/H^- current up to 50/60A on a wide surface (more than $1m^2$) with uniformity within 10%. The second experimental device is the prototype of the whole ITER injector, MITICA (Megavolt ITeR Injector and Concept Advancement), aiming to develop the knowledge and the technologies to guarantee the successful operation of the two injectors to be installed in ITER, including the capability of 1MV voltage holding at low pressure. The beam source is the key component of the system, whose design results from a tradeoff between requirements of the optics and real grids with finite thickness and thermo-mechanical constraints due to the cooling needs and the presence of permanent magnets. The experimental effort is supplemented by numerical simulations devoted to the optimisation of the accelerator optics and to the estimation of heat loads and currents on the various surfaces.

In the paper the main requirements will be discussed and the design and the status of the main components and systems will be described. Particularly a review of the accelerator physics and a comparison between the designs of the SPIDER and MITICA accelerators are presented. This work was set up in collaboration and financial support of F4E.

Recent Studies of Hydrogen Negative Ion Source and Beam Production for NBI in Large Helical Device

K. Ikeda^a, P. Agostinetti^c, M. Brombin^c, U. Fantz^d, S. Geng^b, O. Kaneko^a, M. Kisaki^a,
K. Nagaoka^a, H. Nakano^a, M. Osakabe^a, E. Sartori^c, G. Serianni^c, Y. Takeiri^a,
K. Tsumori^a, P. Veltri^c, C. Wimmer^d, and D. Wunderlich^d

^a*National Institute for Fusion Science, 322-6 Oroshi-cho, Toki 509-5292, Japan*

^b*The Graduate University for Advanced Studies, Toki Gifu, 509-5292, Japan*

^c*Consorzio RFX (CNR, ENEA, INFN, Università di Padova, Acciaierie Venete SpA) Corso Stati
Uniti 4 - 35127 Padova (Italy)*

^d*Max-Planck-Institut für Plasmaphysik, Boltzmannstraße 2, 85748 Garching, Germany*

Neutral beam injector (NBI) is an indispensable device to produce high-density and hot plasmas in fusion development machine. We have developed negative-ion-based NBI (N-NBI) in LHD, that have been operated continuously since 1998. Three N-NBIs are arranged tangentially, and was equipped with a negative hydrogen ion (H^-) source which enabled high energy and high power beam injection. The nominal specification of beam energy and beam power for each N-NBI was 180 keV and 5 MW, respectively. We had achieved 16 MW beam injection by three N-NBIs in LHD experiment. Moreover, we installed two positive-ion-based neutral beam injector (P-NBI) arranged perpendicularly to the LHD. High-power (12 MW) with lower energy (40 ~ 60 keV) beam injection allowed effective ion heating and profile measurement of ion temperature by charge exchange recombination spectroscopy.

A hydrogen negative ion source is a key component in N-NBI system, that will also use future NBI in ITER. Understanding of H^- behavior from cesiated metal production surface to extraction aperture is an important issue to maintain high power negative ion beam. We have researched distribution of H^- ions and its extraction behavior by cavity ring-down spectroscopy and a spectrally-selective imaging system, respectively, in the 1/3 scaled ion source (NIFS-RNIS). We found that H^- ions widely distributed in the extraction region, and these ions constituted H^- beam.

Recently, we have a lot of domestic and international collaboration program for H^- source. We applied a spectrally-selective imaging system in RF hydrogen negative ion source in ELISE test facility in Max-Planck-Institut für Plasmaphysik (IPP) Garching (Germany). We found clear signal response on H_α emission during beam extraction. This observation will contribute to obtain behavior of H^- ions in RF source which is variable output for production high power beam and optimization of beam shape in ITER source. We also observed an extracted H^- beam shape in NIFS-RNIS used the mini-STRIKE system which consists of a carbon-fibre-carbon-composite (CFC) tiles and an infrared camera collaborated with Consorzio RFX (Italy). We found the clear dependence between the beam shape and operating parameters. These findings have contributed to the high performance and safety NBI operation in the LHD.

Advances in 2-D Millimeter-Wave Plasma Imaging of Magnetic Fusion Plasmas

N.C. Luhmann, Jr., Yu-Ting Chang, Ming Chen, Xi Chen^a, C.W. Domier, J. Gu, Fengqi Hu, Xing Hu, G.J. Kramer^b, Meijiao Li, X. Liu, M. Mamidanna, A.-V. Pham, T. Phan, Xiaoxin Ren, L. Shi^b, A.G. Spear, B. Tobias^b, Yilun Zhu

University of California at Davis, Davis, CA 95616, USA

^a*General Atomics, San Diego, CA 92127, USA*

^b*Princeton Plasma Physics Laboratory, Princeton University, Princeton, NJ 08543*

UC Davis and PPPL are developing advanced millimeter wave technologies for imaging density and temperature fluctuations in magnetic fusion plasmas. A high resolution 12×8 MIR system is under development for use on the EAST tokamak in Hefei, China. The diagnostic is similar to the DIII-D Microwave Imaging Reflectometer (MIR) system operating on the DIII-D tokamak [1, 2] and will co-exist with the Electron Cyclotron Emission (ECE)-Imaging system developed by UC Davis and currently operating on EAST [3]. Unique to the EAST MIR system, which, is the ability to independently tune all 8 illumination frequencies. In addition to providing unparalleled flexibility in the selection of plasma cutoff surfaces to monitor, this capability also allows the frequencies to be continuously varied so as to maintain optimum focusing in the presence of time-varying density profile changes.

UC Davis also has an active mm-wave technology development program that aims to revolutionize the state-of-the art in transmitter and receiver systems for ECE-Imaging and MIR. CMOS systems-on-a-chip (SOC) are being pursued for use as a compact, multi-frequency MIR transmitter. Next generation receiver arrays feature “on-board” multiplication, amplification and delivery of local oscillator drive, eliminating long, costly runs of overmoded waveguide and reducing low frequency noise. Pre-amplification of signals in-band with MMIC LNAs significantly reduces system noise temperature, while reliability is enhanced through the use of liquid crystal polymer (LCP) hermetic packaging and modules. Wide bandgap GaN MMICs exhibit larger breakdown voltage, allowing for very high power density, necessary for robust, low-noise operation in harsh environments. Digital beamforming systems using high speed field programmable gate array (FPGA) controllers as well as direct digital synthesis will provide active beam steering and beam focusing/defocusing capabilities to MIR.

The plasma imaging program is supported by an aggressive program in synthetic modelling. A robust MIR synthetic diagnostic platform has been developed by integrating the PPPL full-wave reflectometer code and a diffraction-based optical code to simulate the full diagnostic process using either experimentally determined perturbed density profiles or from plasma simulations [4]. A similar synthetic diagnostic is also being developed for ECE-Imaging. This work is supported by US DoE grants DE-AC02-09CH11466 and DE-FG02-99ER54531.

- [1] C.M. Muscatello, C.W. Domier, X. Hu, G.J. Kramer, N.C. Luhmann, Jr., X. Ren, P. Riemenschneider, A. Spear, B.J. Tobias, E. Valeo, L. Yu, *Rev. Sci. Instrum.* **85**, 11D834702 (2014).
- [2] A.G. Spear, C.W. Domier, X. Hu, C.M. Muscatello, X. Ren, B.J. Tobias, N.C. Luhmann, *Rev. Sci. Instrum.* **85**, 11D834 (2014).
- [3] C. Luo, B.J. Tobias, B. Gao, Y. Zhu, J. Xie, C.W. Domier, N.C. Luhmann, T. Lan, A. Liu, H. Li, C. Yu and W. Liu, *J. Instrum.* **9**, P12014 (2014).
- [4] X. Ren, C.W. Domier, G. Kramer, N.C. Luhmann Jr., C.M. Muscatello, L. Shi, B.J. Tobias and E. Valeo, *Rev. Sci. Instrum.* **85**, 11D863 (2014).

Recent results from the H-1 heliac on MHD activity, fluctuations and RF propagation

B.D. Blackwell, C.A. Michael, S.R. Haskey, A. Thorman, F.J. Glass, D.G. Pretty, C. Nührenberg^a, A. Konies^a, M.Cole^a, M.J. Hole^b, V. Moiseenko^c, B. Seiwald and J. Howard

Plasma Research Laboratory, RSPE, ANU, Canberra, ACT 0200, Australia

^a *Max-Planck-Institut für Plasmaphysik, Greifswald, Germany*

^b *RSPE, ANU, Canberra, ACT 0200, Australia*

^c *IPP, National Science Center "Kharkiv Institute of Physics and Technology", Ukraine*

H-1 is a medium-sized ($R \sim 1\text{m}$, $\langle a \rangle \sim 0.15\text{-}0.2\text{ m}$) 3 field period flexible heliac with access to a wide range of magnetic configurations. Plasma generated in H-1 (H/D/He mixtures, $B \sim 0.5$, $n_e \sim 10^{18}$) by RF at ω_{cH} shows a very complex dependence on configuration; both the electron density and the nature of fluctuations vary in a manner correlated with the presence of low order rational values of rotational transform. Results from both coherent, MHD range fluctuations and broadband fluctuations in the range 1-200kHz are reported, and a new method for visualising RF waves is described.

Coherent modes $\sim 5\text{-}100\text{kHz}$ are detected by three magnetic probe arrays, displaying Alfvénic scaling in many cases. New results separating the effects of magnetic field, rotational transform, number and mass density will be presented. The accompanying density fluctuations have been imaged by tomography of three views of carbon ion optical emission, revealing their 2D structure. This is in good agreement with the mode structure of BAEs predicted by the CAS3D MHD code, induced by the strong shaping of H-1. Mode identification using data mining techniques (Figure 1) and possible drive mechanisms will be discussed. For example, the strong shaping produces a large $n=6$, $m=2$ component in the $|B|$ spectrum allows excitation of the $5/4$ mode by populations \sim one order slower than $V_{\text{Alfvén}}$.

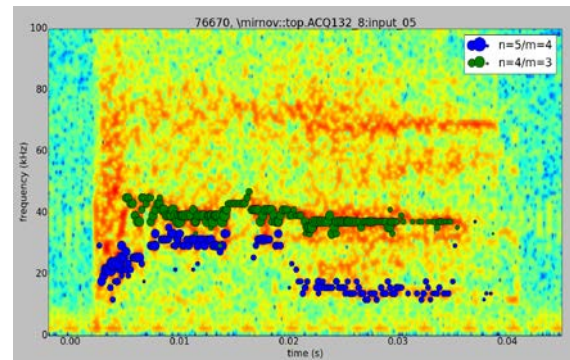


Figure 1: Identification of the dominant MHD modes in H-1, $n/m = 5/4$ and $4/3$

Measurements of the structure of edge turbulence using twin Langmuir probes have revealed poloidally extended structures in both density and potential at low frequencies. Their narrow radial extent resembles zonal flows found in both Ar discharges in H-1 and other devices. Fluctuation-induced flux has been evaluated for higher frequency modes, including BAEs and broadband turbulence, and correlated with changes in overall confinement. Langmuir probes have also been used to determine the configuration dependence of confinement in the vicinity of the $7/5$ resonance. When the resonance is located near the plasma edge in a magnetic hill region, the plasma density exhibits strong dithering type behaviour as well a decrease in edge density, characteristic of flattening in the $7/5$ island or ergodic region.

The first images of propagating radiofrequency waves were obtained by an RF-synchronised camera viewing the H-1 plasma under the RF antenna, illuminated by a localised supersonic gas puff. The observed waves appear to have a wavelength smaller than the fast wave, and are strongly affected by the position of the ion-cyclotron resonance layer. Observations will be compared with predictions of a finite element cylindrical RF code, and plans for a compact Uragan-type Alfvén heating antenna will be presented.

Friday, 6th November, 2015

PL-4

Commissioning and First Plasma Operation at the Wendelstein7-X Stellarator

H.P. Laqua, W7-X team,

Max Planck Institute for Plasma Physics, EURATOM Association, 17491 Greifswald, Germany

Wendelstein7-X is the first large Stellarator with super-conducting modular coils. Its design and construction has been a technologic, engineering and logistic challenge. 50 non-planar coils and 10 planar coils had been produced and assembled with high precision and quality requirements. Thermal insulation was fault-free placed in a narrow 3-dimensional space in between the cold coil casing and the plasma vessel. Even more the components inside the plasma vessel required precise positioning in the 3-dimensional environment. Most of the components need a full steady state design for continuous heat loads and have to take into account the additional load by microwave stray radiation of the electron cyclotron heating (ECRH) with a power of 10 MW for 30 minutes. High heat load components have been developed and tested for steady state operation at a maximal power load of up to 10 MW/cm². The plasma start-up and long pulse operation will be sustained by a 10 MW ECRH system at a frequency of 140 GHz. The ECRH will be supported by NBI and ICRH for short pulse (<20 s) operation.

The main machine assembly, in particular closing the cryostat, had been finished in March 2014. The consecutive commissioning runs with in its schedule. First the cryo-vessel was successfully pumped down and the coils cool down was performed within 4 weeks. When the coil temperature was below 4°K the commissioning of the super conducting system started. The nominal magnetic field strength of 2.5 T on axis could be achieved, which is the pre-condition for ECRH plasma operation at the second harmonic electron cyclotron resonance. The safety system for the coil current fast shut down was successfully tested. In parallel the plasma vessel was pumped down. Next the magnetic flux surfaces could be measured. Different coil currents generate different magnetic field configurations. The characteristic magnetic flux surfaces and island structure were found as theoretically predicted. Therefore major misalignments could be excluded. This demonstrates already the feasibility of the modular stellarator concept.

For the first test plasma operation (OP1.1 [1]) W7-X is equipped with a graphite limiter in each of the five modules. A set of most important diagnostics is installed. The ECRH system is commissioned. Six of seven gyrotrons with a power of up to 5 MW are in operation.

Further preparation work is ongoing now. The central safety system and radiation protection is presently evaluated by the government authorities in order to receive the operation license soon.

[1] T. Sunn Pedersen et. al., "Plans for first plasma operation of Wendelstein 7-X", submitted to Nuclear Fusion

Progress of Gyrokinetic Turbulence Simulation in Helical Plasmas

M. Nunami, A. Ishizawa, M. Nakata, S. Toda, T.-H. Watanabe^a, and H. Sugama

National Institute for Fusion Science, 322-6 Oroshi-cho, Toki 509-5292, Japan

^a*Department of Physics, Nagoya University, Nagoya, 464-8602, Japan*

nunami.masanori@nifs.ac.jp

Quantitative evaluations of anomalous transport fluxes of particles and heat in magnetically confined plasmas are critical issues for the design of fusion reactors. The gyrokinetic approaches are powerful to analyze the transport phenomena, which are considered to be driven by the drift-wave plasma turbulence. Numerical simulations based on the gyrokinetics, however, requires a huge computational resources for calculations of turbulent transport in toroidal plasmas. Especially, in three-dimensional system such as Large Helical Device (LHD), the higher spatial resolutions are required to cover the complicated three-dimensional field structure, which are obtained from the equilibrium calculation corresponding to the experimental observations.

In the past few years, a number of gyrokinetic codes which are available for simulating the turbulence phenomena in the three-dimensional field configurations have been developed, e.g., GENE-GIST[1] and GKV/GKV-X[2], and the codes were verified each other in the benchmarking calculations. Using the codes, the turbulence simulations have been performed. The ion temperature gradient (ITG) turbulence simulations, for example, showed significant results that the simulations reproduced the turbulent spectra and the transport coefficient in the LHD experiment, and the optimized field configurations may reduce the transport levels [3, 4]. Recently, we extend the GKV/GKV-X code to include the electromagnetic effects [5], and multi-species plasmas with precise collisions [6, 7].

On the other hand, it is strongly demanded to establish a reduced transport model that can quickly reproduce the nonlinear simulation results, because the gyrokinetic simulations in helical systems tend to consume huge computational resources. Using linear instability analyses, a primitive reduced model has been constructed for pure ITG turbulent transport in helical plasmas under the collisionless limit [8]. Linear growth rates of the instabilities and the linear zonal flow responses in the model, we applied the model to integrated transport simulations, and it can predict the plasma profiles in LHD plasmas.

- [1] P. Xanthopoulos *et al.*, Phys. Plasmas **16** (2009), 082303.
- [2] M. Nunami *et al.*, Plasma Fusion Res. **5** (2010) 016.
- [3] M. Nunami *et al.*, Phys. Plasmas **19** (2012), 042504.
- [4] T.-H. Watanabe *et al.*, Phys. Rev. Lett. **100** (2008), 195002.
- [5] A. Ishizawa *et al.*, Nucl. Fusion **55** (2015), 043024
- [6] M. Nunami *et al.*, Plasma Fusion Res. **10** (2015), 1403058.
- [7] M. Nakata *et al.*, Compt. Phys. Comm. (2015) in press.
- [8] M. Nunami *et al.*, Phys. Plasmas **20** (2013), 092307.

Kinetic physics of magnetic reconnection in collisionless plasmas

C. Z. Cheng^a, S. Inoue^b, Y. Ono^a, and R. Horiuchi^c

^a *Department of Advanced Energy, University of Tokyo, Kashiwa, Chiba 277-8561, Japan*

^b *Japan Atomic Energy Agency, 801-1, Mukoyama, Naka 311-0193, Japan*

^c *National Institute for Fusion Science, 322-6 Oroshi-cho, Toki 509-5292, Japan*

Highlights of the collisionless plasma kinetic physics during driven magnetic reconnection are presented. In particular, we explain the physical pictures of (1) how electron and ion dynamics decouple and how the charge separation and electrostatic electric field are produced in the magnetic field reversal region (reconnection current layer and outflow exhaust) and around the separatrix regions, (2) how electrons and ions gain energy in the reconnection current layer, (3) why the electron outflow velocity in the reconnection exhaust reaches super-Alfvénic speed and the ion outflow velocity reaches Alfvénic speed and how the parallel electric field is produced, (4) how electrons are accelerated by the parallel electric field around the separatrix region, and (5) how ions gain energy when they move across the separatrix region into the downstream. We also show that electrons and ions gain energy mainly from the inductive reconnection driven electric field and less from the electrostatic electric field. Applications to understand space observations and laboratory experiments will be discussed.

Geospace Exploration Mission: ERG

Y. Miyoshi^a, I. Shinohara^b, T. Takashima^b, K. Asamura^b, N. Higashio^b, H. Matsumoto^b,
T. Mitani^b, S. Kasahara^b, S. Yokota^b, Y. Kazama^c, M. Hirahara^a, Y. Kasaba^d,
A. Matsuoka^b, H. Kojima^c, Y. Katoh^d, K. Shiokawa^a and K. Seki^a

^a *Solar-Terrestrial Environment Laboratory, Nagoya University, Nagoya 464-8601, Japan*

^b *ISAS/JAXA, Sagami-hara 252-5210, Japan*

^c *ASIAA, Taipei, Taiwan*

^d *Tohoku University, Sendai 980-8578, Japan,*

^e *RISH, Kyoto University, Uji 610-0011, Japan*

We present the geospace exploration project: ERG (Energization and Radiation in Geospace). Relativistic electrons of the outer belt largely change associated with the solar wind variations, and often increase largely particularly during the storm recovery phase. Several wave-particle interactions have been proposed as plausible acceleration processes. The inward radial diffusion driven by the interaction between the MHD mode waves and drifted electrons around the Earth provides significant accelerations via the betatron acceleration. The acceleration caused by the wave-particle interactions with whistler mode waves also contributes the large flux enhancement of relativistic electrons. In order to investigate the acceleration mechanism of relativistic electrons of the outer radiation belt as well as the space storm dynamics, the ERG project is going [1]. The ERG project consists of the satellite program, the ground-based network observations, and the integrated study group. The ERG satellite will be launched in 2016 that is a declining phase of solar cycle 24. The planned apogee altitude is about 4.5 Re and the perigee is about 300 km. The ERG satellite is designed to have a comprehensive set of plasma/particle sensors that can measure electrons from 12 eV to more than 10 MeV and ions from 10 eV/q to about 200 keV/q with a mass discrimination. The satellite can also measure field and waves from DC to 10 MHz (electric field) and to 100 kHz (magnetic field) in order to observe several plasma waves in the inner magnetosphere that are essential for the particle acceleration, transportation, and loss. Besides these instruments, newly developed wave-particle interaction analyser that can measure directly energy exchange process between electrons and whistler mode waves [2], which provides essential data sets to understand the non-linear wave particle interactions in the space plasma.

[1] Y. Miyoshi et al. AGU Monograph 199, 2012.

[2] Y. Katoh et al., JPS, 1, 015100, 2014.

Magnetized plasma modelling: common approach interesting for fusion and processing plasmas

T. Minea¹, A. Revel¹, S. Mochalsky², A. Lifschitz³

¹*Laboratoire de Physique des Gaz et Plasmas, UMR 8578 CNRS, Université Paris-Sud, 91 405 Orsay Cedex, France*

²*Max-Planck-Institut für Plasmaphysik, Garching, Germany*

³*Laboratoire d'Optique Appliquée, ENSTA/CNRS/Polytechnique UMR 7639, Palaiseau, France*

Magnetized plasmas operate at low pressure and due to the efficient trap of electrons they lead to a high ionization degree of the neutral gas, even if they remain partially ionized. Hence a large variety of sources of charged particles exploits magnetized plasmas to produce electrons and positive or negative ions, often (i) extracted from the plasma and further accelerated to higher energies for several applications or (ii) used directly in interaction with the electrodes, the substrate or plasma immersed surfaces for technological processing.

As an example for the first case, the future experimental reactor ITER will use the energy delivered to the core plasma by two beams of neutral Deuterium particles of 16 A @ 1 MeV each. In addition to energy, they should provide also momentum to the tokamak plasma, allowing to reach the H-mode (High advanced confinement mode) by current drive. The neutralization reaction by simple stripping of the negative ions (D⁻) has a significantly high cross section at 1 MeV than the electron attachment on energetic deuterons. Definitely, the ITER's negative beam injector (NBI) is designed to operate with negative ions extracted from a low pressure-high density plasma through a complex (3D) magnetized structure.

Another example for the second category is taken among the recent technologies of ionized physical vapor deposition (I-PVD) processing, known as High Power Impulse Magnetron Sputtering (HiPIMS) and used for specific coatings. In spite of the large scale industrial mastering of the deposition process, the further optimizations of the HiPIMS demand necessarily the fundamental understanding of the plasma phase and the transport of particles in the reactor volume, at different moments.

Analogously, the NBI optimization requires a deeper understanding of the meniscus formation and the 3D extraction of NI together with the co-extracted electrons, and the intrinsic relationship with the gas kinetics in the accelerator, as well as in the plasma source volume and at the surface.

Fully 3D Particle-in-Cell numerical modelling coupled with the Monte Carlo treatment of collisions (PIC-MCC) can effectively simulate these types of complex situations involving time dependence, complex gas kinetics, self-consistent 3D evolution of the plasma or beam particles in the presence of 3D magnetic field traps. Even if these two cases are apparently very different, the same numerical approach proved their efficiency giving valuable results on the mechanism of extraction of negative ions, the geometry and expected extracted current of the beams produced, the transport of these beams and the role of the plasmas created in the accelerator and in the neutralization region and provides information at nanosecond scale on the plasma instabilities ('spokes', flares, etc.) governing the electron transport across the complex magnetic structures related with co-called anomalous transport.

Self-Organization and Heating by Inward Diffusion in Magnetospheric Plasmas

N. Sato, Z. Yoshida, and Y. Kawazura

Graduate School of Frontier Sciences, The University of Tokyo, Kashiwa, Chiba 277-8561, Japan

In magnetospheric plasmas, spontaneous confinement is achieved by self-organization of charged particles through the process of inward diffusion. The resulting creation of density gradients appears as a violation of the entropy principle. Recent studies [1] have suggested that foliation of phase space resulting from topological constraints imposed by adiabatic invariants is consistent with maximization of entropy on the associated symplectic leaves [1-2]. Consequently, description of the dynamical process leading to the formation of the plasma clump requires the formulation of an appropriate diffusion operator on the distorted metric of the foliation. This work is carried out in [3] where a Fokker-Planck equation for inward diffusion is obtained. Here, with the aid of numerical simulations, we investigate the heating mechanism associated with the above diffusion process and study the resulting temperature anisotropy.

An interesting relationship between temperature anisotropy and conservation of the second adiabatic invariant J_{\parallel} emerged. Our research suggests that time-scale and strength of electromagnetic fluctuations responsible for inward diffusion drastically change the behavior of the Fokker-Planck equation in [3]: fast and strong diffusion destroys the second adiabatic invariant ($J_{\parallel} \propto v_{E \times B} / \omega_b$ with $v_{E \times B}$ the $E \times B$ velocity generated by fluctuations and ω_b the bounce frequency). This results in preferential heating of the perpendicular temperature as particles climb up the magnetic field by preserving the first adiabatic invariant. The opposite scenario is observed for slow, weak diffusion, where no preferential heating occurs. This situation is represented in figure 1.

From a theoretical perspective, we expect the ratio between time-scale of fluctuations and period of bounce oscillations to determine the definition of the stochastic integral that has to be taken in the Fokker-Planck equation.

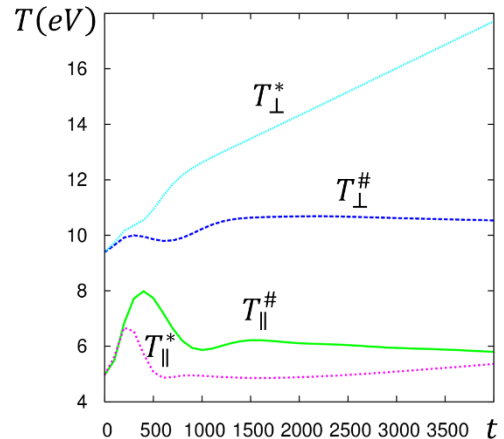


Figure 1: spatially averaged plasma temperatures versus time. *: fast, strong diffusion. #: slow, weak diffusion.

- [1] Z. Yoshida and S.M. Mahajan, Prog. Theor. Exp. Phys. 2014 (2014), 073J01.
- [2] N. Sato, N. Kasaoka, and Z. Yoshida, Phys. Plasmas 22 (2015), 042508.
- [3] N. Sato and Z. Yoshida, J. Phys. A: Math. Theor. 48 (2015), 205501.

Development and Initial Cruise Operation of the Hayabusa2 Ion Engine System

K. Nishiyama, S. Hosoda, R. Tsukizaki, H. Kuninaka

Japan Aerospace Exploration Agency, 3-1-1 Yoshinodai, Chuo-ku, Sagami-hara 252-5210, Japan

Hayabusa2 is the second asteroid sample return mission by JAXA [1]. The ion engine system (IES) for Hayabusa2 is based on that developed for Hayabusa with modifications necessary to improve durability, to slightly increase thrust, and to reflect on lessons learned from Hayabusa mission [2]. Hayabusa2 will rendezvous with a near-earth asteroid 1999 JU3 and will take samples from its surfaces. More scientific instruments than Hayabusa including an impactor to make a crater and landers will be on board thanks to the thrust enhancement of the IES. An improved neutralizer with stronger magnetic field for longer life has been under endurance test in diode mode since August 2012 and has accumulated the operational hours of 25800 h (> mission requirement: 14000 h) until August 2015. The IES flight model and the spacecraft was developed within 2.5 years (Figure 1). The spacecraft was launched from Tanegashima Space Center in Kagoshima Prefecture on-board an H-IIA launch vehicle on December 3, 2014. The IES was quickly checked out in orbit and cruise operation by ion propulsion for the electric delta-V Earth gravity assist (EDVEGA) was almost completed in the first week of June 2014. Accumulated operating times for four ion thrusters are 594 h, 11 h, 54 h and 592 h, respectively. Trajectory correction maneuvers by IES and reaction control system (RCS) will be executed after September if necessary before the planned earth swing-by on December 3, 2015.

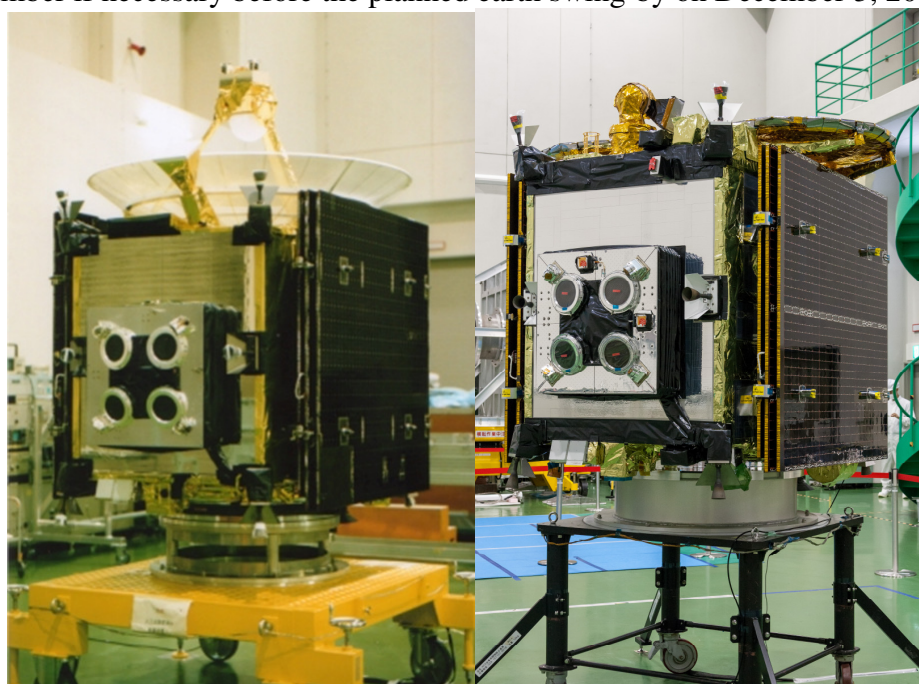


Figure 1. Asteroid explorer Hayabusa launched in 2003 (Left) and its successor Hayabusa2 launched in 2014 (Right).

[1] H. Kuninaka and Hayabusa-2 Project, 30th International Symposium on Space Technology and Science, 2015-k-61, 2015.

[2] K. Nishiyama, H. Kuninaka, Trans. JSASS Aerospace Tech. Japan **10**, No ists28, (2012) pp. Tb_1-Tb_9.

The origin and the impact of stochasticity resulting from edge localized perturbations.

Michael Tendler

Fusion Plasma Physics, Alfvén Laboratory, Royal Institute of Technology,
Sweden

Abstract

Stochastization of the magnetic fields resulting from overlapping magnetic islands has been addressed because of the importance of the 3 D effects caused by perturbation fields and currents at the edge and in the scrape-off layer in a tokamak. The main mechanism results from the emergence of the radial electron stochastic conductivity in a braided magnetic field. This electron current is closed by the ion radial current well known from biasing experiments and causing a significant pump-out effect. The impact of the stochastization is demonstrated to affect ELM's events via RMP and/or filaments existing within the SOL. The resulting electric fields from the balance of currents are strongly affected changing their value and even the sign under certain conditions. The impact on the momentum balance is also important because convective fluxes emerge due to the axial $j_{ir} \times B$ torque.

Poster Session 1
Tuesday, 3rd November, 2015

Change in Reynolds stress induced by end-plate biasing in a cylindrical laboratory plasma

T. Kanzaki^a, Y. Nagashima^b, S. Inagaki^b, T. Yamada^c, Y. Miwa^a, F. Kin^a, A. Fujisawa^a,
N. Kasuya^b, Y. Kosuga^d, M. Sasaki^b, M. Lesur^a, S.-I. Itoh^b and K. Itoh^e

^a*Interdisciplinary Graduate School of Engineering Sciences, Kyushu University,
Kasuga, Fukuoka 816-8580, Japan*

^b*Research Institute for Applied Mechanics, Kyushu University, Kasuga, Fukuoka 816-8580, Japan*

^c*Faculty of Arts and Science, Kyushu University, Fukuoka, Fukuoka 819-0395, Japan*

^d*Institute for Advanced Study, Kyushu University, Kasuga, Fukuoka 812-8581 Japan*

^e*National Institute for Fusion Science, Toki, Gifu 509-5292. Japan*

e-mail address: kanzaki@riam.kyushu-u.ac.jp

Formation of the shear flow structure in magnetized plasmas is now widely recognized to be important because it is accompanied by the reduction of turbulence-driven transport. Thus prediction capability of flow structure is strongly required to control the turbulence transport. The Reynolds stress is a candidate for the fundamental driving force for the self-consistent flow generation in magnetized plasmas by micro-scale turbulent fluctuations [1]. The determination of the Reynolds stress requires specific diagnostics. In small laboratory plasmas, probe measurement allows us to evaluate the ExB flow and its fluctuations. A multi-channel Reynolds stress probe system has been developed in a linear device, PANTA [2]. Each probe has six tungsten tips. Four of them are simultaneously used to measure the radial and azimuthal electric field and the others are used for ion saturation current measurement. To understand the flow formation mechanism, end-plate biasing experiments have been performed in PANTA and change in the drift-wave characteristics during biasing are found[3].

Here we report changes in *radial profiles* of the Reynolds stress induced by end-plate biasing. The drift wave amplitude is significantly reduced during the biasing [3] while few changes in the azimuthal flow in the central region are observed. The impact of the end-plate biasing on the radial structure of the Reynolds stress will be discussed.

This work is partly supported by a grant-in-aid for scientific research of JSPS, Japan (15H02335, 15H02155, 23244113, 26420852) and by the collaboration programs of NIFS (NIFS13K0CT001) and of the RIAM of Kyushu University and Asada Science foundation.

[1] P. H. Diamond, et al., Plasma Phys. Control. Fusion 47 (2005) R35

[2] Y. Nagashima, et al., Rev. Sci. Instrum. 82 (2011) 033503

[3] T. Yamada, et al., Nucl. Fusion 54 (2014) 114010

How to Identify Ion Temperature Gradient Mode in Cylindrical Plasma

Y. Miwa^a, S. Inagaki^b, Y. Nagashima^b, N. Kasuya^b, T. Kobayashi^c, Y. Kosuga^d,
T. Yamada^e, M. Sasaki^b, H. Arakawa^f, F. Kin^a, K. Itoh^c and S.-I. Itoh^b

^a*Interdisciplinary Graduate School of Engineering Sciences, Kyushu University,
Kasuga, Fukuoka 816-8580, Japan*

^b*Research Institute for Applied Mechanics, Kyushu University, Kasuga, Fukuoka 816-8580, Japan*

^c*National Institute for Fusion Science, Toki, Gifu 509-5292, Japan*

^d*Institute for Advanced Study, Kyushu University, Kasuga, Fukuoka 812-8581 Japan*

^e*Faculty of Arts and Science, Kyushu University, Fukuoka, Fukuoka 819-0395, Japan*

^f*Teikyo University, Omuta, Fukuoka, 836-8505, Japan*

e-mail address: yudai_miwa@riam.kyushu-u.ac.jp

In fusion plasmas, a radial ion heat transport driven by Ion Temperature Gradient (ITG) modes is considered to be dominant [1]. For improvement of confinement, comprehensive understanding of features of ITG turbulence is necessary. The ITG turbulence has been studied theoretically [1] and substantial progress in the study has been made in numerical simulation [2]. In experiments, a few observations in tokamak indicated that fluctuations propagating in the ion diamagnetic drift direction were the candidate for ITG modes [3], and some spectrum analyses under a particular condition indicated an excitation of the ITG mode in the linear plasma [4]. However, other evidences are needed for a full identification of the ITG mode, such as the ion temperature fluctuation measurement. It is difficult in core region of toroidal plasmas. The impact of ITG turbulence on heat transport has not been fully verified as well. In linear plasmas, multi point measurement of these to confirm corresponding to the density/ITG whole distribution is much easier.

In the basic linear plasma: Plasma Assembly for Nonlinear Turbulence Analysis (PANTA) in Kyushu University, we have succeeded in observing a fluctuation propagating in the ion diamagnetic drift direction, which co-exists with drift waves propagating in the electron diamagnetic drift direction. The linear wave analysis by using the fluid simulation indicated possibility of excitation of ITG modes in PANTA and an optimum condition to excite the ITG mode was obtained, which depends on not only ITG but plasma scales [5]. The excitation region of a fluctuation (propagating in the ion diamagnetic drift direction) in the space of plasma radius and magnetic field was in good agreement with the prediction by the simulation. Here we report the details of excitation condition and identification of spatiotemporal structure of the observed modes. The parallel wavenumber of these modes was evaluated to be finite (order of the inverse of plasma length) from a phase difference between probes on the same magnetic field line at distant locations. Cross-correlation technique was applied to experimental data observed by multiple Langmuir probes aligned along the magnetic field line. In addition, we have developed a conditional averaging method to estimate electron/ion temperature fluctuations by using the probes. Observation of temperature fluctuations allows us to evaluate heat flux driven by these modes. Behaviors of temperature fluctuations and heat flux will be discussed.

- [1] W. Horton, *Rev. Mod. Phys.* **71**, 735 (1999)
- [2] W. Dorland *et al.*, *Science* **275**, pp. 289-292 (1997).
- [3] A. K. Sen *et al.*, *Phys. Rev. Lett.* **66**, pp. 429-432 (1991)
- [4] D.W. Ross *et al.*, *Phys. Fluids B* **3** 2251 (1991)
- [5] Y. Miwa *et al.*, *Plasma Fusion Res.* **8**, 2403133 (2013)

Observation of radial scale length of fluctuations in PANTA

T. Tarumi^a, S. Inagaki^b, Y. Nagashima^b, T. Yamada^c, Y. Miwa^a, F. Kin^a, A. Fujisawa^b,
N. Kasuya^b, Y. Kosuga^d, M. Sasaki^b, M. Lesur^b, K. Itoh^e and S.-I. Itoh^b

^a*Interdisciplinary Graduate School of Engineering Sciences, Kyushu University,
Kasuga, Fukuoka 816-8580, Japan*

^b*Research Institute for Applied Mechanics, Kyushu University, Kasuga, Fukuoka 816-8580, Japan*

^c*Faculty of Arts and Science, Kyushu University, Fukuoka, Fukuoka 819-0395, Japan*

^d*Institute for Advanced Study, Kyushu University, Kasuga, Fukuoka 812-8581 Japan*

^e*National Institute for Fusion Science, Toki, Gifu 509-5292, Japan*

e-mail address : tarumi@riam.kyushu-u.ac.jp

Radial scale of turbulence in magnetized plasmas characterizes transports driven by turbulence and thus a scaling law of the radial length of turbulence is of central importance. The characteristic radial scale length of micro-fluctuations, e. g. the drift waves, is considered to scale with the drift scale (the ratio of sound speed to ion cyclotron frequency) which is of the order of an ion gyro-radius [1]. Many experiments, however, have shown that transport does not simply scale the gyro-radius [2]. A closer experiment–theory comparison for turbulence structure size is strongly required to predict the turbulence driven transport in the large fusion plasma. While at the same time, the stationary small laboratory plasma allows better diagnostics accessibility. Probe arrays have proven already successful as a diagnostic for turbulence studies in fusion and magnetized low-temperature plasmas [3]. Thus we studied the spatial structure of the turbulence in the low-temperature plasma by probe arrays. In order to vary the drift scale in a wide range, we changed the magnetic field strength from 500 G to 1500 G and ion mass number by using helium and argon as working gases in the linear plasma device PANTA [4].

Here we report the experimental observations of the radial correlation length of fluctuations. The correlation lengths of the drift waves will be compared with the drift scales. We will also vary the plasma radius from 2 cm to 8 cm and discuss about its effect on radial transport scaling.

This work is partly supported by a grant-in-aid for scientific research of JSPS, Japan (15H02335, 15H02155, 23244113) and by the collaboration programs of NIFS (NIFS13KOCT001) and of the RIAM of Kyushu University and Asada Science foundation.

[1] W. Horton, Rev. Mod. Phys. 71 (1999) 735

[2] C. C. Petty, et al., Phys. Rev. Lett. 74 (1995) 1763

[3] A. Latten, et al., Rev. Sci. Instrum. 66 (1995) 3254

[4] H. Arakawa, et al., Plasma Phys. Control. Fusion 52 (2010) 105009

Reconstruction of Cross-Sectional Structure of Reynolds Stress in End-Plate Biasing Experiment in PANTA

F. Kin, Y. Nagashima^{1,2}, T. Yamada^{1,3}, S. Inagaki^{1,2}, T. Kanzaki, Y. Miwa,
H. Arakawa⁴, T. Kobayashi⁵, N. Kasuya^{1,2}, M. Sasaki^{1,2}, M. Lesur²,
Y. Kosuga^{2,6}, A. Fujisawa^{1,2}, K. Itoh^{1,5}, S.-I. Itoh^{1,2}

*Interdisciplinary Graduate School of Engineering Sciences, Kyushu University, 6-1 Kasuga-koen,
Kasuga 816-8580, Japan*

¹*Research Center for Plasma Turbulence, Kyushu University, 6-1 Kasuga-koen, Kasuga 816-8580,
Japan*

²*Research Institute for Applied Mechanics, 6-1 Kasuga-koen, Kasuga 816-8580, Japan*

³*Faculty of Arts and Science, Kyushu University, 744 Motoooka, Nishi-ku, Fukuoka 819-0395, Japan*

⁴*Teikyo University, 6-22 Misakimachi, Omuta 836-8505, Japan*

⁵*National Institute for Fusion Science, 322-6 Oroshi-cho, Toki 509-5292, Japan*

⁶*Institute for Advanced Study, Kyushu University, 6-10-1 Hakozaki, Higashi-ku, Fukuoka 812-8581
Japan*

In magnetized plasmas, micro-scale plasma turbulence interacts with meso-scale structures such as zonal flow and streamer. Evaluation of momentum transport between different scales of fluctuations is important to understand the structure formation in plasma turbulence. Spatial gradient of Reynolds stress is a main mechanism for flow generation by turbulence. In magnetized plasmas, axial-scale length of plasma is assumed to be much longer than azimuthal- and radial-scale lengths, observations of the dynamics of turbulence, flow and Reynolds stress in the azimuthal cross-section allow us to identify the causal relation among them. Direct measurement of Reynolds stress has been performed in linear plasma devices [1], and has also been performed in PANTA (Plasma Assembly for Nonlinear Turbulence Analysis) with Reynolds stress probe [2]. For reconstructing two-dimensional patterns of Reynolds stress, cross-correlation analysis between azimuthal 64-channel probe array and the radial movable Reynolds probe is used. The azimuthal probe array sets 250 mm away from Reynolds stress probe in magnetic field direction, and measures floating potential for azimuthally. Conditional averaging methods are used to reconstruct azimuthal mode structures. Here we report the details of the reconstruction method and observed 2-dimensional structures of density and potential fluctuations, mean flows and the Reynolds stress. We also carried out the end-plate biasing experiment in PANTA [3] to induce perturbations to the plasma. During biasing, turbulence was suppressed and Reynolds stress was drastically changed. The changes in two-dimensional patterns will be discussed.

This work is partly supported by a grant-in-aid for scientific research of JSPS Japan (15H02335, 15H02155, 23244113, 26420852) and by the collaboration programs of NIFS (NIFS13KOCT001) and of the RIAM of Kyushu University and Asada Science foundation.

[1] C. Holland, et al., Phys. Rev. Lett. 96, 195002 (2006)

[2] Y. Nagashima, et al., Rev. Sci. Instrum. 82, 033503 (2011)

[3] T. Yamada, et al., Nucl. Fusion 54, 114010 (2014)

Evaluation of flow velocity with a frequency comb Doppler Backscattering in PANTA

R. Minato^a, S. Inagaki^b, T. Mizokami^a, T. Yamada^c, Y. Nagashima^b, T. Tokuzawa^d,
Y. Miwa^a, F. Kin^a, A. Fujisawa^b, N. Kasuya^b, K. Itoh^d and S.-I. Itoh^b

^a*Interdisciplinary Graduate School of Engineering Sciences, Kyushu University,
Kasuga, Fukuoka 816-8580, Japan*

^b*Research Institute for Applied Mechanics, Kyushu University, Kasuga, Fukuoka 816-8580, Japan*

^c*Faculty of Arts and Science, Kyushu University, Fukuoka, Fukuoka 819-0395, Japan*

^d*National Institute for Fusion Science, Toki, Gifu 509-5292, Japan*

e-mail address: minato@riam.kyushu-u.ac.jp

A multi-channel Doppler backscattering diagnostics is the most promising to observe the flow structures and their dynamic behaviors simultaneously in magnetized plasmas [1]. We have applied the microwave frequency comb technique to the reflectometry in the linear plasma device PANTA and succeeded to observe density fluctuations at 29 different radii simultaneously [2]. We also applied this technique to the Doppler backscattering diagnostics. Typical operational parameters of PANTA are as follows; plasma diameter of about 120 mm, axial magnetic field of 0.09 T, and filling argon pressure of 3 mTorr. Typical central density and electron temperature are $1.0 \times 10^{-19} \text{ m}^{-3}$ and 3 eV, respectively. Reflectometer and probe measurements indicated that the electron density gradient is steep in the radius of $r = 30\text{-}40$ mm, and produces drift waves, which propagates in the nearly perpendicular direction to the magnetic field (in the electron diamagnetic direction) with finite axial wavelength. The Doppler backscattering wavenumber is selected via an adjustable launch angle. In this study, the incident and reflected wave signals are directly transferred to the digital storage oscilloscope, which has a frequency band of 33/50 GHz (the sampling frequency is 80/160 GHz), so the waveforms of the incident and reflected signals are detected in the form of digital signals with very high temporal resolution [2]. The Doppler frequency is calculated by the delta-phase method [3]. Advanced digital signal processing techniques (e.g. Hilbert transform and convolution) allow us to improve the signal-to-noise-ratio of evaluating the Doppler frequency. Results obtained with a Backscattering diagnostics will be compared with probe measurements.

This work is partly supported by a grant-in-aid for scientific research of JSPS, Japan (15H02335, 15H02155, 23244113) and by the collaboration programs of NIFS (NIFS13KOCT001) and of the RIAM of Kyushu University and Asada Science foundation.

- [1] T. Tokuzawa et.al., Plasma Fusion Res.9(2014)
- [2] T. Mizokami et. al., 24th International Toki conference (2014)
- [3] S. Inagaki et.al., Plasma Fusion Res. 8 (2013).
- [4] G. D. Conway et al., Plasma Phys. Control. Fusion47(2005)

Helium volumetric recombining plasma formation for energetic ion injection in a radio-frequency plasma device DT-ALPHA

H. Takahashi, A. Okamoto^a, T. Miura, D. Nakamura, P. Boonyarittipong,
S. Sekita, S. Kitajima

Dept. of Quantum Science and Energy Engineering, Tohoku Univ., Sendai 980-8579, Japan

^a*Dept. of Energy Engineering and Science, Nagoya Univ., Nagoya 464-8603, Japan*

In magnetically confined fusion devices, heat flux mitigation by detached plasma formation is important issue. Because reaction rate of the volumetric recombination becomes large in a low electron temperature plasma, sufficient plasma-neutral interactions are required to maintain stable plasma detachment. On the other hand, energetic particles are exhausted from confinement region and then transported in divertor region by edge localized modes in a high confinement mode plasma. Therefore, understanding of the divertor plasma dynamics that coexists with intermittently inflowing energetic particles is recognized as an important subject in fusion related studies. A divertor plasma simulator with radio-frequency (RF) plasma source offers some advantages for such divertor plasma dynamics study because cylindrically wound RF antenna permits the penetration of the energetic particles.

Experiments were performed with the RF plasma device DT-ALPHA [1]. Plasma production method is a 13.56 MHz RF discharge. Typical electron temperature produced in the DT-ALPHA device is several eV, so helium secondary gas is supplied into the device at the downstream region to form helium recombining plasma [2].

To investigate the volumetric recombining plasma dynamics which coexists with energetic ions by beam injection, radial distribution of the volumetric recombination is important because beam components pass around central axis of a cylindrical target plasma. In a low electron temperature and high electron density plasma, electrons lose their energy through energy exchange between ions. Therefore, electron-ion temperature relaxation time τ_T^{ei} is important to induce volumetric recombination [3]. τ_T^{ei} is dependent on the electron temperature and density. In the DT-ALPHA device, the electron temperature and electron density are controlled by changing RF heating power or neutral pressure distribution. Spectroscopic and Langmuir probe measurements indicate that τ_T^{ei} affects helium volumetric recombining plasma formation. In this presentation, we will discuss about helium volumetric recombining plasma formation required for beam injecting experiment based on the electron-ion temperature relaxation.

This work is partly supported by JSPS KAKENHI Grant numbers 22740357, 26420848 and by JSPS Fellows Grant number 264331.

- [1] A. Okamoto, *et al.*, Plasma Fusion Res. **7** (2012) 2401018
- [2] H. Takahashi, *et al.*, Fusion Sci. Technol. **63** 1T (2013) 404
- [3] N. Ezumi, *et al.*, J. Nucl. Mater. **241-243** (1997) 349

Development of linear plasma device for proof of principle of energetic ion injection

S. Tsubota, A. Okamoto^a, K. Shimizu, D. Nakamura, T. Kobayashi, H. Takahashi, S. Kitajima

Department of Quantum Science and Energy Engineering, Tohoku University, Sendai 980-8579, Japan

^a *Department of Energy Engineering and Science, Nagoya University, Nagoya 464-8603, Japan*

In the study of magnetically confined fusion plasma, confinement of the fusion products is important. One of the possible methods to investigate confinement performance of fusion products experimentally is using energetic ions produced by neutral beam injection [1]. However, the above method has some restrictions for energetic ion production due to fixed beam line and ionization point. Moreover it is difficult to apply this method to smaller devices and lower density target plasmas. We have been developing a compact ion injector, which consists of hydrogen storage material containing hydrogen molecules. It is expected to accelerate hydrogen ions by using the electron sheath potential between the plasma and the surface of positively biased electrode. Using the injector inside the last closed flux surface, more flexible experiments are expected. It has been observed that emission of hydrogen atom line increased according to increase in bias voltage of the electrode in the small standard heliac device (Tohoku University Helic) [2].

The linear plasma device, in which a target plasma for proof of principle of the above-mentioned method is produced, has been developed. The plasma is produced by the electron cyclotron resonance (ECR) heating using a microwave of frequency 2.45 GHz. Maximum injection power is 6 kW. Total length and inner diameter of the device are 2.2 m and 0.2 m, respectively. Two groups of magnetic coils are located. One produces a magnetic beach configuration ($B \sim 0.1$ T) for ECR heating in a plasma production region [3], and the other produces uniform configuration of 0.3 T in a measurement region. Components for the plasma production region have been constructed, and the plasma was successfully produced. We measured the electron temperature and density of the helium plasma in the plasma production region using Langmuir probe (typically $T_e \sim 10$ eV, $n_e \sim 1 \times 10^{17}$ m⁻³) and obtained their radial profiles. Dependence of the T_e and n_e on plasma heating power, magnetic field strength, and neutral pressure was also investigated. In the measurement region, we have a plan to produce the magnetic field by a pulse operation. Therefore, we developed a circuit consists of capacitors and inductors for a pulse forming network of current source (~ 1.2 kA). In preliminary experiments the flat top of the magnetic field (~ 10 ms) was successfully produced, and the current in the magnetic coils in the plasma production region induced by the pulse operation in the measurement region was investigated quantitatively.

This work is supported by Grant-in-Aid for Scientific Research (KAKENHI), 24246152.

[1] R. K. Fisher *et al.*, *Rev. Sci. Instrum.* **81**, 10D307 (2010).

[2] A. Okamoto *et al.*, *Rev. Sci. Instrum.* **85**, 02B302 (2014).

[3] M. Tanaka *et al.*, *J. phys. Soc. Jpn.* **60** 1600 (1991).

Observation of Plasma Dynamics in TPD-sheet IV

T.Onda, S. Kajita^a, A. Tonegawa^b, T. Iijima^b, and N. Ohno

Graduate School of Engineering, Nagoya Univ, Furo-cho, Chikusa-ku, Nagoya, 464-8603, Japan

^aEcoTopia Science Institute, Nagoya Univ, Furo-cho, Chikusa-ku, Nagoya, 464-8603, Japan^bDepartment of Physics, School of Science, Tokai Univ, 4-1-1 Kitakaname, Hiratukai, 259-1292, Japan

Sheet plasmas have been used in various fields of researches such as a divertor simulator in fusion plasmas and, negative ion production [1, 2]. For ex., previously studies, negative ion density in a sheet plasma was controlled with aim of reducing the heat flux to the divertor plates [3]. Furthermore, the temperature and density associated with the generation of negative ion were investigated [4]. Although expensive experiments have been conducted in sheet plasmas up to now, the dynamic behavior of sheet plasma has not been fully understood yet. In order to utilize the sheet plasma more efficiently and meaningfully, it is of interests to investigate the dynamic behavior and understand the physics of the sheet plasma. In this work, we have observed dynamic behaviors of a sheet plasma with a high-speed camera. The dynamic behavior of sheet plasmas and corresponding releases of blob-like plasmas to the periphery of the sheets are shown.

The experiment was performed in the linear divertor plasma simulator TPD Sheet-IV. The plasma was divided into two regions: a plasma source region and an experimental region for divertor simulator [2]. In order to observe the dynamic behavior of sheet plasma structures, a high-speed camera (ULTRA CAM HS-106E : NAC Image Technology, Inc.) was used at a frame rate of 100000 fps. A heat-resistant glass was installed at the end of TPD Sheet-IV to observe the plasma in parallel to the magnetic field. A Langmuir probe was installed from the upper side of the device and measured the ion saturation current at the periphery of the plasma. We observed the dynamic behavior of a pure helium plasma or helium argon mixture plasma. Additional hydrogen gas was injected in the experimental region.

Figure 1 (a) and (b) shows fast framing camera images of He and Ar mixture plasmas and pure He plasma, respectively, observed with the high-speed camera. It is seen in Fig.1(a) that the plasma column moves back and forth horizontally at a frequency of about 4 kHz in He/Ar mixture plasma. However, in case of pure He plasma, the plasma column did not exhibit such a dynamic behavior. In addition, intermittent transport which is similar to plasma blob was observed. The temporal evolution of I_{sat} in the peripheral plasma supported the fact that blob like plasma was released at the same frequency of ~ 4 kHz.

This work was supported by JSPS KAKENHI Grant Number (25289337). This work is partially supported by NIFS/NINS under the project of Formation of International Network for Scientific Collaborations and NIFS Collaboration Research Program NIFS14KUGM094

[1] A. Ando, T. Kuroda, et al. : Rev.Sci. Instrum., Vol 61, No 1, January (1990)442-444

[2] A. Tonegawa, K. Kumita, et al.: Jpn. J. Appl. Phys., Vol. 45, No. 10B (2006)8212-8216

[3] M. Ono, A.Tonegawa, et al.: Journal of Nucl. Mater 337-339 (2005) 261-265

[4] S. Matumoto, et al.: JPS Conf.Proc. 1, 015042(2014)

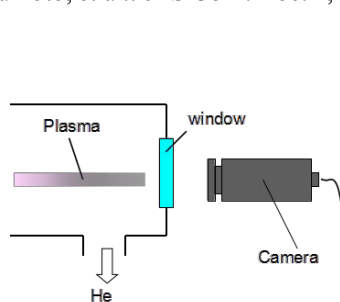


Fig. 1 Experimental setup

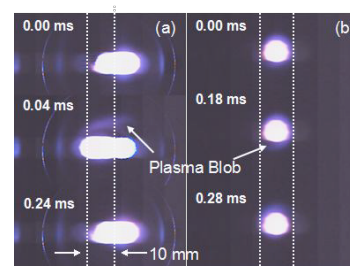


Fig. 2 A snapshot of image captured by the high-speed camera:(a)He and Ar plasma (b)He plasma

Experimental and Numerical Studies of Hall Effect on Merging Formation process of a Field-Reversed Configuration

Y. Kaminou, X. Guo, M. Inomoto, Y. Ono, and R. Horiuchi^a

Graduate School of Engineering, the University of Tokyo, 7-3-1 Yayoi, Bunkyo-ku, Tokyo, Japan

^a*National Institute for Fusion Science, 322-6 Oroshi-cho, Toki 509-5292, Japan*

Counter-helicity spheromak merging[1] is one of the formation methods of a Field-Reversed Configuration(FRC). In counter-helicity spheromak merging, two spheromaks with opposing toroidal fields merge together, through magnetic reconnection events and relax into a high-beta FRC, which has no or little toroidal field. This process contains magnetic reconnection and a relaxation phenomena with energy conversion from magnetic energy to kinetic or thermal energy, and the Hall effect has some essential effects on these process because the X-point in the magnetic reconnection or the O-point of the FRC has no or little magnetic field. In this poster, we conducted 2D/3D Hall-MHD simulations and experiments of counter-helicity spheromak merging. We found that the Hall effect enhances the reconnection rate, and reduces the generation of toroidal sheared-flow. The suppression of the “slingshot effect” may affect the relaxation process. We will discuss their details in the poster.

[1] M. Inomoto et al, Phys. Rev. Lett., **97** (135002) 2006

Generation of Energetic Electrons during Spherical Tokamak Merging in UTST

T. Ushiki, X. Guo, H. Furui, K. Matsuyama, H. Koguchi^a, M. Inomoto

Graduate School of Frontier Sciences, The University of Tokyo, 5-1-5, Kashiwanoha, Kashiwa, Chiba 277-8656, Japan

^a National Institute of Advanced Industrial Science and Technology, 1-1-1, Umezono, Tsukuba, Ibaraki 305-8586, Japan

Spherical tokamak (ST) merging method has been studied as one of the CS-less start-up schemes in START, MAST (UKAEA), TS-3/TS-4 (Univ. Tokyo). In merging start-up high-power plasma heating through magnetic reconnection is expected to form high beta STs in short period, but a small number of experimental studies have been carried out on the electron acceleration/heating during reconnection in ST merging. In this paper, experimental investigation of electron acceleration during reconnection in the presence of strong guide field will be presented.

In recent experimental result in MAST, extremely localized electron heating was observed near the X-point during magnetic reconnection [1]. The heating mechanism is unclear, but recent numerical work with 3-D PIC model suggests that electrons are effectively accelerated in toroidal direction by reconnection electric field in presence of the strong guide field [2]. These accelerated electrons may contribute to the electron heating observed in MAST. The goal of this research is to verify the electron acceleration during magnetic reconnection with strong guide field.

Surface barrier detector (SBD) was employed to observe soft x-ray emission by electron bremsstrahlung during magnetic reconnection. 2 μm thickness polycarbonate foil was equipped in front of the SBD as X-ray absorption filter to eliminate photon with low energy ($< 200\text{eV}$).

Sharp soft x-ray burst was observed only during magnetic reconnection with good correlation with reconnection electric field. This suggests that electron acceleration by toroidal electric field accounts for the soft x-ray emission. Fig.1 shows dependence of soft x-ray intensity on toroidal guide field and toroidal electric field. Soft x-ray intensity showed clear dependency on both toroidal electric field and guide field. These results suggest that the efficiency of the electron acceleration could be roughly evaluated by the effective electric field $E_t (B_t/B_p)$, which is employed to predict the electron acceleration in torus break down near a null point [3].

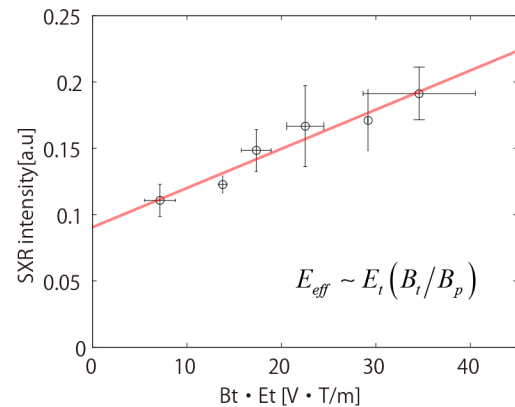


Fig.1 Dependence of soft X-ray (polycarbonate 2 μm) intensity on toroidal guide field and toroidal electric field.

[1] Y. Ono. Et al, Plasma Phys and Control. Fusion **54** (124039) 2012.

[2] P. L. Pritchett and F. V. Coroniti, J. Geophys. Res. **109** (A01220) 2004.

[3] B. Lloyd. Et al, Nuclear Fusion. **31** (2031) 1991.

Characterization of an atmospheric pressure plasma by a Gerdien condenser

M.C.C. Lacdan and M. Wada

*Graduate School of Science and Engineering, Doshisha University, 1-3 Tatara Miyakodani,
Kyotanabe-shi, Kyoto-fu 610-0394, Japan*

A diagnostic instrument based on the Gerdien condenser [1] principle is being developed as a new characterization method for laboratory-produced atmospheric pressure plasma. The Gerdien condenser instrument is capable of determining the ion density and mobility, thus ion species composition of the plasma. In this study, a miniaturized Gerdien condenser has been designed and fabricated to measure parameters of atmospheric plasma produced by an RF excited atmospheric pressure plasma pen.

The condenser has a 1.0 cm diameter 6 cm long cylindrical collector electrode mounted in a bias electrode of 1.7 cm inner diameter. The entire condenser is mounted in an aluminum made rectangular shield box. An atmospheric pressure plasma pen produces a plasma by 13.56 MHz RF power source. The plasma produced with 30 W discharge power was analyzed by the Gerdien condenser while supplying Ar and N₂ gases at 5 and 3 liters per minute flow rates, respectively.

In Fig. 1 are shown typical current-voltage (*I-V*) characteristics obtained by applying voltage sweep from 0 V to 12 V at the Gerdien condenser's bias electrode and measuring the collected current by the inner electrode. The flow rate of fan attached at the end of the condenser was set at 1.88, 3.75, 5.63 and 7.5×10^{-4} m³/s.

The figure clearly indicates the saturation current of the condenser increases with the flow rate that determines the intake of atmospheric ions by the condenser. The values of ion mobility calculated from the condenser *I-V* characteristics are identified to be those of O₂⁺, Ar⁺, Ar⁺⁺ and N₂⁺. The determined ion densities are in the range from 1.93×10^5 to 2.24×10^6 cm⁻³.

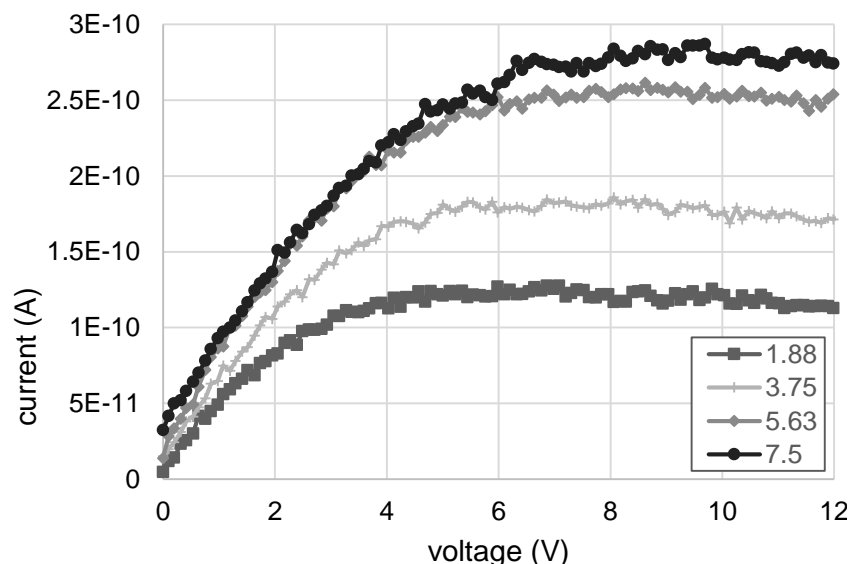


Figure 1. Current-voltage characteristics of atmospheric pressure plasma pen for varying fan flow rate of 1.88, 3.75, 5.63 and 7.5×10^{-4} m³/s.

[1] J.A. Chalmers, *Atmospheric Electricity* 2nd edition, (Pergamon Press, Oxford, 1967) p. 53-53, p. 128-130.

Supersonic Gas Injection for High Density Operation and Associated Development of 140 GHz Interferometer in RELAX RFP

S. Nakanobo, S. Masamune, A. Sanpei, G. Ishii, Y. Aoki, T. Nagano, M. Higuchi, K. Jikuhara, R. Tsuboi, H. Himura, T. Akiyama¹, H. Okada², T. Mizuuchi²

Kyoto Institute of Technology, Matsugasaki, Sakyo-ku, Kyoto 606-8585, Japan

¹National Institute for Fusion Science, Oroshi-cho, Toki 509-5292, Japan

²Institute for Advanced Energy, Gokasho, Uji 611-0011, Japan

nakano14@nuclear.es.kit.ac.jp

Reversed-Field Pinch (RFP) is one of the magnetic confinement systems for high-temperature, high-beta fusion plasmas. In the RFP, as the aspect ratio (A) is lowered, the self-induced bootstrap current tends to increase, which may lead to a reduction of the external source for current drive.

RELAX [1] is a low-aspect-ratio RFP whose major radius R is 0.5 m and the minor, a , 0.25 m. The objectives include geometrical optimization of the RFP configuration, so, the aspect ratio A was designed as low as 2. The equilibrium analysis [2] showed that we could expect sizable fraction of the bootstrap current with beta of $\sim 30\%$ at $I_p \sim 100\text{kA}$ with T_e of $\sim 200\text{-}300\text{ eV}$ in $A=2$ RFP, the details depending on the equilibrium profiles. Figure 1 shows the central electron poloidal beta $\beta_{pe}(0) = n_e(0)T_e(0)/(B_p^2(a)/2\mu_0)$ vs. electron density n_e normalized to the Greenwald density n_G achieved in RELAX to date, where the central electron temperature and density were measured with Thomson scattering [3]. We should note that since $B_p \gg B_t$ in the RFP, the poloidal beta is almost equal to the total beta. Figure 1 shows that the beta increases with density, whose upper bound is $\sim 30\%$ of n_G . It is therefore important to achieve higher density region to see if higher beta could be realized there.

We have developed a supersonic gas injection system for higher density operation in RELAX. The system consists of a fast-acting electromagnetic gas valve with a Laval nozzle to produce directed supersonic gas flow with Mach number of up to 5 ($M=5$). A 140 GHz heterodyne interferometer was also developed to measure n_e in higher regime than before [4]. The system consists of two oscillators and an IQ detector, which provide orthogonal components of the phase shift arising from the difference in optical path lengths for plasma and reference legs. In Fig. 2, a gas-puff fueled discharge is compared with a non-fueled case in the initial experiments. The electron density is almost doubled near the current flat top at $\sim 1.5\text{ms}$ into the discharge. Details of the fuelling efficiency will be discussed along with the results from further optimized cases.

[1] S. Masamune et al., IAEA FEC25, EX/P3-52 (2014).

[2] A. Sanpei et al., J. Phys. Soc. Jpn. 78 013501 (2009).

[3] R. Ueba et al., PFR 9, 1302009 (2014).

[4] M. Sugihara et al., PFR 5, S2061 (2010).

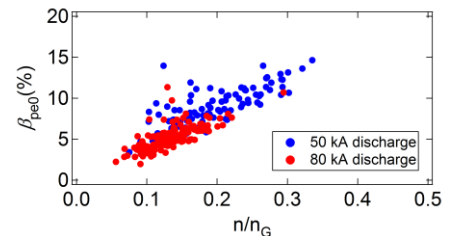


Fig.1 Electron poloidal beta vs. density

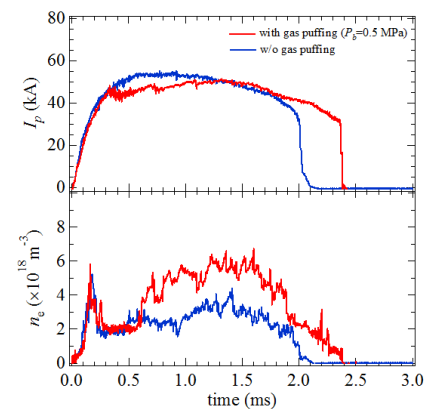


Fig.2 Results from initial gas-puff experiment

Evidence of increased ion temperature by slow wave heating in RT-1

M. Nishiura, Z. Yoshida, Y. Yano, Y. Kawazura, T. Mushiake, H. Saitoh, M. Yamasaki,
A. Kashyap, N. Takahashi, M. Nakatsuka, A. Fukuyama^a

*Graduate School of Frontier Sciences, The University of Tokyo, 5-1-5 Kashiwanoha, Kashiwa
277-8561, Japan*

^a*Department of Nuclear Engineering, Kyoto University, Nishikyo-ku, Kyoto 615-8540, Japan*

nishiura@ppl.k.u-tokyo.ac.jp

The ring trap 1 (RT-1) device realizes a "laboratory magnetosphere" created by a levitated superconducting ring magnet. The physical processes in the vicinity of a magnetic dipole are studied for magnetosphere dynamics and advanced thermonuclear fusions.

The electron cyclotron resonance (ECR) heating with 8.2 GHz and ~50 kW produces the plasmas with hot electrons in the range of a few ten keV. We reported that the local electron beta exceeds 1 in RT-1 plasmas. In such situation, the ions still remain cold at a few ten eV, because the heating source is dominated by Coulomb collisions between cold electrons and ions. Heating ions is expected to access high ion beta state and to improve the plasma confinement theoretically. Therefore the ion cyclotron range of frequencies (ICRF) heating with 2 - 4 MHz and 10 kW was prepared in RT-1. Based on the results of the TASK-WF2 code, the \square shape loop antenna was designed for a slow wave excitation, and was implemented in the RT-1.

In the ICRF heating experiments, a base plasma was sustained by 8.2 GHz-ECRH for 1 s, and an ICRF heating was applied with the delay of 0.2 ms from the plasma startup. We observed the clear increase in diamagnetic signals and impurity ion temperature (C III) in helium plasmas at the neutral gas pressure of 3 mPa, if the ICRF power of ~ 10 kW is comparable to the ECRH one. The increases of ion temperatures for C III and He II were observed near the levitation coil (the coil did not levitate in this case), where the ion cyclotron layer for H⁺ is located. The result is the first time in a magnetosphere plasma device, although the heating effect has a possibility of electron heating by a fast wave that results in the ion heating by Coulomb collisions. The results during the ICRF heating will be discussed in detail.

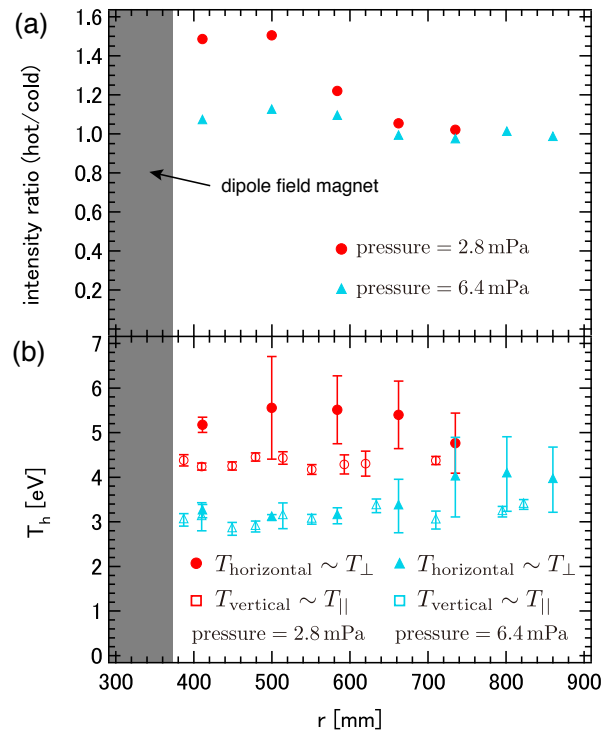
Anisotropy in tail component of $H\alpha$ in RT-1

Y. Kawazura, Z. Yoshida, M. Nishiura, Y. Yano, H. Saitoh, T. Nogami, T. Mushiake, M. Yamasaki, A. Kashyap, N. Takahashi and M. Nakatsuka

Graduate School of Frontier Sciences, The University of Tokyo, 5-1-5 Kashiwanoha, Kashiwa 277-8561, Japan

Magnetospheres are self-organized plasma confinement device commonly seen in the space. Inhomogeneous magnetic field causes inward diffusion which gives rise to planetward density gradient. The ring trap 1 (RT-1) device simulates *laboratory magnetosphere* by the levitated superconducting magnet. Plasma is produced by electron cyclotron resonance heating. The inward diffusion in RT-1 was proved by the interferometric measurement of the peaked electron density profile [1].

Recently the ions in RT-1 were found to be energized by betatron acceleration concomitant with inward diffusion [2]. The heating power was higher than that by the relaxation with the electrons. In this study, we decomposed the emission line profile of $H\alpha$ with double Gaussian distribution to obtain the radial profile of hot component of neutral hydrogen. The primary loss mechanism for ions, in RT-1, is considered to be charge exchange with neutral particles, whose mean free path is longer than the device size. The tail component of $H\alpha$ emission may inherit the information of protons since the spontaneous emission occurs much faster than the time scale of thermal motion of the neutral hydrogen particles. Figure (a) shows the radial profile of the ratio of line integrated emission intensity (hot/cold) for two different filling gas pressure operations. For the low filling gas pressure, the emission intensity of the hot component surpassed that of the cold component near the dipole magnet, while little increase of intensity ratio was seen for the high gas pressure. At the same time, we observed temperature anisotropy estimated by Doppler broadening of tail component only for low filling gas pressure operation (Fig. (b)), which is consistent with the preceding ion energy transfer model.



[1] H. Saitoh et al., Nucl. Fusion **51**, 063034 (2011).

[2] Y. Kawazura et al., arXiv:1507.03692.

Studies on power dependence of plasma production and ion heating by a single helical antenna for a simple thruster

Y. Nakatsuka, F. Kurashita, S. Nakamoto, H. Takeno

*Department of Electrical and Electronic Engineering, Kobe University,
1-1, Rokkodai-cho, Nada-ku, Kobe 657-8501, Japan*

Recently, technologies for long distance and long time missions are required in the space engineering such as a farther space exploration or a sample return, so development of an efficient electrical propulsion engine is necessary. The conventional electrical propulsion engine cannot control a thrust and a specific impulse individually because they are inversely proportional to each other under the condition of the constant input power. It also has a durability problem because electrodes are abraded by plasma.

The VASIMR engine was researched and developed in NASA and AD ASTRA Co. It can control a thrust and a specific impulse individually by separating a plasma production section and an ion heating section. A radio frequency (RF) power is inductively used, so the problem of the durability on electrodes can also be avoided [1]. However, the device is not necessarily efficient on the aspects of size and structure as it uses two RF power supplies and two antennas for individual control of plasma production and ion heating.

For downsizing of the device, a new method was proposed in which plasma production and ion heating were performed simultaneously by using one helical antenna [2]. The helical antenna has a bi-directional excitation characteristic. For a right helical antenna, R wave, so-called fast wave, is excited in the $-z$ direction under the magnetic field in the $+z$ direction. On one hand, L wave, so-called slow wave, is also excited in the $+z$ direction simultaneously. The R wave has right-rotating field and a higher cut-off frequency, so high density plasma could be produced. The L wave has left-rotating field and could couple with ion motion, so acceleration of ions could be expected in the ion cyclotron resonance frequency. The high density plasma production and the ion heating are corresponding to a strong thrust and a high specific impulse, respectively, thus it is expected that a single helical antenna with one RF power supply can control a thrust and a specific impulse individually by controlling a magnetic field. This scenario was qualitatively confirmed experimentally [3], however, the quantitative examination is necessary to design an actual engine. In this paper, we will show an RF power dependence of plasma production and ion heating in this scheme.

The power dependence of plasma production and ion heating is not considered to be a simple one. Even if the magnetic field is in the ion heating condition, a part of the input power is consumed for plasma production. Moreover, increase of plasma production power results in an increase of plasma density which may make ion heating complex as more power is required for the higher density plasma heating and the propagation characteristic of L wave will be changed according to the density increase. The heating characteristic to RF input power would become complex, and a thrust and a specific impulse would be controlled by combined adjustment of magnetic field and RF input power.

This paper would clarify those heating characteristics experimentally. The calibrated power monitor system was installed in the experimental device, and the experiments are in progress. The detailed experimental results and discussion will be shown in the conference.

- [1] F. R. Chang Diaz, *Trans. Fusion Sci. Tech.* **43** (2003) 3.
- [2] H. Wakabayashi, et al., *21st Int. Toki Conf.* (2011) P1-103.
- [3] Y. Hayashi, et al., *Trans. Fusion Sci. Tech.* **63**(1T) (2013) 389.

Characteristics of Magnetic Fluctuations during Magnetic Reconnection in Counter-helicity Spheromak Merging Experiment

R. Yanai, A. Kuwahata^a and M. Inomoto^a

Graduate School of Engineering, The University of Tokyo, Bunkyo, Tokyo, Japan

^a*Graduate School of Frontier Sciences, The University of Tokyo, Kashiwa, Chiba, Japan*

Magnetic reconnection is an important phenomenon in magnetized plasmas because it leads to sudden release of magnetic energy and global changes of magnetic field structure. Fluctuations generated during magnetic reconnection are likely to affect reconnection speed and energy conversion process [1,2] as well as energy/helicity transport. We investigated magnetic fluctuation spectra during TS-4 counter-helicity merging experiment in which both poloidal and toroidal fields reconnect (no guide field case). The fluctuations had different characteristics in the downstream region and at the reconnection X-point. The fluctuation power with 0.5-5.0 MHz frequency component concentrated on outboard-side downstream region (Fig. 1 (a)), whereas the fluctuation power with 7-20 MHz frequency component was localized around the X-point (Fig. 1 (b)) and propagated almost radially. Since the lower hybrid frequency near the X-point was lower than 15 MHz, this higher frequency mode detected near the X-point is supposed to belong to the whistler mode. Dispersion relation of the fluctuations near the X-point indicated that the angle between the wave vector and magnetic field was about 60-80 degrees. The fluctuation power spectral density (PSD) observed in the outboard-side downstream region and near the X-point are shown in Fig. 1 (c). Since the observed fluctuation has higher frequencies than the ion cyclotron frequency and the reconnection structure is smaller than the ion inertia length, the turbulence could be expressed in electron MHD framework. The PSD near the X-point clearly shows inverse cascade occurring in the imbalanced turbulence driven by the whistler waves[3]. These fluctuation characteristics could play a key role in vanishment of the helicity during counter-helicity merging.

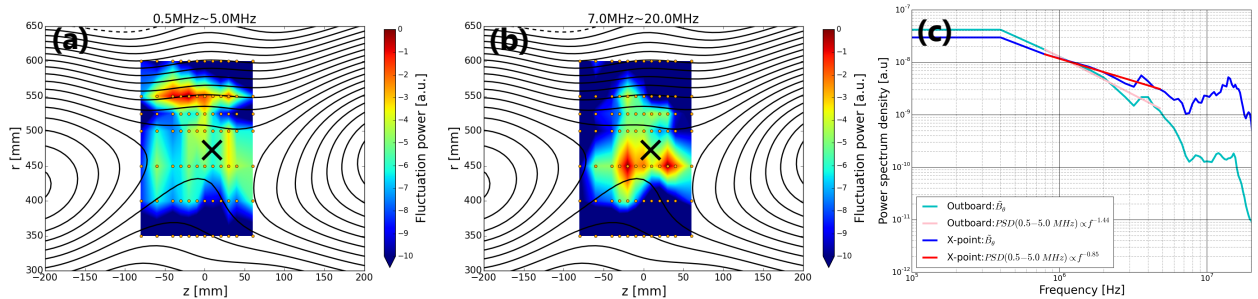


Fig. 1: Spatial distribution of magnetic fluctuation power of (a) 0.5-5 MHz and (b) 7-20 MHz components during counter-helicity spheromak merging. Orange dots indicate measurement points and cross mark represents the X-point. (c) Power spectral density (PSD) of the toroidal component fluctuations measured at different radial point of (blue) near X-point and (cyan) outboard side.

- [1] H. Ji *et al.*, *Phys. Rev. Lett.* **92** (2004) 115001.
- [2] M. Inomoto *et al.*, *Phys. Plasmas.* **20** (2013) 061209.
- [3] H. Kim and J. Cho, *Astrophys. J.* **801** (2015) 75.

Role of Kinetic Alfvén Wave in Energy Transportation in Magnetopause

Abstract

The transportation of energy is the vital subject in space physics. Magneto hydrodynamic waves are known to play very important role in plasma transportation. In the present work, we have studied the localization of kinetic Alfvén wave (KAW), which is three dimensionally propagating. These localized structures might be a possible candidate for transported energy at small scales in dissipation range of turbulent spectra. For this scenario, governing dynamical equation of KAW has been derived taking ponderomotive nonlinearity into account. Furthermore, these equations are solved numerically using pseudo spectral method in magnetopause regime to analyse the localized structures of KAW and corresponding turbulent spectrum. Spectrum shows steeper scaling followed by inertial range and this steepening is due to the transportation of energy from large to small scale, which eventually contributes to heating of plasma. The present mechanism may be useful for explaining the plasma heating and particle acceleration in magnetopause. The present study is correlated with the observations made by Chaston et al. [2008] using THEMIS data.

Reference

Chaston, C., et al. (2008), Turbulent heating and cross-field transport near the magnetopause from THEMIS, *Geophys. Res. Lett.*, 35, L17S08, doi:10.1029/2008GL033601.

Numerical study of spectral line shapes in high-density He plasmas

H. Kawazome, S. Namba^a

Department of Information Engineering, National Institute of Technology, Kagawa College, 551 Kohda Takuma-cho, Mitoyo 769-1192, Japan

^a *Graduate School of Engineering, Hiroshima University, 1-4-1 Kagamiyama, Higashihiroshima 739-8527, Japan*

In order to determine electron temperature and density in plasmas, spectral line intensity ratio of appropriate transitions provides a useful method for plasma diagnostics, in which the experimental ratio is compared with the value calculated by using a collisional-radiative (CR) model. However, in high-density plasmas, such as atmospheric thermal plasmas and divertor plasma of magnetically confined devices, an optical depth becomes significantly thick. For example, although He arcjet plasmas have been studied extensively for fundamental research of arcjet thrusters and atomic/molecular physics, it is found that the radiation trapping of resonance transitions alters the population distribution. Consequently, we cannot apply the intensity ratio method for determinations of plasma temperature and density. In this study, therefore, coupled rate equations incorporating the radiation transport are solved to derive the population densities and analyze spectral line shapes of the resonance spectra. The transitions considered are $1s^2\ ^1S - 1s2p\ ^1P$, $1s^2\ ^1S - 1s3p\ ^1P$ and $1s^2\ ^1S - 1s4p\ ^1P$, and the respective wavelength are 58.4 nm, 53.7 nm and 52.2 nm. In the calculation, a slit function is not taken into account. The plasma is a cylinder shape having a radius of 0.25 cm and a length of 0.5 cm and divided by four regions. The spatial profiles of the electron temperature and density are given by $Te(l) = T_0(1 - (l/0.5)^2)^2$ eV $n_e = n_0(1 - (l/0.5)^2)^2$ cm⁻³, respectively, where T_0 and n_0 are 0.5 eV and 1.0×10^{13} cm⁻³, respectively. The ion density is equivalent to that of electron density, and gas temperature is set to electron temperature. The atomic density ($=1.0 \times 10^{15}$ cm⁻³) and temperature (Gaussian: 300 K) are constant throughout the volume. Figure 1 shows the time evolution of calculated line profiles for $1s^2\ ^1S - 1s2p\ ^1P$ transition. As clearly seen, the profiles change to flat top shape with time, because the line

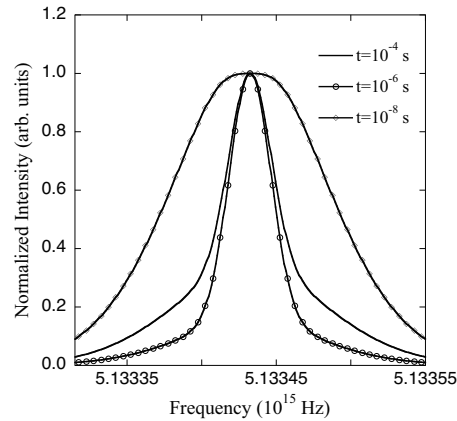


Figure 1: Time evolution of spectral line profiles for $1s^2\ ^1S - 1s2p\ ^1P$ transition.

center has the highest absorption probability. Details of the results will be discussed.

Doppler reflectometer system for measuring plasma rotation velocity in GAMMA 10

J. Kohagura, T. Tokuzawa^a, M. Yoshikawa, Y. Nakashima

Plasma Research Center, University of Tsukuba, 1-1-1 Tennodai, Tsukuba, Ibaraki 305-8577, Japan

^a National Institute for Fusion Science, 322-6 Oroshi-cho, Toki 509-5292, Japan

kohagura@prc.tsukuba.ac.jp

Doppler reflectometry is currently used as a powerful technique to measure the perpendicular velocity of density fluctuations, the radial electric field, and the perpendicular wave number spectrum in many fusion plasma devices [1-3]. In GAMMA 10 a Doppler reflectometer has recently been installed to measure perpendicular rotation velocity of density fluctuations in the cylindrical plasma at the central cell as shown in Fig. 1. The Doppler reflectometer has an antenna system with a launching/receiving scalar feed antenna and focusing mirrors. It gives a quasi-Gaussian beam with beam waist ω of ~ 5 cm at the plasma edge. By rotating one of the mirrors the tilting angle of the incident microwave can be controlled against the normal of cutoff layers. A frequency synthesizer is used in the range 11.5–18 GHz as the stable microwave source of x-mode probing beam for GAMMA 10 plasma having typical peak density $\sim 2 \times 10^{18} \text{ m}^{-3}$. Simple direct conversion microwave circuit is built using I-Q mixer which combines the reference signal from the synthesizer and the back-scattered signal from plasma and produces in-phase ($I=A\cos\phi$) and quadrature ($Q=A\sin\phi$) signals. The I and Q signals are sampled at 1MHz by a fast digitizing oscilloscope. Spectrum analyzer has poor time resolution but it helps to confirm the frequency spectrum of the back-scattered signal directly. The first preliminary results of Doppler shifted complex spectra and radial profiles of the perpendicular velocity of density fluctuations are presented for ICRF start-up plasma with additional ECH. The rotation of fluctuations during additional ECH period is found to become opposite direction comparing to the case of ICRF heating alone.

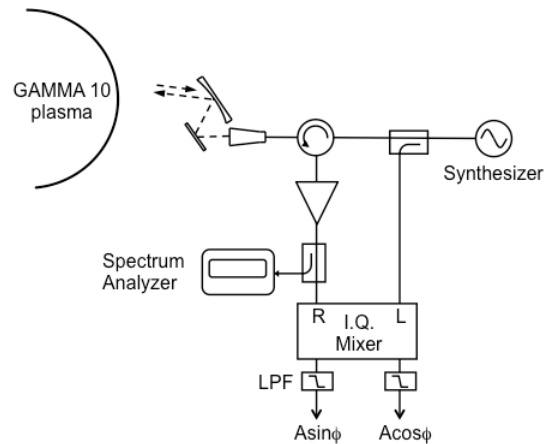


Fig. 1 Schematic drawing of the Doppler reflectometer system in GAMMA 10.

- [1] M. Hirsh *et al.*, Plasma Phys. Contral. Fusion **43** (2001) 1641.
- [2] G. D. Conway *et al.*, Nucl. Fusion **46** (2006) S799.
- [3] T. Tokuzawa *et al.*, Plasma Fusion Res. **9** (2014) 1402149.

Co-extraction of Low Energy Ar⁺ and C₂H₂⁻ Ions for Space Charge Effect Mitigation and Increased Beam Intensity

C.L.S. Mahinay, M. Wada^a

Department of Physics, School of Science and Engineering, Ateneo de Manila University, Quezon City 1108, Philippines

^aGraduate School of Science and Engineering, Doshisha University, Kyotanabe, Kyoto 610-0321, Japan

Low energy ion beams, especially negative ion beams, have fairly low intensities due to the space charge effect. Negative ions generated from a target surface by plasma sputtering typically yield very low intensities. To significantly increase the beam intensity of negative ion beams, Cs is introduced into the plasma volume which lowers the work function of the target surface and increase negative ion yield [1]. However, Cs is difficult to handle and is a hazardous substance. To increase the intensity of positive ion beams, electrons are introduced to neutralize the beam and mitigate the space charge effect [2]. In this study, positive and negative ion beams are co-extracted from a hot cathode filament-type DC plasma source as a means to increase the intensities of either beam. The positive ions consists mainly of Ar⁺ ions and the negative ions are C₂H₂⁻ ions. Energies do not exceed 800eV. A Wien filter mass analyzer is used to obtain the mass spectra of the ion beam and a 127° sector electrostatic energy analyzer (ESA) is used to measure the ion energy distribution function. The ESA and Wien filter can be coupled to measure the ion energy distribution function of specific ion masses. The co-extraction of the positive and negative ions increased the beam intensity of the Ar⁺ ions to a maximum of 10⁻⁸A from 10⁻⁹A. The C₂H₂⁻ beam intensity also increased from 10⁻¹¹A to 10⁻⁹A. Hence, we have a devised a simple way of increasing the intensity of either low energy positive or negative ion beams by means of co-extracting both beams simultaneously. This method of co-extraction is a much safer alternative than using Cs in increasing the negative ion intensity especially at low energies.

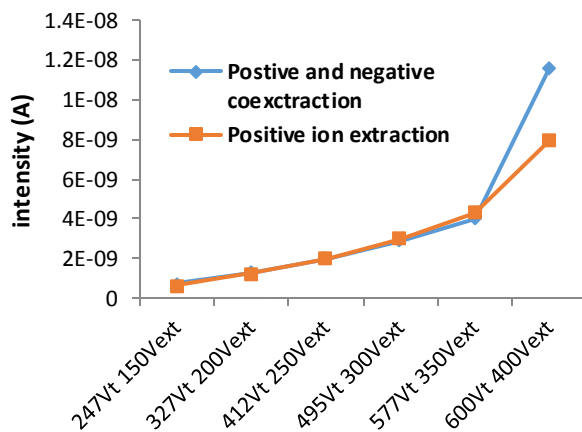


Fig. 1. Comparing intensities from both co-extracted ion beam and positive only ion beam.

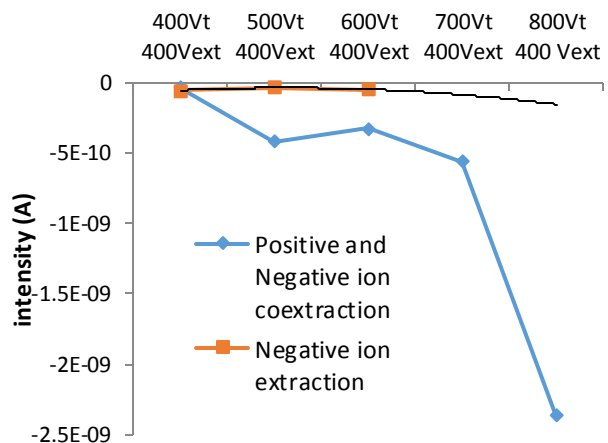


Fig. 2. Comparing intensities from both co-extracted ion beam and negative only ion beam. A geometric trend line is fitted to the negative ion extraction intensities

[1] J.R. Hiskes, A.M. Karo, P.A. Willmann and W.J. Stevens, Physics Letters A, **68** (1978) 221.

[2] V. Dudnikov and A. Dudnikov, Rev. Sci. Instrum. **73** (2002) 995.

Synthesis of hydrogenated amorphous carbon nitride using DC graphite hollow cathode discharge

Catherine Joy M. Dela Cruz, Sidney M. Palardonio, and Henry J. Ramos^a

^a*Plasma Physics Laboratory, National Institute of Physics,
University of the Philippines Diliman, Quezon City, Philippines*

Hydrogenated amorphous carbon nitride (a-C:H:N) was synthesized on Si substrates in a plasma-enhanced chemical vapour deposition (PECVD) facility operating in direct current graphite hollow cathode discharge (HCD) mode. Methane percentage, filling pressure and discharge voltage of the CH₄/N₂/Ar mixture plasma were varied. Prior to deposition, optical emission spectroscopy (OES) was used to determine the presence of active species in plasma that are needed for carbon nitride synthesis, such as CN radicals, N₂⁺ first negative, N₂ second positive and Ar II. Electron temperature was obtained using the slope of the Boltzmann plot of ten Ar I lines. The optical emission spectra has showed that carbon nitride synthesis is favoured with high discharge voltage, 6% methane and 1.0 Torr filling pressure. Changes induced in the elemental composition, surface morphology, crystallographic structure, and structural disorder in the deposited a-C:H:N were analysed by FTIR, SEM, XRD and Raman spectroscopy, respectively. As an application, surface free energy was determined using the Owen Wendt method.

For all the samples, FTIR showed the presence of a strong broad band peak in 3000-3500 cm⁻¹ corresponding to OH, medium strength peaks on 2800-2900 cm⁻¹ and 2150-2250 cm⁻¹ corresponding to (sp³) C-H and (sp) CN triple bond, respectively. The intensity for C-H bond increases while the CN triple bond decreases with increasing methane percentage. Raman spectra analysis showed that I_D/I_G intensity ratio decreases with increasing methane percentage for 0.6 and 0.7 Torr filling pressures. XRD and SEM confirmed the amorphous properties of a-C:H:N deposits. There is an increase in the surface free energy for the treated samples ranging from 37.5-41.9 compared to the untreated sample with 35.3.

Study on operating principle of Cockcroft-Walton circuit to produce plasmas using high-voltage discharge

T. Fukuyama, K. Sugihara ^a

Faculty of Education, Nagasaki University, 1-14 Bunkyo-machi, Nagasaki 852-8521, Japan

^a *Graduate School of Education, Ehime University, 3 Bunkyo-cho, Matsuyama, Ehime 790-8577, Japan*

The basis of operating principle of Cockcroft-Walton (CW) circuit [1] as shown in Fig. 1 in order to produce high-voltage is studied using SPICE which is simulator of electrical circuit. CW circuit experimentally contributed to breakthrough of nuclear physics to be applied to the development of particle accelerator [2]. High-voltage discharges obviously play an important role not only in producing plasmas but also a wide variety of fields. However, studies on operating principle of CW circuit are not enough, though improvement and application of it have been studied [3, 4].

As a result of our studies, we have found that: part of electrical charge stored in capacitors remains, output value of voltage can be expressed in recurrence formula, and more time is needed in order to boost concerning circuit which has higher number of steps as shown in Fig. 2. Furthermore, we have studied combination between frequency of alternating current and capacitance in capacitor in order to boost effectively as shown in Fig. 3.

[1] J.D.Cockcroft and E.T.S.Walton, Proc. Roy. Soc. Lond., A. **136** (1932) 619.
 [2] J.D.Cockcroft and E.T.S.Walton, Proc. Roy. Soc. Lond., A. **137** (1932) 229.
 [3] N.Marium, D.Ismail, K.Anayet, N.Khan, and M.Amran, Amer. J. Appl. Sci. **3** (2006) 2178.
 [4] K.Sur, and E.Bloodworth, IEEE Trans. Circuits Syst. **37** (1990) 432.

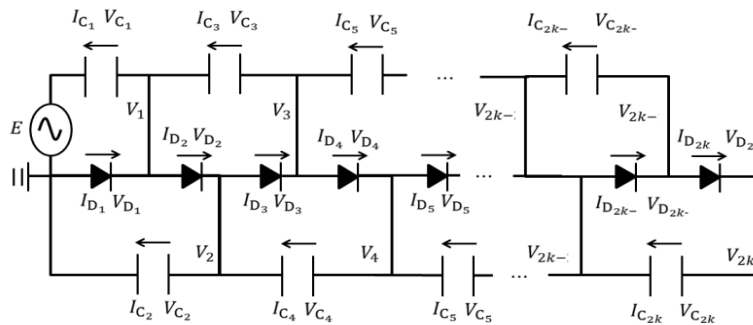


Fig. 1: CW circuit which has k steps

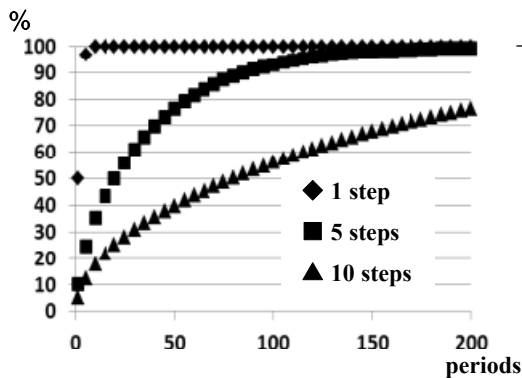


Fig. 2: Boost rate of CW circuit with 1, 5, and 10 steps

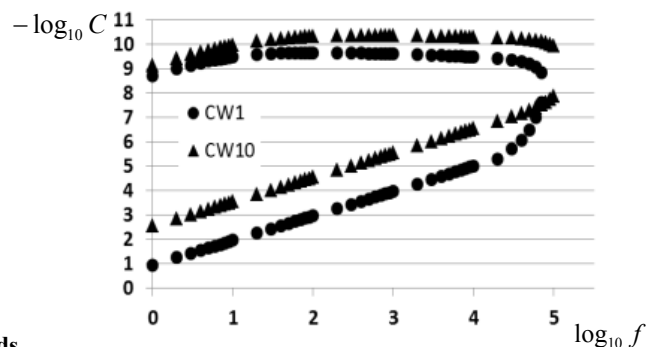


Fig 3: Frequency of power source and capacity (If combinations of frequency and capacity enter in the domain surround in a plot, CW circuit can work)

P1-23

Nonthermal and geometric effects on the dual-mode surface waves in a Lorentzian dusty plasma slab

Myoung-Jae Lee

Department of Physics

Hanyang University, Seoul 04763, South Korea

mjlee@hanyang.ac.kr

Kyu-Sun Chung

Department of Electrical Engineering

Hanyang University, Seoul 04763, South Korea

kschung@hanyang.ac.kr

Young-Dae Jung

Department of Applied Physics and Department of Bionanotechnology

Hanyang University, Ansan, Kyunggi-Do 15588, South Korea

ydjung@hanyang.ac.kr

The nonthermal and geometric effects on the propagation of the surface dust acoustic waves are investigated in a Lorentzian dusty plasma slab. The symmetric and anti-symmetric dispersion modes of the dust acoustic waves are obtained by the plasma dielectric function with the spectral reflection conditions the slab geometry. The variation of the nonthermal and geometric effects on the symmetric and the anti-symmetric modes of the surface plasma waves is also discussed.

High density plasma sustainment in microwave plasma source with slot antennas

S. Kogoshi, Y. Kanesaka, H. Araya, Y. Takahashi, S. Nakatui, N. Katayama

Department of Electrical Engineering, Faculty of Science and Technology, Tokyo University of Science, 2641 Yamazaki, Noda, Chiba, 278-8510, Japan

kogoshi@ee.noda.tus.ac.jp

It has been shown experimentally that TM waves and near field from the antennas can sustain high density plasma in a microwave plasma source with slot antennas, in which surface waves was not excited judging from mode numbers. It is well known that surface wave plasma (SWP) can sustain high density (and low electron) plasma [1]-[3]. A resonant absorption model has been proposed as the mechanism of the high density plasma sustainment of SWP [4]. The model suggests that high density plasma (and low electron temperature) would be sustained if there exists oscillating E-field parallel to a density gradient, its density is higher than the cut-off density, and the space between the cut-off density point and the sheath edge is wide enough for electron plasma waves to be excited. It has shown that a microwave plasma source with a resonant cavity for a TM mode was able to sustain high density plasma when it was satisfied with above conditions [5]. Here, we show that the same microwave plasma source as the reference (5) except for the air gap length (see Fig.1), which was different from the resonant cavities for TM waves. New air gap lengths, which are corresponding to near field ($L=2$ mm) and far field ($L=15$ mm, TM mode) irradiation, can also sustain high density plasma. Figure 2 shows that when plasma density reached cut-off density, the increasing rate of plasma density becomes more rapid and the electron temperature starts to drop. It suggests that the energy absorption mechanism changed from normal one to the resonant absorption at the point. The picture of the plasma taken from the bottom is shown in Fig.3. The mode pattern suggests the plasma was not sustained by SWP.

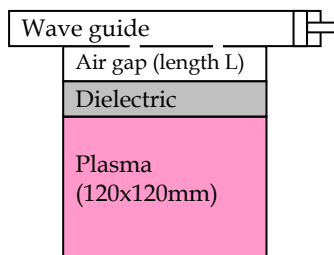


Fig.1 Schematic experimental setup.

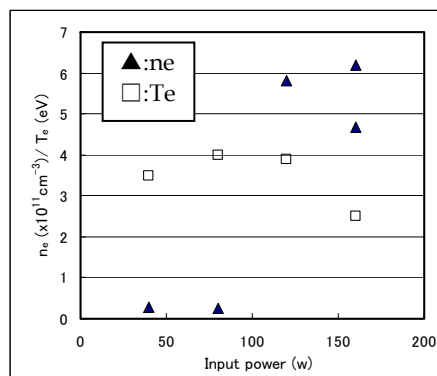


Fig.2 Dependence of n_e and T_e on input power ($P=0.6$ Torr, $L=2$ mm).

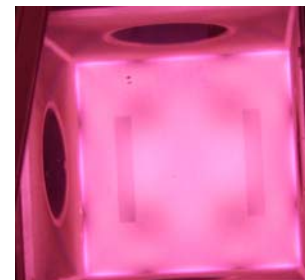


Fig.3 Picture of plasma ($P_{in}=200$ W, $P=0.6$ Torr $L=2$ mm).

- [1] K. Komachi, J. Vac. Sci. Technol. A11(1993) 164.
- [2] M. Nagatsu, G. Xu, I. Ghanashev, M. Kanoh, and H. Sugai, Plasma Sources Sci. Technol. 6(1997)427.
- [3] J. Kudela, T. Terebessy, and M. Kando, Appl. Phys. Lett. 76(2000)1249.
- [4] T. Omaru, F. Komiyama, and S. Kogoshi, Jpn. J. Appl. Phys. 43(2004)2690.
- [5] S. Kogoshi, Y. Yoshioka, N. Katayama, and Y. Kudo, Jpn. J. Appl. Phys. 48(2009)08HB01.

P1-25

Formation of Diamond-Like Carbon (DLC) on Silicon using Low Energy Ion Beam Deposition

by

Juan Paulo N. Gonda, and Dr. Christian Lorenz S. Mahinay

This study focuses on the synthesis and yield of a Diamond-Like Carbon thin film deposited on silicon slides using low energy ion beams, with acetylene as the carbon source. The plasma source used is a tungsten filament with current passing through. The characteristics of the plasma and ion beam generated, such as discharge voltage, discharge current, extraction voltage and ion current, are varied and related to the yield of DLC on the surface of the silicon. The yield is to be determined by using an SEM.

As of writing, only argon plasma has been generated. Using the argon plasma, the ion and plasma characteristics were tested and related to one another. It has been observed that as discharge current and extraction voltage increases, the ion current increases as well, indicating an increase in the number of argon ions flowing. This could lead to a greater DLC yield when using carbon ions.

Another aspect tested was how the pressure of the vacuum chamber affected the generation of ions. It was determined through tests that the optimum pressure for this particular setup is at $5e^{-4}$ torr as at that pressure. Less than that amount would require more current in the filament to produce the same discharge current, and more would also show the same effects.

The extraction voltage (EV) was used to determine if what was being harvested was the desired positive ions. As the EV increased, the ion current changed from negative to positive, meaning that the faraday cup was catching positive ions. The ion current also increased gradually, indicating that if a higher yield is to be desired, a greater EV is the optimum setting.

Further tests will be run using an acetylene argon mixture to produce plasma to coat the slides. Also, tests will be run to see how the changes in characteristics relate to the yield deposited on the surface.

Parallel electric fields in nonlinear magnetosonic waves in a multi-ion-species plasma

M. Toida

National Institute for Fusion Science, 322-6 Oroshi-cho, Toki 509-5292, Japan

Theory and particle simulations have revealed that nonlinear magnetosonic waves can strongly accelerate particles with various nonstochastic mechanisms [1]. The electric field parallel to the magnetic field in a magnetosonic shock wave plays crucial roles in some of the mechanisms. For example, the parallel electric field can cause trapping and acceleration of electrons in an oblique shock wave. In a plasma containing electrons, positrons, and ions (e-p-i plasma), the parallel electric field can accelerate positrons.

The parallel electric field E_{\parallel} and its integral along the magnetic field, $F = -\int E_{\parallel} ds$, were quantitatively analyzed with theory and electromagnetic particle simulations [2]. The theory and simulations showed that F can be large (E_{\parallel} can be strong) when the external magnetic field is strong. The value of F can be estimated as $eF \sim \epsilon^2 m_i v_A^2$ in small-amplitude pulses in a cold plasma, where ϵ is the amplitude of the pulse, m_i is the ion mass, and v_A is the Alfvén speed. This work was also extended to e-p-i plasmas [3].

In this study, we theoretically analyze E_{\parallel} and F in nonlinear magnetosonic waves in a plasma containing two species ions. In such a plasma, there exists two magnetosonic modes, which we call high-frequency mode and low-frequency mode. Nonlinear behavior of these modes can be described by Korteweg-de Vries equations for the frequency regions, $\omega \ll \Omega_i$ of the low-frequency mode and $\Omega_i \ll \omega \ll (\Omega_i \Omega_e)^{1/2}$ of the high-frequency mode [4, 5]. It is found the value of F for the high-frequency-mode pulse can be estimated as $eF \sim \epsilon^2 m_i v_A^2$, whereas that for the low-frequency-mode pulse as $eF \sim \epsilon^2 (m_e m_i)^{1/2} v_A^2$. Thus, F for the high-frequency-mode pulse is (m_i/m_e) times as strong as F for the low-frequency-mode pulse. It indicates that E_{\parallel} of the high-frequency-mode pulse may influence particle acceleration in a multi-ion-species plasma. We also derived the parallel electric field of nonlinear magnetosonic pulses in e-p-i plasmas for the region $\Omega_i \ll \omega \ll (\Omega_i \Omega_e)^{1/2}$, which was not obtained in Ref. [3] where the expansion method for the region $\omega \ll \Omega_i$ was used.

- [1] Y. Ohsawa, Phys. Reports **536** (2014) 147
- [2] H. Takahashi, Y. Ohsawa, Phys. Plasmas **14** (2007) 112305
- [3] H. Takahashi, M. Sato, Y. Ohsawa, Phys. Plasmas **15** (2008) 082309
- [4] M. Toida and Y. Ohsawa, J. Phys. Soc. Jpn. **63** (1994) 573
- [5] M. Toida and Y. Kondo, Phys. Plasmas **18** (2011) 062303

P1-27

withdrawal

Design study on double layer type interface structure for heat exchanger of Fusion DEMO blanket

M. Kondo¹⁾, T. Tanaka²⁾, Y. Hishinuma²⁾, N. Suzuki³⁾, Y. Kawamata³⁾, H. Chikaraishi²⁾, T. Muroga²⁾, A. Sagara²⁾

1) Tokyo Institute of Technology, 2-12-1, O-okayama, Meguro-ku, Tokyo 152-8550 Japan,

2) National Institute for Fusion Science, Toki, Gifu 502-5292, Japan,

3) Tokai university, 4-1-1 Kitakaname, Hiratsuka-shi, Kanagawa 259-1292, Japan

The design of heat exchanger for the liquid breeders, which can achieve a large coefficient of heat transfer and a small permeability of tritium (T), is important issues for the development of fusion DEMO reactors. The tritium permeability in the heat exchanger can be improved by the coating with tritium permeation barrier (TPB) by metal organic decomposition (MOD) method or metal organic chemical vapor decomposition (MOCVD) method. Several ceramic coatings having high thermodynamic stability, such as Y_2O_3 , Er_2O_3 and ZrO_2 , are the candidates of the TPB material for the liquid breeder blanket. The function of the TPB must be kept during the life time of the heat exchanger. Therefore, these coatings should be protected in the liquid breeders by so-called multi-layer structure as shown in Fig.1 (a). The thickness of the outer layer corresponds to the corrosion margin, and the thinning of the outer layer does not influence on the TPB performance. The purpose of the present study is to design the double layer type interface structure, which achieves the function of TPB and the corrosion resistance in the same time during the long-term operation. The allowable thickness of the double layers was evaluated based on the estimation of the coefficient of overall heat transfer. The online monitoring technology for this type of functional layers must be established. The electrochemical impedance spectroscopy (EIS) is proposed as the online monitoring method and the response for the degradation and the layer thinning by the corrosion was simulated by Z-view code. The double layer structures were preliminary fabricated on SUS316L steel by the MOD coating method and the thermal spraying method. The fabrication conditions are presented in Table 1. Figure 1 (b) shows the results of surface cross sectional observation for the specimen of test ID 5 by FE-SEM. It was found that thermal spray layer of Al_2O_3 with the thickness of approximately $20\mu m$ was successfully fabricated on the Al_2O_3 MOD layer.

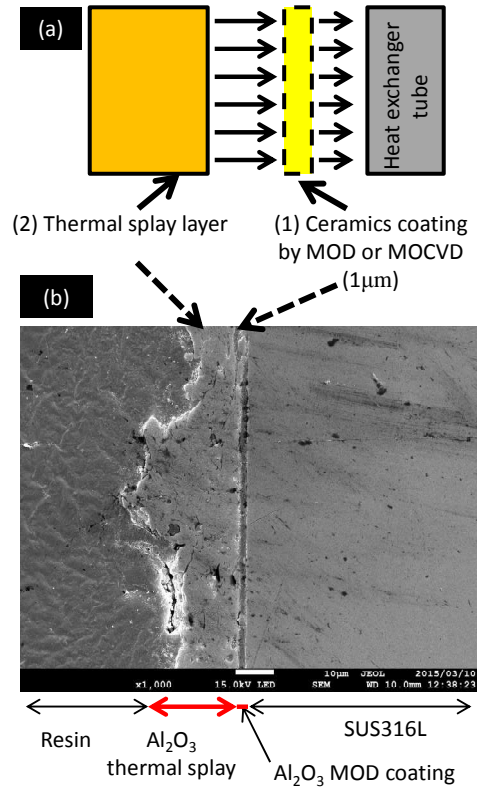








Fig. 1 (a) schematic of double layer structure, (b) Surface cross section of specimen of TEST ID 5 observed by FE-SEM

Figure 1 (b) shows the results of surface cross sectional observation for the specimen of test ID 5 by FE-SEM. It was found that thermal spray layer of Al_2O_3 with the thickness of approximately $20\mu m$ was successfully fabricated on the Al_2O_3 MOD layer.

Table 1 Fabrication conditions of double layer structure

	Test ID 1	Test ID 2	Test ID 3	Test ID 4	Test ID 5	Test ID 6
	Disc type specimen ($\Phi 20mm \times t7mm$)			Bullet type ($\Phi 20mm \times$ length 40 mm)		
Substrate	SUS316L	Al_2O_3 MOD/ SUS316L	Y_2O_3 MOD/ SUS316L	SUS316L	Al_2O_3 MOD / SUS316L	Y_2O_3 MOD / SUS316L
Substrate temperature	$30^\circ C - 60^\circ C$	$30^\circ C - 60^\circ C$	$30^\circ C - 60^\circ C$	$30^\circ C - 60^\circ C$	$30^\circ C - 60^\circ C$	$30^\circ C - 60^\circ C$
Thermal spray layer	Al_2O_3	Al_2O_3	Y_2O_3	Y_2O_3	Al_2O_3	Y_2O_3
Average size of powders [μm]	30	30	30	30	30	30
Spray distance [mm]	130	130	130	130	130	130
Plasma output [kW]	44	44	44	44	44	44
Repeated times	7	7	7	2	7	2
Photo after thermal spray						

Thermal quench of ion-beam induced luminescence of Er₂O₃

D. Kato, H.A. Sakaue, T. Tanaka, I. Murakami, T. Muroga, and A. Sagara

National Institute for Fusion Science, 322-6 Oroshi-cho, Toki 509-5292, Japan

Er₂O₃ is a prospective material for electric insulation and tritium permeation barrier of advanced blanket systems with liquid breeders and coolants, e.g., Li, Fliebe, and Li-Pb [1, 2]. It is undertake to develop optical methods for *in-situ* characterization of radiation-induced defects in Er₂O₃ by using energetic ion bombardment. The Er₂O₃ crystals exhibit an ion-induced luminescence band in 640-690 nm which is identified as $4f^{11} 4F_{9/2} \rightarrow 4I_{15/2}$ transition of Er³⁺ at C₂ cation sites. It has been demonstrated that the luminescence intensity is reduced significantly by the energetic ion bombardment with plasma splay coating samples [3] and sintered bulk samples [4]. The intensity reduction can be associated with decrystallization of surfaces by the energetic ion bombardment.

In the present work, we addressed for the first time measurements of the ion-induced luminescence with a heated sample up to 873 K. As shown in Fig. 1, it is found that the luminescence intensity vanishes above 670 K. Excited electrons in the upper levels of Er³⁺ ions are dissipated non-radiatively due to interaction with ambient thermal phonons at high temperatures. Indeed, a characteristic rate of the non-radiated depopulation of the upper levels deduced from the emission line broadening increases with temperatures. However, this drastic thermal quench of the luminescence is hardly to reconcile with the measured rate of the non-radiative depopulation.

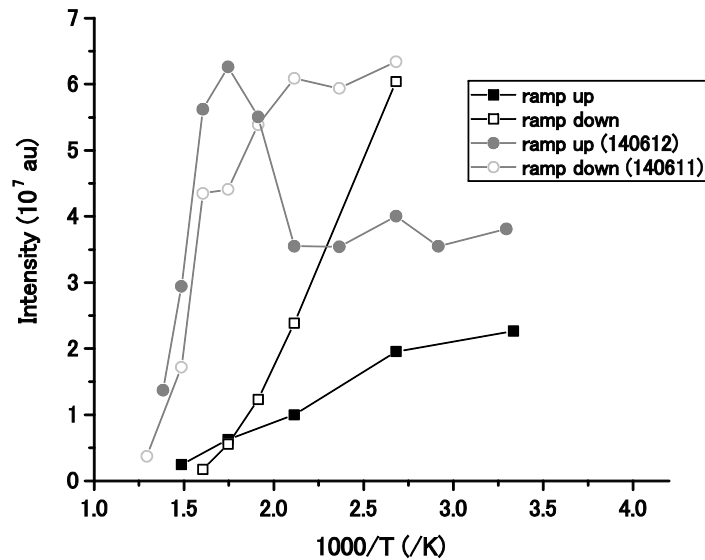


Fig.1. Temperature dependence of the luminescence intensity induced by an Ar⁺ ion-beam (35keV, 10 μ A). Solid squares and circles stand for measurements ramping up the temperature, and open squares and circles for those ramping down the temperature.

- [1] T. Muroga et al.: J. Nucl. Mater. **367–370** (2007) 780.
- [2] D. Levchuk et al.: J. Nucl. Mater. **367–370** (2007) 1033.
- [3] T. Tanaka et al.: J. Nucl. Mater. **417** (2011) 794.
- [4] D. Kato et al.: Plasma Fusion Res. **7** (2012) 2405043.

Hydrogen solubility in molten salt FLiNaK mixed with nano-Ti powder

J. Yagi, A. Sagara, T. Tanaka, S. Takayama, T. Muroga

National Institute for Fusion Science, 322-6 Oroshi-cho, Toki 509-5292, Japan

Molten salts including FLiNaBe, FLiBe, and FLiNaK have attracted strong interests as candidate liquid breeding material for a magnetic fusion reactor due to the low electric conductivity, light density, and chemical stability. Their major concerns are the very low hydrogen solubility (i.e. risk for tritium leakage) and the enhanced corrosivity by impurities such as moisture, oxygen, and generated TF in neutron field. Considering these points, the concept of mixing a hydrogen-absorbing metal powder with the molten salt has been proposed by A. Sagara [1]. A hydrogen-absorbing metal such as Ti or Zr increases the effective hydrogen solubility of the molten salt. If the mixing fraction of the metal powder is small, the advantages of the molten salt (low conductivity, light density, chemical stability, etc.) would be retained. J. Yagi has already confirmed the 5 order increase of effective solubility [2] using FLiNaK mixed with Ti powder whose grain size is below 38 μm . However, there was no increase for the powder exposed to air [2]. The aim of this paper, therefore, is to make clear the effect of surface contaminations by comparing with ideally clean powder. Fortunately, The nano-Ti powder (0.1wt%) was directly electrocrystallized in FLiNaK by I'MSEP, Japan [3]. In this work, practical hydrogen solubility of nano-Ti powder mixed FLiNaK (Fig. 1) is investigated using the device shown in Fig.2. Detailed results will be presented and discussed in the conference.



Fig.1. nano-Ti powder mixed FLiNaK

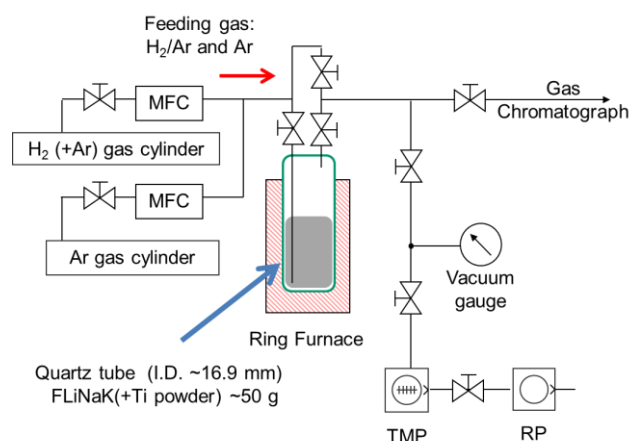


Fig.2. Experimental setup

- [1] A. Sagara, H. Tamura, T. Tanaka, N. Yanagi, J. Miyazawa, T. Goto, R. Sakamoto, J. Yagi, T. Watanabe, S. Takayama, the FFHR design group, *Fusion Engineering and Design*, **89** (2014) 2114-2120
- [2] J. Yagi, A. Sagara, T. Watanabe, T. Tanaka, S. Takayama, T. Muroga, *Fusion Engineering and Design*, in press
- [3] Y. ITO, T. Nishikiori and M. Tokushige, *Plasma-Induced Discharge Electrolysis for Nanoparticle Production*, *Molten Salts Chemistry: From Lab to Applications*, 269-286 (2013)

Fabrication and characterization of MOD ceramic coatings on coolant duct materials

T. Tanaka, T. Chikada^a, Y. Hishinuma, J. Morimoto^b, T. Muroga

National Institute for Fusion Science, 322-6 Oroshi-cho, Toki, Gifu 509-5292, Japan

^aShizuoka University, 836 Ohya, Suruga-ku, Shizuoka, 422-8529, Japan

^bThe Graduate University for Advanced Studies, 322-6 Oroshi-cho, Toki, Gifu 509-5292, Japan

Studies of ceramic coating on low activation ferritic/martensitic (RAFM) steels have been conducted mainly for suppression of tritium permeation from blanket components. However, the coating technologies are also considered important for coolant ducts to minimize tritium leakage during the transport to a hydrogen recovery system. Coating fabrication on candidate duct materials and characterization are performed in the present study.

Coatings of Er_2O_3 were fabricated on stainless steel 316, Inconel 600 and HASTELLOY C-276 substrates by the metal organic decomposition (MOD) method. After painting the MOD organic liquids on the substrate surfaces, the oxide ceramic coatings were obtained by baking the substrates in air for 1 hour at 650 °C. Depth profiles of atomic concentrations and energy spectra obtained by X-ray Photoelectron Spectroscopy (XPS) showed that Fe_2O_3 and Cr_2O_3 were produced on all the three substrate surfaces under ~50 nm thick Er_2O_3 coating layers. In our previous studies, the production of Fe_2O_3 on substrate surfaces degraded hydrogen permeation barrier performances and corrosion resistance properties of the ceramic coatings on RAFM steel substrates [1]. Also in the present fabrication, growth of Fe_2O_3 was found to break the coating layer (stainless steel 316) or make the coating layer rough (Inconel 600) in scanning electron microscope (SEM) observation. On the HASTELLOY substrate, influence of the Fe_2O_3 production on the coating layer was moderate compared with the others. However, since Fe_2O_3 is reduced by hydrogen at high temperatures, the production should be suppressed in all the substrates to obtain stable coating performances.

In the previous studies, preprocess to suppress the production of Fe_2O_3 in the coating baking process has been examined for RAFM steel substrates and preferable coating performances have been obtained [2]. Similar preprocess was applied to a HASTELLOY substrate. The substrate was heated up to 700 °C in a vacuum of $<7 \times 10^{-3}$ Pa and heat treatment was performed at 700 °C in air of 5 Pa for 30 minutes. Atomic concentrations obtained by XPS after the heat treatment showed that the surface was covered with ~200 nm thick Cr_2O_3 layer and the production of Fe_2O_3 was suppressed successfully. This indicates that the preprocess can be applied to the Ni-based alloy substrates and coatings with superior performances could be obtained on the Cr_2O_3 -covered substrate surfaces.

Regarding coating fabrication on rounded duct surfaces, test fabrication of a MOD ZrO_2 coating was performed on an outer surface of an Inconel 600 pipe of 26 mm in outer diameter. In the present study, the MOD liquid was painted on the pipe surface by silk screen printing and smooth coating was successfully obtained after baking in an Ar flow.

Optimization of the preprocess conditions to suppress the Fe_2O_3 production in coating baking on the coolant duct materials and characterization of the obtained coatings are being performed at present.

[1] D. Zhang et al., Fusion Sci. Technol. 60 (2011) 1576–1579.

[2] T. Tanaka, T. Muroga, Journal of Nuclear Materials 455 (2014) 630–634.

Investigation of the selective heating of the metal powder with hydrogen in the molten salts using by microwave

S. Takayama, J. Yagi, T. Tanaka, A. Sagara

National Institute for Fusion Science, 322-6 Oroshi-cho, Toki 509-5292, Japan

In this paper, we will discuss with experiments the selective heating behavior of the molten salts and metal powders absorbed hydrogen in a single-mode cavity at 2.45GHz microwave. The new developed experimental device has the structure that two single-mode cavity intersected perpendicularly. In the crossing of two single-mode cavities, one becomes in the maximum electric field of microwave, and another becomes in the maximum magnetic field of microwave. For that reason, the sample at the crossing can control an inputting electric field and magnetic field separately.

In FFHR design studies, the molten-salt Flinabe (LiF-NaF-BeF₂) is the first candidate for a self-cooled liquid breeding blanket due to its superior safety (e.g., low MHD pressure loss, low reactivity with air, low-pressure operation, and low hydrogen solubility) [1]. In particular, low hydrogen solubility is advantageous for keeping the tritium inventory low and for simplifying the tritium recovery system. However, due to the high equilibrium pressure of tritium in the liquid (a few kPa at 600°C for 3 GW fusion), the following two aspects have been major issues: reduction of tritium permeation through a heat exchanger, and the use of low radio-activation vanadium alloys that have high mechanical strength up to and over 700°C but high hydrogen solubility (i.e., hydrogen storage metal). In order to resolve those two issues simultaneously, Sagara proposed to mix hydrogen-absorption metal powders (e.g., Ti, Zr, and V) in molten salt to effectively increase hydrogen solubility, where the MHD pressure loss is negligible, and also proposed to use selective heating with microwave in order to recover hydrogen from powders [1]. Yagi confirmed experimentally that a hydrogen-soluble Ti powder mixed with FLiNaK can increase the effective hydrogen solubility for more than 5 orders [2].

On the other, microwave has characteristics of the selective heating, internal heating, volumetric heating and rapid heating. For the reasons, since 1960th, we have been successfully applied microwave energies for cooking foods, drying woods, heating rubbers, medicines and textiles, sintering of ceramics etc. During the last decade, the use of microwave sintering technology for production of sintered composite materials with components of high electric conductivity such as metals has intensively been investigated. It is well known that metallic materials reflect microwaves rather than absorb them. However, it has been demonstrated that sintering of metal powder compacts by using microwave heating is possible. Systematic experimental investigations on microwave sintering of metal powder compacts in a single mode microwave applicator operating at 2.45 GHz revealed that heating may strongly depend on the sample position in the electromagnetic mode. In addition, selective heating occurs in different absorption ratios of materials each other. In selective heating, the local temperature difference is made in materials and the thermally non-equilibrium state occurs in macro-state. We expect the selective heating of metal powders in molten salts using by the magnetic field of microwave.

[1] A. Sagara, H. Tamura, T. Tanaka, N. Yanagi, J. Miyazawa, T. Goto, R. Sakamoto, J. Yagi, T. Watanabe, S. Takayama, the FFHR design group, *Fusion Engineering and Design*, **89** (2014) 2114-2120

[2] J. Yagi, A. Sagara, T. Watanabe, T. Tanaka, S. Takayama, T. Muroga, *Fusion Engineering and Design*, in press

Performance evaluation of a three-surface-multi-layered channel with a reinforced metal layer

D. Isshiki^a, S. Ito^a, T. Muroga^b, H. Hashizume^a

^aTohoku University, 6-6-02-1 Aramaki Aza Aoba, Aoba-ku, Sendai 980-8579, Japan

^bNational Institute for Fusion Science, 322-6 Oroshi-cho, Toki 509-5292, Japan

disshi@karma.qse.tohoku.ac.jp

Reducing MHD pressure drop is one of the most important R&D issues in liquid metal fusion blankets. A three-surface-multi-layered channel which is a rectangular channel and consists of a thin metal layer and a ceramic insulating layer on three of the four inner surfaces of the channel, is an advanced concept to reduce the MHD pressure drop [1]. The three-surface-multi-layered channel reduces the MHD pressure drop to an acceptable value if the thickness of the inner metal layer is less than 0.02 mm. However, this thickness is too small to sustain strength of the inner metal layer. To solve this problem, we have proposed a new design for the channel in which the inner metal layer is partially reinforced by attaching reinforcing structures as shown in Fig. 1 [2]. The study demonstrated that the attached reinforcing structure not only increases rigidity but also increases pressure drop which, however, can change flow field and enhance heat transfer. Therefore, this study evaluates the effect of the geometry of reinforcing structures on the pressure drop, rigidity of inner metal layer, and heat transfer performance by 3D finite element analysis depending on geometry of the reinforcing structure. And then we will discuss optimized geometry of the inner metal layer. Additionally, we fabricate prototype of the channel.

Fig. 2 illustrates numerical model used in this study to consider a reinforced three-surface-multi-layered channel. In this figure, the width, thickness, and the angle of the reinforcing structures are denoted as w , h , and θ . Navier-Stokes equation with Lorentz force and charge conservation equation are solved to evaluate pressure drop under conditions of a magnetic field of 1 T and an average velocity of 0.10 m/s. To evaluate rigidity of inner metal layer, we consider it as cantilever and evaluate the maximum displacement. We also analyze temperature field at inflow condition of a heat flux of 1 MW/m² from the first wall, and obtain the maximum temperature to discuss heat transfer performance.

As a result, when $w = 2.0$ mm, $h = 0.140$ mm, $\theta = 34$ degree, the pressure drop is only 1.16 times larger but the rigidity is 128 times larger than an unreinforced channel. Detail of results including heat transfer performance and fabrication of the prototype will be presented in the full paper.

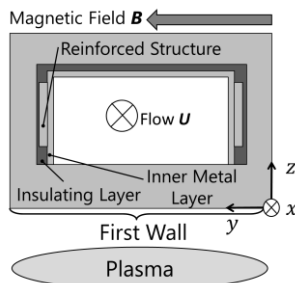


Fig. 1 Reinforced three-surface-multi-layered channel

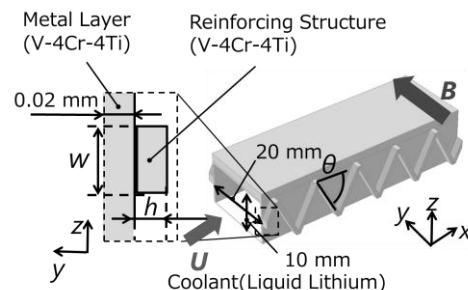


Fig. 2 Assumed geometry of the reinforcing structure attached inner metal layer

[1] H. Hashizume, Fusion Engineering and Design, Vol. 81, (2006), 1431-1438.

[2] Y. Inage et al., Proceedings of NTHAS8, (2012), N8P1107.

Adhesion strength of Er_2O_3 /buffer stacked MOCVD coating for advanced breeding blanket

Y. Hishinuma, T. Tanaka, Y. Tanaka^a, K. Matsuda^a, T. Muroga and A. Sagara

National Institute for Fusion Science, 322-6 Oroshi-cho, Toki 509-5292, Japan

^a *University of Toyama, 3190, Gofuku, Toyama 930-8555, Japan*

The electrical insulator and tritium permeation barrier are key components to realize liquid metal (Li or Pb-Li) and molten-salt typed breeding blanket systems. We investigated the Er_2O_3 coating as the one of the candidate material for the electrical insulator and tritium permeation barrier. Because Er_2O_3 coating has higher electrical resistivity and barrier effect of hydrogen permeation compared with the other oxide materials. Recently, we succeeded to form the homogeneous Er_2O_3 coating on the large area, for example the interior surface of the 600 mm length stainless tube, using MOCVD process [1]. Furthermore, the double-stack structured Er_2O_3 coating layer with oxide buffer material was also easily formed using MOCVD process. It is well known that the crystal growth direction can be controlled by the crystal orientation of the substrate. Generally, the physical soundness of coating material was evaluated by the hardness, abrasion and adhesion properties. The scratch test is often used to evaluate the adhesion strength of hard coating and car paint layer. The schematic image of the scratch mechanism is shown in fig.1. The coating material is actually broken by the diamond scratch stylus, and the adhesion strength is obtained by the shearing stress on the interface of coating and substrate shown in fig.2.

In this study, we carried out the scratch test to the single and double-stacked coating, and the adhesion strength comparisons between single and double-stacked coating were investigated as functions of thickness and crystallinity of Er_2O_3 coating. Furthermore, the thermal cycling up to 973 K in Ar atmosphere was also carried out, and the changes of microstructure and adhesion strength will be reported.

Acknowledgement

This study was mainly performed and supported by the Fusion Engineering Project in NIFS (UFFF026)

[1] Y. Hishinuma, T. Tanaka, T. Tanaka, T. Nagasaka, Y. Tasaki, A. Sagara and T. Muroga, Fusion Engineering and Design, 86, 2011, 2530.

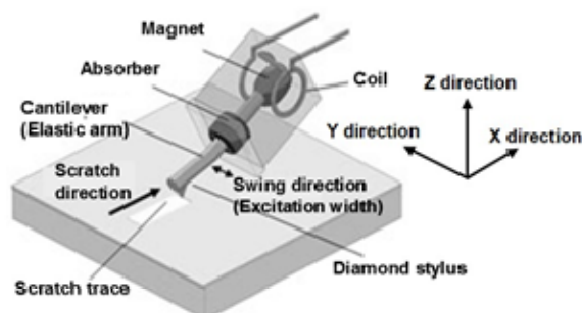
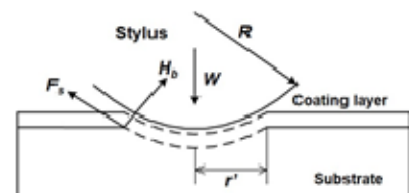


Fig.1 The schematic image of the scratch mechanism on the scratch test.



W : The vertical dynamic load applied by the stylus to the coating layer
 F_s : The shearing stress between coating layer and substrate
 R : The curvature radius of the stylus tip
 r' : The radius in the contacted region with the stylus tip
 H_b : Brinell hardness of the substrate

Fig.2 The configuration and interaction between the diamond scratch stylus and surface of the coating layer

Proposal of the maintenance method of breeder blankets of LHD-type helical fusion reactor FFHR

T. Goto, J. Miyazawa, H. Tamura, T. Tanaka, N. Yanagi, A. Sagara and the FFHR Design Group

National Institute for Fusion Science, 322-6 Oroshi-cho, Toki 509-5292, Japan

Conceptual design activity of LHD-type helical fusion reactor FFHR has been advanced under the Fusion Engineering Research Project in NIFS. One of the important design issues is the method of construction and maintenance of the in-vessel components with a three-dimensional shape. In particular, breeder blankets should be replaced periodically due to the neutron damage of the structural material. To enable the replacement of the breeder blankets with a short time, module structure of the breeder blankets should be designed with a consideration of the maintenance method.

In the latest conceptual design of FFHR, molten salt (FLiBe or FLiNaBe) is considered as a breeder material. Because electric conductivity of the molten salt is significantly lower than that of other liquid breeder candidates (liquid metals), flexible design of the flow channels of breeder blankets can be adopted. Therefore, we proposed Toroidally-Sliced, HELically-Linked (T-SHELL) breeder blanket system. The helical shape breeder blanket is cut by the plane of constant toroidal angle. By considering the mass of each module, division per 2-3 degree is assumed. With such a narrow range of the toroidal angle, the degree of torsion of the blanket is not so large and the shape of each module is similar to the bananas-like blanket modules of tokamak reactors. Because large areas between superconducting coils of FFHR can be used as a port structure, most of these toroidally-sliced modules can be extracted by a simple movement with radial and vertical directions. In the presentation, the detailed shape of each module is given and a baseline replacement method will be discussed.

Observations of gas stream from fusion test device for the design of exhaust detritiation system

M. Tanaka^{a,b}, N. Suzuki^a, H. Kato^a, T. Kondo^a and LHD Upgrade Team

a. National Institute for Fusion Science

*b. SOKENDAI (The Graduate University for Advanced Studies)
322-6 Oroshi-cho, Toki 509-5292, Japan*

e-mail address: tanaka.masahiro@nifs.ac.jp

The development of nuclear fusion system is remarkably progressed in recent years. Owing to advance of the plasma performance, the deuterium gas is used as the operation gas in a fusion test device. Under the deuterium plasma experiments by large fusion test device equipped with NBI heating systems, a small amount of tritium is produced by D-D reactions in the vacuum vessel. Then, a part of tritium is exhausted from the vacuum vessel and the rest is retained in the first wall and the diverter tiles. From the viewpoints of radiation protection and public acceptance, exhausted tritium from the vacuum vessel may be recovered by an exhaust detritiation system. The exhaust gas streams are classified into: (1) plasma discharge operation; (2) the regeneration of cryopumps and ice pellet injection systems; (3) rough pumping for main and NBI vacuum vessels; (4) a purge gas in the vacuum vessel during the maintenance. For example, the plasma discharge for a few seconds is operated intermittently with a cycle per several minutes. Thus, the average gas flow rate would be very low and the concentration of gaseous hydrogen isotopes in the exhaust gas may be higher. On the other hands, the cryopump systems would be regenerated with the purging of nitrogen gas over a period of hours once a week. Thus, the gas flow rate under the regeneration operation and the total gas volume would be much larger than that under the plasma discharge operation. In the case of rough pumping, the flow rate is large but transitory. To design of the exhaust detritiation system, therefore, the behavior of exhaust gas stream from large fusion test device under each operation has to be understood quantitatively. In this study, we observed the gas stream from the large fusion test device under the various operation conditions such as plasma discharges, the regeneration of cyopump system and the rough pumping of the vacuum vessels. Then, the conceptual design of exhaust detritiation system, which has enough capacity to treat the various gas streams, will be shown.

Development of Soft-X Ray Computed Tomography Diagnostic System for MHD Dynamics Study in RELAX RFP

Y. Aoki, A. Sanpei, H. Makizawa, M. Higuchi, T. Nagano, S. Nakanobo, R. Tsuboi,
H. Himura, S. Masamune

Kyoto Institute of Technology, Department of Electronics, Kyoto 606-8585, Japan

aoki13@nuclear.es.kit.ac.jp

The reversed-field pinch (RFP) is one of the magnetic confinement systems for high-beta fusion plasmas. One of the topics is a spontaneous transition of RFP configuration from axisymmetric to non-axisymmetric helical structure dubbed quasi-single helicity (QSH) state. In this QSH state, improved confinement was realized in the helical core, either inside a large magnetic island or helically deformed nested flux surfaces having helical axis, with increased electron temperature and/or higher density [1].

RELAX is an RFP machine with major radius $R = 0.5$ m and the minor radius $a = 0.25$ m. The aspect ratio $A = 2$ in RELAX, whose research objectives include geometrical optimization of the RFP configuration [2]. Generally speaking, the q value on axis increases as the aspect ratio is lowered, while the edge value does not change so much because the field reversal surface ($q = 0$) is close to the edge. Therefore, if we could avoid the resonance near the core, relatively large space is available in the core region without major resonance; the single island of a core resonant tearing mode can grow without interacting neighboring islands associated with the tearing modes. This picture has been demonstrated experimentally in RELAX in which transition to QSH occurs at lower current density and lower Lundquist number than in other machines such as RFX-mod and MST [3].

When the plasma is in equilibrium, the Soft-X ray (SXR) emissivity contours coincide with magnetic flux surfaces because both the electron temperature and density can be regarded as surface quantities. Therefore, the SXR computed tomography (CT) is a powerful tool to identify the thermal or magnetic structure inside high temperature plasmas. We are developing a new SXR CT system consisting of two 20-channel photodiode arrays. The cross-sectional view of the diagnostic system is shown in Fig.1 where two arrays are set at the top and bottom at a single toroidal location. Our interest includes time evolution of the SXR emissivity contours at transition to and back-transition from the QSH in RELAX; the process was studied by magnetic diagnostics and SXR camera, the latter providing SXR images with 10- μ s time resolution. We expect to obtain time evolution of the magnetic flux surfaces with 1- μ s time resolution (typical sampling time), which would be useful to study the dynamic processes of transition or self-organization associated with QSH.

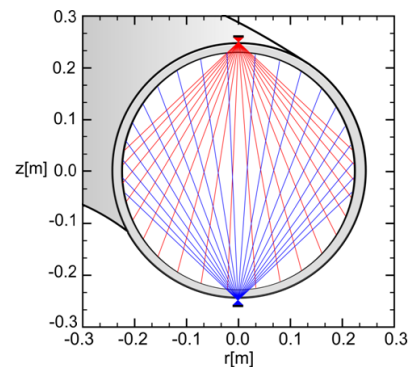


Fig.1 Poloidal cross-section of RELAX with lines of sight covered by two photodiodes.

[1] D. Escande, "What is a reversed field pinch?" 2013 <hal-00909102>.

[2] S. Masamune et al., J. Phys. Soc. Jpn. 76, 123501 (2007).

[3] K. Oki et al., PFR 7, 1402028 (2012); Fusion Sci. Technol. 63, 1T, 386 (2013).

Studies on the effect of radio frequency field in a cusp-type charge separation device for direct energy conversion

M. Hamabe, H. Izawa, H. Takeno, S. Nakamoto, K. Ichimura^a, Y. Nakashima^a

*Department of Electrical and Electronic Engineering, Kobe University,
1-1, Rokkodai-cho, Nada-ku, Kobe 657-8501, Japan*

^a *Plasma Research Center, University of Tsukuba, 1-1-1, Tennodai, Tsukuba 305-8577, Japan*

Direct energy conversion can be applied to D-³He fusion power generation in which high plant efficiency can be expected because the majority of the produced energy in D-³He reaction is kinetic energies of charged particles. This power generation method is also advantageous in the environmental aspects because harmful high energy neutrons are hardly generated. For direct energy conversion, charged particles escaping from the reactor should be separated from each other in energy and electrical polarity. For this purpose, application of a cusp-type direct energy converter (CuspDEC) is expected to be used [1].

Previous studies show that cusp magnetic field is effective for particle separation to low density plasma [2]. Although the effectiveness was also examined to high density plasma, separation performance was insufficient for high efficiency direct energy conversion and some methods to improve separation performance were required. As one of these methods, using a radio frequency (rf) electric field was proposed. The ponderomotive force is well known as a non-linear effect of high frequency electric field [3], and is expressed by $F_{NL} = -(\omega_p / \omega)^2 \nabla \langle \varepsilon_0 E^2 \rangle / 2$, where ω is the angular frequency of rf, $\langle E^2 \rangle$ is time-averaged square of the rf electric field, and other symbols are as in Ref. 3. This force influences electrons much stronger than ions. An rf field with an appropriate distribution may have a function to assist charged separation in a CuspDEC.

In this study, we experimentally examine the effect of rf field in a CuspDEC simulator following to the previous reports [4,5]. Two ring-type electrodes were newly installed in the simulator, and electrostatic rf field was formed near the electron collector and the collector current was measured. The collector current increased or decreased according to the enhancement of field. We could not find difference of the variation to the change in rf frequency although the strength of the ponderomotive force depends on rf frequency as shown in the equation above. On one hand, we found clear difference of the variation to the change in magnetic field strength. We also found some differences on the field curvature and on the relative phase difference between rf voltages of the two electrodes. The detail of the experimental results with discussions will be presented in the conference.

This work is partially supported in part by a Grant-in-Aid for Scientific Research (C) (25420255) from Japan Society for the Promotion of Science and by the bilateral coordinated research program (NIFS13KUGM082) between PRC, University of Tsukuba, NIFS, and Kobe University.

- [1] H. Momota, et al., Proc. 14th IAEA **3** (1993) 319.
- [2] Y. Yasaka, et al., Nucl. Fusion **49** (2009) 075009.
- [3] F. F. Chen, Introduction to Plasma Physics and Controlled Fusion, 2nd Ed. **1**, Plenum Press (1984) 305.
- [4] H. Takeno, et al., 23rd ITC (2013) P1-53.
- [5] H. Takeno, et al., PLASMA2014 (2014) 18PB-031.

Studies on the axial position of the decelerator in traveling wave direct energy converter

T. Katsura, T. Wakaizumi, H. Takeno, K. Ichimura^a, Y. Nakashima^a

*Department of Electrical and Electronic Engineering, Kobe University,
1-1, Rokkodai-cho, Nada-ku, Kobe 657-8501, Japan*

^a Plasma Research Center, University of Tsukuba, 1-1-1, Tennodai, Tsukuba 305-8577, Japan

In D-³He fusion, most of fusion energy is carried by kinetic energy of created protons, so direct energy conversion can be applied. Traveling wave direct energy converter (TWDEC) was proposed as an energy recovering system for these protons [1], which was composed of a modulator and a decelerator. Incident protons are velocity modulated by radio frequency (RF) field in the modulator and are density modulated in the downstream. Then, they are decelerated by traveling RF field and their kinetic energy is converted into electricity in the decelerator.

The axial position of the decelerator is one of the important device parameters for energy conversion efficiency and device size. The best position for conversion efficiency is considered to be the bunching position in which ion density is the highest. In the previous study, the authors conducted numerical calculations and simulation experiments by setting a decelerator at the bunching position [2]. The highest experimental record of the efficiency was obtained, however, the optimum axial position was not confirmed experimentally.

In this study, we investigate the dependence of deceleration efficiency on the axial position of the decelerator. By using numerical calculations and simulation experiments, we examine the efficiency by changing the distance between the modulator and the decelerator (L), and discuss the optimum position of the decelerator based on the results.

We examined the dependence by numerical calculations. Figure 1 shows deceleration efficiency versus L . The conditions are the same as those in the previous simulation experiment. As shown in the figure, the highest deceleration efficiency of 61.5 % is obtained for $L = 22$ cm, and this is much higher than 55 % for the bunching length of $L = 11.9$ cm. Therefore, the bunching position is not necessarily the optimum position of the decelerator. This may be because that the decelerator is designed based on the constant deceleration scheme [3]. The corresponding simulation experiments are in preparation. We will present the results and discussion in the conference.

This work is supported in part by the bilateral coordinated research program (NIFS13KUGM082) between PRC, University of Tsukuba, NIFS, and Kobe University..

[1] H. Momota, LA-11808-C, Los Alamos Natl. Lab. (1990) 8.

[2] Y. Togo, et al., 24th ITC (2014) P6-33.

[3] Y. Togo, et al., Plasma and Fusion Research **10** (2015) 345013.

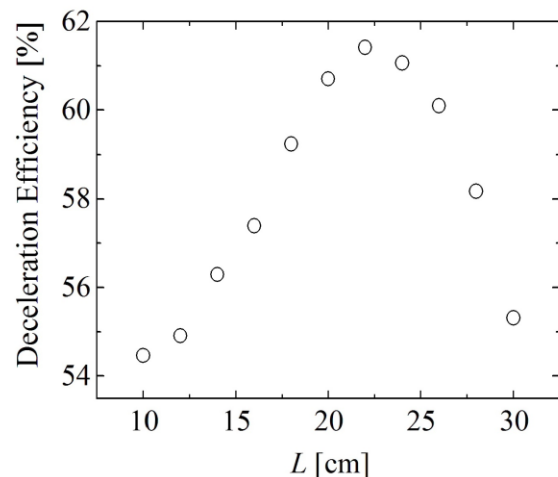


Fig. 1 Deceleration Efficiency versus distance between the modulator and the decelerator.

Improvement of charge separation by increase of magnets in a PM-CuspDEC simulator

T. Watanabe, Y. Kitahara, H. Takeno, S. Nakamoto, K. Ichimura^a, Y. Nakashima^a

*Department of Electrical and Electronic Engineering, Kobe University,
1-1, Rokkodai-cho, Nada-ku, Kobe 657-8501, Japan*

^a *Plasma Research Center, University of Tsukuba, 1-1-1, Tennodai, Tsukuba 305-8577, Japan*

Cusp-type direct energy converter (CuspDEC) was proposed as a charge separation device for D-³He fusion power generation [1]. It separates charged particles based on the difference of Larmor radii. The authors proposed an application of this function to divertor plasma to reduce thermal loads on a divertor plate [2]. For the application to divertor plasma, the device should be miniaturized as the divertor region is not so wide. The authors proposed use of permanent magnets (PMs) and composition of CuspDEC with them (PM-CuspDEC) [2].

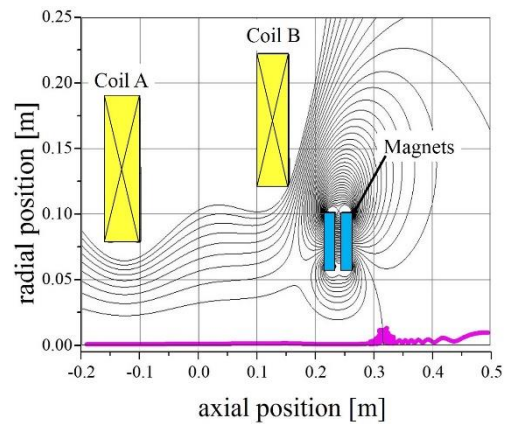
Some core units of PM-CuspDEC were examined experimentally, showing a good performance [3]. Based on the results, a PM-CuspDEC simulator, composed of two magnetic coils and two cylindrical hollow ferrite magnets, was constructed, which was assumed to be applicable to GAMMA 10. By using a test plasma source, the charge separation performance of the simulator was examined, however, it was not sufficient [4]. In this paper, an improvement of the performance of the simulator is treated by increasing the number of PMs.

Figure 1 shows results of numerically calculated electron orbits. Cross sections of two magnetic coils and PMs are shown in r - z plane. Thin curves are field lines, and electrons are expected to be deflected in the cusp field in the downstream of the PMs although ions go through the region. Orbits of electrons incident at $(r, z) = (0.1 \text{ cm}, -20 \text{ cm})$ are shown by thick (magenta) curves.

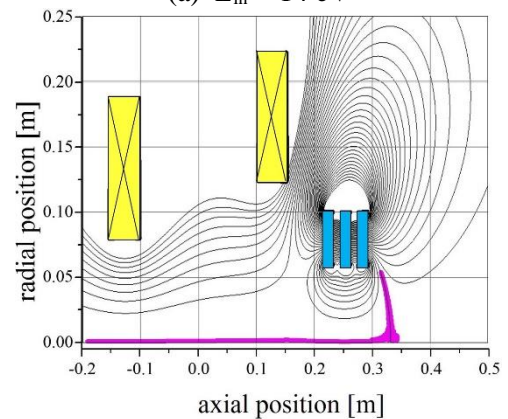
In Fig. 1(a) and (b), two and three PMs are installed corresponding to the conditions of the former simulator and an improved one, respectively. The incident energy of the electron (E_{in}) also differs: 14 eV and 20 eV for (a) and (b), respectively. Although the electron in (a) goes straight, that in (b) is deflected in spite of its higher energy. In other calculations, electrons with much higher E_{in} are also deflected when four PMs are installed, which is preferable for efficient separation. An increase of PMs would improve separation performance of the simulator. The corresponding experimental results and discussion will be presented in the conference.

This work is supported partially by the NIFS collaboration research program (NIFS13KUGM082), and by a Grant-in-Aid for Scientific Research (C) (25420255) from JSPS.

- [1] Y. Tomita, et al., NIFS Series (1993) NIFS-252.
 [2] H. Takeno, et al., Trans. Fusion Sci. Tech. **63** (2013) 131.
 [3] K. Nishimura, et al., 9th APFA (2013) TP-33.
 [4] Y. Tomita, et al., 24th ITC (2014) P6-32.



(a) $E_{in} = 14 \text{ eV}$



(b) $E_{in} = 20 \text{ eV}$

Fig. 1 Orbits of electron.

Development of high strength W/V/Au/ODS-Cu joint using HIP process

H.Noto^a, T.Yamada^b, Y.Hishinuma^a, T.Muroga^a

^a National Institute for Fusion Science, 322-6 Oroshi-cho, Toki 509-5292, Japan

^b Nagoya University, Graduate School of Engineering, 509-5292 Gifu, Japan

e-mail address of submitting author: noto.hiroyuki@nifs.ac.jp

The divertor with higher heat removal capabilities and heat resistance to severe heat and particle load are one of the key components to operate fusion reactors. In the designing of helical DEMO reactor FFHR-d1, the steady thermal load is assumed to exceed 20 MW/m². One of the candidate material combination for fabricating the divertor is tungsten (W) and copper (Cu) alloy because W and Cu have promising properties for the divertor application. W has high melting point, low hydrogen isotope retention, low sputtering yield, and so on. Cu alloy has higher thermal conductivity compared with the other metal materials. In fact, copper alloy (Cu-Cr-Zr) pipes are tried to join with W by conventional brazing on the ITER project. However, toughness of the copper alloy drastically decreased at a high temperature over 450 °C due to instability of strengthening precipitated particle. On the other hand, oxide dispersion-strengthened copper alloys (ODS-Cu) such as GlidCop[®] (Cu-0.3wt%Al₂O₃) has superior mechanical properties at high temperatures than Cu-Cr-Zr because the metal has thermally-stable oxide particle, and thus can be an advanced candidate for the divertor components.

Therefore, the establishment of the bonding process between W and ODS-Cu is an essential technology to succeed the divertor system using ODS-Cu. W and Cu are almost insoluble with each other and they have very different coefficient of thermal expansion (CTE). Thus, the insert materials between W and ODS-Cu is expected to be effective to the bonding.

In this study, vanadium (V) and gold (Au) are selected as interlayers to the joint between W and ODS-Cu. These layers have advantage for the W/ODS-Cu bonding such as high solubility, plasticity and thermal conductivity, and low activation. V and Au have extremely different melting points, these metal expected to use as a new bonding material based on diffusion reaction. The new bonding proceeded with two steps. The first step is the W/V bonding by solid-phase diffusion reaction. The second step is the W-V/Au/ODS-Cu bonding using the Hot Isostatic Press (HIP). The HIP process condition was 950 °C for 1 hr in argon atmosphere of 200 MPa. The melting point in the interface between Au and ODS-Cu is decreased by the eutectic reaction, and referred as the Transient Liquid Phase bonding.

The smooth interfaces without reaction layers and large defects were observed in the W/V and Au/ODS-Cu interface. However, the partial-coverage by reaction layer (approx.20μm) that differ from each inset metals (V,Au) were observed in the V/Au interface region. The homogeneous hardness profiles showed around the hardening area at V/Au interface. In addition, the overall bending strength of the W/V/Au/ODS-Cu joints using HIP process and the depressant method of hardening area at V/Au interface will be reported.

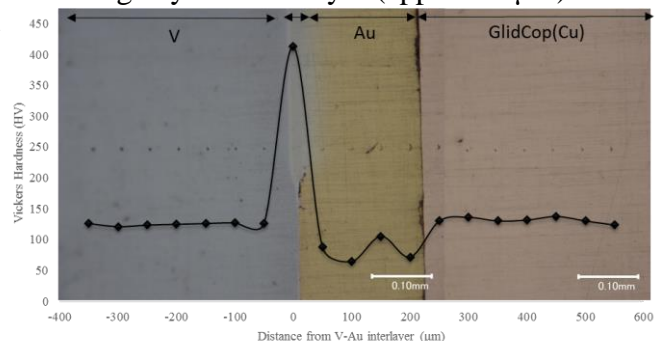


Figure 1. OM image of the cross section of V/Au/GlidCop joint, showing hardness profile.

Development of Oxide Dispersion Strengthened-Copper Using MA-HIP Method

T. Yamada ^a, H. Noto ^b, Y. Hishinuma ^b, H. Nakamura ^{a, b}, T. Muroga ^b

^a Graduate School of Engineering, Nagoya University, 509-5292, Japan

^b National Institute for Fusion Science, 322-6 Oroshi-cho, Toki 509-5292, Japan

yamada-tetsuya14@ees.nagoya-u.ac.jp

The divertors of fusion reactors are subject to a high thermal heat load. In the helical DEMO reactor FFHR, the steady thermal load is assumed to exceed 20 MW/m². Thus development of heat sink materials having a high heat removal capability is required. For this purpose, copper alloys have a large advantage in thermal conductivity. Although copper alloys are susceptible to neutron irradiation and thus were not considered as DEMO candidates, the reduced neutron fluence in the recent FFHR design has led to revisiting them as heat sink materials. In ITER, use of precipitation strengthened (PS)-Cu (CuCrZr) is being considered. However PS-Cu has issues such as instability of microstructure at high temperatures. On the other hand, dispersion strengthened (DS)-Cu is known to have higher stability in microstructure and strength at high temperature. The conventional DS-Cu has been produced by internal oxidation and extrusion, which, however, can cause inhomogeneity and coarsening of dispersed particles and formation of anisotropic microstructure.

In this study, we research into improvements of DS-Cu using Mechanical Alloying (MA) followed by Hot Isostatic Pressing (HIP) method. MA can disperse particles finely and homogeneously, and HIP can form dense microstructure. In this study, effects of additive elements (Al, Zr) and MA conditions (rotation speed and duration) are investigated. Cu-1wt.% Al (Cu-Al) and Cu-1wt.% Zr (Cu-Zr) are alloyed using planetary ball mill, with rotation rates of 50, 200 and 250 rpm for 1 to 40 hours. During MA, the state of the powder is observed with Optical Microscopy (OM), a Scanning Electron Microscopy (SEM) and X-Ray Diffractometer (XRD). HIP is carried out at 950C for 1 hour in an argon atmosphere of 150MPa. Vickers hardness tests are also carried out.

Examination of particles after MA shows that the original particles start to combine with each other around 200-250 rpm for 1 hour, which is considered to be the starting point of alloying. An examination with XRD shows the peak of Al, which is present before the MA treatment, disappear after the MA treatment. HIPed materials following MA show reduced grain size and increased hardness relative to those of the unalloyed copper HIPed in the same condition. Large precipitates or inclusions are not observed either in matrix or on grain boundaries.

The present study has demonstrated that MA-HIP of Cu with Al or Zr addition can produce homogeneous structure with refined grains.

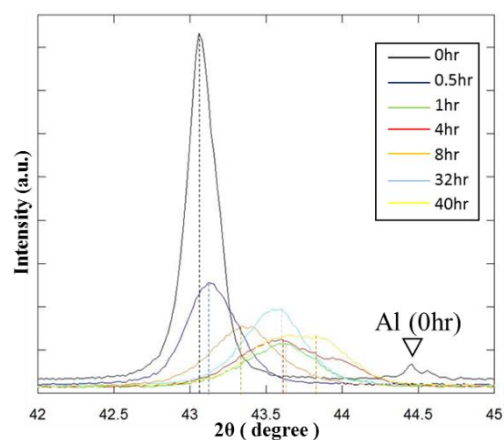


Figure : The shift of Cu(111) peak during MA process

Real-Time Display System of the Equilibrium Reconstruction for Long Time Discharge in QUEST

M. M. Alam, K. Nakamura^a, M. Hasegawa^a, F. Xia^b, O. Mitarai^c, K. Tokunaga^a,
K. Araki^a, H. Zushi^a, K. Hanada^a, A. Fujisawa^a, H. Idei^a, Y. Nagashima^a,
S. Kawasaki^a, H. Nakashima^a, A. Higashijima^a, T. Nagata^a

IGSES, Kyushu University, 6-1 Kasuga-koen, Kasuga, Fukuoka, 816-8580 Japan

^aRIAM, Kyushu University, 6-1 Kasuga-koen, Kasuga, Fukuoka, 816-8580 Japan

^bCFS, SWIP, P.O. Box 432, 610041 Chengdu, P. R. China

^cTokai University, Kumamoto, 862-8652 Japan

Cost effective, efficient, precise and faster real-time display system design and development has become an important issue of QUEST (Q-shu University Experiments with Steady-State Spherical Tokamak) for advanced operations. For the construction of real time display system, data acquisition is one of the most important issues. Most of the cost is required for the construction of the real-time data acquisition system. But due to having the promise of cost effectiveness for the construction of real-time display system, data acquisition has been carried out from reflective memory. In QUEST, it is reported that a distributed feedback control system has been developed with a reflective memory [1]. So for the design and develop of the real-time display system of the equilibrium reconstruction for long time discharge in QUEST, the reflective memory of the distributed control system will be used.

For the equilibrium reconstruction, CCS (Cauchy-Condition Surface) method will be used. The CCS method has suitable precision for equilibrium reconstruction in conventional tokamak. But for spherical tokamak good precision can be obtained by CCS method if we solve the inverse problem of flux loop measurement by using least square method [2]. On the other hand to remove noise we can introduce singular value decomposition on CCS method so that the CCS method can reproduce plasma boundary shape more precisely and faster for the real-time system by using the data from magnetic sensors [3]. The plasma equilibrium reconstruction parameters such as position, minor radius, elongation and triangularity will be calculated by using this CCS method and will be carried out in real-time operating system (LabVIEW). The RTOS (Real-time Operating System) will ensure precise timing and high reliability. Finally, the real-time data profiles and plasma shape will be displayed in real-time I/O and third party PC.

[1] Makoto Hasegawa et al., Fusion Eng. and Des. 95 (2015).

[2] K. Nakamura et al., J. Plasma Fusion Res. SERIES, 9 (2008).

[3] K. Nakamura et al., IEEE Trans. on Plasma Sci. 42 (9) (2014).

W7-X ECRH plant - Control System Design Features

H. Braune¹, V. Erckmann¹, H. Laqua¹, S. Marsen¹, F. Noke¹, F. Purps¹, N. Schneider¹, T. Schulz¹, T. Stange¹, P. Uhren¹ and the W7-X ECRH teams at IPP, IGVP Stuttgart and KIT Karlsruhe

¹*Max-Planck-Institut für Plasmaphysik, Garching and Greifswald, Germany*

Electron Cyclotron Resonance Heating (ECRH) is the main heating system for steady-state operation and will be the only available heating system during the first operation phases of the stellarator W7-X [1]. The ECRH is going to be used for different tasks at the W7-X such as wall conditioning, controlled plasma start-up from the neutral gas up to steady state plasma control [2] and performance optimization by plasma profile shaping. The ECRH plant is equipped with 10 gyrotrons with a frequency of 140 GHz and a microwave output power of 1 MW each [1]. The microwave beams are guided quasi optical via copper coated mirrors toward the W7-X vessel. The prospective W7-X operation requires an ECRH system as a whole, only controlled by some high level parameters such as heating power, launch direction, polarisation and timing. The main challenges and developed solutions will be discussed.

Challenges and Requirements

Up to 10 gyrotrons have to be controlled simultaneously as well as 10 different wave guides and two additional remote steering launchers apart from the 10 ordinary front steering launchers. Each gyrotron is equipped with a superconducting magnet, high voltage power supplies, collector sweep systems, different cooling circuits filled with water as well as with oil. Response times between 1 μ s and 100 ms are necessary in order to control the different auxiliaries reliable. The control system has to provide the interface between the ECRH-plant and the W7-X main control system as well as the W7-X data acquisition system.

The support of error diagnostics for each ECRH component part is a further mandatory control system function.

Solutions

The human-machine interface is based on the Siemens WinCC software and has been redesigned in order to meet the W7-X requirements. Each part of the ECRH installation such as magnet, high voltage power supplies, water cooling system etc. is controlled separately by Siemens S7 PLC [3] and the controller software has been completed with several functions that relieve the ECRH operators from many periodical tasks.

The ECRH remote control system has been connected to the central W7-X control system in a reliable and easily maintainable way.

An ECRH fast interlock system monitors all devices within timescales less than 5 μ s, which are able to achieve a dangerous state in particular arcs and gyrotron failures.

- [1] V. Erckmann et al. "ECRH and W7-X – an intriguing pair" Radio Frequency Power in Plasmas, Proc. 20 Topical Conference, Sorrento, Italy, AIP Conference Proceedings 1580 (2013) page 542
- [2] M. Preynas et al. "Characterization of plasma start-up using ECRH in preparation of Wendelstein 7-X operation" Conference Proceedings 18th Joint Workshop on ECE and ECRH, 22-25.04.2014, Nara, Japan
- [3] H. Braune et al. "Architecture of central control system for the 10 MW ECRH-plant at W7-X" Fusion Engineering and Design 82 (2007) 677–685

Experimental Study on W-Band Oversized Surface Wave Oscillator Driven by Weakly Relativistic Electron Beam

Min Thu San, K. Ogura, K. Yambe, Y. Annaka, S. Gong, J. Kawamura, T. Miura,
S. Kubo^a, T. Shimosuma^a, S. Kobayashi^a, K. Okada^a

Graduate School of Science and Technology, Niigata University, Niigata 950-2181, Japan

^a *National Institute for Fusion Science, 322-6 Oroshi-cho, Toki 509-5292, Japan*

High power microwave sources utilizing high current relativistic electron beam such as backward wave oscillator consist of slow-wave structure (SWS). The SWS reduces the phase velocity of electromagnetic waves below the vacuum speed of light so that the electrons in the relativistic beam can interact with the wave. To increase the operation frequency, SWS is oversized with the diameter larger than the free-space wavelength of output electromagnetic wave by several times or more. And microwave generators with oversized SWS have attracted much attention as a compact terahertz wave source [1], [2]. In oversized SWS cases, the slow wave becomes a surface wave concentrated on the SWS wall. And the interaction may result in backward wave or travelling wave operation depending on the group velocity of the surface wave. At high electron energy, the group velocity of this wave is positive and the device operates in the manner of a travelling wave tube (TWT), at low electron energy, the group velocity is negative and operates like a backward wave oscillator (BWO). And at an intermediate energy, called the Bragg condition or π point, the group velocity of the evanescent wave vanishes. The overall operation from BWO to TWT has been studied theoretically and it has been shown that there is no operation near the π point [3]. Up to now, the theoretical prediction has not been validated against experimental results.

In this work, we studied a W-band oversized surface wave oscillator driven by weakly relativistic electron beams of less than 100kV. The overall operations from BWO to TWT including π point operation were studied experimentally. Rectangular corrugations are used as the SWS having surface waves with upper cutoff frequency about 100GHz. Parameters of SWS: average radius R_0 , corrugation amplitude h , corrugation width d and periodic length z_0 , determine dispersion characteristics of the structure. To get the upper cutoff frequency about 100GHz, the structure parameters of $R_0 = 15.1\text{mm}$, $h = 0.3\text{mm}$, $d = 0.3\text{mm}$ and $z_0 = 0.5\text{mm}$ are used. Uniformly distributed annular electron beams generated by a disk-type cold cathode are injected into the oscillator. In the study, the operations of the oscillator were investigated experimentally by injecting the electron beams into various structure lengths of 40, 80 and 120 periods. Driven electron beam energies are of 10~80keV. The operations of the oscillator depend on the energy level and the structure length. The experiments showed that the operations of the oscillator are mainly concerned with the structure length.

- [1] V. L. Bratman, B. S. Dumesh, A. E. Fedotov, P. B. Makhaliy, B. Z. Movshevich, and F. S. Rusin, *IEEE Trans. Plasma Sci.* **38** (2010) 1466.
- [2] S. Gong, K. Ogura, S. Nomizu, K. Yamazaki, K. Yambe, S. Kubo, T. Shimosuma, S. Kobayashi, and K. Okada et al., accepted for publication in *IEEE Trans. Plasma Sci.*
- [3] H. L. Andrews, C. H. Boulware, C. A. Brau, and J. D. Jarvis, *Phys. Rev. ST Accel. Beams* **8**, (2005) 050703.

Experimental Study on Slow Cyclotron Interaction under Anomalous Doppler Effect in W-Band Backward Wave Oscillator

Y. Annaka, K. Ogura, J. Kawamura, T. Miura, T. Kawamura, S. Takanashi,
S. Gong, Min Thu San, and K. Yambe

Graduate School of Science and Technology, Niigata University, Niigata 950-2181, Japan

Backward Wave Oscillator (BWO) has been studied as one of high power microwave sources. BWO has a slow-wave structure (SWS) to reduce the phase velocity of microwave to the beam velocity and is driven by axially streaming electron beams. The electron beams are propagating along the direction of an axial magnetic field and have four beam modes: slow and fast space charge modes and slow and fast cyclotron modes [1]. The microwave radiation may occur near the intersection point between the slow beam modes and slow-wave modes in SWS. In this paper, we refer the intersection of slow space charge mode to “Cherenkov interaction” and that of slow cyclotron mode to “slow cyclotron interaction”. The latter occurs at the anomalous Doppler shifted cyclotron frequency [2]-[4]. The resonance condition between the slow wave and the beam is given by $\omega = kv + S\Omega$ ($S = 0, -1, -2, \dots$). Here, ω and k are respectively the angular frequency and the wave number of slow wave, v is the velocity of electron along the magnetic field, Ω is cyclotron angular frequency, and S is harmonic number. At $S = 0$, Cherenkov interaction takes place. At $S = -1, -2, \dots$ slow cyclotron interaction occurs due to the anomalous Doppler effect. It has been pointed out by numerical analyses that the slow cyclotron interaction provides high efficiency operations and the potential for large frequency up-shift with moderate magnetic field and beam energy.

In this work, we examine experimentally microwave generations by the slow cyclotron interaction in a W-band BWO. We use rectangularly corrugated waveguide as SWS with corrugation amplitude $h = 0.15$ mm, period length $z_0 = 0.5$ mm and corrugation width $d = 0.3$ mm. The upper cutoff frequency of surface wave is about 100 GHz. We prepare two SWSs. They have different periods of 40 and 80. We also compose 120 periods SWS of 40 and 80 periods SWSs. BWOs with various length SWS are driven by non-relativistic beams less than 30 keV. To help electrons go through SWS, the magnetic field of 0.8 T is provided by 10 solenoid coils. In this magnetic field, electron cyclotron frequency is 22.9 GHz. Frequency of electromagnetic field can be predicted from the resonance condition and dispersion characteristics of SWS. The microwave from BWOs is detected by two detect systems, F-band and D-band. The cutoff frequency of F-band is about 74 GHz. D-band is about 91GHz. We investigate the slow cyclotron interaction in BWOs based on the frequency of detected microwave by comparing numerically obtained dispersion characteristics and resonance conditions.

- [1] K. Ogura, K. Yambe, K. Yamamoto, and Y. Kobari, *IEEE Trans. Plasma Sci.* **41** (2013) pp.2729-2734.
- [2] T. H. Kho and A. T. Lin, *Phys. Rev. A*, **38** (1988) pp.2883-2888.
- [3] K. Ogura, M. R. Amin, K. Minami, X. D. Zheng, Y. Suzuki, and W. S. Kim, *Phys. Rev. E*, **53** (1996) pp.2726-2729.
- [4] G. S. Nusinovich, M. Korol, and E. Jerby, *Phys. Rev. E*, **59** (1999) pp.2311-2321.

Depth of Influence on the Plasma by Beam Extraction in a Negative Hydrogen Ion Source for NBI

Shaofei Geng, Katsuyoshi Tsumori^a, Haruhisa Nakano^a, Masashi Kisaki^a, Katsunori Ikeda^a, Masaki Osakabe^a, Ken-ichi Nagaoka^a, Yasuhiko Takeiri^a, Osamu Kaneko^a, Masayuki Shibuya^a

SOKENDAI (The Graduate University for Advanced Studies), 322-6 Oroshi, Toki, Gifu 509-5292, Japan

^{a)} National Institutes for Fusion Science, 322-6 Oroshi, Toki, Gifu 509-5292 Japan

Experimental results obtained with single-Langmuir probe and laser photodetachment measurements in beam extraction region of a cesium-seeded negative ion source for NBI are described. It is unclear how negative ions are extracted from plasmas at the extraction region, and we investigated the response of charged particles to applied external field. The profiles of probe saturation currents and H^- ion density in the direction normal to the plasma grid (PG) surface are measured by scanning the tip positions. By comparing the results before and during beam extraction, the charged particle responses due to the beam extraction are analyzed. During beam extraction, probe saturation current increases since H^- ions are extracted and electrons flow into the extracting region for compensation. The maximum increment of the probe saturation current due to electron flow appears at 14-24 mm apart from the PG surface. Meanwhile, the maximum decrement of the local H^- ion density is in the same region. In the region far from the plasma grid, probe saturation current increment is low as well as the decrement of the local H^- ion density. The extrapolation of the profile suggests that the depth of the influence on the plasma by beam extraction is around 40 mm from the plasma grid surface.

Power and polarization monitor developed for ECRH and ECCD on LHD

R. Makino^a, S. Kubo^{a,b}, K. Kobayashi^b, T. Ii Tsujimura^a, S. Kobayashi^a, T. Shimosuma^a,
Y. Yoshimura^a, H. Igami^a, H. Takahashi^{a,c}, T. Mutoh^{a,c}

^a National Institute for Fusion Science, 322-6 Oroshi-cho, Toki 509-5292, Japan

^b Nagoya University, Nagoya 464-8603, Japan

^c SOKENDAI (The Graduate University for Advanced Studies), 322 Oroshi-cho, Toki 509-5292, Japan

Polarization states of injected EC waves significantly affect the mode excitation purity, therefore, power absorption and current drive in plasmas. A power and polarization monitor has been developed for electron cyclotron resonance heating (ECRH) and electron cyclotron current drive (ECCD) on the Large Helical Device (LHD).

The power and polarization monitor is installed at the miter-bend in the 77GHz ECRH transmission line system. The monitor is composed of a miter-bend mirror with coupling holes, orthomode transducer, heterodyne systems and ADC with FPGA (Field Programmable Gate Array). A part of EC wave is picked-up from main corrugated waveguide to square sub-waveguide through the coupling holes in a miter-bend. The EC waves are separated to two orthogonal polarization by orthomode transducer. Two orthogonal waves are down-converted to a few hundred MHz by heterodyne systems. The IF signals are detected by ADC with FPGA (Field Programmable Gate Array). Amplitudes and phase difference of the electric field of the two orthogonal polarizations are obtained by applying fast Fourier transforming to the IF signal data. Polarization angle α and polarization ellipticity β can be calculated from amplitudes and phase difference of the electric field of the two orthogonal polarizations.

To investigate the performance of the power and polarization monitor, polarization scan experiments were performed on LHD. Amplitudes and phase difference of two orthogonal electric field, which are needed for calculation of the polarization angle α and polarization ellipticity β , were successfully detected. We will present the configuration of the monitor and results of performance tests.

withdrawal

Absorption Behavior of Nitrogen in Nitrogen Hot Trap

E. Wakai, H. Tanaka, Y. Ito, H. Sakasegawa^a, T. Higashi^b, A. Suzuki^b, T. Tera^b, J. Yagi^c, K. Nakaniwa, H. Kondo, F. Groeschel^d, H. Tanigawa^a, M. Sugimoto^a, S. Ohira^a

Japan Atomic Energy Agency, Tokai-mura, Ibaraki 319-1195, Japan

^a *Japan Atomic Energy Agency, Rokkasho, Aomori 039-3212, Japan*

^b *The University of Tokyo, Tokyo 113-8654, Japan*

^c *National Institute for Fusion Science, Toki, Gifu 509-5292, Japan*

^d *Karlsruhe Institute of Technology, Karlsruhe, Germany*

e-mail address: wakai.eiichi@jaea.go.jp

The main function of the International Fusion Materials Irradiation Facility (IFMIF) is to generate the intense fusion neutrons by injecting the deuteron beams accelerated to high energy onto the liquid lithium flow. Guiding the lithium flow along the concave back plate at a speed of 15 m/s is required to increase the pressure in the lithium flow by centrifugal force, to avoid boiling by the heat input about 1 GW of the deuteron beams, and to remove heat by the lithium flow circulation under lithium purification control by N hot trap, H hot trap, and cold trap. In this study, the absorption behaviour of nitrogen using N hot trap and the trap system are mainly evaluated in IFMIF/EVEDA project, and the fabricated nitrogen hot trap system is also presented.

The validation test of the N hot trap using Fe-5Ti getter under nitrogen gas atmosphere was performed at 500°C or 450°C. Almost 70% of the introduced nitrogen gas into the N hot trap container was seemed to be absorbed by the Fe-5Ti pebble during this test for 115 h. That is, about 18 g of nitrogen in the N hot trap container have been absorbed by the Fe-5Ti pebble of 95 kg and by another area in the N hot trap container. The surfaces of the pebbles, which were as-received Fe-5Ti pebble and its tested one, were observed by a scanning electron microscopy, and the distribution of nitrogen and the elements were analysed by EPMA. In the chemical analysis of nitrogen content in the specimen, the 65 wppm of nitrogen was quantified for the Fe-5Ti pebble tested under 500°C for 115 hours. That is, about 6.2 g of nitrogen was absorbed by the Fe-5Ti pebble of 95 kg. Accordingly, the rest 11.8 g of nitrogen would be absorbed by another area, for example, by the inner wall of N hot trap container. Moreover, it was succeeded to maintain the temperature of the hot trap at 500°C or 450°C in a total time about 800 hours. The other results will be also presented.

The getter materials for nitrogen hot trap system in the lithium facility of IFMIF are proposed to use the getter materials of Fe-Ti alloy or pure Ti, and the nitrogen hot trap system for Li purification of the lithium facility was also evaluated in this study.

Materials Test Plan and Design Summary in PIE Facility of IFMIF

E. Wakai, T. Kikuchi^a, T. Yutani, M. Soldaini^b, M. Shingala^c

Japan Atomic Energy Agency, Tokai-mura, Ibaraki 319-1195, Japan

^a *Japan Atomic Energy Agency, Rokkasho, Aomori 039-3212, Japan*

^b *CEA, Paris, France*

^c *IFMIF/EVEDA Project Team, Rokkasho, Aomori 039-3212, Japan*

e-mail address: wakai.eiichi@jaea.go.jp

Under the frame of the Broader Approach Agreement between Europe and Japan, the intermediate engineering design of the International Fusion Materials Irradiation Facility (IFMIF) plant has accomplished in the middle of 2013 in the IFMIF/EVEDA (Engineering Validation and Engineering Design Activity). The IFMIF plant has five specific facilities such as Accelerator Facility (AF), the Lithium Target Facility (LF), the Test Facility (TF), the Post Irradiation Examination Facility (PIEF), and the Conventional Facilities (CF). The main function of the IFMIF plant is to give the demanded design database for the licensing, and the operation and maintenance of the Fusion DEMO reactor, and it is achieved from the materials data set obtained from the high, medium, and low flux test modules (HFTM, MFTM, and LFTM) of the IFMIF.

For materials to be tested in IFMIF, databases on irradiation properties should already pre-exist. The candidate (structural) materials to be tested in IFMIF should undergo a rigorous pre-selection procedure, including evidence on radiation resistance to be proven in other irradiation campaigns including fission reactor, multi-ion beam facilities and spallation sources. Expected contributions will include: (a) Engineering design for fusion DEMO reactor, (b) Definition of performance limits, (c) Completion and validation of (existing) databases, (d) Selection or optimization of materials, (e) Validation of fundamental understanding of radiation response of materials, and (e) Tests of blankets and functional materials prior to or complementary to Test Blanket Modules (TBMs) of the Internal Thermonuclear Experimental Reactor (ITER).

The contents of KIT (A. Moeslang) report for test matrix of IFMIF, a comprehensive design report (CDR) for IFMIF and a report of the Specification Working Group of the IFMIF/EVEDA team are very important, however, the details of information for the schedule and test plan, and methodology of PIE in IFMIF in order to produce database for the design of fusion DEMO reactor is not necessarily enough in them. Further requirement and guidelines from users will be needed to prepare and construct them. The main function of IFMIF facility is, off course, to produce the database for the design of fusion DEMO reactors, while this facility may be also useful for materials and biological researches of neutron scattering with continuous neutron beams with high intensities. In this study, the materials tests and the engineering design for the post irradiation examination (PIE) facility of the IFMIF was evaluated.

Installation and commissioning of components for IFMIF/EVEDA Prototype Accelerator

R. Ichimiya, J. M. Ayala^{A)}, Ph. Cara^{C)}, R. Heidinger^{C)}, A. Jokinen^{C)}, A. Kasugai, J. Knaster^{A)},
H. Kobayashi^{B)}, K. Kondo, S. Ohira, Y. Okumura^{A)}, G. Phillips^{C)}, K. Sakamoto and
M. Sugimoto

Japan Atomic Energy Agency (JAEA), Rokkasho Fusion Research Institute, Rokkasho, Aomori, Japan

^a *IFMIF/EVEDA Project Team, Rokkasho, Aomori, Japan*

^b *High Energy Accelerator Research Organization (KEK), Tokai, Ibaraki, Japan*

^c *F4E, Fusion for Energy, BFD Department, Garching, Germany*

International Fusion Materials Irradiation Facility (IFMIF) is a projected accelerator-driven-type neutron source for qualifying fusion reactor materials, characterized by its beam current frontier accelerator producing two sets of 125 mA/CW deuterium ion beams up to 40 MeV. Under the framework of the Broader Approach (BA) agreement between Japan and Europe, Engineering Validation and Engineering Design Activities (EVEDA) for IFMIF were launched in 2007 to validate the key technologies on which the IFMIF design is based. In order to realize such a high current CW accelerator, Linear IFMIF Prototype Accelerator (LIPAc) has been developed and is constructed in Rokkasho, Japan. LIPAc components are to a major part developed and contributed by European Institutes (CEA, CIEMAT, INFN, SCK-CEN) and consist of an injector, a RFQ accelerator, a superconducting RF linac (SRF), a Low, a Medium and High Energy Beam transport and a beam dump. Its target is to produce 125 mA/CW deuterium ion beam up to 9 MeV adequate to validate the 40 MeV deuteron beam of IFMIF. The accelerator building of LIPAc, central control system and other facilities are developed and contributed by JAEA. Commissioning and operation are taken by JAEA with tight collaboration with European Institutes, Fusion For Energy (F4E) and Project Team (PT). In order to achieve the target performance, various technologies including limit design have been implemented and also thus special care is required when installation and commissioning them. Therefore, we are developing installation/commissioning procedures and improving them towards the optimum. In this paper, we will introduce the design scheme of LIPAc and discuss the installation and commissioning scheme/plan.

Evaluation of dark current profile for prediction of voltage holding capability on multi-aperture multi-grid accelerator for ITER

R. Nishikiori, A. Kojima, M. Hanada, M. Kashiwagi, K. Watanabe, N. Umeda, H. Tobari, M. Yoshida, M. Ichikawa, J. Hiratsuka, Y. Yamano^a and NB Heating Technology Group.

Japan Atomic Energy Agency, 801-1, Mukoyama, Naka 311-0193, Japan
^aSaitama University, 255, Shimo-Okubo, Sakura-ku, Saitama 338-8570, Japan

Stable high energy beam acceleration is required in neutral beam injectors for JT-60SA and ITER where 22- 40 A D⁺ ions are accelerated up to 0.5-1MeV by a large electrostatic accelerator with multi-aperture multi-grid (MAMuG). One of critical issues for such high-energy high-current beam acceleration is the high voltage holding which is dominated by vacuum discharges. In order to improve and design the voltage holding capability of MAMuG accelerators based on the physics understanding, the physics of vacuum discharge is being investigated. The past results suggest that vacuum discharge occurs beyond the threshold of the dark current due to the field emitted electrons from cathode to anode [1]. Therefore, analytical estimation of the dark current plays an important role to evaluate the voltage holding capability.

The dark current can be derived from F-N theory [2] where electric field enhancement factor β is included. Though, β could only be evaluated from the experiment previously. Therefore, the method to decide β without experiment was considered.

β can be evaluated from the F-N plots with measured dark current. This time dark currents were measured at three different areas in the MAMuG accelerator to compare β in different electric field. Fig.1 shows schematic view of each measured areas and the electrical field distribution between the electrodes. As a result the effective electric field βE_{ave} , where E_{ave} is average electric field, were found to be almost constant for different areas although the β is largely different as shown in fig. 2. By applying $\beta E_{ave} \sim 10^3$ kV/mm β can be evaluated analytically, leading to the analytical prediction of the dark current without the measurements. This prediction will enable the estimation of voltage holding capability by evaluating the threshold of the dark current.

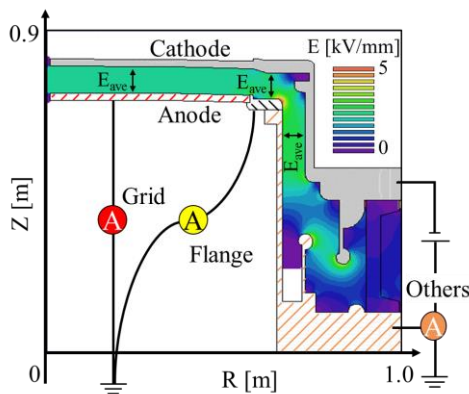


fig. 2 Schematic view of measured areas and the electrical field distribution between the electrodes.

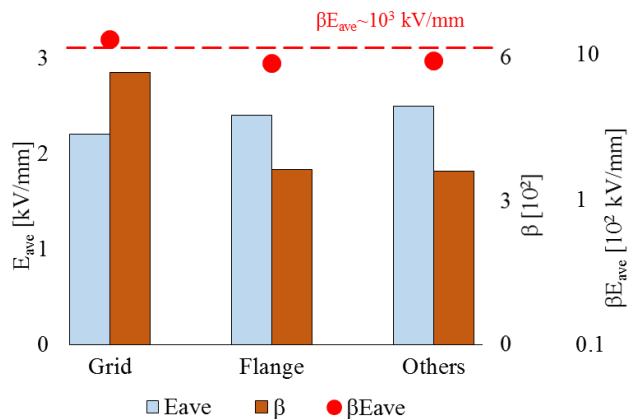


fig. 1 Comparison of measured β and effective electric field at each area.

- [1] A. Kojima, M. Hanada, A. Hilmi et al., Rev. Sci. Instrum. 83, 02B117 (2012).
 [2] R.H. Fowler, L.W. Nordheim, Proc. Roy. Soc. London A, 119 (1928) p. 3.

Variation in secondary electron collection and energy recovery concerning electrode angle in a high energy ion penetration scheme

T. Wada, S. Konno, S. Nakamoto, H. Takeno, Y. Furuyama^a, A. Taniike^a

*Department of Electrical and Electronic Engineering, Kobe University,
1-1, Rokkodai-cho, Nada-ku, Kobe 657-8501, Japan*

*^a Graduate School of Maritime Sciences, Kobe University,
5-1-1, Fukae-minamimachi, Higashinada-ku, Kobe 658-0022, Japan*

D-³He nuclear fusion has been expected as an energy source for next generation because most of the energy obtained in this reaction is kinetic energy of charged particles and direct energy conversion can be applied. An energy recovery device from produced protons by using traveling wave (TWDEC) was proposed [1], but some protons were not decelerated and efficiency of the device was limited. In order to recover those protons passing through the TWDEC, an additional device was proposed to be settled in the downstream, which was called secondary electron (SE) direct energy converter (SEDEC) [2]. In SEDEC, a lot of metal foil electrodes are aligned in the direction of the proton beam. The incident protons penetrate the electrodes where SEs are emitted. Collectors settled on both sides of the foil electrodes catch the SEs and those energy is recovered by appropriately biased voltage.

A series of experiments were performed. In an SEDEC with a simple structure, SEs arrived at not the collectors, but the anteroposterior electrodes [2]. A magnetic field perpendicular to the proton beam by permanent magnets (PMs) was introduced, but magnetic mirror effect in front of PMs disturbed SEs arrival at the collectors [3]. Finally, PMs were aligned on one side and an appropriate distance to the collector plate was taken as shown in Fig. 1. In this structure, the amount of the recovered energy exceeded that without PMs [4].

Although the final structure succeeded in the improvement of SE collection, optimization of the structure has not been studied yet. The structure has many parameters. Concerning foil electrodes, parameters such as thickness, interval between electrodes, angle to the incident beam, etc. can be considered. In this paper, we investigate variation in SE collection on the aspect of angle to the incident beam as a first step for optimization of the structure.

The angle of the electrode to the incident beam affects SE collection in many points of view. It changes equivalent thickness of the foil. The amount of SE emission may change according to the incident angle to the foil. The distribution of initial velocity of SEs may also change. The SE motion is disturbed by the electrode and may change because the angle to the magnetic field is changed. The experiments of SE collection by changing the angle of the foil electrodes are in progress, and detail results and discussion will be presented in the conference.

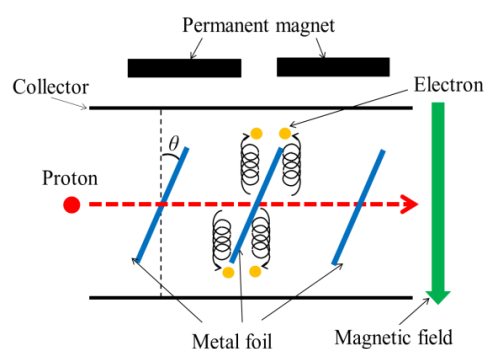


Fig. 1 Structure of SEDEC with PMs aligned on one side.

- [1] H. Momota, LA-11808-C, Los Alamos Natl. Lab. (1990) 8.
- [2] D. Akashi, et al., Trans. Fusion Sci. Tech. **63**(1T) (2013) 301.
- [3] Y. Takeshita, et al., 9th APFA (2013) TP-36.
- [4] S. Hagihara, et al., Plasma and Fusion Res. **10** (2015) 3405025.

Numerical Study on New Steering Grid of Negative Ion Source for NBI

K. Tsumori, M. Kisaki, O. Kaneko, Y. Takeiri, M. Osakabe, K. Ikeda, O. Kaneko,
K. Nagaoka and NIFS NBI group

National Institute for Fusion Science, 322-6 Oroshi-cho, Toki 509-5292, Japan
e-mail: tsumori@nifs.ac.jp

New steering grid (SG) for a beam accelerator equipping multi-slot grounded grid (MSGG) has been investigated using beam-trajectory simulation. A long circular shape with 13 mm (width) and 10 mm (height) is adopted for the SG to correct the asymmetric focal characteristics of MSGG [1, 2]. Extracted hydrogen/deuterium-negative-ion (H^-/D^-) beam scratches inner wall of the narrower opening of the SG in the high current density of H beam. Scratched beam produces secondary electrons, which damage the grounded grid.

The new SG has $\phi 13$ mm circular apertures with so-called kerbs surrounding each horizontal row of the apertures. The kerb has a similar shape of the slot of MSGG, and the beamlet trajectories are controlled by sifting the vertical and horizontal centerlines of the kerb. In the previous SG without the kerbs, coulomb repulsion between beamlets was corrected only by displacing the aperture center of the SG to inner direction. On the other hand, the beamlet interactions are compensated with shifting the edge of kerbs in the new SG. This makes the design for arrangement of the aperture much easier.

The SG is made of ferromagnetic material, nickel-plated iron, to short the magnetic circuit induced with electron deflection magnets imbedded in extraction grid (EG), and is installed at the exit side of the EG. By reduce the return magnetic field, the field strength on the opposite side, plasma-grid side, of the EG increases and more electron suppression is expected in the case of D^- extraction. Influences of the ferromagnetic SG to the other magnetic field and that to the beamlet trajectories are indicated with simulation result.

- [1] K. Tsumori, O. Kaneko, Y. Takeiri et al., *Proceedings of the 10-th International Symposium on Production and Neutralization of Negative Ions and Beams, AIP Conference Proceedings* **763** (2005) pp.35-46.
- [2] K. Tsumori, Y. Takeiri, O. Kaneko et al., *Rev. Sci. Instrum.*, **79** (2008) pp. 02C107-1 - 02C107-3

Fabrication and property investigation of metal hydride blocks for neutron shielding in a fusion reactor

T. Tanaka, H. Muta^a, M. Yoshino^b, Y. Hishinuma, T. Muroga, A. Sagara

National Institute for Fusion Science, 322-6 Oroshi-cho, Toki, Gifu 509-5292, Japan

^a*Graduate School of Engineering, Osaka University, 2-1 Yamadaoka, Suita, Osaka 565-0871, Japan*

^b*Graduate School of Engineering, Nagoya University, Furo-cho, Chikusa-ku, Nagoya 464-8603, Japan*

Hydride materials such as ZrH₂ and TiH₂ have been adopted as superior neutron shielding materials in neutronics designs of fusion reactors. However, for investigation of a detailed shield design, material studies on fabrication and properties of the hydride blocks, and hydrogen desorption behaviors in accident conditions are required.

In neutronics benchmark experiments using a DT neutron source, the minimum size of blocks used to construct an irradiation assembly is ~50 x 50 x 50 mm³ [1]. Therefore, test fabrication of blocks from commercially available TiH₂ powder has been performed with the dimensions of ~25 x 25 x 5 mm³ and ~25 x 25 x 12.5 mm³ in the present study. Cold-pressed blocks were prepared by using a die at 80-100 MPa and following densification were performed by cold isostatic pressing (CIP) at 200 MPa to apply pressure to the blocks from all directions. The densities of the TiH₂ blocks after the CIP process were ~75 % of the theoretical density of 3.75 g/cm³. These densities are almost same as those of small thin TiH₂ discs (10 mmφ x ~2 mm thick) fabricated by cold-pressing using a die at 200 MPa [2]. If a CIP apparatus with 400 MPa is used, the densities of the TiH₂ blocks is expected to be ~85 % of the theoretical density from relation between pressures and densities obtained in our previous fabrication of small cold-pressed TiH₂ discs [2]. Test fabrication of ZrH₂ blocks and study on a densification method are being conducted at present.

Regarding behaviors of the hydride materials in accident conditions, oxidation of the TiH₂ and ZrH₂ powders in an air flow is examined by thermogravimetry and differential thermal analysis (TG/DTA) up to 1000 °C. Composition in the flowing air was analyzed simultaneously by quadrupole mass spectrometer (QMS) to examine desorption of hydrogen under the oxidizing condition. The TG data showed that oxidation started from ~300 °C in both the powders and significant increase in weight were observed at 600-900 °C in the TiH₂ powder and at 400-900 °C in the ZrH₂ powder. In the QMS data, hydrogen desorption from the TiH₂ powder was detected in the range of 400-600 °C and this is considered almost independent from the oxidation process. In the ZrH₂ powder, hydrogen desorption was detected in the range of 350-800 °C and might be affected by the oxidation process. After the heating up to 1000 °C in air, the flat surface of the ZrH₂ powder packed in a specimen cup became significantly rough. Deformation of the hydride blocks under oxidation conditions is required to be examined especially for ZrH₂ for discussion of a shield design.

[1] T. Tanaka et al., *Fusion Science and Technology* **60** (2011) 681-686.

[2] H. Muta et al., *Plasma and Fusion Research* **10** (2015) 3405021.

The present study is being conducted under supports of KAKENHI 25289344 and NIFS UFFF0251.

Improvement of weight density and thermal conductivity of hydride neutron shielding material using metal coated powder

H. Muta, T. Tanaka^a, R. Nishikane, Y. Ohishi, K. Kurosaki, Y. Hishinuma^a,
S. Yamanaka, T. Muroga^a

Osaka University, 2-1 Yamadaoka, Suita, Osaka 565-0871, Japan

^a National Institute for Fusion Science, 322-6 Oroshi-cho, Toki 509-5292, Japan

muta@see.eng.osaka-u.ac.jp

To reduce a fusion reactor size, a thinner radiation shield layer with high density neutron shielding materials must be installed. Metal hydrides are promising as the shielding materials because they can include higher density of hydrogen atoms than liquid hydrogen [1]. However, it is known that the bulk non-crack metal hydride is difficult to fabricate due to the brittleness and the large volume change in the hydrogenation. Previously, to simplify the fabrication process, we tried to make dense hydride pellets by cold-pressing from their powders [2]. More than 80 % of theoretical density and acceptable thermal conductivity could be obtained by the simple process. In the present study, to improve the density and the thermal conductivity, metal coating on the hydride powders were examined.

Commercial ϵ -titanium hydride (TiH_2) (Aldrich, 99 % purity) was used as a starting material. The powders were coated by copper (Cu) by using electroless Cu plating process at room temperature. The plating solution was C-200LT (Japan Pure Chemical Co., LTD). After plating, the powder was washed by ethanol. Then the powder was pelletized by cold-pressing with pressure of 400 MPa. The density was calculated from the weight and dimensions. The thermal diffusivity, α , was measured by laser flash method using Netzsch LFA457 to calculate the thermal conductivity, κ , from the equation of $\kappa = \alpha C_p d$. C_p and d are heat capacity and sample density, respectively.

Figure 1 shows SEM image of the Cu-coated TiH_2 pellet. Small particles of Cu are distributed in gap of the large TiH_2 particles. Due to the Cu coating, the relative density of the pellets increases from 83 % [2] to > 90 %. The Cu particles appears to act as lubricant, which might promote the particle displacement at the cold-pressing. The thermal conductivity is shown in figure 2. In spite of the increase of sample density, the thermal conductivity is almost same as that for the pure TiH_2 pellet because of decrease of the thermal diffusivity.

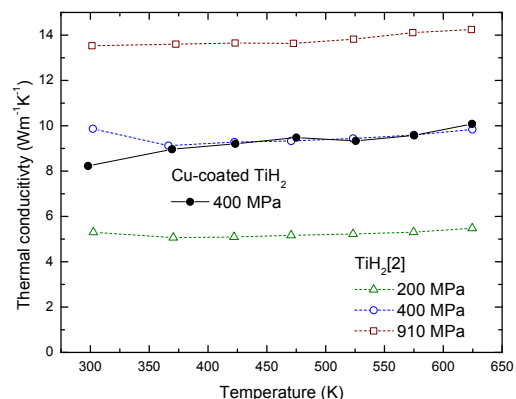
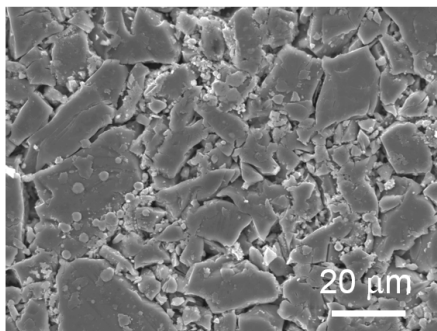


Fig. 1 SEM image of Cu-coated TiH_2 pellet. Fig. 2 Thermal conductivity of the TiH_2 pellets.

[1] T. Tanaka et al., to be published in Fusion Science and Technology.

[2] H. Muta et al., Plasma and Fusion Research **10** (2015) 3405021.

The present study is being conducted under supports of KAKENHI 25289344, 26420871 and NIFS14KEMF060.

Environmental Effects on V-4Cr-4Ti Alloy during IrradiationH. Watanabe¹, T. Nagasaka², T. Muroga²,² *Research Institute for Applied Mechanics, Kyushu University, Kasuga, Fukuoka, Japan*¹ *National Institute for Fusion Science, 509-5292 Gifu, Japan*

In the V-4Cr-4Ti alloy, it is well established that interstitial impurities such as oxygen and nitrogen play an important role in radiation effects such as microstructure change, irradiation hardening and embrittlement. Among them, oxygen is regarded as the most effective atom in the alloy. Furthermore, the alloy is considered to be used as a fusion blanket structural material that face to a vacuum and helium gas, which may contain a low partial pressure of oxygen. Recently, our ion irradiation experiments on V-4Cr-4Ti alloys at 473-973K revealed that oxygen pick-up from irradiation environment (namely, vacuum) is very minor up to the levels of 1 dpa. But at higher dose levels, the effects might cause degradation of mechanical properties due to enhanced formation of titanium oxide precipitates during irradiation. To understand the radiation induced phenomena related with oxygen, such as oxide formation in the matrix, not only oxygen level in the alloy but also oxygen pick-up from radiation environment must be considered. To reduce the oxygen concentration in the V-4Cr-4Ti alloy, oxygen gettering using Zr foil and Y addition on V-4Cr-4Ti alloy were a well-known technique. The objective of the present study is, therefore, to understand the detailed mechanisms of oxygen pick-up from irradiation environment which related with titanium oxide.

For neutron and ion irradiation, NIFS HEAT 2 and welded joint samples by YAG laser, Y doped V-4Cr-4Ti alloys were used in this study. The samples were irradiated with 2.4MeV copper ion irradiation with a tandem accelerator at Kyushu University. The TEM specimens were sliced from welded materials and irradiated at 573 and 873K up to the dose of 12 dpa. After irradiation, the specimen was electro-polished by a back thinning method, and the area near the peak damage region (at about 700 nm) was observed. These samples were also irradiated in JMTR and BR2 in the temperature range of 563-873K. After the irradiation, conventional TEM (CTEM) observation and detailed chemical analysis by Cs corrected microscopy were performed by using a JEOL ARM200FC located in a radiation controlled area in Kyushu University.

ACT2: a high heat flux test facility using electron beam for fusion application

Y. Hamaji, M. Tokitani, R. Sakamoto, H. Tamura, A. Sagara

National Institute for Fusion Science, 322-6 Oroshi-cho, Toki 509-5292, Japan

ACT2 (Active Cooling Teststand 2), a high heat flux test facility has been upgraded from ACT facility and started operation. A newly installed electron gun and data acquisition systems of ACT2 enables powerful and flexible experiments for R&D activities of plasma facing components (PFCs) for DEMO and beyond such as FFHR-d1[1]. The beam profile and heating performance were characterized by measurements using a pyrometer, thermocouples, fast visible camera and graphite probes.

Thermo-mechanical properties, heat removal performance and reliability of plasma facing components (PFCs) are crucial for long-term operation in future fusion reactors such as FFHR-d1. High heat flux testing with reactor relevant heat flux with actively cooled PFCs is essential for R&D of PFCs and fundamental researches of material response to high heat flux. A high flexibility of electron beam control is also required to test components in various scale and shape. The original ACT facility was established in 1994[2]. Nominal power and flexibility of beam control system of ACT was not sufficient for recent requirement for heat flux test facility. ACT was upgraded into the ACT2 to satisfy these demands. Technical characteristics of ACT2 are listed in Table 1. Focused electron beam scans defined area using high frequency deflection lenses. 300 kW beam power and 60 degree of deflection angle of ACT2's electron gun allow to apply reactor relevant heat flux ($\sim 30 \text{ MW/m}^2$) into defined area up to $100 \times 100 \text{ mm}^2$. Both steady state and transient ($\sim \text{ms}$) heat load are capable. Cyclic heat loads for thermal fatigue test are achieved by automatic routinely beam transfer between defined areas with each dwell time. In order to remove the effect of inhomogeneous heating at the edge of scanned area, a water-cooled "beam limiter" made of copper with specific aperture is located above the sample surface. The edge of scanned area is scraped by the limiter. Absorbed heat flux is calculated from electron current through the sample and irradiated area defined by limiter's aperture. To characterize electron beam of ACT2 facility, beam profile and local heat flux is measured by 2 mm diameter graphite probes that are embedded in a target tile at a high time resolution. Beam profile was obtained as Gaussian-like peaked profile with the spot size about 23 mm. Peak value of local heat flux during each pass of scanned beam was also obtained.

[1] A. Sagara, T. Goto, et al., *Fusion Eng. Des.* 87 (2012) 594–602.

[2] Y. Kubota, N. Noda, A. Sagara, O. Motojima, *Vacuum* 47 (1996) 955–957.

Table 1. Technical Characteristics of ACT2

<i>Parameter</i>	<i>Value</i>	<i>unit</i>
<i>Max. beam power</i>	300	kW
<i>Accelerating voltage</i>	40	kV DC
<i>Max. beam current</i>	7.5	A
<i>Beam deflection frequency in x direction</i>	500	Hz
<i>Beam deflection frequency in y direction</i>	5000	Hz
<i>Max. heated Area</i>	500×500	mm
<i>Beam spot diameter</i>	~ 20	mm
<i>Typical flow rate of the cooling water</i>	42	l/min.

Conceptual design of a new liquid metal divertor REVOLVER-D

J. Miyazawa^{a,b}, T. Goto^{a,b}, T. Ohgo^b, N. Yanagi^{a,b}, T. Murase^a, H. Tamura^a, A. Sagara^{a,b},
and the FFHR Design Group

^a National Institute for Fusion Science, 322-6 Oroshi, Toki 509-5292, Japan

^b SOKENDAI (The Graduate University for Advanced Studies), 322-6 Oroshi, Toki 509-5292, Japan

A divertor system with easy maintenance and low radioactive wastes is desired for a fusion reactor. It is also important that the divertor can handle a high heat load exceeding 20 MW/m^2 . A liquid metal divertor is one of the promising candidates. Especially, a continuous flow of the liquid metal of the order of $\sim 1 \text{ m/s}$ will be effective to remove the high heat load in steady state. According to these demands, a new liquid metal divertor system named the REVOLVER-D (Reactor-oriented Effectively VOLumetric VERTICAL Divertor) is proposed.

The REVOLVER-D is composed of the vertical free-surface stream (VFSS) as shown in Fig. 1, where two VFSS of the molten solder (60 % tin + 40 % lead) with and without a ball-chain inside are shown. The landing points of the two VFSS were different although these were ejected from the same nozzle at the same flow rate with an identically slanted angle, showing a reduced velocity in the case with the ball-chain. Instead of the solder, pure tin (Sn) is considered to be the first candidate for the REVOLVER-D because of its low melting temperature, low vapor pressure, low material cost, high safety (low toxicity and no explosive reaction with water), and high nuclear stability.

The top-view of the REVOLVER-D showing its nozzle layout is shown in Fig. 2. In this example, 52 nozzle units drawn by large circles are used. Each of the nozzle unit has 10 nozzles drawn by small circles, to generate 520 VFSS in total. Ball chains or something equivalent to them will be installed on each nozzle, to slow down the VFSS against the gravity. As seen in the figure, the magnetic field lines slanted through cannot penetrate the REVOLVER-D. Many magnetic field lines hit the VFSS *inside* the REVOLVER-D and the heat load is absorbed there. This is why we call this the “effectively volumetric divertor”. On the other hand, the neutral particles generated inside the REVOLVER-D can easily move to the vacuum pump side, since the conductance in this direction is larger than those of the other directions.

In the case of a helical fusion reactor FFHR-d1, it is calculated that 10 REVOLVER-D set at the inner side of the torus to intersect with the ergodic layer can correct more than 80 % of the magnetic field lines directed toward the divertor region. Applying the REVOLVER-D, it becomes possible to design a helical fusion reactor without complicated full-helical tungsten divertors. Easy maintenance and reduced radioactive wastes together with the high-safety of the REVOLVER-D are attractive for the fusion reactor.

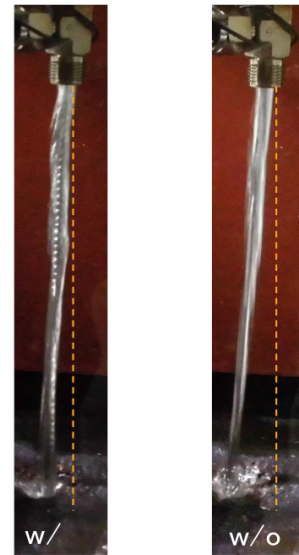


Fig. 1. Photos of VFSS w/ and w/o a ball-chain inside. The height of the VFSS is $\sim 170 \text{ mm}$.

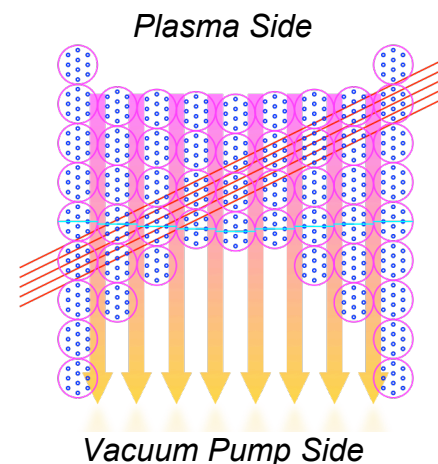


Fig. 2. An example of the REVOLVER-D nozzle layout.

Experimental simulations for detached plasma with Super-X divertor using a liner divertor simulator TPD-Sheet IV

Y. Tanaka^a, T. Iijima^a, T. Hase^a, A. Tonegawa^a, K. N. Sato^b and K. Kawamura^a

^aTokai University, 4-1-1 Kitakaname, Hiratsuka, Kanagawa, 259-1292, Japan

^bChubu Electric Power Co. Inc., 20-1 Kitasekiyama, Ohdaka-cho, 459-8522, Japan

E-mail: tanachu09@gmail.com

In the magnetic confinement fusion reactor for high power and long pulse operation, enormous heat flux (exceeding 10 MW/m^2) is expected to flow onto divertor plates from core plasma. In order to reduce this heat load, the divertor geometry on stationary detached plasma formation must be realized. In addition, the neutral particle flowback into the core plasma is necessary to suppress by the divertor geometry. The Super-X divertor has been proposed by DEMO divertor concept, investigated using simulations. Its optimization needs detail information on confined neutral particles and their physical process. An experimental simulation on the V-shaped, long-leg and baffled long-leg target for closed divertor has been conducted by a liner divertor plasma simulator TPD-Sheet IV [1]. Experimental simulations of divertor geometries for the formation of detached hydrogen sheet plasma using the linear divertor plasma simulator TPD-Sheet IV. In order to understand the basic mechanism of detached plasma, we have carried out an experiment using two target geometries (V-shaped target, super-X target). In this experiment, the ionization and recombination rate are discussed by using the collisional-radiative (CR) model. The electron density and temperature were measured using a Langmuir probe. Ionization and recombination ratio (P_{Ion} , P_{Rec}) are discussed from experimental data of T_e and n_e , using the collisional-radiative (CR) model. The results expect that a Super-X divertor with a Super-X target effectively enhances plasma detachment.

[1] S. Tanaka, et al., Fusion Sci. Tech. 63 (2013) 420

Effects of gamma-ray irradiation on electronic and non-electronic equipment of the Large Helical Device

K. Ogawa^{a,b}, T. Nishitani^a, M. Isobe^{a,b}, M. Sato^a, M. Yokota^a, H. Hayashi^a
T. Kobuchi^a, T. Nishimura^a, S. Imai^c

^a National Institute for Fusion Science, 322-6 Oroshi-cho, Toki 509-5292, Japan

^b SOKENDAI (The Graduate University for of Applied Advanced Studies), School of Physical Sciences, 322-6 Oroshi-cho, Toki 509-5292, Japan

^c Nagoya University, Furo-cho, Chikusa-ku, Nagoya 464-8603, Japan

kogawa@nifs.ac.jp

Deuterium operation will be started from 2017 on the Large Helical Device (LHD). In deuterium campaign, measurement and control equipment of the LHD must be survive under radiation environment. The LHD is controlled by means of many semiconductor integrated circuits. The circuit is regularly replaced latest highly-integrated one. The circuit becomes weaker against radiation year by year because of higher integration. Water sealing gaskets made of polytetrafluoroethylene are used on the LHD to serve the cooling water. Radiation resistance polytetrafluoroethylene should be studied to avoid the leakage of water. Neutrons are mainly generated by deuterium reactions, on the other hands, gamma-rays are generated by materials activated by neutrons. Equipment of the LHD is irradiated with gamma-rays, regardless of the presence or absence of plasma discharges. Both transient effect and permanent effect can be caused by irradiation on equipment. Permanent effect is more serious because the damage cannot be removed forever. So, understanding of permanent effect of gamma-ray irradiation on equipment being used for the LHD is very important for the deuterium operation.

Gamma-ray irradiation on the programmable logic controllers (PLCs), PC, flow meters composed of a light-emitting diode and a photodiode, isolation amplifiers, media converters, and water sealing gaskets are done at the ⁶⁰Co irradiation facility of Nagoya University. The integrated dose is from 100 to 500 Gy. We found that analogue to digital and digital to analogue converter module of PLC does not work after 100 Gy irradiation, and Ethernet connection of the PC is failed after 300 Gy irradiation. Flow meters, isolation amplifiers and media converters work after 100 Gy irradiation. In this presentation, detailed results of gamma-ray irradiation on electronic equipment and water sealing gaskets will be reported.

Desorption of non-metal impurities from Pb and Pb-Li alloy

M. Kondo¹⁾, Y. Nakajima²⁾, T. Tanaka³⁾, T. Nozawa⁴⁾, T. Yokomine⁵⁾

1) Research laboratory for nuclear reactors, Tokyo Institute of Technology, 2-12-1, O-okayama, Meguro-ku, Tokyo 152-8550 Japan

2) Department of Nuclear Engineering, Tokai university 4-1-1 Kitakaname, Hiratsuka-shi, Kanagawa 259-1292, Japan

3) National Institute for Fusion Science, Toki, Gifu 502-5292, Japan

4) Japan Atomic Energy Agency, 2-166 Omotedate, Obuchi, Rokkasho, Aomori 039-3212

5) Kyoto University, Kyotodaigaku-Katsura, Kyoto, Japan

Liquid lithium lead alloy (Pb-Li) is one of the promising candidates of the tritium breeders for fusion DEMO reactors. The study on the fabrication methodology of the alloy having high purity has been studied [1]. However, the control of some non-metal impurities such as hydrogen, oxygen, nitrogen, water and carbon dioxide dissolved in the alloy is an important issue. The low oxygen concentration in the alloy should be kept to suppress the depletion of Li by its selective oxidation. The hydrogen in the alloy should be removed to keep the solubility of tritium. Though the effect of the nitrogen on the chemical characteristics of the alloy is not made clear, nitrogen also should be removed from the alloy to suppress the loss of Li due to the selective nitriding of Li in the alloy. The information on these non-metal impurities such as hydrogen and oxygen in the alloy is quite limited. The control of the non-metal impurity in the Pb-Li alloy is not made clear so far. The purpose is to investigate the potentiality of the high temperature desorption method for the removal of the non-metal impurities from the Pb-Li alloy.

The temperature-programmed desorption (TPD) experiments were performed at the test conditions summarized in Table 1. Figure 1 shows the test section connected to the Temperature Programmed Desorption and Mass Spectrometer (TPD-MS). The test cylinder was connected through some stainless steel tubes, the cold trap and valves into the TPD-MS. The valve (A) was used for the evacuation of the TPD-MS system. The valve (B) was opened and the temperature of the test cylinder was raised at a temperature rising rate of 2.5K/min, starting at 308.5 K and finishing at 774.5 K.

Large desorption of CO₂, O, C and H₂O from Pb samples (types A and B) even below the melting point. The result for Pb-Bi test indicated that the desorption behavior of the non-metal impurities was close to that from the Pb samples. The standard Gibbs free energies for the formation of oxides indicated that PbO is more stable than H₂O and CO₂ in these cases. The molecules were attached on the surface and dissolved in the alloy.

Hydrogen and oxygen were desorbed from the Pb-Li alloy around 700K. The desorption of H₂O and CO₂ from Pb-Li alloy was much smaller than that from Pb and Pb-Bi samples. This is because Li in the alloy react with H₂O and CO₂, and LiH, LiOH and Li₂O are formed and dissolved in the alloy. Some part of hydrogen and oxygen must be dissolved in the fabrication procedure of the alloy due to the chemical reaction between Li and H₂O in Pb [1]. It was indicated that hydrogen and oxygen can be removed from the Pb-Li alloy by TPD method.

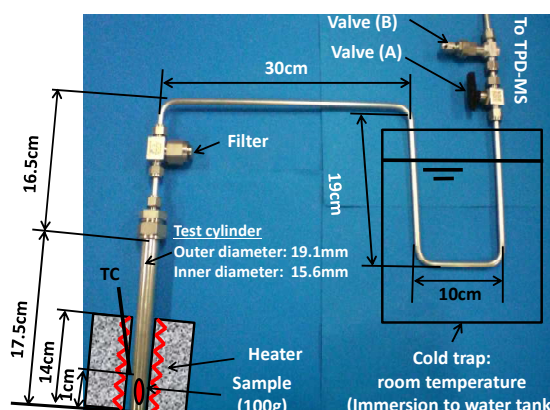


Fig. 1 Test section of TPD system

Table 1 Test conditions

Test material	Purity	Sample quantity [g]
Pb (type A) [1]	99.999%	100
Pb (type B) [1]	99.9%	100
Pb-Bi	-	100
Pb-17Li	Li (99%) + Pb (99.9%)	100
Pb-17Li	Li (99%) + Pb (99.9%, Baking)	1
Pb-15Li [1]	Li (99%) + Pb (99.999%)	100
Pb-28Li [1]	Li (99%) + Pb (99.999%)	100
TiH ₂	Calibration of hydrogen desorption	0.011

Reference [1] Y. Nakajima, M. Kondo, T. Nozawa, Study on fabrication method of lithium alloys with metal grain, Fus. Eng. Design in press (2015).

Conceptual design of temporarily storage area in hot cell for fusion DEMO reactor

M. Kondo^a, Y. Someya^b, M. Tsuji^c, S. Yanagihara^d, T. Kato, Y. Sakamoto^b, K. Tobita^b, S. Matsuda^a

^a Tokyo Institute of Technology, 2-12-1, 2-12-1 O-okayama, Meguro-ku, Tokyo 152-8550, Japan

^b Japan Atomic Energy Agency, Rokkasho-mura, Kamikita-gun, Aomori 039-3212, Japan

^c Tokai University, 4-1-1, Kitakaname, Hiratuka, Kanagawa, 502-5292, Japan

^d Research Institute of Nuclear Engineering, University of Fukui, Fukui 914-0055, Japan

The maintenance scenario and the waste management of fusion DEMO reactor having a fusion output of 1.35GW have been proposed. In the maintenance procedure of the reactor, used in-vessel components were removed from the reactor vessel for their replacement. Then, the low-level radioactive wastes (LLW) of approximately 6000 t are generated. The reuse and the recycle of the blanket components can reduce the quantity of the LLW by 60% in total. However, these components are radioactivated and having a large decay heat. Their dismantlement is available by the remote handling (RH) only after their temporarily storage for a certain period in the hot cell till their radiation level decreases to allowable level for the RH. Therefore, the temporarily storage of the blanket components in the hot cell is the important procedure for the waste management of the fusion reactors. However, the information for the temporarily storage of the used blanket components in the hot cell is quite limited. The used blankets are removed as multi module segments from the vacuum vessel (VV) through the vertical port. The segments are the back plate integrated blanket modules. These segments must be stored temporarily in the hot cell after the removal of residual tritium by thermal detritiation process. During the temporarily storage of the segments, their decay heat must be removed. The segments must be kept at the adequate temperature to suppress the effect of the heat treatment on their reuse and recycle. In the present study, it is proposed that the used blanket segments are stored dispersively in the plural compartments of the temporarily storage area in the hot cell. The motivation for this system is to achieve the reduction of the risk, the simplification of the hot cell structure and the mitigation of the cooling conditions of the decay heat in the same time without the increase of total floor space required for the storage. The changes of the dose rate and the temperature distribution in the compartment with time were investigated by means of gamma ray transport calculation and thermofluid calculation. The purpose of the present study is to propose the effective scenario and design of the temporarily storage area in the hot cell.

The used segments are stored dispersively in the plural compartments in the hot cell for the following dismantle step. The total floor space required for the temporarily storage of the segments are estimated less than 1500 m². The compartment, which is made of a heavy concrete, has high shielding performance and cooling performance. Fig. 1 shows the schematic drawing of the compartment. The temporarily storage of the segments with the pentagonal arrangement in the compartments, which can make the gentle distribution of the dose rate without the formation of the hot spot in the compartment, is proposed in the present study. The change of the dose rate in the compartment with time was evaluated by means of the gamma ray transport calculation performed by PHITS Monte Carlo analysis code. It was found that the dismantle process by the remote handling can be available after the temporarily storage for 10 years. The decay heat during the temporarily storage of the segments can be removed by the flowing He. The segments can be kept at the temperature lower than 550 °C, which does not affect the mechanical properties of the back plate as the heat treatment for their reuse in the other operation of the reactor.

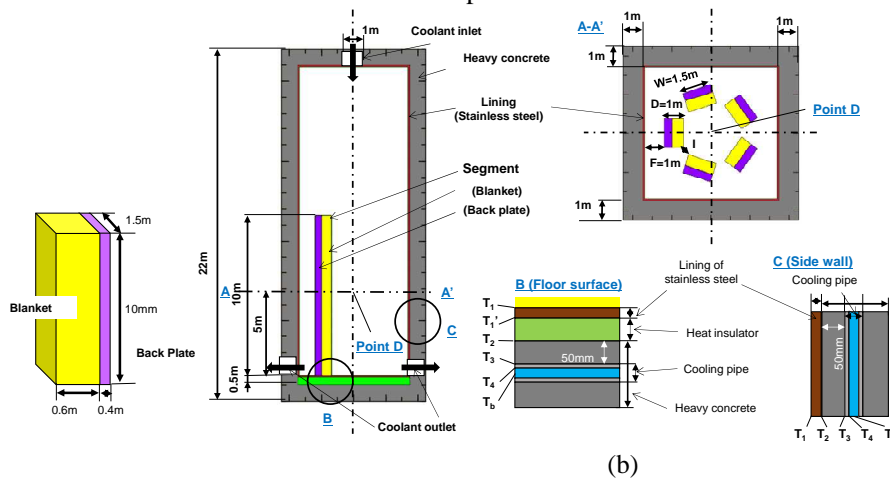


Fig. 1 Structure of (a) Simplified model of the segment having a rectangular parallelepiped shape and (b) Compartment for temporarily storage of plural segments in hot cell

Effect of HIP temperature and cooling rate on the microstructure and hardness of dissimilar-metal joints between ODS-RAFM steels and JLF-1 steel

Haiying Fu, Takuya Nagasaka ^a, Takeo Muroga ^a, Akihiko Kimura ^b, Shigeharu Ukai ^c

SOKENDAI (The Graduate University for Advanced Studies), 322-6 Oroshi-cho, Toki 509-5292, Japan

^a National Institute for Fusion Science, 322-6 Oroshi-cho, Toki 509-5292, Japan

^b Institute of Advanced Energy, Kyoto University, Uji 611-0011, Japan

^c Graduate School of Engineering, Hokkaido University, N13, W18, Kita-ku, Sapporo 060-8628, Japan

Because of excellent high-temperature mechanical properties, ODS-RAFM (oxide-dispersion-strengthened reduced activation ferritic/martensitic) steels can be used partly for the surface of fusion blanket by bonding with conventional RAFM steels to enhance the acceptable temperature of the blanket surface by 100-150°C. In this work, candidate ODS-RAFM steels, such as 9Cr-ODS and 12Cr-ODS, were diffusion bonded to a conventional RAFM steel JLF-1 by hot isostatic pressing (HIP) for the purpose of the connection between ODS-RAFM steel and conventional RAFM steel components. A previous investigation revealed that JLF-1 base metal (BM) was hardened by quenching with martensite transformation after the HIP at 1000°C in a commercial furnace with 5°C/min in cooling rate, however the 9Cr-ODS BM was softened due to no quenching and carbides coarsening. Since nano-oxide particles impede the martensite transformation, rapid cooling after HIP is required for 9Cr-ODS to keep their strengthening by martensite. However, the cooling rate is generally decreased due to the increase in heat capacity for the large mass of blanket itself and also the large mass of HIP furnace for it. On the other hand, higher content of Cr in 12Cr-ODS can strengthen the steel instead of martensite and stabilize its ferrite phase, and thus can avoid the degradation of strength in the HIP process. However, microstructural change with carbide coarsening is also an issue for strengthening of 12Cr-ODS. In the present study, therefore, the effects of HIP temperature and the subsequent cooling rate on the microstructure and hardness were investigated to obtain the optimum HIP bonding conditions and proper strength at the whole part of the joints.

HIP bonding was examined at 1000°C, 1050°C, and 1100°C under a pressure of 191MPa for 3h with a cooling rate of 5°C/min. In addition to the conditions for a commercial HIP furnace, various isochronal annealing was carried out at 800-1100°C with controlled cooling rate of from 0.5 to 36°C/min by a laboratory-scale furnace.

Quench with hardening was observed for 9Cr-ODS after the annealing at 1000°C with 36°C/min in cooling rate, however was not induced with 0.5°C and 5°C/min. While, the annealing at 1050°C induced quench hardening with 5°C/min in cooling rate in addition to 36°C/min. Based on these results, HIP temperature can be low as 1000°C under rapid cooling condition, 36°C/min in cooling rate, to get quenched martensite and avoid softening of 9Cr-ODS BM. On the other hand, the cooling rate 0.5°C/min never induced quench hardening even up to 1100°C. The quench is enhanced not only by rapid cooling after the HIP, but also by carbide decomposition and carbon dissolution at the HIP temperature. Therefore the critical cooling rate for quench, which should be between 5°C/min and 36°C/min for the 1000°C HIP, is increased with decreasing the HIP temperature.

The proper HIP conditions for 12Cr-ODS will also be investigated, and will be compared with that for 9Cr-ODS.

Investigation on the Magnetic Field Distortion by Ferromagnetism of the Blanket for the Helical Fusion Reactor

Xiang Ji^{a, b}, Nagato Yanagi^a, Takuya Goto^a, Hitoshi Tamura^a, Junichi Miyazawa^a,
Akio Sagara^a, Songke Wang^b, Minzhong Qi^b, Yuntao Song^b

^a *National Institute for Fusion Science, 322-6 Oroshi-cho, Toki 509-5292, Japan*

^b *Institute of Plasma Physics, Chinese Academy of Sciences, P.O.BOX 1126, Hefei 230031, China,*

In the future fusion reactors, ferritic steel is a realistic candidate to be used as a structural material of the blanket, because of the low activation characteristics after neutron irradiation which can reduce the issue of radioactive waste disposal. However, since the ferritic steel is a ferromagnetic material, distortion of magnetic field produced by the magnet coils is a concern on the plasma confinement due to island formation and partial changes of magnetic surfaces.

The conceptual design studies on the LHD-type helical fusion reactor (FFHR) are progressing at National Institute for Fusion Science (NIFS) by employing the heliotron magnetic configuration with continuous helical coils. In order to include the distortion of magnetic field produced by the ferritic steels in the blanket, the numerical calculation code ANSYS based on the finite element method (FEM) is incorporated. First, the precise structure of the magnet coils, vacuum vessel, and blanket is input to establish the 3D modelling for the finite element calculation. Second, the magnetic field by assuming nonmagnetic materials in the blanket is calculated as a reference. In this phase, the magnetic field-line tracing code is combined to obtain the magnetic surfaces and their associated parameters, such as the rotational transform and magnetic well. Third, the nonmagnetic material is changed to ferritic materials and the new magnetic fields are calculated. Comparison of magnetic field properties by changing the permeability of the structural material is investigated. The calculation results will be described in the presentation.

Feasibility study of react-and-wind method for helical coils wound from cable-in-conduit conductors.

S. Imagawa

*National Institute for Fusion Science, 322-6 Oroshi, Toki, GIFU 509-5292, Japan
SOKENDAI, Department of Fusion Science, 322-6 Oroshi, Toki GIFU 509-5292, Japan*

imagawa@LHD.nifs.ac.jp

Cable-in-conduit (CIC) conductors made of a multi-strand cable of superconducting wires within a tube-like conduit have been developed for large superconducting magnets. Major features of the CIC conductors are a large current up to 100 kA, high mechanical strength with a thick conduit, small AC losses, and high cryogenic stability by forced-flow cooling with supercritical helium. Since the technology related to high-field CIC conductors with Nb₃Sn wires has been widely advanced through the construction of ITER, they should be the first candidates for the magnets of next fusion reactors. The major disadvantage is the reduction of critical current (I_c) caused by large thermal strain due to heat treatment up to 650°C for production of the A15 phase. In the case of SS316 conduit, the compressive thermal strain in the superconductor such as Nb₃Sn or Nb₃Al exceeds 0.7%, and their critical current is considerably degraded. In order to prevent the further increase of the strain, the heat treatment is usually carried out after winding, which is called a "wind-and-react" method. A "react-and-wind" method, however, is preferred for a helical coil to avoid a huge oven for the heat treatment. In this concept, the heat treatment of a CIC conductor is carried out on a conventional bobbin, the circumference of which is the same as the length of one pitch of the helical coil [1]. After that, the conductor is wound into the helical coil case with being pulled aside, that is, being twisted. Since the superconducting wires in the conduit are multi-stage twisted, the effect of twisting the conductor on the strain of the wires is considered to be small. Furthermore, if the compressive thermal strain of the wires is reduced by being twisted, I_c of CIC conductors can be increased with the react-and-wind method.

In order to examine the effect of twisting the conductor on the strain of the wires, experimental study with a sub-size CIC conductor sample has been carried out. Three copper wires are twisted together, and 6×4 sets of the triplets are wound around a SS304 pipe of the diameter of 6 mm that simulates a center channel for coolant. The whole assembly is inserted into a SS304 conduit of the diameter of 17.3 mm. The wires are fixed to the conduit with epoxy resin at both the ends. The longitudinal strains of the wires are measured with strain gauges on the copper wires. The experimental results show that the tensile or compressive strain is induced in the wire by twisting the conduit in the same or counter direction to the wire twisting direction. In this experiment, the amounts of change in strain of wires are in the order of 1/10 of the torsional strain of the conduit. The strain of the wires is considered to depend on the change of their lengths. In order to examine the change of I_c of Nb₃Sn wires by twisting the conductor, small CIC conductor samples in spring-shape are under preparation. The torsion strain is induced on the conduits by changing the length of the spring. In this paper the concept of react-and-wind method for a large helical coil and the expected effect on I_c are discussed.

[1] S. Imagawa et al., Concept of Magnet Systems for LHD-type Reactor, Nuclear Fusion, Vol. 49 (2009) 075017(7pp).

Evaluation of Shear Strength in Soldered and Mechanical Lap joints of High-Temperature Superconducting tapes Intended for a Remountable Magnet

L. Aparicio, S. Ito, H. Hashizume

Tohoku University, 6-6-02-1 Aramaki Aza Aoba-Ku, Sendai 980-8579, Japan

lapa@karma.qse.tohoku.ac.jp

Remountable and joint-winding high-temperature superconducting (HTS) magnets have been proposed for a helical fusion reactor FFHR-d1. Mechanical lap joint (MLJ) and soldered lap joint (SLJ) of HTS coated conductors (CC) are joint method candidates for the joint above magnets. These joints must have sufficiently large mechanical strength to be tolerant to electromagnetic forces. Tensile test of MLJ between two HTS CC having copper (Cu) stabilizer with a contact area of 25 mm² was performed in a previous study [1], whose results suggested a linear dependency between joint conductivity and shear strength of the joint. Also, shear strength with joint pressure >50 MPa was higher than the required value. On the other hand, in tensile test for a SLJ of HTS CC having no Cu stabilizer with a contact area 200 mm², fracture in the joint occurred due to stress concentration at the edge of the joint [2].

Furthermore, evaluation of the mechanical behavior of SLJ of HTS CCs with Cu stabilizer has not been reported yet. Therefore this study performs tensile test on both MLJ and SLJ using HTS CCs with Cu stabilizer, to analyze and compare their mechanical behavior and fracture mechanism based on contact and friction theories.

Figure 1 shows the experimental setup for the tensile test performed in liquid nitrogen. Joint area for MJL and SLJ used in this study were 50 and 25 mm², respectively. In fabrication of MLJ, pressure of 100 MPa is applied at joint section where a 100 μm indium film is inserted between joint surfaces, then the pressure is once released and after that the pressure was kept a certain value.

SLJ was fabricated using Tin-lead (Sn₆₃Pb₃₇) solder. Normalized tensile test results plotted in figure 2 show a good agreement with those given in ref. [1] for the MLJ with contact area of 50 mm². Also, notable discrepancy between both joint methods is seen, that is, in the SLJ the maximum stress is almost constant due to different failure mechanism reported in [2]. Further results will be shown in full paper.

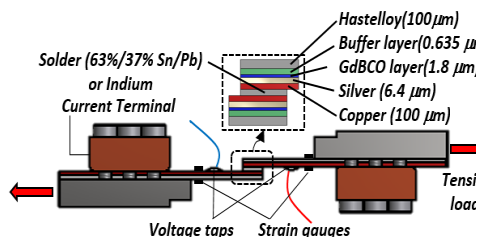


Fig. 1. Sample holder set-up.

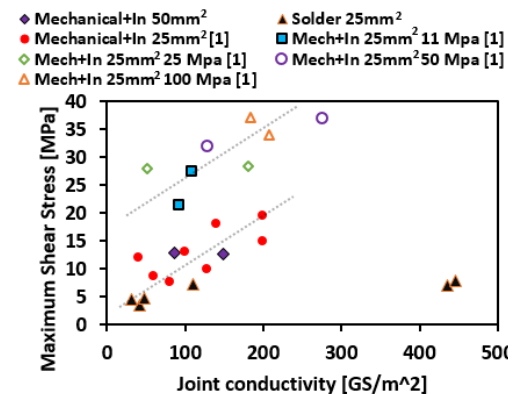


Fig. 2. Maximum tensile load vs Joint conductivity of mechanical and soldered lap joint with different joint pressure values.

[1] S. Ito et al., IEEE Trans, Appl. Supercond, Vol 25, 2015, 4201025.

[2] M, Sugano et al, IEEE Trans, Appl. Supercond, Vol. 17, 2007, 9606863

NITA Coil —Innovation for Enlarging the Blanket Space in the Helical Fusion Reactor

Nagato Yanagi, Takuya Goto, Hitoshi Tamura, Junichi Miyazawa, Akio Sagara

National Institute for Fusion Science, 322-6 Oroshi-cho, Toki 509-5292, Japan

Conceptual design studies of the LHD-type helical fusion reactor FFHR-d1 are progressing steadfastly. A multi-path strategy is being pursued for securing the design foundation, and it presently specifies FFHR-d1A as the base option for promoting the 3D engineering design [1]. In d1A, a pair of helical coils (major radius: 15.6 m) has the helical pitch parameter γ_c of 1.20 (the corresponding minor radius: 3.744 m), which was changed from the previous value of 1.25 for the original d1 (minor radius: 3.9 m) [2]. Due to the γ_c decrease, the “blanket space” Δ_{cp} at the inboard side of the torus is enlarged from 890 mm (for d1) to 950 mm (for d1A). Here Δ_{cp} is defined as the distance between the innermost layer of the helical coil windings and the ergodic layer outside the last closed flux surface (LCFS). In order to further improve the structural integrity and to lower the neutron flux, it is preferable to further enlarge Δ_{cp} .

Four methods were considered for enlarging Δ_{cp} in the previous studies. The first is to choose a smaller γ_c , such as 1.15 for FFHR-2m1 [3], but it gives a smaller minor radius of LCFS (plasma volume). The second is to set high current density in the helical coil, which intensifies the engineering challenge. The third is to make an outward shift of LCFS (together with the magnetic axis) and cut the remnant ergodic layer by target plates on X-points [3, 4]. In the outward shifted configuration, the alpha particle confinement and neoclassical transport are deteriorated, and thus, an inward shifted configuration is employed for FFHR-d1. The fourth is to split the helical coils at the outboard side of the torus which improves the poloidal symmetry of magnetic surfaces [5], but the outward shifted configuration is again the problem.

In 2014, another innovative method was proposed to shed a new light on this problem. The idea is to vary the current density within the helical coil by subdividing the coil windings into multi blocks [6]. The proposed method was, however, later determined to be almost infeasible from the engineering viewpoint since the current density was unrealistically high. Then, a modified version of the similar concept was proposed, in which a pair of sub-helical coils, presently named NITA (Newly Installed Twist Adjustment) coils, is employed at about two times the minor radius of the main helical coils [7]. An oppositely directed current of 5-10% of the main helical coil current is applied to the NITA coils and this combination effectively lowers γ_c . As the main helical coils have the original minor radius of FFHR-d1, Δ_{cp} can be resultantly enlarged to 1100-1200 mm. We should emphasize that the minor radius of LCFS is still comparable to that of FFHR-d1A, which is a contrast to choosing a smaller γ_c for the main helical coils. Presently, the electromagnetic stress analysis is being carried out and the result will be compared with that for FFHR-d1A to examine the effect of inclusion of NITA coils.

- [1] A. Sagara, H. Tamura, T. Tanaka, et al., *Fusion Eng. Des.* **89** (2014) 2114.
- [2] H. Tamura, T. Goto, T. Tanaka, et al., *Fusion Eng. Des.* **89** (2014) 2336.
- [3] A. Sagara, O. Mitarai, S. Imagawa, et al., *Fusion Eng. Des.* **81** (2006) 2703.
- [4] T. Morisaki, S. Imagawa, A. Sagara, O. Motojima, *Fusion Eng. Des.* **81** (2006) 2749.
- [5] N. Yanagi, K. Nishimura, T. Goto, et al., *Contrib. Plasma Phys.* **50** (2010) 661.
- [6] T. Watanabe, N. Yanagi, A. Sagara, *Plasma Fusion Res.* **9** (2014) 3403089.
- [7] T. Watanabe, *private communication*.

Summary of conductor and joint test results of JT-60SA CS and EF coils using NIFS test facility

T. Obana, K. Takahata, S. Hamaguchi, K. Kizu^a, H. Murakami^a, H. Chikaraishi, H. Noguchi, T. Kobuchi, S. Moriuchi, S. Imagawa, T. Mito, K. Tsuchiya^a, K. Natsume^a, K. Yoshida^a

National Institute for Fusion Science, 322-6 Oroshi-cho, Toki 509-5292, Japan

^a Japan Atomic Energy Agency, 801-1, Mukoyama, Naka 311-0193, Japan

The JT-60 tokamak is being upgraded to an advanced superconducting tokamak referred to as the JT-60 super advanced (JT-60SA) at the Japan Atomic Energy Agency (JAEA) Naka site in Japan. [1,2]. The JT-60SA magnet system consists of a central solenoid (CS) coil, 18 toroidal field (TF) coils and six plasma equilibrium (EF) field coils. Nb₃Sn cable-in-conduit (CIC) conductors are used for the CS coil, and NbTi CIC conductors are used for the TF and EF coils. JAEA was taking charge of conductor production for the CS and EF coils, and the conductor production was started from 2008 at Naka site [1,3].

In 2007, the collaborative project between JAEA and the National Institute for Fusion Science (NIFS) was launched to evaluate the performance of the CIC conductors and conductor joints using a conductor test facility in NIFS [3,4]. Conductor tests for four types of coil conductor and joint tests for seven types of conductor joints have been conducted for the past eight years. In this paper, all of the conductor and joint test results are summarized.

[1] K. Yoshida, K. Tsuchiya, K. Kizu, H. Murakami, K. Kamiya, T. Obana, et al., *Physica C*, **470** (2010) 1727-1733.

[2] H. Murakami, K. Kizu, K. Tsuchiya, Y. Koide, K. Yoshida, T. Obana, et al., *IEEE Transactions on Applied Superconductivity*, **24** (3) (2014) 4200205.

[3] K. Kizu, K. Tsuchiya, T. Obana, K. Takahata, R. Hoshi, S. Hamaguchi, et al., *Fusion Engineering and Design*, **84** (2009) 1058-1062.

[4] T. Obana, K. Takahata, S. Hamaguchi, N. Yanagi, T. Mito, S. Imagawa, et al., *Fusion Engineering and Design*, **84** (2009) 1442-1445.

Effect of Laval Nozzle in the GAMMA 10 SMBI Experiments

M. M. Islam, Y. Nakashima, S. Kobayashi^a, Y. Nakano^a, N. Nishino^b, K. Hosoi, K. Ichimura, M. S. Islam, K. Shimizu, K. Fukui, M. Ohuchi, A. Terakado, M. Yoshikawa, J. Kohagura, R. Ikezoe, X. Wang, M. Ichimura and T. Imai

Plasma Research Center, University of Tsukuba, Tsukuba, Ibaraki 305-8577, Japan

^a*Institute of Advanced Energy, Kyoto University, Gokasho, Uji 611-0011, Japan*

^b*Graduate School of Engineering, Hiroshima University, Higashi-Hiroshima, Japan*

In GAMMA 10, supersonic molecular beam injection (SMBI) has been carried out at the central-cell where the main plasma is confined as shown in Fig.1 [1]. The proper control of gas fueling is very important to obtain good performance plasma. The results of SMBI experiment with plenum pressure from 0.4 MPa to 2.0 MPa were obtained. The electron line density in the central-cell (NLcc) of the plasma was increased during SMBI as well as with the increase of plenum pressure (Fig.2). In Fig.2, NLcc was also increased before injecting SMBI because of gas-puffing. H α intensity was measured by H α detector at different position along z-axis. The H α line intensity was increased by SMBI (Fig.3). The neutral particle behavior was investigated based on 2-dimensional image captured by a high speed camera which is installed at the central-cell (Fig.4). The distribution of the emission intensity were also investigated by the image captured by the camera as an index of the neutral transport. The full width at half maximum (FWHM) value with laval nozzle was lower than that of straight nozzle. This means that the effect of laval nozzle reduces the diffusion of injected hydrogen molecules. Detailed results of SMBI experiments will be presented in the poster session.

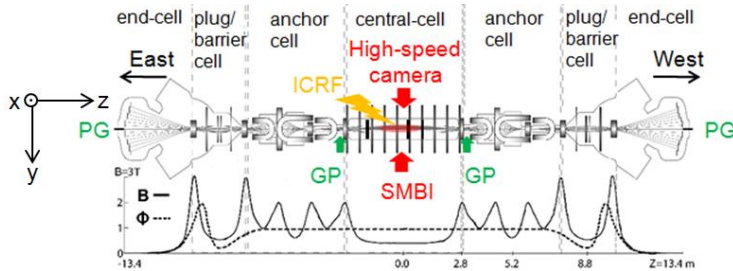


Fig. 1 Overview of GAMMA 10 experimental set-up

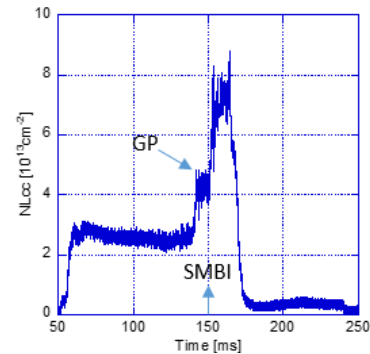


Fig. 2 Time responses of line density in central cell

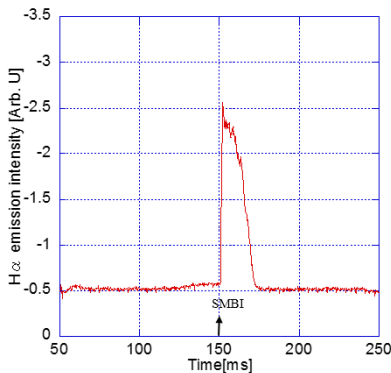


Fig. 3 Variation of H α with time in central-cell

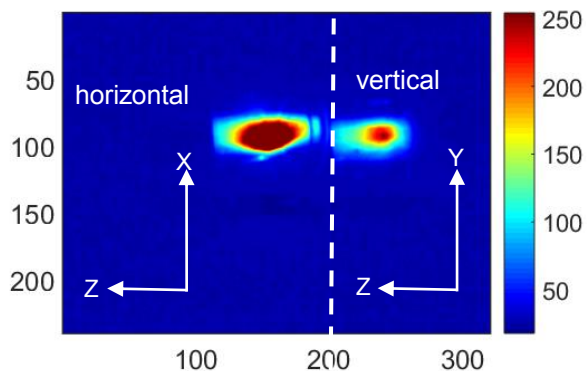


Fig. 4 2-D image by the high-speed camera

[1] K. Hosoi, et al., J. Plasma Fusion Res. 7 (2012) 2402126

Speedup of shielding current analysis in high-temperature superconducting film: implementation of \mathcal{H} -matrix method

A. Kamitani, T. Takayama, A. Saitoh, H. Nakamura^a

Yamagata University, 4-3-16, Jōnan, Yonezawa, Yamagata 992-8510, Japan

^aNational Institute of Fusion Science, 322-6, Oroshi, Toki, Gifu 509-5292, Japan

Two types of numerical methods have been investigated for analyzing the shielding current density in a High-Temperature Superconducting (HTS) film: differential-algebraic-equation method [1] and virtual-voltage method [2]. If an initial-boundary-value problem of the shielding current density is discretized with n nodes, both methods require $O(n^2)$ operations at each time step. In order to further accelerate the virtual-voltage method, the \mathcal{H} -matrix method [3–5] is applied to matrix-vector multiplications in its linear-system solver, GMRES.

A numerical code for calculating the shielding current density has been developed on the basis of both proposed methods and, by means of the code, the influence of the \mathcal{H} -method on the performance of the shielding current analysis has been numerically investigated.

Conclusions obtained in the present study are summarized as follows.

- When GMRES is implemented as a linear-system solver, the virtual-voltage method can realize a high-speed shielding current analysis in an HTS film with cracks.
- Acceleration by the \mathcal{H} -matrix method is effective especially for a large-sized shielding current analysis in a high-aspect-ratio HTS film.

- [1] A. Kamitani, T. Takayama, A. Saitoh, H. Nakamura, *Plasma Fusion Res.* **10** (2015) 3401059.
- [2] A. Kamitani, T. Takayama, S. Ikuno, *IEEE Trans. Magn.* **49** (2013) 1877.
- [3] S. Kurz, O. Rain, S. Rjasanow, *IEEE Trans. Magn.* **38** (2002) 412.
- [4] Y. Takahashi, C. Matsumoto, S. Wakao, *IEEE Trans. Magn.* **43** (2007) 1277.
- [5] V. Le-Van, B. Bannwarth, A. Carpentier, O. Chadebec, J.M. Guichon, G. Meunier, *IEEE Trans. Magn.* **50** (2014) 7010904.

Fuelling effect by axial injection of torus plasma into ST plasmaS. Koike, T. Takahashi, N. Mizuguchi¹, and O. Mitarai²*Division of Electronics and Informatics, Gunma University, Kiryu, Gunma 376-8515, Japan*¹*National Institute for Fusion Science, Toki, Gifu 509-5292, Japan*²*Tokai University, 9-1-1 Toroku Higashi-ku, Kumamoto 862-8652, Japan*

Development of fuelling technique for supplying fuel particles in the core region of a burning plasma is of great importance to realize nuclear fusion power generation. Experiments of compact torus (CT) injection into a relatively large-scale torus plasma [1] have explored an innovative deep-fuelling method. However, the experiments have found retard of an accelerated CT plasma by the vertical field of a target torus plasma is a technological problem. Recently, a new fuelling technique using the merging of two plasmas with the same plasma current directions (Merging Fueling) has been proposed for a D-³He spherical tokamak (ST) reactor [2]. In this scheme, a smaller-scale torus plasma produced by the auxiliary poloidal coils is vertically accelerated toward a main ST plasma by controlling the external field. In a fact, the C-2 experiment shows two field-reversed configurations (FRCs) are successfully merged after the head-on collision, and the merged FRC is found to exhibit a better confinement property [3]. If the merging process completes, steady state operation of a fusion reactor is available by intermittent injection. We study here feasibility of fuelling by a compact-size torus plasma merging with a ST plasma by the magnetohydrodynamic (MHD) simulation code MHD Infrastructure for Plasma Simulation (MIPS) [4]. Detailed results will be shown in our presentation.

[1] L. J. Perkins, S. K. Ho, and J. H. Hammer, *Nucl. Fusion* **28**, 1365 (1988).

[2] O. Mitarai, "Impacts of STOR tokamaks on fusion research", W2-6 (June 17), Invited talk, CAP Congress 2015 (University of Alberta, Edmonton, Canada June 15-19, 2015).

[3] M. W. Binderbauer *et al.*, *Phys. Rev. Lett.* **105**, 045003 (2010).

[4] Y. Todo *et al.*, *Plasma Fusion Res.* **5**, S2062 (2010).

Progress in development of TE_{31,11} mode gyrotron for ITER EC system

Ryosuke Ikeda, Yasuhisa Oda, Takayuki Kobayashi, Masayuki Terakado,
Ken Kajiwara, Koji Takahashi, Shinichi Moriyama and Keishi Sakamoto

Japan Atomic Energy Agency (JAEA), Naka, Ibaraki 311-0193, Japan

iked.ryosuke@jaea.go.jp

A 20 MW electron cyclotron resonance heating and current drive (EC H&CD) system is planned in ITER. ITER EC system is composed of 24 gyrotrons including superconducting magnets and matching optics units (MOU), high voltage power supplies, 24 set of transmission lines, 4 upper port launchers and equatorial port launcher. The required specifications of a gyrotron are 170 ± 0.3 GHz oscillation frequency, > 1 MW continuous wave operation and > 50 % electrical efficiency. To suppress a neo-classical tearing mode, 5 kHz high-speed power modulation is required. In addition, to achieve low loss transmission, HE₁₁ mode purity at the MOU exit demands > 95 %. In JAEA, the gyrotrons with a triode magnetron injection gun has been developed. In TE_{31,8} mode gyrotron, the output power, the electric efficiency and the pulse width achieved 1 MW / 55 % / 800 s and 0.8 MW / 57 % / 3600s [1, 2]. The demand performance was almost filled by these results. Moreover, 5 kHz full power modulation was demonstrated by an electron beam modulation using an anode voltage switching [3]. To decrease the heat load on the cavity resonator for > 1 MW CW operation, TE_{31,11} mode gyrotron is under development. The cavity radius at its straight section was increased from 17.90 mm to 20.87 mm to excite TE_{31,11} mode and the cavity wall loading becomes considerably low. Therefore, high power operation of 1.5 MW is expected.

In last campaign, maximum output power and the total electric efficiency were 1.19 MW and 43%. And, in steady-state operation, a 1000 s oscillation length and output power of 0.5 MW was achieved [4]. In last campaign, electron beam radius injected in a cavity resonator was 9.1 mm. This value corresponds to peak radius of coupling coefficient between electron beam and electric field. However, mode coupling with counter-rotating modes such as TE_{28,12} mode and TE_{29,12} mode was observed. Especially, TE_{28,12} mode which is excited in low field side interferes with high efficiency oscillation region in TE_{31,11} mode. To avoid excitation of counter-rotating TE_{28,12} mode, it has extended the electron beam radius to 9.3 mm. As the results, TE_{31,11} mode was oscillated in a hard-self excitation region without mode coupling. Maximum efficiency at 0.6 MW operation reached 50 %. In this campaign, 1.24 MW/45 %/2 sec and 1.13 MW/49 %/2 sec were obtained in high power experiments. In steady-operation, 0.6 MW/1000 sec and 1.0 MW/200 sec were achieved.

[1] K. Sakamoto *et al.*, Nat. phy. **3** (2007) 411.

[2] K. Sakamoto *et al.*, Nucl. Fusion **49** (2009) 095019.

[3] K. Kajiwara *et al.*, Nucl. Fusion **53** (2013) 043013.

[4] R. Ikeda *et al.*, Fusion Eng. Des., High-power and long-pulse operation of TE_{31,11} mode gyrotron, ARTICLE in PRESS (2015).

Characteristics of a Large diameter RF negative hydrogen ion source

Yuko Sasaki¹, Sho Takayama¹, Haruhisa Nakano², Atsushi Komuro¹, Kazunori Takahashi¹
and Akira Ando¹

¹*Department of Electrical Engineering, Tohoku University, Sendai 980-8579, Japan*

²*National Institute for Fusion Science, 322-6, Orishi-cho, Toki, 509-5292, Japan*

e-mail address of submit author: yukosasaki@ecei.tohoku.ac.jp

Negative Neutral Beam Injection system (NNBI) is a powerful tool for fusion plasma heating and is planned to be installed in ITER. A negative ion source is a key technology to develop the high performance NBI. A long-pulsed negative-ion-based NBI is required to be operated with the D⁻ beam energy of ~1 MeV and beam current of 200 A/m². From the view point of the stable and long-pulsed operation, development of an radio frequency (RF) negative ion source is one of the vigorous research issues [1].

In our previous researches a high density plasma production ($\sim 10^{19}$ m⁻³) and the resultant increase in a negative beam current have been performed in the RF negative ion source driven with the RF frequency of 100-400 kHz and the RF power of 10-30 kW [2,3,4]. The inner diameter of the driver region of the source is 70 mm and the axial magnetic field is applied to improve the source performance.

In this research we have investigated a larger RF source with the inner diameter of the driver region is 230 mm, which is the same diameter as the ITER NBI. Two solenoids to create the axial magnetic field are installed in the driver region. Permanent magnets are also installed at the source back plate and around a diffusion chamber, eliminating plasma loss to the wall. Efficient plasma production was obtained and effects of Cs vapor evaporation on the ion source performance will be shown.

[1] U. Frantz, *et al.* AIP Conference Proc. **1655**, 040001 (2015)

[2] A.Ando, *et al.* Rev. Sci. Instrum. **83**, 02B122 (2012).

[3] K.Oikawa, *et al.* Rev. Sci. Instrum. **85**, 02B124 (2014).

[4] A.Ando, *et al.* AIP Conf. Proc. 1390, 322 (2011).

Temperature dependence of tritium enrichment by electrolysis with solid polymer electrolyte

N. Ikemoto^a, N. Akata^{a, b}, M. Tanaka^{a, b}, N. Shima^c, H. Kakiuchi^d

^a SOKENDAI (The Graduate University for Advanced Studies), 322-6 Oroshi-cho, Toki 509-5292, Japan

^b National Institute for Fusion Science, 322-6 Oroshi-cho, Toki 509-5292, Japan

^c Fukushima University, 1 Kanayagawa, Fukushima 960-1296, Japan

^d Institute for Environmental Science, 1-7 Obuchi-ienomae, Rokkasho 039-3212, Japan

ikemoto.norihito@LHD.nifs.ac.jp

In the future fusion facilities, tritium will be released from the facility. It is important to understand the impact of tritium in the environment. Tritium exists as water in the environment. However, recently the tritium concentration in environment is almost lower than the detection limit of a liquid scintillation counter (LSC). Therefore, sample water must be enriched by electrolysis for tritium measurement. It is known that tritium enrichment is affected by the temperature of the sample water [1]. The purpose of this study is obtaining a relation between tritium enrichment and the temperature of the sample water.

In this study, the temperature of sample water is cooled from outside of water tank with cooling chiller. An electrolytic apparatus (TRIPURE XZ001, Permelec Electrode Ltd.) with solid polymer electrolyte (SPE) is utilized for tritium enrichment. The temperature of sample water is measured by thermocouple attached near the SPE. The sample water is electrolyzed from 800 mL to 75 mL. The electrolytic current is 55 A for 35 hours, then it is reduced to 20 A. The total operational time is approximately 48 hours. Distilled sample water is mixed with scintillator (ULTIMA GOLD LLT, PerkinElmer) in a polyethylene vial. The tritium concentration of the sample is measured by low background LSC (LSC-LB5, Aloka).

Fig. 1 shows the relation between the average temperature of sample water and the enrichment factor. The enrichment factor is defined as:

$$\text{Enrichment factor} = \frac{T_f}{T_i}, \quad (1)$$

where T_i and T_f are the initial and final tritium concentration, respectively. The enrichment factor is increased when the average temperature is low. In addition, the most stable enrichment is confirmed by cooling to 15 °C. It is suggested that tritium enrichment by SPE method with cooling water circulator is effective for high and stable enrichment.

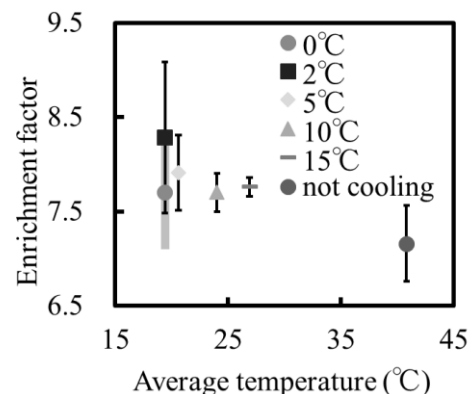


Fig. 1. Relation between the average temperature and the enrichment factor.

[1] Y. Ogata et al. J. Radioanal. Nucl. Chem. 255 (2003) 539-541

Study of tritium release behavior from soil particle

Hiroyuki Date^a, Kazunari Katayama^a, Kazuya Furuichi^a, Tatsuro Hyuga^b, Toshiharu Takeishi^b, Satoshi Fukada^a

^a Department of Advanced Engineering, Kyushu University
6-1, Kasuga-koen, Kasuga, Fukuoka, Japan, 816-8580

^b Faculty of Engineering, Kyushu University, 744 Motoooka, Nishi-ku, Fukuoka, Japan, 819-0395

Recently, the demand on requirements to assess the risk for severe accidents in nuclear facilities is increasing and countermeasures for various accidents are being reconsidered. The spill of tritiated water to the ground is one of accidents which should be assumed because a large amount water containing tritium is handled in a fusion facility. The transport model of tritiated water under the ground is required from a viewpoint of safety of a fusion reactor and nuclear facilities but studies on tritium behavior in natural soil are limited. In this study, the present authors discuss how tritium is trapped in soil particles.

Sample soil of 39.2g was immersed in tritiated water of 2.5×10^5 Bq/cc for 62 days. 3.0g of wet tritiated soil was packed in a quartz tube and Ar gas was passed in it for 18 hours at room temperature in order to dry. After that, soil bed was heated to 1000°C at 5°C/min and heated at 1000°C constant for 30 minute while Ar gas passing. The released tritium was collected in a double-water bubbler and tritium concentration was measured by LSC. In addition, non-tritiated soil was heated on the same condition and released water was measured by moisture meter.

The amount of tritium in water decreased and 12% of them are resorbed in soil. Sample soil resorbed tritium of 1.2×10^6 Bq and tritium concentration of tritiated water became 2.2×10^5 Bq/cc. It is because isotope exchange reaction. After 18 hours Ar gas purging, the mass of soil decreased 0.318g. The amount of tritium in released water was calculated with 7×10^4 Bq and it conformed to amount of tritium collected in bubbler. Fig.1 shows the amount of released tritium and water content every 100°C. Total amount of released tritium was 6×10^3 Bq. This is 6% of all tritium trapped in soil sample. Generally, it is said that the soil particles have 3 kinds of water: surface water, interlayer water, and structural water. These water have different release peaks. Among released tritium, it is thought that surface water and interlayer water had most. However, it is difficult to recover all tritium resorbed in soil by heating.

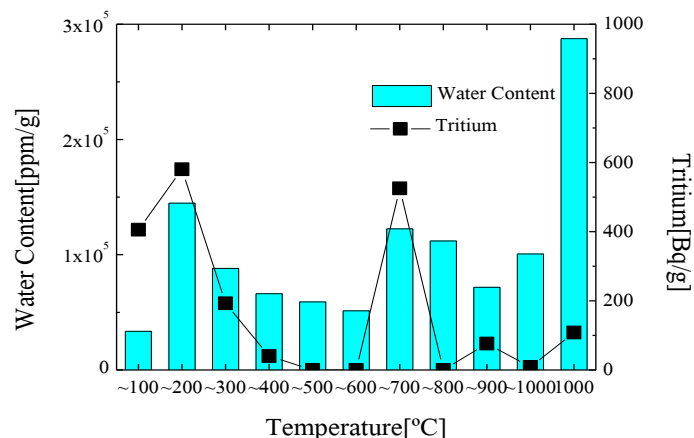


Fig. 1 Released tritium and water content every 100°C

Evaluation of tritium sorption rate in soil packed bed by numerical analysis

Kazuya Furuichi, Kazunari Katayama, Hiroyuki Date, Taturo Hyuga, Satoshi Fukada

*Department of Advanced Energy Engineering Science, Kyushu University,
6-1, Kasugakoen, Kasuga-shi, Fukuoka 816-8580, Japan*

From a viewpoint of safety, understanding of tritium behavior in the environment is an important issue for the development of a fusion reactor. Because a large amount of tritiated water will be handled in the fusion plant, the accidental spill of tritiated water to the natural soil around the plant should be assumed. When the tritiated water is penetrating into the ground, a part of tritium is considered to be retained in the soil particles by absorption, adsorption and isotope exchange reaction. In our previous study, the percolation experiment of tritiated water into the soil packed bed were performed and it was found that a part of tritium is sorbed by the isotope exchange reaction [1]. In this study, a simplified transfer model for tritium in a soil packed bed was proposed and experimental results were numerically analyzed.

Sample soils were collected in the Hakozaki campus of Kyushu University. The soils were separately packed in the fluoroplastic tube and tritiated water was poured to the top of the packed bed. The percolated water was drained into a tray which was put on an electric balance. Weight change of the tray was continually monitored to measure the weight of the effluent water. The effluent water was periodically sampled and tritium concentration was quantified by a liquid scintillation counter. The detail of experimental system and procedure was reported in [1]

The present authors have been proposed a transfer model for tritiated water vapor in concrete materials [2]. This model was simplified for analysis of tritium behavior in the soil packed bed. In our previous study [1], it was found that the Darcy's law is valid for the water percolation in the soil packed bed. Additionally, the saturated hydraulic conductivity was obtained. This means that the percolation behavior of water can be calculated by using the obtained hydraulic conductivity assuming Darcy's law. In this work, total isotope exchange capacity and the overall sorption rate by isotope exchange reaction in soil particles were assumed and tritium concentration in the effluent water in the tray was calculated. The comparison of experiment and calculation are shown in Fig.1. The overall sorption rate was evaluated to be $6 \times 10^{-4} \text{ s}^{-1}$. By using obtained sorption rate and water percolation rate, tritium penetration rate into the ground can be estimated approximately.

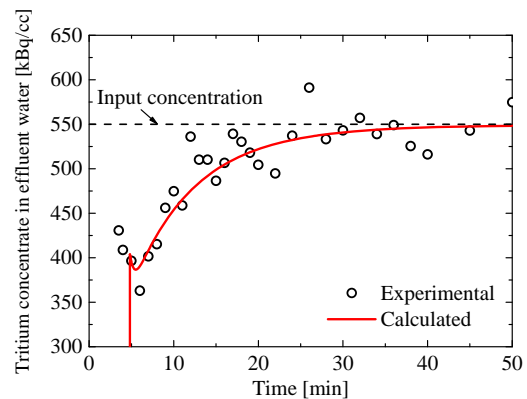


Fig.1 Comparison of experiment and calculation for the change of tritium concentration in the effluent water in the percolation of tritiated water into the soil packed bed.

This work is supported by KAKENHI Grant-in-Aid for Young Scientists (A) 25709087.

[1] T. Honda, K. Katayama et al., *Fusion Sci. Technol.*, **67** (2015) 382-385.

[2] K. Furuichi, H. Takata et al., *J. Nucl. Mater.*, **367-370** (2007) 1243-1247.

Effects of gas-liquid ratios on separative performance of dual-temperature water hydrogen chemical exchange column

T. Sugiyama^a, K. Kotoh^b, K. Munakata^c, A. Taguchi^d, T. Kawano^e, M. Tanaka^e, N. Akata^e

^aNagoya University, Fro-cho 1, Chikusa-ku, Nagoya 464-8603, Japan

^bKyushu University, Moto-oka 744, Nishi-ku, Fukuoka 819-0395, Japan

^cAkita University, Tegata-gakuen-machi 1-1, Akita 010-8502, Japan

^dUniversity of Toyama, Gofuku 3190, Toyama 930-8555, Japan

^eNational Institute for Fusion Science, Oroshi-cho 322-6, Toki, Gifu 509-5292, Japan

One of the primary components for Water Detritiation System (WDS) of DEMO fuel cycle is Combined Electrolysis and Catalytic Exchange (CECE). A simple CECE process is, however, not feasible to treat the huge amount of tritiated water, because very large electrolyzer will be required. In the case of WDS for ITER, some combination processes, such as CECE combined with water distillation or vapor phase chemical exchange, have been proposed and investigated [1-3]. Dual temperature system is a typical method to produce a reflux without any chemical conversion. A dual temperature water-hydrogen chemical exchange (DT-CE) can be, then, a candidate method to combine with CECE, because the process does not require an electrolyzer. A DT-CE was investigated as the method of deuterium recovery [4]. The optimal pressure of the method explained in the literature was very high as 69 atm and the method seems to lose the feasibility.

In the present study we propose a system which consists of two liquid phase chemical exchange (LPCE) columns operated under different pressures each other as well as different temperatures. The system is named 'DTDP-CE' hereinafter. By changing the operating pressures of the columns each other, we can examine the possibility to reduce the optimal pressures and to accomplish a feasible combination of operating conditions. Although there are some reports on the system like DTDP-CE for the limited cases of operating conditions [5, 6], variety effects of operating parameters on separative performance are not sufficiently investigated. The purpose of the present study is to investigate effects of gas-liquid ratios on separative performance of a DTDP-CE process. Detail results and discussions about effects of hydrogen-vapor flow ratio as well as hydrogen-water flow ratio on concentration profiles in the columns were presented using McCabe-Thiele diagram.

- [1] J. M. Miller, S. L. Celovsky *et al.*, Fusion Sci. Technol., **41** (2002) 1077.
- [2] Y. Iwai, Y. Misaki, T. Hayashi *et al.*, Fusion Sci. Technol., **41** (2002) 1126.
- [3] R. Michling, I. Cristescu, L. Doerr *et al.*, Fusion Eng. Des., **84** (2009) 338.
- [4] M. Benedict *et al.*, Nuclear Chemical Engineering 2nd Edition, McGraw-Hill, Inc. (1987).
- [5] I.A. Alekseev, S.D. Bondarenko *et al.*, Fusion Eng. Des., **69** (2003) 33.
- [6] T.V. Vasyanina, I.A. Alekseev *et al.*, Fusion Eng. Des., **83** (2008) 1451.

Preparation of hydrophobic platinum catalyst with porous silica supports for water hydrogen chemical exchange

Y. Morita, T. Sugiyama, K. Sawada, Y. Enokida

Nagoya University, Fro-cho 1, Chikusa-ku, Nagoya 464-8603, Japan

Hydrogen isotope separation by water-hydrogen chemical exchange is one of the candidate methods for Water Detritiation System. In order to accelerate the isotopic exchange reaction between hydrogen and water vapour molecules, a hydrophobic platinum catalyst is indispensable. Many kinds of catalysts have been developed using hydrophobic porous supports such as polytetrafluoroethylene, polyethylene, polystyrene and styrene-divinylbenzen [1]. In the present study, a porous silica support was employed in order to improve heat resistance and hydrophobicity under pressurized condition.

Platinum catalysts were prepared using porous silica beads (Fuji silysia chemical Ltd., CARiACT Q-50) as a support. A number of silane coupling agents was tested for hydrophobic treatment of the beads. Among them a catalyst treated with hexadecyltrimethoxysilane provided superior performance in hydrophobicity and isotope exchange. The catalyst performances for isotopic exchange between hydrogen and water vapour molecules were measured with tritiated water of 1 MBq/kg, and the overall mass transfer coefficient was obtained as $84 \pm 5 \text{ s}^{-1}$. Figure 1 shows a relationship between the overall mass transfer coefficient k and the alkyl chain length of the silane coupling agents. The mass transfer process in the catalyst bed was also examined theoretically.

[1] J. P. Butler, J. H. Rolston, W. H. Stevens, A.C.S. Symposium Series, **68** (1978) 93.

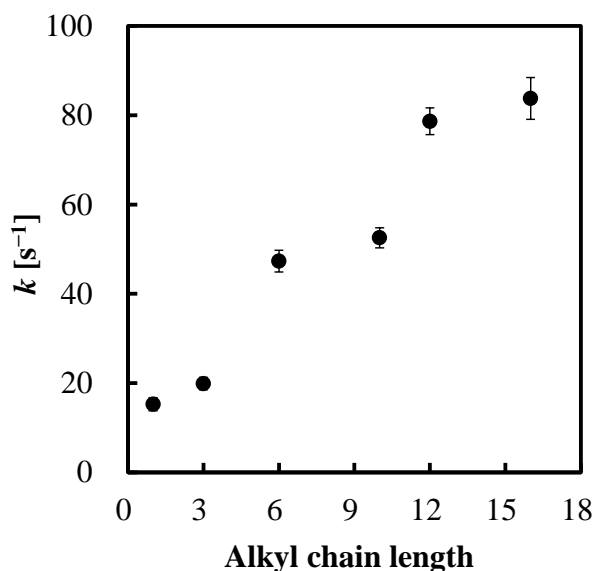


Fig. 1

A new pretreatment technique for environmental tritium analysis with microwave heating method

N. Akata^{a,b}, M. Tanaka^{a,b}, S. Takayama^a, H. Kakiuchi^c, T. Tamari^d, S. Sano^e

^a National Institute for Fusion Science, 322-6 Oroshi-cho, Toki 509-5292, Japan

^b SOKENDAI (The Graduate University for Advanced Studies), 322-6 Oroshi-cho, Toki 509-5292, Japan

^c Institute for Environmental Sciences, 1-7 Ienomae, Obuchi, Rokkasho, Aomori 039-3212, Japan

^d Kyushu Environmental Evaluation Association, 1-10-1 Matsukadai, Higashi-ku, Fukuoka 813-0004, Japan

^e Advanced Industrial Science and Technology, 2266-98 Anagahora, Shimoshidami, Moriyama, Nagoya, Aichi 463-8560, Japan

akata.naofumi@LHD.nifs.ac.jp

The deuterium plasma experiment is being planned to produce higher performance plasma using the Large Helical Device (LHD) of National Institute for Fusion Science (NIFS) [1]. In the experiments, a small amount of tritium will be produced by the D(d, p)T reaction in deuterium plasma. Therefore, it is important to understand the tritium concentration in environmental samples for radiation safety and environmental impact assessment. Tritium in environmental organic samples usually consists of free water tritium (FWT) and organically bound tritium (OBT). The FWT exists as HTO form, and its behavior is similar to natural water. On the other hand, OBT is tritium bounded to organic molecules (or carbon). The OBT has a longer biological half-life and higher incorporation to organic materials than the FWT [2]. The conventional method for FWT and OBT analysis is a liquid scintillation counting method after freeze-drying and combustion of the sample as summarized in MEXT report [3]. However, pretreatment for FWT and OBT analysis are complicated and time consuming processes over a week. Thus, we propose the application of microwave heating technique to save time and effort of the pretreatment of plant samples for FWT analysis.

To understand the behavior of the combustion and drying of organic samples, we conducted TG/DTA analysis of pine needle samples. It is found that the sample has to be heated up to 100-110 °C for complete drying under N₂ gas flow condition. Then, we tried the water recovery from fresh pine needle samples by the multi-mode microwave heating system. The recovery rate was achieved more than 97% under these experimental conditions (microwave output: 1.0kw, time: 30 min, N₂ flow: 2L/min). This result shows more preferable for the pretreatment of organic samples than the conventional method.

[1] A. Komori et al. Fusion Science Technol, 58, 1 (2010)

[2] C. Boyer et al., Environmental and Experimental Botany, 67, 34-51 (2009)

[3] MEXT, Radioactivity Measurement, Series No. 9 (2002)

Tritium decontamination from carbon deposited layer by baking

N. Ashikawa^a, Y. Torikai^b, K. Nishimura and the LHD experiment group

National Institute for Fusion Science, Toki, Gifu, 509-5292, Japan

^a*SOKENDAI (The Graduate University for Advanced Studies), Toki, Gifu, 509-5292, Japan*

^b*Toyama University, Toyama, Toyama, 930-8555, Japan*

Investigations on hydrogen isotope inventories in plasma facing walls are important with the view of controls of fuel recycling and in-vessel tritium inventories in fusion devices. But, removal processes of hydrogen isotopes have not been optimized yet and still serious problems in ITER and DEMO. In particular, retained hydrogen isotopes in deposition layers are higher than that in bulk materials. Depth profiles in target materials are different between the retained hydrogen isotopes originating from energetic hydrogen isotopes during plasma discharges and the molecular hydrogen isotopes [1]. In tokamaks, high-level tritium retentions were observed under the dome regions and this phenomenon is the trappings of molecular hydrogen isotopes into deposition layers. Thus, investigations of the trapped molecular tritium are also required. In this study, tritium retentions by the molecular gasses into the deposition layers are analyzed, and the removal methods for these tritium from the deposition layers are investigated.

A target deposition layer, namely sample S2, was produced on stainless steel (SS) 316 target samples which was set near the graphite divertor targets during one experimental campaign in LHD. On the sample S2, the thickness of deposition layer was 382 nm and the atomic concentrations were 80 %C, and 15 % Fe. The retained hydrogen from the deposition layers were 1.03×10^{22} mol./m² on sample S2. The hydrogen was mainly trapped into the deposition layers through the main plasma discharges and the glow discharges in LHD. The hydrogen-carbon (H/C) ratio for the sample S2 was 0.23. The ratio of sp²/sp³ bonded carbon is 0.1-0.2 measured by X-ray photoelectron spectroscopy (XPS). Based on the ellipsometry analysis, single C-H bonds in the carbon deposited layers were observed. Four kinds of analytical parameters, H/C, sp²/sp³ ratio, Raman spectroscopy, and the ellipsometry show that these carbon deposited layers have characterizations of hydrogenated amorphous carbon with single C-H bonds [2].

The tritium imaging plate technique is one of the useful tools for tritium measurement. The LHD deposition layer on sample S2 was exposed to 7% of tritium gasses at 423K for 3 hours. After the tritium gas exposure, the amount of retained tritium into the deposition layer was evaluated by β -ray-induced X-ray spectrometry (BIXS) and the detected tritium amount was 5.25×10^{17} molecular/m². Molecular tritium was confirmed to be trapped near the surface of deposition layers.

Long-term tritium desorption from the deposition layer after the tritium gas exposure measured by the tritium imaging plate technique. The target was kept at the room temperature in the air. The released tritium amount from the deposition layer was about 30% for 3 months. After that time to one year, the released tritium is negligible. After the observation of long-term tritium desorption, the baking experiments were done at 368K, 423K, 573K and 773K. The effective temperatures for the tritium removal are from 425 K to 573 K, and the tritium desorption reached a background level at 773K.

This study reveals the fundamental processes for tritium decontaminations from carbon deposited layers by the baking. Molecular tritium trapped near the surface regions of the LHD deposition layers has a limitation to long-term tritium desorption, and the baking using an isochronal annealing is effective for the tritium decontamination from the deposition layer.

[1] T. Tanabe, et al., Journal of Nuclear Materials 313 (2003) 478.

[2] N. Ashikawa, et al., JPFRR-SERIES 11 (2015) 015.

Microstructural and Microchemical Evolution of V-4Cr-4Ti under Heavy Ion Irradiation

T. Muroga¹, H. Watanabe², T. Miyazawa³, T. Nagasaka¹

¹*National Institute for Fusion Science, 509-5292 Gifu, Japan*

²*Research Institute for Applied Mechanics, Kyushu University, Kasuga, Fukuoka, Japan*

³*Japan Atomic Energy Agency, Rokkasho, Aomori, 039-3212, Japan*

V-4Cr-4Ti alloy is a promising candidate low activation structural material for fusion blankets. For this material, it is pointed out that the factor determining its low temperature operation limit is hardening and loss of elongation by irradiation. Since it is known that initial defects formed by irradiation are interstitial dislocation loops at the lower boundary temperature region (<673K), the kinetics of dislocation loop evolution needs to be investigated. It is also pointed out that precipitates highly enriched with Ti and O are formed in the matrix and on the dislocation sites, which can influence the dislocation evolution. The precipitation is known to be highly dependent on irradiation temperature. This study investigates the dislocation and precipitate evolution and their mutual interactions in V-4Cr-4Ti during heavy ion irradiations.

The material used was NIFS-HEAT-2, a reference V-4Cr-4Ti alloy. The ion irradiations were carried out with 2.4 MeV Cu²⁺ ions at 408K, 473K, 573K, 673 and 773K to 0.15 to 10 dpa and at 4.5x10⁻³ dpa/s at the damage peak depth (800nm from the surface) using Tandem accelerator of RIAM, Kyushu University. Microstructural and microchemical evolution was characterized by a TEM and a high resolution STEM-EDS of Kyushu University, respectively.

Dislocation loops were observed at 573K and below. The loop density decreased with temperature. At 473K the loop growth rate was low. It was not until 10 dpa that tangled dislocation was observed. Enriched region with Ti or O was not observed in the matrix at 573K and 1 dpa. At 673K a complex dislocation network structure was observed. The contribution of the precipitation to the complete difference in dislocation structure between 573k and 673K is investigated.

Transport properties of high-beta plasmas in the inward shifted configurations on LHD

H. Funaba, K.Y. Watanabe, S. Sakakibara, S. Murakami ^a, R. Seki, S. Ohdachi,
Y. Suzuki, I. Yamada, R. Yasuhara, K. Tanaka, T. Tokuzawa, M. Osakabe, H. Yamada,
Y. Takeiri and LHD Experiment Group

National Institute for Fusion Science, 322-6 Oroshi-cho, Toki 509-5292, Japan

^a *Kyoto University, Department of Engineering, Kyoto 606-8501, Japan*

funaba@lhd.nifs.ac.jp

The local transport property of high beta plasmas on the Large Helical Device (LHD) is studied by referring the ISS04 scaling [1], since the plasmas in the low beta range of LHD have the similar local transport property as χ^{ISS04} , which is a modeled transport coefficient with the same non-dimensional parameter dependence of ISS04. In the previous analysis [2], high beta plasmas were mainly produced in the conditions of the magnetic field strength, $B \leq 0.75$ T, the pitch parameter of the helical coils, $1.197 \leq \gamma_c \leq 1.254$ and the magnetic axis position in vacuum, $R_{\text{ax}}^{\text{vac}} = 3.50 \sim 3.90$ m. Recently, the high beta experiments of LHD are mainly carried out with $B = 1$ T and $R_{\text{ax}}^{\text{vac}} = 3.56$ m in order to produce high beta plasmas in the lower collisionality region. The configurations with $R_{\text{ax}}^{\text{vac}} < 3.60$ m are called 'inward shifted configurations' since the standard $R_{\text{ax}}^{\text{vac}} = 3.60$ m. In this study, it is intended to investigate how the high beta is achieved by comparing the thermal transport coefficients in the plasmas with different β , γ_c , heating schemes, fueling methods and so on.

The thermal transport coefficients χ^{exp} is evaluated with the TASK4LHD system [3], where the power balance analysis in the steady state is made by TR-snap which is a modification of one module in TASK code [4], TR by including the 3D equilibrium. Then, χ^{exp} is compared with $g_{\text{ren}\chi}^{\text{int}} \chi^{\text{ISS04}}$, where $g_{\text{ren}\chi}^{\text{int}}$ is a renormalization factor for transport coefficients, which corresponds to the renormalization factor, f_{ren} in ISS04 and represents the effects of devices or configurations. The coefficient $g_{\text{ren}\chi}^{\text{int}}$ includes the effect of the change of the magnetic configuration due to the increment in beta.

From the first results, the ratio $\chi^{\text{exp}} / (g_{\text{ren}\chi}^{\text{int}} \chi^{\text{ISS04}})$ is compared with unity, where the transport property is similar to the ISS04 scaling, at the normalized average minor radius $\rho = 0.5, 0.7$ and 0.9 . In a high beta plasma of the volume-averaged beta value, $\langle \beta \rangle = 3.4\%$ which were produced in the magnetic configuration of $B = 1$ T, $\gamma_c = 1.254$ and $R_{\text{ax}}^{\text{vac}} = 3.56$ m and with the gas-pu fueling, $\chi^{\text{exp}} / (g_{\text{ren}\chi}^{\text{int}} \chi^{\text{ISS04}})$ becomes smaller than unity at $\rho = 0.5$ and 0.7 . This indicates reduction in thermal transport at main plasma region in the beta range around $\langle \beta \rangle \simeq 3\%$.

- [1] H. Yamada *et al.*, Nucl. Fusion **45**, 1684 (2005).
- [2] H. Funaba, K.Y. Watanabe, *et al.*, Plasma Fusion Res., **3**, 022 (2008).
- [3] R. Seki, H. Funaba, *et al.*, Plasma Fusion Res., **6**, 2402081 (2011).
- [4] A. Fukuyama, *et al.*, Proc. of 20th IAEA Fusion Energy Conf. (Villamoura, Portugal, 2004) IAEA-CSP-25/CD/TH/P2-3.

Heat Transport Characteristics of High Temperature Discharges in LHD - Dependence on Hydrogen/Helium Ratio -

K. Nagaoka^{1,2}, H. Takahashi^{1,2}, K. Tanaka¹, M. Osakabe^{1,2}, S. Murakami³, M. Yokoyama¹, K. Fujii⁴, H. Nakano^{1,2}, H. Yamada^{1,2}, Y. Takeiri^{1,2}, K. Ida^{1,2}, M. Yoshinuma^{1,2} and the LHD experiment group

¹National Institute for Fusion Science, Toki, 509-5292, Japan

²SOKENDAI(The Graduate University for Advanced Studies), Toki, 509-5292, Japan

³Department of Nuclear Engineering, Kyoto University, Kyoto 606-8501, Japan

⁴Department of Mechanical Engineering and Science, Kyoto University, Kyoto 615-8540, Japan

Deuterium experiment is planned in the Large Helical Device (LHD) project, and the isotope effect is one of the most important subjects in the deuterium experiment. The ion heat transport is expected to be improved by the isotope effect due to the reduction of damping rate of zonal flow [1].

In order to investigate the physics mechanism of the isotope effect, the comparison of the ion heat transports of high temperature discharges (ion ITB plasmas) [2-3] between the helium dominated and hydrogen dominated plasmas in LHD. The central ion temperature is higher in helium dominated plasma than that in hydrogen dominated plasmas, while electron temperatures are almost identical between them, which are shown in Fig. 1. The transport analysis indicates that the ion heat transport increases with the ratio of hydrogen ions (n_H/n_{H+He}), while the turbulent characteristics are almost unchanged. The heating efficiency, impurity content, neutral density profile will be presented in detail. The comparison of heat transport in the electron ITB plasma will be also discussed in the paper.

- [1] T. H. Watanabe, et al., Nucl. Fusion **51** 123003 (2011).
 [2] K. Nagaoka, et al., Nuclear Fusion **51** 083022 (2011).
 [3] H. Takahashi, et al., Nuclear Fusion **53** 073034 (2013).

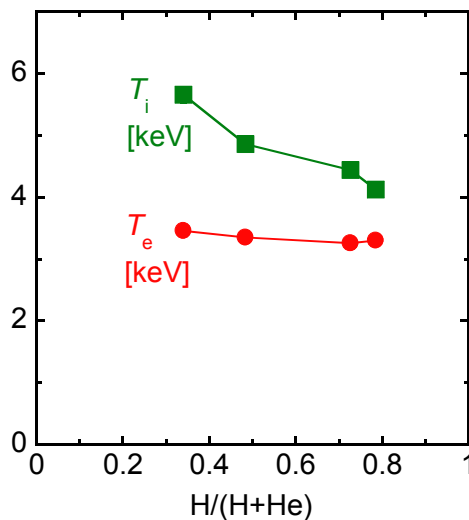


Figure 1. The central ion-temperature and electron-temperature as a function of hydrogen ration (n_H/n_{H+He}). The plasma density is $n_e = 1.3 \times 10^{19} \text{m}^{-3}$.

Analysis of LHD NBI-plasma interaction with upgraded FIT3D module of TASK3D-a analysis transport suite

P. Vincenzi^{1,2}, S. Murakami³, M. Osakabe⁴, R. Seki⁴, M. Yokoyama⁴, T. Bolzonella¹

¹*Consorzio RFX, Corso Stati Uniti 4 - 35127 Padova, Italy*

²*Università degli Studi di Padova, 35122 Padova, Italy*

³*Department of Nuclear Engineering, Kyoto University, Kyoto 606-8501, Japan*

⁴*National Institute for Fusion Science, 322-6 Oroshi-cho, Toki 509-5292, Japan*

LHD [1] is a superconducting helical device running at NIFS. The experiment is equipped with different auxiliary heating systems such as electron cyclotron resonance heating (ECRH), ion cyclotron resonance heating (ICRH) and neutral beam injection (NBI). 5 NBI systems currently working with H gas and carrying a maximum total power of 28MW are installed: 2 perpendicular positive injectors (40-50 keV) and 3 tangential negative injectors (180-190 keV). At present it is the only machine worldwide running negative NBI systems.

TASK3D-a analysis suite [2] is a tool for interpretative transport analysis of LHD experiments, built for the analysis of hydrogen and multi-ion species plasma [3, 4]. FIT3D is the module of TASK3D-a code which performs the analysis of LHD NBI-plasma interaction, calculating radial profiles of NBI absorbed power, beam pressure, beam source and induced momentum.

LHD will be run with deuterium (D) gas in the next future instead of the current hydrogen (H) experiments, and at least 3 of the NBI systems will be upgraded to D neutral particle injection. For this reason an upgrade of TASK3D-a code has started to enable the analysis of D experiments. In particular FIT3D NBI code has been updated [5] with a more recent and comprehensive ionization cross section formula for treating NBI neutral particle ionization process by plasma and impurities [6], suitable for the case of D injection in D plasma. A routine which estimates the neutron production from background plasma and beam-plasma fusion reactions has been implemented too.

The upgrade of FIT3D with the improved ionization cross section allows also a detailed analysis of H discharges with relevant presence of He impurity. In recent similarity H experiments with different concentration of He, better confinement properties have been observed with He majority. The upgraded FIT3D code is here used to investigate how the different background gas composition influences the ionization of the NBI particles, in order to understand the contribution of NBI power deposition on the increased general confinement properties. First results indicate that the ionization of the injected neutral particles is not dramatically affected by the gas composition change and the ionization of the NBI does not seem to play a direct role in the observed confinement properties.

[1] O. Motojima et al, Nucl. Fusion 40 (2000) 599

[2] M. Yokoyama et al., Plasma Fusion Res. 8 (2013) 2403016

[3] A. Sakai et al., Plasma Fusion Res. 9, (2014) 3403124

[4] H. Yamaguchi and S. Murakami, Plasma Fusion Res. 9 (2014) 3403127

[5] P. Vincenzi et al., 42nd EPS Conf. on Plasma Physics (Lisbon, Portugal, 2015), P1.150, <http://ocs.ciemat.es/EPS2015PAP/pdf/P1.150.pdf>

[6] S. Suzuki et al, Plasma Phys. Control. Fusion 40 (1998) 2097

Design study for high spatial resolution of beam emission spectroscopy viewing from 6-O port on large helical device

H. Nakano, M. Yoshinuma, K. Ida

National Institute for Fusion Science, 322-6 Oroshi-cho, Toki 509-5292, Japan

Beam emission spectroscopy (BES) is one of the powerful diagnostics to measure local density with high time resolution for turbulence and transport studies in toroidal plasmas. BES systems has been installed several toroidal devices (PBX-M, DIII-D, CHS, LHD, etc.). Sample volume (SV) is defined by Doppler-shifted H-alpha emission (beam emission) region where line of sight (LOS) and neutral beam cross in the plasma. High spatial resolution of minor radius can be performed by aligning the SV along magnetic flux surface. To detect small scaled fluctuation, the SV has to be also aligned with magnetic field line. In BES on large helical device (LHD), although low frequency mainly less than 10 kHz and large scale fluctuations have been observed with some BES systems, high frequency and small scale fluctuations have not been detected. Candidates of reasons for this are followings: the magnetic field line curvature changes along toroidal direction, and accessibility of LOS to the plasma is not high due to complicate vacuum chamber and large distance between the plasma and ports. Recently, we designed a new BES system where the emission from the tangential neutral beam of beam line 3 (BL3) on 7-T port in the plasma was viewing from the 6-O port through mirrors. The LOS of this BES was set mostly along the magnetic field in periphery plasma. Measure region is limited until outer area of 0.8 in normalized minor radius due to prevent the final mirror from touching with main plasma. The calculated spatial resolution was around 0.03 in normalized minor radius. An angle between the LOS and BL3 is 32 degree. When the beam is injected with energy of 188 keV which is maximum beam energy, the Doppler shift is 11 nm which is enough far to separate the beam emission from background H-alpha.

Preliminary design of an imaging bolometer for W7X

Byron J. Peterson^{a,b}, Daihong Zhang^c, Marcin Jakubowski^c, Yuhe Feng^c, Ryuichi Sano^a,
Kiyofumi Mukai^{a,b} and the W7X experiment group.

^a National Institute for Fusion Science, 322-6 Oroshi-cho, Toki 509-5292, Japan

^b SOKENDAI (The Graduate University for Advance Studies), 322-6 Oroshi-cho, Toki 509-5292, Japan

^c Max Planck Institute for Plasma Physics, Greifswald, Germany

The InfraRed imaging Video Bolometer (IRVB) measures plasma radiation images, which can be directly compared with the results of impurity radiation models to provide a quantitative understanding of the spatial distribution of the plasma radiation [1]. In a three-dimensional (3D) device such as W7X, the two-dimensional (2D) images provided by the IRVB are necessary to understand the complicated divertor radiation pattern. The ten-fold W7X divertor is divided into two sections, designated as the ‘low iota’ divertor and the ‘high iota’ divertor, referring to the magnetic configuration under which the divertor flux to those sections is dominant. In this paper we give information on the design of the imaging bolometer for the ‘high iota’ divertor from the AEM30 port of W7X. This design assumes a 640 x 480 pixel, 30 fps, 100 mK, IR camera imaging the IRVB foil. The bolometer camera consists of a 9 cm x 7 cm x 2 micron thick Pt foil blackened with graphite which is located 119 mm from a 5.2 mm x 5.2 mm aperture. This provides a view of almost the entire ‘high iota’ divertor as shown in Figure 1. The 8 cm x 6 cm central section of the foil is divided into 20 x 15 IRVB channels each consisting of 726 IR camera pixels. Using a previously derived expression [1] the noise equivalent power of the IRVB is given as 90 microwatts/cm². Assuming 5 MW of radiated power uniformly emanating from the 30 m³ plasma, the signal level is estimate as 3 mW/cm² giving a signal to noise ratio of 33. In the paper more details and ongoing work on the design of an IRVB for the ‘low iota’ divertor region and corresponding synthetic images derived from impurity transport models will be presented. This work was supported by NIFS budget code ULHH026 and the NIFS International Collaboration budget.

[1] B. J. Peterson *et al.*, Rev. Sci. Instrum. **74** (2003) 2040.

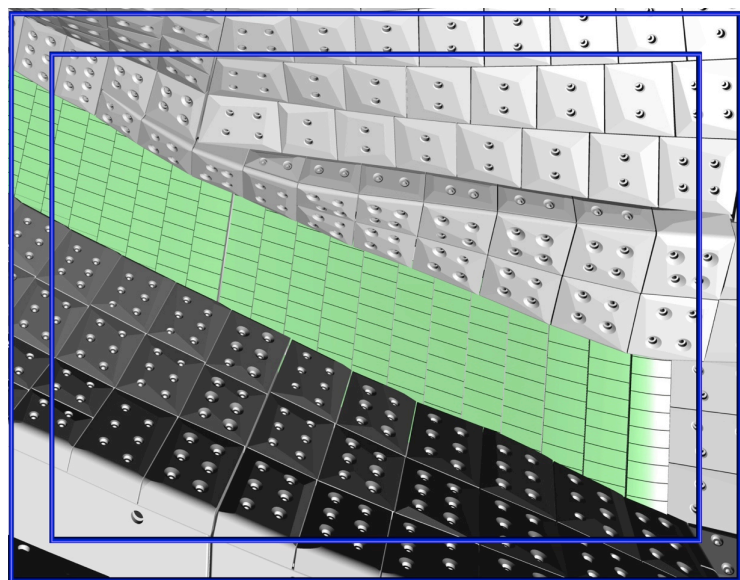


FIG. 1. Designed field of view of IRVB at Port AEM30 in W7X. The inner blue rectangle corresponds to the 6 cm x 8 cm central portion of the foil.

Development of in-situ calibration system for foil detector of infrared imaging video bolometer in Large Helical Device

K. Mukai^{a,b}, B. J. Peterson^{a,b}, R. Sano^a

^a National Institute for Fusion Science, 322-6 Oroshi-cho, Toki 509-5292, Japan

^b SOKENDAI (The Graduate University for Advance Studies), 322-6 Oroshi-cho, Toki 509-5292, Japan

The InfraRed imaging Video Bolometer (IRVB) is a useful diagnostic for the measurement of plasma radiation profiles [1] to investigate phenomena such as plasma detachment [2]. The fundamental schematic of an IRVB is a combination of a pinhole camera and an IR camera. The profiles of the plasma radiation are collimated by an aperture (e.g. 8 mm × 8 mm) in the pinhole camera and are projected onto a thin platinum foil (e.g. 130 mm × 100 mm, $t = 2.5 \mu\text{m}$) as a two-dimensional temperature distribution. The IRVB has many channels by dividing the large foil into many bolometer pixels (~ 1000). The foil detector is coated by carbon on both sides to increase the emissivity, then, the distribution can be observed from the opposite side of the foil using an IR camera as an IR image. Considering the heat-diffusion effect of the foil, the heat characteristics of each bolometer pixel should be calibrated to estimate the radiation profile using the two-dimensional heat diffusion equation. For the application of the IRVB measurement to the neutron environment of deuterium plasma experiments in the Large Helical Device (LHD), the effect of the neutron irradiation on the heat characteristics should be investigated. In this study, an in-situ calibration system was developed.

The schematic of the in-situ calibration system [3] is shown in Figure 1. A periscope system must be applied to protect the IR camera detector from the damage by the direct irradiation of X-rays, neutrons, and gammas from the plasma. A He-Ne laser as the known radiation power source is injected to the foil. Laser irradiation points can be scanned using a mirror with two motorized goniometers, which correspond to the center of the each bolometer pixel. The visible laser can be transmitted to the foil and the IR radiation from the foil can be reflected to the IR camera using a hot mirror since it has the transmittance of $> 85\%$ for visible light and the reflectance of $> 95\%$ for IR signal. The results of the characteristic tests of important components and the effect of uniform and reproducible graphite coatings by vacuum evaporation on the heat characteristics will be presented.

[1] B. J. Peterson *et al.*, Rev. Sci. Instrum. **74** (2003) 2040.

[2] K. Mukai *et al.*, Nucl. Fusion **55** (2015) 083016.

[3] K. Mukai *et al.*, Rev. Sci. Instrum. **85** (2014) 11E435.

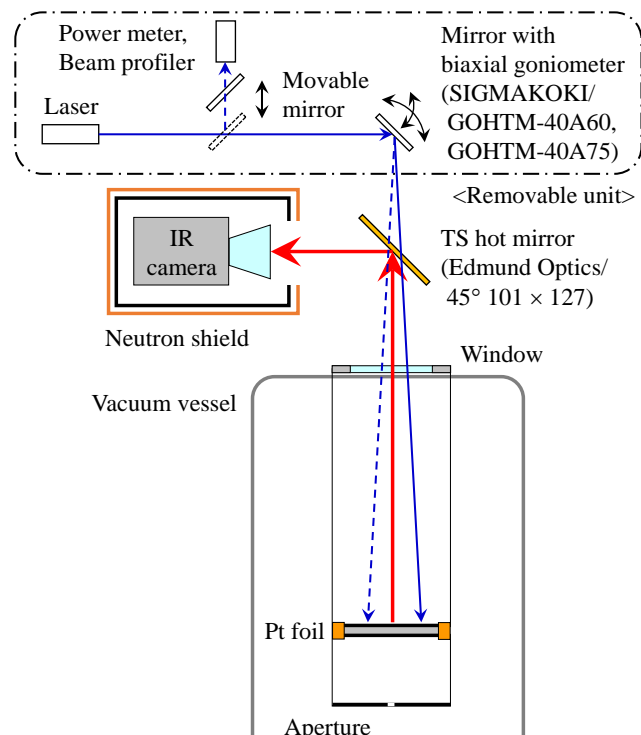


FIG. 1. Schematic of in-situ calibration system for IRVB foil detector. Thin arrows and thick arrows indicate paths of visible light and IR, respectively.

Improvement of 3D radiation imaging using Euclidean distance from model phantom in LHD

Ryuichi Sano^{1,2}, Masaru Teranishi³, Naofumi Iwama¹, Masahiro Kobayashi^{1,4},
Byron J. Peterson^{1,4}, Kiyofumi Mukai^{1,4}

¹*National Institute for Fusion Science, 322-6 Oroshi-cho, Toki, Gifu 509-5292, Japan*

²*JSPS Research Fellow*

³*Hiroshima Institute of Technology, 2-1-1, Miyake, Saeki-ku, Hiroshima Japan*

⁴*SOKENDAI (The Graduate University for Advanced Studies), Hayama, Kanagawa 240-0193, Japan*

Radiation which is emitted from impurities is one of the major paths of power loss from fusion plasmas. Heat load reduction on the divertor in future devices requires the detached plasma produced by the enhancement of the radiation loss from the divertor plasma. Because of a 3D complicate structure of radiation from the outside of the last closed flux surface (LCFS), a 3D understanding of radiation is necessary for radiation control. Therefore, the study of 3D dynamic behavior of the plasma radiation is important for the control of fusion plasmas. In LHD, 3D radiation imaging using four InfraRed imaging Video Bolometers (IRVBs) and standard solvers for inverse problems had been developed. Current reconstructed images by 3D radiation imaging still have artifacts caused by the ill-conditions of Field of View (FoV) for the IRVBs. To avoid this kind of artifact, mechanical and numerical approaches for improvement of the 3D radiation imaging are in advance. The mechanical approach is an addition of IRVB. Numerical approach is the use of alternative solvers for image reconstruction. In this study, an alternative solver using model phantoms is applied for the 3D radiation imaging and numerically examined.

The alternative solver employs model phantoms in the constraint for image reconstruction. In the solver, the Euclidean distance between the model phantom and the reconstructed image is employed as a penalty function. Image reconstructions of a simulated radiation phantom by EMC3-EIRENE have been carried out using various model phantoms. The image reconstruction using an appropriate model phantom, such as the simulated phantom itself, provides a sufficiently smaller amount of artifacts. Even with use of inaccurate model phantoms such as a simple elliptic cylinder, the solver also provide smaller amounts of artifacts than the standard solver. These results indicate that the alternative solver works well in the 3D radiation imaging. The method of model selection for image reconstruction from experimental data will also be presented at the meeting.

[1] B. J. Peterson et al., *Rev. Sci. Instrum.* **74**, 2040 (2003).

[2] R. Sano et al., *Plasma Fusion Res.* **7**, 2402041(2013).

[3] R. Sano et al., *Plasma Science, IEEE Transactions on*, **42**, 10, 2860 (2014).

Design and evaluation of broad-band high pass filter using metal perforated plates with circular holes

A. Tani, M. Koga, H. Tsuchiya^a, Y. Nagayama^a

Graduate School of Engineering, University of Hyogo, 2167 Shosha, Himeji 671-2280, Japan

^a *National Institute for Fusion Science, 322-6 Oroshi-cho, Toki 509-5292, Japan*

e-mail: er15e007@steng.u-hyogo.ac.jp

ECE (Electron Cyclotron Emission) measurement is useful method in observation of electron temperature profile and its local fluctuations. Generally ECE is detected by heterodyne type filter bank radiometer. The frequency band of radiometer is not broad. It is assumed that two radiometer systems with different local frequency are used for detection of the broad-band ECE in the high-magnetic devices. It is necessary to divide the RF with high precision before radiometer detection to avoid the gain loss. In the case of LHD (Large Helical Device), frequency range of ECE is 50GHz-150GHz. The broad-band high pass filter for such frequency (E-band, W-band) is not commercially available. Therefore, we have developed the broad-band high pass filter originally. The schematic of the filter is shown in Fig.1.

The purpose of this study is to design the porous metal plane type broad-band filters (cut off frequency is 44GHz), and to evaluate their characteristics by 3D-numerical electromagnetic field analysis (E-field). The validity of the numerical analysis is guaranteed by the good agreement with calculated result and measured results shown as fig.2. It is found that the frequency characteristics depend on the filter thickness (see fig.3), and the appropriate thickness is in the range of 0-0.5mm.

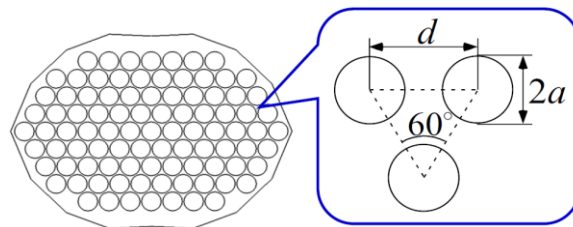


Fig.1 Schematic of the metal perforated plate with circular holes.

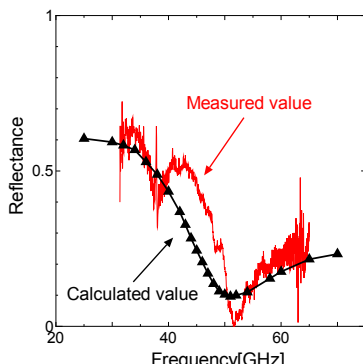


Fig.2 Frequency characteristic of calculated and measured reflectance. (Filter thickness is 1mm.)

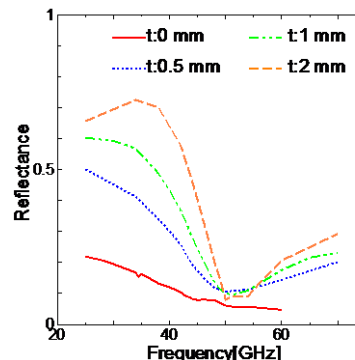


Fig.3 Filter thickness dependence of reflectance.

Development of Electron Bernstein Emission Diagnostic for Heliotron J and LHD

K. Nagasaki, H. Igami^a, G. M. Weir, Y. Nakamura^b, S. Kamioka^b, K. Sakamoto, H. Okada, T. Minami, S. Kado, S. Kobayashi, S. Yamamoto, S. Ohshima, S. Konoshima, N. Kenmochi^b, Y. Ohtani^b, F. Volpe^c, N. Marushchenko^d, S. Kubo^{a,e}, Y. Goto^e, T. Mizuuchi

Institute of Advanced Energy, Kyoto University, Uji, Kyoto 611-0011, Japan

^a *National Institute for Fusion Science, 322-6 Oroshi-cho, Toki 509-5292, Japan*

^b *Graduate School of Energy Science, Kyoto University, Uji, Kyoto 611-0011, Japan*

^c *Department of Applied Physics and Applied Mathematics, Columbia University, New York, USA*

^d *Max-Planck-Institut für Plasmaphysik, EURATOM Association, D-17491, Greifswald, Germany*

^e *Department of Energy Engineering and Science, Nagoya University, Nagoya, 464-8603, Japan*

e-mail address: nagasaki.kazunobu.4x@kyoto-u.ac.jp

Use of electron Bernstein Waves (EBWs) is attractive for heating/current drive, electron temperature diagnostic [1] and magnetic pitch angle profile measurement [2] at high densities where electron cyclotron waves are not accessible. The EBWs have advantage of no density limit and high optical thickness even at low electron temperature. We have been studying Electron Bernstein Emission (EBE) in the Heliotron J and LHD devices in order to measure electron temperature at high density plasmas. A ray tracing code, KRAY, has been developed, which evaluates the power absorption and emission profiles via O-X-B process. The code solves the radiative transfer equations under geometrical optics approximation in the three-dimensional magnetic field structure [3]. The calculation results in the Heliotron J configuration show that the existing EC launcher antenna has an access window for the O-X conversion for Ka-band (24-42 GHz), and the radiation is located at the core region, $r/a \leq 0.5$, for $B=1.25$ T and $n_e=2 \times 10^{19}$ m⁻³. In LHD, a ray tracing calculation also shows that a current horizontal ECRH launcher has an access window for the O-X conversion for the same frequency band. These indicate that a radiometer of Ka-band frequency range is applicable to both the Heliotron J and LHD devices. The designed EBE measurement system consists of a Gaussian optics antenna, a waveguide transmission line and a heterodyne radiometer. As the radiometer is connected to the transmission line and steerable antenna of current ECRH/ECCD system, angular scan is possible to find the best conversion efficiency to measure the EBW radiation. Accessing the EBE by means of B-X-O conversion requires the plasma densities over around 1×10^{19} m⁻³ which are routinely obtained in the Heliotron J and LHD devices. The status of EBE measurement setup will be presented.

[1] F. Volpe, H. P. Laqua and the W7-AS Team, Rev. Sci. Instrum. **74** (2003) 1409

[2] F. Volpe, Rev. Sci. Instrum. **81** (2010) 10D905

[3] K. Nagasaki, N. Yanagi, Plasma Phys. Control. Fusion **44** (2002) 409

Validation of the Digital Correlation ECE measurement technique using low frequency fluctuation in LHD

H. Tsuchiya, S. Inagaki^a, T. Tokuzawa, N. Tamura, Y. Nagayama

National Institute for Fusion Science, 322-6 Oroshi-cho, Toki 509-5292, Japan

^a Research Institute for Applied Mechanics, Kyushu University, Kasuga 816-8580, Japan

We have proposed and developed the Digital Correlation Electron Cyclotron Emission (DCECE) Measurement Technique [1] with a Giga Hertz sampling digitizer [2] in LHD. In the conventional radiometer type ECE measurement [3], the power detector with filter bank for intermediate frequency (IF) is used. In case of the ECE measurement in the magnetized plasma, generally, the frequency band is up to tens of Giga Hertz. Instead of filter bank system, the IF digitizing technique is applied for DCECE. The conceptual diagram of DCECE is shown in Fig.1. One of the advantages of this technique is to enable to choose the spatial and temporal resolutions after the plasma experiment. This characteristic is considered to be useful for the study of the multiscale dynamics which should determine the whole confinement in plasmas.

The IF digitizing technique was applied to the ECE of LHD plasmas. We can reconstruct the electron temperature fluctuation profile and compare the analysis results of conventional radiometer type ECE and DCECE about 5 kHz fluctuation as shown in Fig.2. The data length of DCECE is 51 msec. The sampling rate is 10GHz. The IF resolution is 166MHz which corresponds to 3mm resolution in radial direction. It is confirmed that several kHz fluctuation with strong correlation is detected more sharply than conventional radiometer ECE. It is also found that the aspect of fourie analysis result depends not only on the sampling rate of digitizer but also the parameter of DCECE analysis such as IF resolution and time resolution. In this presentation, the parameter dependence will be shown as example of the analysis results of actual LHD plasma data.

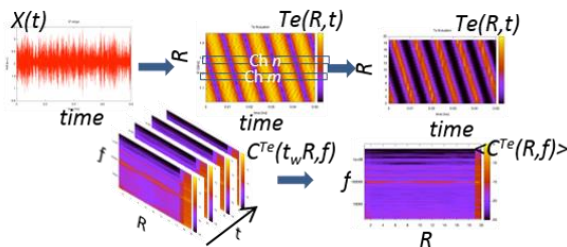


Fig.1 Conceptual diagram of DCECE analysis.

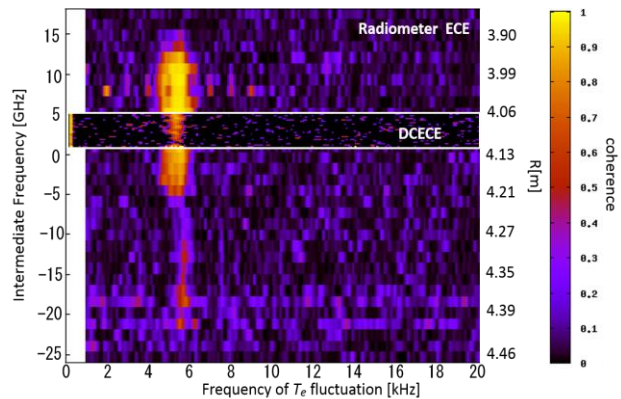


Fig.2 The coherence profile of T_e fluctuation by conventional radiometer type ECE and DCECE. The profile by DCECE (IF= 0.5 to 4.5GHz) is drawn on the profile by radiometer ECE (IF=-25GHz to 17.5GHz). The IF resolution (left axis) is 166MHz in DCECE, and 1GHz in radiometer ECE. The radial position R [m] (right axis) is derived from ECE frequency.

[1] H. Tsuchiya, *et al.*, Plasma Fusion Res. **9**, (2014) 021.

[2] <http://teledynelecroy.com/>

[3] Y. Nagayama, *et al.*, Rev. Sci. Instrum. 70, (1999) 1021

Development of OXB mode conversion window searching method using inverse emission process in the LHD

Y. Goto^a, S. Kubo^{a,b}, H. Igami^b, M. Nishiura^c, T. Shimozuma^b, Y. Yoshimura^b, H. Takahashi^b, T. Tsujimura^b, R. Makino^b, T. Mutoh^b and the LHD experiment group

^aDept. of Energy Eng. and Sci., Nagoya Univ., Furo-cho. Chikusa-ku. Nagoya, 464-8603, Japan

^bNational Institute for Fusion Science, 322-6 Oroshi-cho, Toki, 509-5292, Japan

^cGraduate School of Frontier Sciences, The University of Tokyo, Kashiwanoha, Kashiwa, 277-8561, Japan

goto-yuuki14@ees.nagoya-u.ac.jp

Electron cyclotron resonance heating (ECRH) using an Electron Bernstein Wave (EBW) is an effective method for the RF heating of the over-dense plasma. The EBW can be excited via the ordinary(O)-extraordinary(X)-EBW(B) (OXB) mode conversion process from low field side. The OX mode conversion window is known to be narrow because the conversion rate depends on the propagating angle of the EC wave. In the Large Helical Device (LHD), EBW heating experiments using the OXB mode conversion process have been carried out, but the achieved heating efficiency had been stayed at almost 10 percent. For improving the heating performance and the experimental efficiency, it is essential to tune the injection direction precisely to aim the OXB mode conversion window experimentally. The contour lines in Fig. 1(a) indicate the calculated OX mode conversion efficiency projected on a lower port (1.5L port) antenna target plane. Since a thermally excited EBW in the plasma core region can be emitted as the O-mode via the inverse OXB mode conversion mechanism, a method to find out the window by measuring the O-mode emission intensity near the heating frequency using a fast steerable antenna is developed. This method can be used as a reference to execute a real time optimization of the injection angle in the future. As a first step, a change of the emission intensity near 77 GHz O-mode was measured by scanning the receiving angle. Figure 1(b) shows the time variation of the radiation intensity when the antenna is scanned along the path indicated by a straight line in Figure 1(a). The increase in the radiation intensity near this region is confirmed experimentally when an over-dense plasma is sustained.

Antenna scan time is shifted by 0.4 sec for both shots, and the increase of the radiation intensity is shifted correspondingly. Since plasma parameters for both shots are kept identical and constant from $t=4.7$ to 6.3 sec, we can conclude this radiation is distributed spatially. A ray-tracing code is extended to simulate the electron cyclotron emission (ECE) including the emission originated from the EBW (EBE) to understand the observed change in the radiation using experimentally obtained plasma profiles for each time slice during the antenna steering.

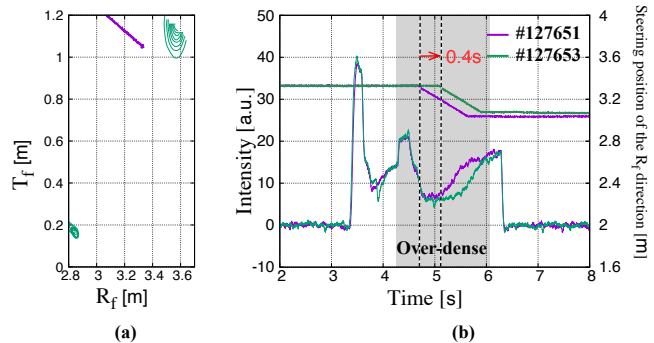


Figure 1: (a) Calculated mode conversion efficiency and steering path. (b) Time variation of the radiation for the shots 127651 and 127653.

Magnetic flux surface measurements on TOKASTAR-2

Y. Shimooka, H. Arimoto, T. Fujita, A. Okamoto, T. Sakito, H. Itou,
K. Muraoka, R. Sugioka, K. Yasuda, R. Yokoyama

*Department of Engineering and Science, Nagoya University,
Furo-cho, Chikusa-ku, Nagoya 464-8603, Japan*

shimooka-yuusuke14@ees.nagoya-u.ac.jp

TOKASTAR-2 device was constructed to study the influence of helical magnetic field application to the tokamak plasma and the influence of plasma current to helical plasma [1]. It has two coil systems, one for tokamak and the other for stellarator.

The stellarator coil system is designed to make closed magnetic flux surfaces without any plasma current. However, due to the influence of manufactural accuracy and installational accuracy of coils, the location and shape of the helical magnetic flux surface can be deviated from the analytical one. The object of this study is to measure the magnetic flux surfaces experimentally.

There are mainly two methods to measure magnetic flux surface, one using a fluorescent screen [2] and the other using a probe [3] for detecting electrons emitted by an electron gun. The method using a fluorescent screen can trace a magnetic flux surface faster than the other one and does not need a mechanical driving system. So, we examined whether the method using a fluorescent screen can be applied to TOKASTAR-2.

Figure 1 shows the conditions for detecting fluorescence in the preliminary experiment done in a test chamber without magnetic field. P15 and P24 (ZnO:Zn) are used for the fluorescence agent. We detected fluorescence by eye. It was found that the electron energy needed to be larger than about 80 eV to detect the fluorescence of P15 and P24.

Figure 2 shows the orbit of electrons with different energies in the typical magnetic configuration condition. It was found that the orbit of the electron with 80 eV differs largely from the magnetic flux surface. From these results, we concluded that the method using a fluorescent screen cannot be applied to TOKASTAR-2.

At the present, we are preparing the method using a probe. It is expected that the electron energy needed for this method is lower than for the method using a fluorescent screen. The required electron energy will be examined in a test chamber while a mechanical driving system of the probe will be developed.

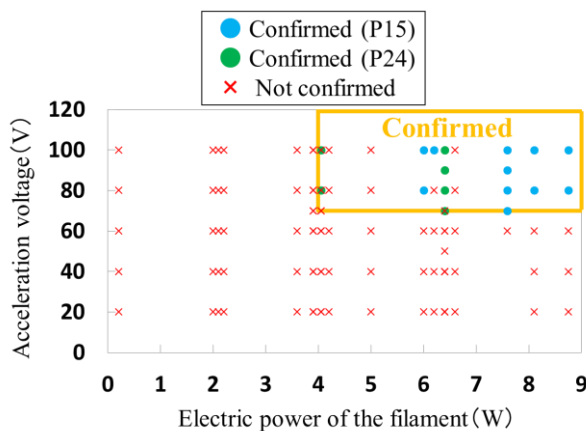


Fig. 1. Conditions for detecting fluorescence in the preliminary experiment.

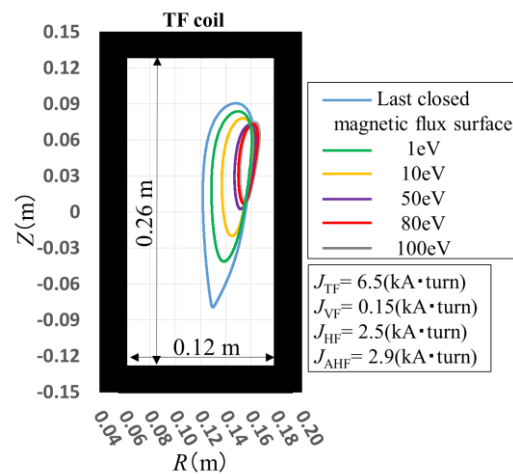


Fig. 2. Orbit of electrons in the typical magnetic configuration condition.

- [1] K. Yamazaki et al., J. Plasma Fusion Res. SERIES 8 1044 (2009).
- [2] R.J. Colchin et al., Review of Scientific Instruments 60 2680 (1989).
- [3] R.M. Sinclair et al., Review of Scientific Instruments 41 1552 (1970).

The development of 2D potential profile measurement with heavy ion beam probe on the Large Helical Device

A. Shimizu^a, T. Ido^{a,b}, M. Nishiura^c, H. Takahashi^a, H. Igami^a,
Y. Yoshimura^a, S. Kubo^{a,b,d}, T. Shimozuma^a, S. Kato^a, M. Yokoyama^{a,d}
and the LHD Experiment Group

^aNational Institute for Fusion Science, 322-6 Oroshi-cho, Toki 509-5292, Japan

^bGraduate School of Engineering, Nagoya University, Chikusa, Nagoya 464-8603, Japan

^cGraduate School of Frontier Science, The University of Tokyo, Chiba 277-8561, Japan

^dGraduate University for Advanced Studies (Sokendai), 322-6 Oroshi-cho, Toki 509-5292, Japan

e-mail: akihiro@nifs.ac.jp

Heavy Ion Beam Probe (HIBP) is a powerful diagnostic tool to study physics related to the electric field in magnetically confined plasmas. By using this tool, we can measure equilibrium and fluctuation of electrostatic potential, and density fluctuation simultaneously in the core region of high temperature plasma. For this unique advantage, many HIBP diagnostic systems have been installed on various devices, such as tokamaks, reversed field pinches, mirror devices, and helical devices.

In the Large Helical Device (LHD), HIBP system was installed and has been developed to study E_r formation physics in the plasma [1]. Although the large size ($R \sim 3.9$ m, $a \sim 0.6$ m) and strong magnetic field strength (~ 3 T) of LHD increase the difficulty of HIBP measurements, we have successfully measured equilibrium potential, and fluctuations of potential and density, in LHD by using tandem accelerator and sensitive micro channel plate detector [2,3].

For HIBP diagnostic, by changing the incident angle of the probe beam, observation point can be changed to obtain one-dimensional profile of plasma potential. If the probe beam energy is additionally changed, two-dimensional potential profile can be measured. However, in LHD-HIBP system, the beam transport line is long (~ 20 m), therefore, beam orbit in the beam transport line has to be adjusted, when the beam energy is changed. This work requires adjusting many deflector voltages and consumes a lot of time. In order to reduce the time for beam adjustment, a PC-based automatic beam adjustment system was developed. By using this system, the alignment of the beam in the beam line can be completed during a discharge cycle of LHD (three minutes), and two-dimensional equilibrium electrostatic potential profile was successfully measured by changing the beam energy shot-to-shot [4]. To measure the two-dimensional potential profile in magnetic islands, trial experiments were conducted by applying rmp field. Although clear island structure was not obtained, a partial flat area was seen in the potential profile. Details of the automatic beam adjustment system and recent analysis of 2-D potential measurement experiments are reported.

- [1] T. Ido, A. Shimizu, M. Nishiura, A. Nishizawa, S. Katoh, K. Tsukada, M. Yokota, H. Ogawa, T. Inoue, Y. Hamada et al., Rev. of Sci. Instrum. **77** (2006) 10F523.
- [2] T. Ido, A. Shimizu, M. Nishiura, S. Nakamura, S. Katoh, H. Nakano, Y. Yoshimura, K. Toi, K. Ida, M. Yoshinuma et al., Nucl. Fusion **51** (2011) 73046.
- [3] A. Shimizu, T. Ido, M. Nishiura, R. Makino, M. Yokoyama, H. Takahashi, H. Igami, Y. Yoshimura, S. Kubo et al., Plasma and Fusion Res. **8** (2013) 2402122.
- [4] A. Shimizu, T. Ido, M. Kurachi, R. Makino, M. Nishiura et al., Rev. Sci. Instrum. **85** (2014) 11D853.

X-Y-t Edge Plasma Reconstruction with Digital Imaging Technique

M. Irie, M. Kubo-Irie^a

Waseda University, 3-4-1 Ohkubo, Shinjyuku Tokyo 169-8555, Japan

^a *The Open University of Japan, 2-11, Wakaba, Mihamaku, Chiba 261-8586, Japan*

The striking high speed CCD camera technique developed under Dr. A. SYKES in late '80s, in START device (Small Tight Aspect Ratio Tokamak : CULHAM laboratory) established the new era in the history of plasma boundary diagnostics.

The refined system has been applied to the spherical tokamaks in early last decade by Prof. N. Nishino and explains the "Actual Plasma Behaviour" in critical issues of the Fusion Engineering, e.g. "L to H transition", "the Edge Local Mode".

In 2013, Dr. L. Zang [1] monitored the movement of edge filamentary structure during Supersonic Molecular-Beam Injection in Heliotron-J device run under Prof. T. Mizuuchi.

In this conference, we would like to mine further quantitative information from these movie data with the state of art "Digital Imaging Technique". This is the third approach to the Fusion Research based on the "Experiment-Simulation" in good old days established by Institute of Fusion Theory: Hiroshima Simulation Group, Prof. Tetsuya SATO and his colleagues.

Reference.

[1] L. ZANG, N. NISHINO, T. MIZUUCHI *et al.*, Plasma Fusion Res. **8** (2013) 1402066

Estimation of total carbon radiation at each ionization stage of C^{2+} to C^{5+} ions in Large Helical Device

H. M. Zhang¹, S. Morita^{1,2}, T. Ohishi^{1,2}, I. Murakami^{1,2}, X. L. Huang¹ and M. Goto^{1,2}

¹Graduate University for Advanced Studies, Toki 509-5292, Gifu, Japan

²National Institute for Fusion Science, Toki 509-5292, Gifu, Japan

Abstract

A detached plasma has been successfully maintained by externally supplying $m/n=1/1$ magnetic island in Large Helical Device (LHD) without introduction of additional impurity gas puffing. The study on the carbon radiation during plasma detachment with edge magnetic island formation is very important to understand the physical mechanism of effective edge plasma cooling because the carbon radiation is believed to be a main part of the total radiation loss in high-density LHD discharges. The total radiation power of carbon ions at each ionization stage of C^{2+} to C^{5+} ions can be analyzed from line spectra of CIII to CVI measured with extreme ultraviolet (EUV: 10-500Å) and vacuum ultraviolet (VUV: 300-2400Å) spectrometers. The resonance lines of CIII (977.02Å, $2s2p - 2s^2$), CIV (1548.2Å, $2p - 2s$), CV (40.27Å, $1s2p - 1s^2$) and CVI (33.73Å, $2p - 1s$) are applicable to estimate the total radiation power at each ionization stage because the resonance transition occupies a considerably large percentage in the total radiation power at each ionization stage. The C^{2+} and C^{3+} ions exist outer side of ergodic layer and the C^{4+} and C^{5+} ions are located near LCFS. It is also very interesting to examine which carbon ions effectively work to create the plasma detachment. The spectral intensity from EUV spectrometers has been absolutely calibrated based on the bremsstrahlung measurement in previous studies, while the VUV spectrometer system has not been yet calibrated. As the first step of the present study, therefore, the spectral intensity from VUV spectrometers has to be calibrated by comparing the spectral intensities between EUV and VUV spectrometers. The ratio of resonance line intensity to total radiation power is calculated at each ionization stage of carbon ions using ADAS atomic code. The total radiation power from C^{2+} to C^{5+} ions can be then estimated by taking account of an effect of electron temperature.

Measurement of tokamak plasma with the external helical field using a high-speed camera in TOKASTAR-2

T. Sakito, H. Arimoto, T. Fujita, A. Okamoto, Y. Shimooka, H. Itou, R. Sugioka, K. Muraoka, K. Yasuda, R. Yokoyama

Department of Energy Engineering and Science, Nagoya University, Furo-cho, Chikusa-ku, Nagoya 464-8603, Japan

sakito-tatsuya14@ees.nagoya-u.ac.jp

TOKASTAR-2 device is designed and constructed to study tokamak-helical hybrid magnetic configuration (TOKASTAR configuration) [1]. The main purpose of TOKASTAR-2 experiment is to evaluate the effect of helical field application on tokamak plasmas and of the plasma current on compact stellarator configurations. The TOKASTAR-2 coil system consists of six kind of coils. The magnetic field strength in the plasma center is $B_t \sim 0.1$ T. To induce plasma current, electron cyclotron resonance (ECR) heating (2.45GHz) is used for the pre-ionization and the ECR injection power is ~ 1.4 kW.

To improve tokamak equilibrium control, we adjusted the charging voltage of the capacitor (V_{PVF}) after determining the optimal parameters of the capacitor for the Pulsed Vertical Field (PVF) coil circuit. In this study, the effect of helical field application on tokamak plasma is evaluated. The plasma position and shape are evaluated by light intensity distribution using a high-speed camera in the tangential direction.

Figure 1 shows the time evolution of the PVF coil current, Ohmic Heating (OH) coil current, one-turn voltage, plasma current of a tokamak discharge and that with the external helical field. Figure 2 shows the peak value and the duration of plasma current as a function of V_{PVF} . From Fig. 1 and Fig. 2, it is found that under the condition of vertical field ($V_{PVF} < 0.30$ kV), the duration and the plasma current of tokamak discharge were improved by the external helical field.

The plasma position was measured by a high-speed camera in the tangential direction, but the field of view was limited. So we are now preparing to expand the field of view using a mirror. In the conference, the result of helical field application on tokamak plasma in other conditions and measurement of plasma behavior by a high-speed camera will be presented.

[1] K. Yamazaki et al. J. Plasma Fusion Res. SERIES 8 (2009) 1044.

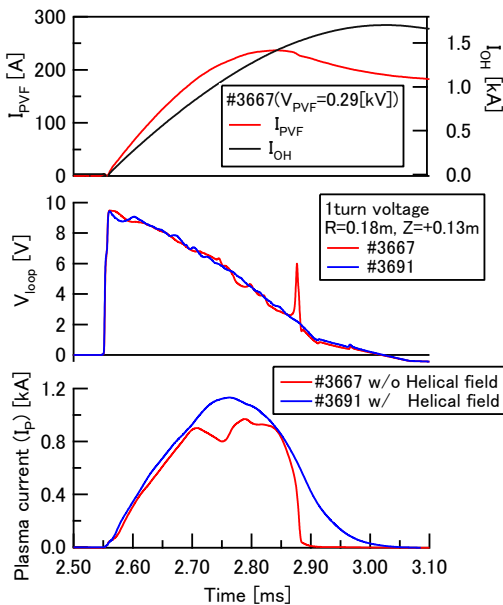


Fig.1 (Top) PVF coil and OH coil current (Middle) loop voltages at the outer legs of TF coil (Bottom) Plasma current

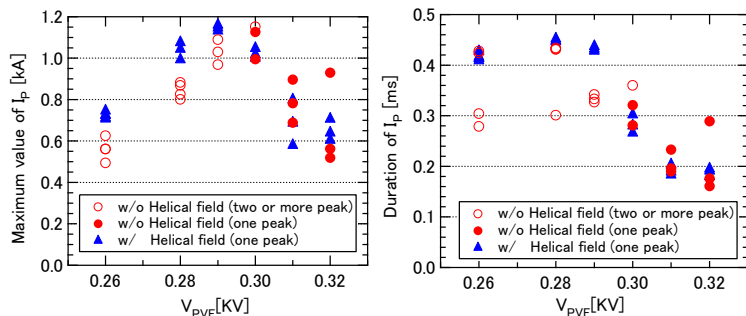


Fig.2 (Left) The peak value of plasma current and (Right) the duration of plasma current as function of the charging voltage of the capacitor for the PVF coil circuit.

Observation of Electron Density Fluctuations by Using the O-mode Microwave Imaging Reflectometry (O-MIR) in LHD

Y. Nagayama, H. Tsuchiya, Y. Soichiro^a, S. Hashimoto,
N. Ito^b, D. Kuwahara^c, S. Sugito^d, Z. B. Shi^e, M. Jiang^e

National Institute for Fusion Science, 322-6 Oroshi-cho, Toki 509-5292, Japan

^a *Faculty of Engineering Science, Kansai Univ., 3-3-35 Yamate-cho, Suita 564-8680, Japan*

^b *Ube National College of Technology, 2-14-1 Tokiwadai, Ube 755-8555, Japan*

^c *Tokyo University of Agriculture and Technology, 3-8-1 Harumi-cho, Fuchu 183-0057, Japan*

^d *Institute for Molecular Science, 38 Nishigo-Naka, Myodaiji, Okazaki 444-0867, Japan*

^e *Southwestern Institute of Physics, P.O.Box 432, Chengdu 610041, China*

Microwave Imaging Reflectometry (MIR) has been intensively developed in Large Helical Device (LHD) [1]. So far the 60 – 65 GHz X-mode MIR (X-MIR) had been developed in order to observe core plasma region in the case of hollow density profile, but the ion ITB plasma was not observable due to high field. In ion ITB plasmas in LHD, the electron density profile is peaked with the central density of $1 - 2 \times 10^{19} \text{ m}^{-3}$. Therefore the O-mode MIR (O-MIR) system has been newly developed in order to observe the ion ITB plasma. In O-MIR, the microwave with four frequencies are simultaneously illuminated the LHD plasma. The illumination wave frequency can be controlled between 26 – 35 GHz. So, the observable density is $0.84 - 1.5 \times 10^{19} \text{ m}^{-3}$. The imaging detector named Horn-antenna Mixer Array (HMA) is newly developed for the Ka-band microwave. In HMA, each printed circuit board (PCB) is installed between aluminum plates, each of which have half cut horn antenna array. The signal wave entering into the horn antenna is transduced from the waveguide to the micro-strip line by the fine-line transducer [2]. The signal wave is amplified by 12 dB before mixing in order to compensate the conversion loss (12dB) of the double balanced mixer (DBM). The half frequency of local wave is divided by Wilkinson power divider on PCB and is doubled by active doublers just before entering into DBM. The optical imaging system of O-MIR is much simpler than that of X-MIR since the local wave is delivered by cables. The sensitivity of O-MIR is significantly improved as the observed noise of O-MIR is 4 mV, while the noise of X-MIR is 800 mV. Intensity of detected power is calibrated by comparing reflections by a plane aluminum plate and by the form absorber (Eccosorb CV3F). By using O-MIR, we have observed electron density fluctuations in the ion ITB plasma and in the H-mode plasma. The k - ω spectra is obtained in the radial direction, the poloidal direction and in the toroidal directions by the use of two point cross power spectrum. Preliminary results are as follows: The density fluctuation near the plasma edge, which is incoherent in the L-mode phase, becomes coherent after L-H transition.

[1] Y. Nagayama, et al: Rev. Sci. Instrum. **83** (2012) 10E305.

[2] D. Kuwahara, et al: Rev. Sci. Instrum. **85** (2014) 11D805.

Examination of efficient electron Bernstein wave heating and measurement scenario with ray-tracing and full-wave calculations in LHD

H. Igami, A. Fukuyama^a, H. Idei^b, K. Nagasaki^c, Y. Goto^d, S. Kubo, T. Shimozuma, Y. Yoshimura, H. Takahashi, T. I. Tsujimura and R. Makino

National Institute for Fusion Science, 322-6 Oroshi-cho Toki 509-5292, Japan

^a*Department of Nuclear Engineering, Kyoto University, Nishikyo-ku, Kyoto 615-8530, Japan*

^b*Research Institute for Applied Mechanics, Kyushu University, 6-1 Kasuga-koen, Kasuga 816-8580, Japan*

^c*Institute of Advanced Energy, Kyoto University, Uji, 611-0011, Japan*

^d*Department of Energy and Technology, Nagoya University, Furo-cho Chikusa-ku Nagoya 464-8603, Japan*

Electron cyclotron resonance heating and current drive (ECRH and ECCD) in over dense plasmas where the electron density is more than the cutoff density are available with use of the electron Bernstein waves (EBWs) excited via the linear mode conversion process inside the plasma by launching the electromagnetic waves from the vacuum region [1]. When the electromagnetic waves are injected from the lower density side, they encounter the evanescent region. A part of the waves' energy can tunnel through the evanescent region and couple with the extraordinary (X-) mode in the higher density side that propagates toward the upper hybrid resonance (UHR) and couples with the EBWs there. It is important to tune the wave incident angle and polarization to obtain high coupling efficiency [2].

To describe the wave propagation around the evanescent region precisely the full wave analysis that solves the Maxwell's equation directly is required with taking into account the non-uniform plasma profiles and distribution of the wave electric field. We are developing a numerical code including TASK/WF2D code that solves the Maxwell's equation by finite elements method (FEM) in two-dimensional space. This numerical code can describe the wave propagation across the evanescent region with taking into account the non-uniform plasma profiles and arbitrary distribution of the electric field of the incident wave. The ray-tracing calculation cannot describe the wave propagation precisely including the reflection and the tunneling around the evanescent region. An expedient manner [3] to restart the ray-tracing calculation at the edge of the higher density side of the evanescent region after tunneling has been used to analyze the wave propagation in the over-dense region. Comparison between the full wave calculation around the evanescent region and the ray-tracing calculation with use of the expedient manner to check the validity of this manner will be reported.

Measurement of the electromagnetic waves originated from thermally emitted EBWs that are radiated via the reversal process of the heating can provide the optimum injection condition of electromagnetic for ECRH/ECCD by EBWs. Examination of the measurement with use of above method will be also reported. With comparing the results of the measurement to the results of the examination, validation of the method can be expected.

[1] H. P. Laqua, Plasma Phys. Control. Fusion **49** (2007) R1

[2] H. Igami, H. Tanaka and T. Maekawa, Plasma Phys. Control. Fusion **48** (2006) 573

[3] H. Igami, H. Idei, S. Kubo, et. al, Plasma Science and Technology, **13** (2011) 405

Improvement in flexibility of ECCD by use of upgraded ECH antenna system on LHD

Y. Yoshimura, Y. Narushima, S. Kubo, T. Shimosuma, H. Igami, H. Takahashi, T. I. Tsujimura, R. Makino, S. Ito, K. Okada, S. Kobayashi, Y. Mizuno, Y. Goto^a, A. Ejiri^b, R. Sakamoto, T. Mutoh, H. Yamada, A. Komori, Y. Takeiri

National Institute for Fusion Science, 322-6 Oroshi-cho, Toki 509-5292, Japan

^a Graduate School of Engineering, Nagoya University, Nagoya 464-8601, Japan

^b Graduate School of Frontier Science, University of Tokyo, Kashiwa 277-8561, Japan

By 2009, three high-power 77 GHz gyrotrons, over 1 MW each, have been installed and applied to large helical device (LHD) experiment [1, 2]. In addition, two 154 GHz gyrotrons of 1 MW each were installed in 2012 and 2014. Corresponding to the increase in the number of the high-power gyrotrons, in 2014, power injection mirror antenna system for electron cyclotron heating (ECH) and electron cyclotron current drive (ECCD) was modified and upgraded. Formerly, an outside port 2-O is furnished with two antenna sets, 2-OLR for power injection from the first 77 GHz gyrotron, and 2-OLL for the first 154 GHz gyrotron. In addition to them, two new antenna systems 2-OUR and 2-OUL were installed in the 2-O port. The second 77 GHz gyrotron changed its power injection port from an upside port 9.5-U to the 2-O port, using the 2-OUR antenna. The second 154 GHz gyrotron uses the 2-OUL antenna. An upside port 5.5-U has been used for power injection from the third 77 GHz gyrotron.

Each antenna in the 2-O port has wide range of EC-wave beam direction control so that these are suitable for ECCD which requires toroidally oblique EC-wave beam injection. In the LHD 18th experimental campaign in 2014-2015, an ECCD experiment with second harmonic resonance condition: on-axis magnetic field of 1.375 T for 77 GHz waves with the magnetic axis position of 3.75 m, was performed in which some combination patterns of two 77 GHz ECCDs were applied. Figure 1 shows waveforms of plasma currents in the discharges of dual co- and counter-ECCDs. 77 GHz EC-wave powers are applied from 2-OUR and 2-OLR for ECCDs, and from 5.5-U for ECH. The injected powers from 2-OUR, 2-OLR and 5.5-U antennas are 365, 366 and 271 kW, respectively. In the discharge #128316, counter-ECCDs and ECH are applied from 1.0 s to 7.6 s, and in #128317 co-ECCDs and ECH from 1.5 s to 7.6 s. Tangential NBIs are applied from 7 s so that plasma currents driven by NBIs are superposed.

The EC-driven currents by the two ECCD systems are evaluated referring to a former ECCD experiment [3], showing that the ECCD abilities of the two antenna systems are nearly identical.

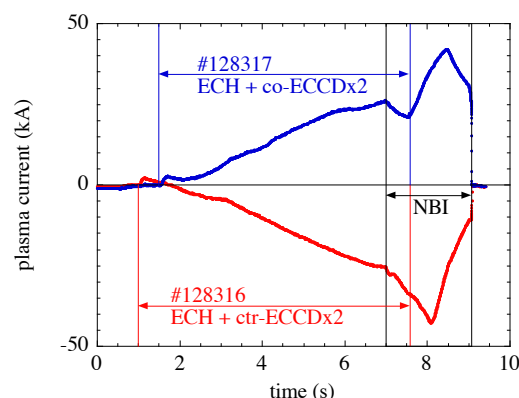


Fig. 1 Waveforms of plasma currents in the discharges of dual co- and counter-ECCDs.

References

- [1] H. Takahashi *et al.*, Fusion Sci. Technol. **57** (2010) 19.
- [2] T. Shimosuma *et al.*, Fusion Sci. Technol. **58** (2010) 530.
- [3] Y. Yoshimura *et al.*, Plasma Fusion Res. **7** (2012) 2402020.

Optimization of ECH injection polarization in real-time polarization scan experiments

T. Ii Tsujimura^a, Y. Mizuno^a, S. Kubo^a, R. Makino^a, T. Shimozuma^a, Y. Yoshimura^a, H. Igami^a,
H. Takahashi^{a,b}, T. Mutoh^{a,b}, the LHD Experiment Group^a

^a*National Institute for Fusion Science, 322-6 Oroshi-cho, Toki 509-5292, Japan*

^b*SOKENDAI (The Graduate University for Advanced Studies), 322-6 Oroshi-cho, Toki 509-5292, Japan*

tsujimura.tohru@nifs.ac.jp

A high central electron temperature with an electron internal transport barrier by use of a highly efficient electron cyclotron resonance heating (ECH) system are required for steady plasma discharge. The operation scenario of the ECH injection system optimally preset before a discharge may result in a high performance plasma. In addition to that, feedback control of the ECH injection system set to an optimum target in real time can create a desired power deposition and reduce the stray radiation level in the vessel.

Experiments were recently performed in the Large Helical Device (LHD) in order to optimize the ECH injection polarization during a single discharge by using the developed fast polarization scan system with the fast rotatable polarizers installed in a transmission line. These fast polarization scan experiments showed clear plasma response to change of the injection polarization in real time and revealed the maximum absorbed power at a certain polarization setting.

The important point is that the polarization was estimated by the upgraded ray-tracing calculation code *LHDGauss*, which includes the mode purity analyses. The calculation indicates that the injected millimeter wave with the polarization setting couples to the plasma wave only with the fundamental ordinary mode. The calculated absorbed power is in good agreement with the experimental value. This suggests that prediction of optimum polarization with the help of the *LHDGauss* can be used for a control model in a real-time feedback control system if information on an electron density profile is available as a sensor for the feedback system.

Ion heating by ECRH through the equipartition process in the LHD

H. Takahashi, K. Nagaoka, R. Seki, M. Osakabe, M. Yokoyama, Y. Yoshimura, R. Sakamoto, S. Murakami^a, A. Ejiri^b and the LHD experiment group

National Institute for Fusion Science, 322-6 Oroshi-cho, Toki 509-5292, Japan

^a *Department of Nuclear Engineering, Kyoto Univ., Kyoto 606-8540, Japan*

^b *Graduate School of Frontier Sciences, The University of Tokyo, Kashiwa 277-8561 Japan*

Burning fusion plasmas are mainly heated by alpha particle as electron heating. Thus we must clarify how much ion temperature T_i is realized through the energy equipartition process under the electron heating dominant situation in order to construct an operation scenario and to predict plasma parameters in prototype fusion reactors.

The ion heating effect by the energy equipartition has been investigated in the Large Helical Device using high power electron cyclotron resonance heating (ECRH). Target plasma was sustained by a perpendicular neutral beam injection NBI (3.8 MW) and on-axis ECRH was superposed in stepwise up to 4.8 MW. Figure 1 shows the radial profiles of (a) the electron temperature T_e and the electron density n_e , and (b) T_i for the moderately high n_e plasma. The solid and the open symbols represent the data with 4.8 MW ECRH and those without ECRH, respectively. The profiles of n_e were approximately same on these two cases. Not only T_e but also T_i clearly increased in whole plasma region during ECRH beam injection. The parabolic shape of T_i profile was not changed by ECRH but the central T_i value increased from 1.6 keV to 2.0 keV.

Increase of T_i by ECRH was observed in wide n_e range ($1.3 \times 10^{19} \text{ m}^{-3} < n_e$). The increment of T_i increased up to $n_e \sim 2.5 \times 10^{19} \text{ m}^{-3}$ and was saturated in higher n_e plasmas. The central ion pressure was found to be expressed as a function of the 0.5 power of the equipartition heat flux.

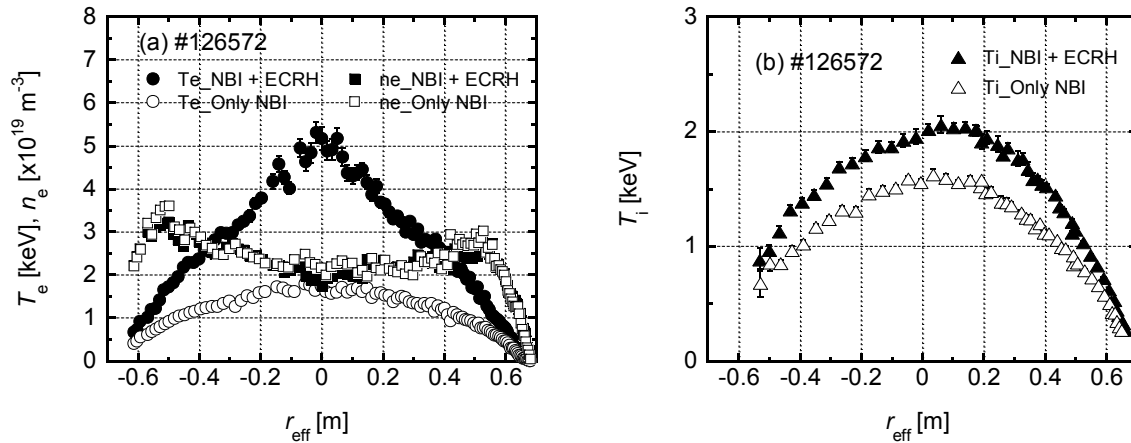


Fig. 1 The radial profiles of (a) T_e and n_e , and (b) T_i for the moderate high n_e plasma. Not only T_e but also T_i clearly increased in whole plasma region during ECRH beam injection.

Experimental Evaluation of Fast-ion Velocity Distribution Produced by Neutral Beam with Si-FNA in LHD

S. Kamio, M. Osakabe, R. Seki, M. Yokoyama, S. Murakami^a, T. Mutoh, and the LHD experiment group

National Institute for Fusion Science, 322-6 Oroshi-cho, Toki 509-5292, Japan

^aKyoto University, Yoshida-honmachi, Sakyo-ku, Kyoto 606-8501, Japan

In order to evaluate confinement property of fast ions, a fast ion measurement system using a Silicon-diode-based Fast Neutral Analyzer (Si-FNA) was developed in the Large Helical Device (LHD) [1]. In evaluating the energy of the fast neutrals, the Pulse Height Analysis (PHA) technique is adopted. This system can measure the fast neutrals one by one and its detection efficiency is almost 100%. A Si-FNA array was newly installed at a tangential port of the LHD in order to evaluate the confinement of fast ions which was produced by tangentially injected Neutral Beam (NB). Since the sight lines of the newly installed Si-FNAs have intersections with a radially injected NB and this NB can be utilized as an active source of charge exchange neutrals, an absolute measurement of fast ion density becomes possible.

Combining the obtained local fast ion information by the Si-FNA with that by the Fast Ion Charge eXchange Spectroscopy (FICXS), verification and validation of fast-ion simulation code such as TASK3D[2], FIFPC, GNET[3], and MORH[4] become possible. The comparison between these experimental data and simulation will reveal the confinement properties of fast ions in helical devices and provide deep understandings of them.

In the NB short pulse injection (NB-blip) experiment, the slowing-down process of mono-energetic fast ions were clearly observed. In addition to the measurement of the slowing-down process, the local energetic particles were measured in three kind of toroidal magnetic field (2.75 T, 1.375T, 0.75 T) and various electron density. By using these experimental results, the orbit effect and the effect of the slowing-down to the velocity distribution are investigated by comparison with the simulation codes.

[1] M. Osakabe et al., Rev. Sci. Instrum. **72** (2001) 788-791.

[2] S. Sato et al., Plasma Fusion Res. **3**, S1063 (2008).

[3] S. Murakami et al., Nucl. Fusion **46**, S425 (2006).

[4] R. Seki et al., Plasma Fusion Res. **5**, 027 (2010).

Developments of millimeter-wave interferometer for electron density measurements with beam extraction in the negative ion source

T. Tokuzawa, M. Kasaki, K. Nagaoka, K. Tsumori, K. Ikeda, H. Nakano, S. Geng^a, M. Osakabe, Y. Takeiri, and O. Kaneko

National Institute for Fusion Science, 322-6 Oroshi-cho, Toki 509-5292, Japan

^a The Graduate University for Advanced Studies, 322-6 Oroshi-cho, Toki 509-5292, Japan

In the NIFS 1/3-scaled negative ion source for LHD [1], the Cavity-Rign-Down (CRD) method and Langmuir probes have been utilized for studying the dynamics of the negative ion and electron during beam extraction, respectively. The Langmuir probe can give the information on the electron density qualitatively, but it has difficulty in obtaining the electron density precisely due to the strong magnetic field in the plasma chamber and the contribution of negative ions to the electron saturation current.

The millimeter-wave interferometer is one of the presumable tools for measuring the electron density under such condition. At first, we had installed the millimeter-wave interferometer to the negative ion source and successfully obtained the electron density in the pure hydrogen and Cs-seeded plasmas [2]. In order to measure the electron density with applying the high voltage on the plasma chamber, the millimeter-wave interferometer has been upgraded. Figure 1 shows the time evolution of the electron density obtained with improved millimeter-wave interferometer in the pure hydrogen plasma. The beam was extracted from 10.8 s to 11.8 s. The electron density changes with the arc power and rapidly rises when the extraction voltage is applied. Amount of the electron density change before and after the beam extraction is $2.6 \times 10^{17} \text{ m}^{-3}$. It has been observed that the negative ion density shows the different response to the extraction voltage and it rapidly drops with beam extraction. In the conference, the improvements on the diagnostic system will be described in detail and the response of the electron to the extraction voltage in other conditions (e.g. Cs-seeded plasma and different bias voltages) will be presented.

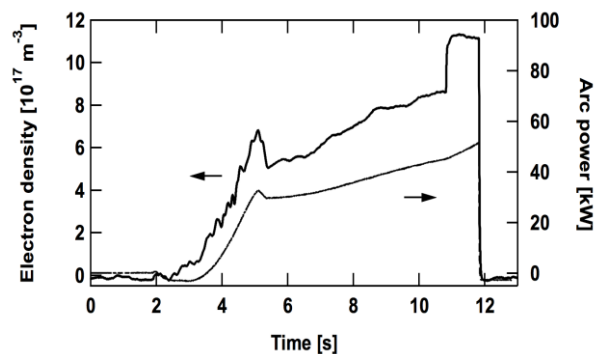


Fig. 1 Time evolution of electron density measured with millimeter-wave interferometer.

[1] K. Tsumori, *et al.*, Rev. Sci. Instrum. **83** (2012) 02B116.

[2] K. Nagaoka, *et al.*, AIP Conf. Proc. **1390** (2011) 374.

Simulation study of NBI beam ion distributions in the presence of magnetic islands in helical plasmas

H. Yamaguchi and S. Murakami

Department of Nuclear Engineering, Kyoto University, Nishikyo, Kyoto 615-8540, Japan

E-mail: yamaguchi@p-grp.nucleng.kyoto-u.ac.jp

Existence of nested closed magnetic flux surfaces is an essential requirement for a good plasma confinement in toroidal configurations. Magnetic perturbations (MHD modes, error fields and etc.) generate magnetic islands and, finally, the nested flux surfaces are broken by the magnetic island overlapping. Thus, these magnetic islands deteriorate the plasma confinement. On the other hand, it is suggested that optimized and controlled magnetic island can have benefit for plasma performance in tokamak plasmas. Therefore a detail study should be done to evaluate the effect of magnetic island on the plasma confinement. The effect of magnetic islands on energetic ion confinement has been studied using several guiding-center codes in tokamak plasmas. They found that the magnetic island enhances the energetic ion loss due to the enhanced radial ripple diffusion. However, the effect of magnetic islands on energetic ion confinement has been studied in helical plasmas.

In the Large Helical Device (LHD) experiments, magnetic island effect and its dynamics in LHD plasmas have been studied applying the resonant magnetic perturbation (RMP) coils [1], and the behaviors such as temperature flattening in the magnetic islands have been observed as in tokamaks. In these experiments three tangential and two perpendicular neutral beam injection (NBI) heating systems are applied. These neutral beams produce energetic ions, which draw variety of passing and trapped orbits more complicated than that in tokamaks. Especially, the confinement of ripple-trapped particles are important for energetic particle confinement in LHD.

In this paper, we study the effect of magnetic islands on the NBI beam ion confinement in LHD plasma. We model the resonant magnetic perturbation as that with a single helicity. Taking into account those magnetic perturbations, we solve the drift kinetic equation for NBI beam ions in 5-D phase space using the GNET-TD code [2], which is based on GNET [3]. The complex guiding-center motion and the pitch-angle and energy scatterings during energy slowing down process are considered in the simulation. We discuss the effect of RMP producing magnetic islands on confinement and velocity space distribution of NBI beam ions in LHD plasmas.

- [1] Y. Narushima *et al.*, Nucl. Fusion **55** (2015) 073004
- [2] H. Yamaguchi *et al.*, Plasma Fusion Res. **8** (2013) 2403099
- [3] S. Murakami *et al.*, Nucl. Fusion **46** (2006) S425

Optimization of helical coil structure for the improved magnetic configuration of LHD

Shoichi Okamura

National Institute for Fusion Science, 322-6 Oroshi-cho, Toki 509-5292, Japan

An optimized magnetic configuration was found for the LHD-type confinement device [1, 2]. The new configuration has a reduced Shafranov shift for high beta equilibria which gives better neoclassical confinement than present LHD configurations. This result was obtained based on the physical understandings of the Fourier components of the boundary shape of LHD plasmas. It was found that two fundamental Fourier components representing the helical excursion of the magnetic axis and the rotating triangularity are important to determine the basic confinement characteristics of magnetic configuration, that are the neoclassical transport and the MHD stability. A new optimized configuration was produced by modifying these two essential components which can not be produced by the present LHD magnetic coils. The magnetic coil design for this new configuration was made using the coil optimization technique and a combination of simple advanced helical coil and the axisymmetric poloidal field was found [3]. The obtained helical coil structure has an additional parameter of the ellipticity of the poloidal cross section of a coil winding surface. In this paper, the coil design study is extended to survey the physical properties of the magnetic configurations created by the advanced helical coil structure with an additional geometric parameters to the existing helical devices.

[1] S. Okamura, Plasma Phys. Control. Fusion **55** (2013) 032002.

[2] S. Okamura, Plasma Fusion Res. **8** (2013) 2402029.

[3] S. Okamura, 41th EPS Conference on Plasma Physics, Berlin (2014) P4.011

Spatial structures of energetic-particle driven geodesic acoustic mode in the LHD

T. Ido^a, A. Shimizu^a, M. Osakabe^{a,b}, T. Watari^a, K. Ogawa^{a,b}, K. Toi^a, M. Nishiura^c, K. Itoh^a,
M. Lesur^d, and the LHD Experiment Group

^a National Institute for Fusion Science, 322-6 Oroshi-cho, Toki 509-5292, Japan

^b SOKENDAI (The Graduate University for Advanced Studies), 322-6 Oroshi, Toki, Gifu 509-5292,
Japan

^c Graduate School of Frontier Sciences, The University of Tokyo, 5-1-5 Kashiwanoha, Kashiwa, Chiba
277-8561, Japan

^d Research Institute for Applied Mechanics, Kyushu University, 6-1 Kasuga-koen, Kasuga, Fukuoka,
816-8580, Japan

Measurement of spatial structures of fluctuations is important for identification of the fluctuations and for investigation of their dynamics and influence on plasmas. In this experiment, spatial structures of energetic-particle driven geodesic acoustic mode (EGAM) have been measured using a heavy ion beam probe (HIBP) and Mirnov probes in the LHD plasmas.

EGAM in the LHD plasmas with normal magnetic shear profiles, where the rotational transform monotonically increases from the center to the edge of the plasmas, is excited in the central region of the plasmas, and is usually accompanied by the frequency up-chirping. Measured spatial structures of the electric potential fluctuation and the density fluctuation associated with the EGAM agree the theoretical prediction: $m = 0$ for the electric potential fluctuation and $m = 1$ for the density fluctuation, where m is the poloidal mode number. The structures are almost same during the frequency chirping[1].

When the frequency of the chirping EGAM reach twice the GAM frequency determined with parameters of bulk plasmas, a mode with the GAM frequency is excited abruptly. The mode is excited in the same region as the chirping EGAM. Because the spatial structures are also same as the EGAM, the abruptly excited mode is identified as a GAM[2] and it is considered to be excited through driven by a cooperative collaboration of fluid nonlinearity and kinetic nonlinearity[3]. The amplitude of the electric potential of the abruptly excited GAM can become roughly twice larger than that of the EGAM, and the GAM may affect transport of background plasmas.

Measurement by both HIBP and Mirnov coils reveals that the chirping EGAM are affected by electron cyclotron heating (ECH) and by resonant magnetic perturbation (RMP). By applying ECH, the density fluctuation of the chirping mode become less up-down antisymmetry, while the structure of the electric potential does not changes. Thus, $m \neq 1$ for the density fluctuation, though $m = 0$ for the electric potential fluctuation. By applying RMP with $m/n=2/1$, where n is the toroidal mode number, n of the chirping mode becomes one. Both results may reflect structures of the magnetic field.

[1] T. Ido, et al., Nucl. Fusion, 55 (2015) 083024

[2] T. Ido, et al., submitted to Phys. Rev. Lett. (2015)

[2] M. Lesur, et al., submitted to Phys. Rev. Lett. (2015)

Slowing down mechanism of instability leading to minor collapse in LHD

Y. Takemura, K.Y. Watanabe, S. Sakakibara, Y. Suzuki, S. Ohdachi, Y. Narushima, K. Ida, I. Yamada and LHD Experiment Group

National Institute for Fusion Science, 322-6 Oroshi-cho, Toki 509-5292, Japan

The MHD instability causing rapid drop in core electron pressure (Minor collapse) is observed in the LHD discharge with the magnetic configuration where the Mercier stability condition is not satisfied [1]. The activity of the instability is changed through three phases divided by behavior of its rotation. In constant rotation phase, rotational frequency and amplitude of the instability's fluctuation is constant and clear flattening of the pressure profile is not observed. In slowing rotation phase, the amplitude increases with the decrease of the rotational frequency and flattening of the pressure profile occurs. In stopping rotation phase, the rotational frequency is zero and the amplitude rapidly grows, the minor collapse takes place. The slowing down of the instability's rotation is believed to lead to occurrence of the minor collapse. However, the reason for the slowing down is not clear. If the LHD experiment with the magnetic configuration where the minor collapse occurs is performed, the rotational frequency of the instability's fluctuation in slowing rotation phase coincides with the rotational frequency of the plasma flow at the resonant surface within the error bar, as shown in Fig.1. This is consistent with the result of the research [2] on the rotational frequency of the typical resistive interchange instability which does not cause the minor collapse. Here the electron diamagnetic drift flow is zero because flattening of the pressure profile appears in this experiment. According to time evolution of the plasma flow profile in Fig.2, the plasma flow is large in edge region but small in core region. The region of the small plasma flow is slowly extended to edge region with the decrease of the rotational frequency. On the other hand, the resonant surface is rapidly moved to the core region. Especially at $R \sim 4.2$ m at an early time in slowing rotation phase, the situation of the fast plasma rotation is kept even with the decrease of the rotational frequency of the instability's fluctuation. These results suggest that the resonant surface moving to the core region is the reason for the slowing down. The move to the core region is believed to be caused by the increase of the Co- plasma current which increase the rotational transform.

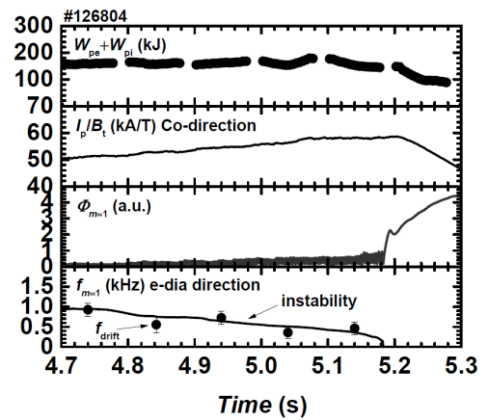


Fig.1 Typical discharge where the minor collapse occurs due to the instability

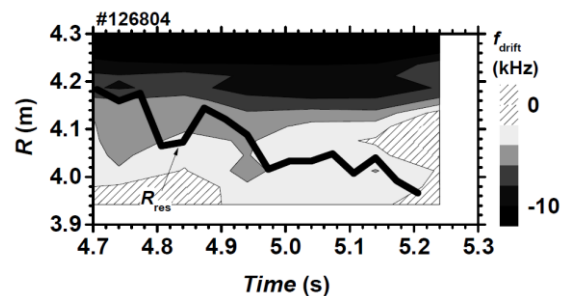


Fig.2 Time evolution of the plasma flow profile and the resonant surface

[1] Y. Takemura, Nucl. Fusion **52** (2012) 102001.

[2] Y. Takemura, Plasma and Fusion Research **8** (2013) 1402123.

Stabilization of Helically Trapped Energetic Ions driven Resistive Interchange Mode by High Power Injection of Electron Cyclotron Resonance Heating

X.D. Du¹, S. Ohdachi^{1,2}, K. Nagaoka^{1,2}, M. Osakabe^{1,2}, Y. Suzuki^{1,2}, K. Toi² and LHD Experimental Group

¹*Department of Fusion Science, Sokendai(The Graduate University for Advanced Studies), 322-6 Oroshi-cho, Toki 509-5292, Japan*

²*National Institute for Fusion Science, 322-6 Oroshi-cho, Toki 509-5292, Japan*

du.xiaodi@lhd.nifs.ac.jp

The resistive interchange mode destabilized through resonant interaction with a characteristic motion of helically trapped energetic ions (EPs) are observed in Large Helical Device (LHD), called the EIC, exhibiting bursting character and rapid frequency chirping down. The EIC strongly impacts the confinement of helically trapped EPs and induces noticeable losses. The loss fraction from the plasma confinement region is crudely estimated to be $\sim 40\%$ over the impact region of the EIC [1]. Therefore, the study on the control of the EIC in LHD is crucial to reduce the losses of helically trapped EPs.

In recent LHD experiment, the clear suppression of the EIC is found during the injection of the high power electron cyclotron resonance heating (ECH). One typical example is shown in Fig. 1. In the so-called high Ti discharge of central electron density $n_e \sim 1 \times 10^{19}$ and temperature $T_e \sim 3keV$, the EIC bursts exhibits the fishbone-shape oscillation in magnetic probes. However, during the time window from 4.65s to 4.85s when the high ECH power of 5.2MW is injected without changing the power of neutral beam injection perpendicular to magnetic field line (PERP-NBI), the strong bursting oscillations in magnetic probes disappear. Moreover, the EIC suppression phase even persists $\sim 100ms$ after switching off the ECH, as seen from Fig. 1. This might be due to the decrease of the deposition power of the PERP-NBI by the strong electron density pump-out induced by the ECH, i.e., $\sim 20\%$ decrease of the electron density in this case, since the destabilization of the EIC strongly correlates with the contents of helically trapped EPs in plasma. The other possibilities of the physics mechanism of the suppression of the EIC by the ECH will also be discussed.

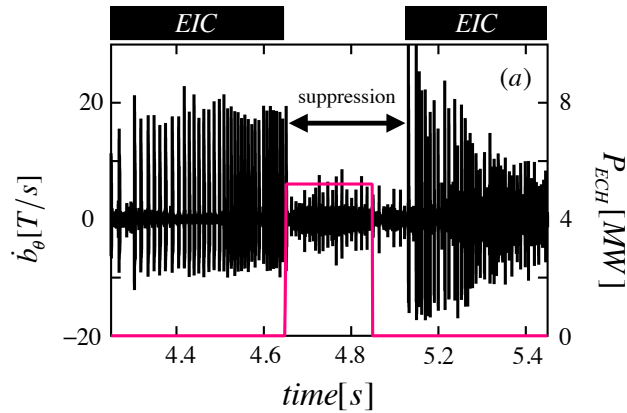


Figure 1: Time evolutions of the magnetic fluctuations measured by a magnetic probe signal and injected ECH power.

[1] X.D. Du, K. Toi et al., Phys. Rev. Lett. **114**, 155003 (2015)

Development of fast-neutron directional detector for fusion neutron profile monitor at LHD

E. Takada^a, N. Nakada^a, M. Isobe^{b,c}, K. Ogawa^{b,c}, T. Nishitani^b, H. Tomita^d

^a National Institute of Technology, Toyama College, 13 Hongo-machi, Toyama 939-8630, Japan

^b National Institute for Fusion Science, 322-6 Oroshi-cho, Toki 509-5292, Japan

^c SOKENDAI (The Graduate University for Advanced Studies), 322-6 Oroshi-cho, Toki 509-5292, Japan

^d Nagoya University, Furo-cho, Chikusa-ku, Nagoya 464-8601, Japan

takada@nc-toyama.ac.jp

In order to measure the incident directions of 14 MeV neutrons, a direction sensitive detector composed of scintillating fibers (Sci. Fi.) has been used[1], [2]. In that system, the signals from the Sci. Fi. were measured with a photomultiplier tube (PMT) where the penetration of recoil proton from one fiber to the other was prevented with the shielding region. The system was applied to TFTR and JT-60U to evaluate the time dependence of 14 MeV neutron emission for the triton burn-up study in deuterium discharges. In the present study, we are trying to optimize the design of the detector to use at LHD. In TFTR and JT-60U, the Sci. Fi. with the length of 10 cm and the diameter of 1 mm has been used. With PHITS code, we calculated the proton flux distribution for 14 MeV neutrons incident parallel to the Sci. Fi. Figure 1 depicts the recoil proton distribution when neutrons are incident parallel to the Sci. Fi. It shows that recoil protons are generated mainly in the region near the inlet, which is caused by the self-shielding by the Sci. Fi. This result suggests the necessity of design optimization.

We calculated the angular dependence of counts over a threshold energy for the case of 1 mm-diameter Sci. Fi. The lengths were set to 10 cm and 5 cm. Also, experiments were carried out at Fusion Neutron Source (FNS) facility of Japan Atomic Energy Agency. It was observed that the measured angular distribution is broader than calculated results. As Sci. Fi. is sensitive to gamma rays, the difference should be due to the background gammas. To reduce the gamma sensitivity, it is effective to adopt smaller core Sci. Fi. In Fig. 2, calculated results are shown for different core size. We can conclude that, by using smaller core Sci. Fi., higher angular resolution can also be achieved. However, smaller diameter causes lower measuring efficiency also for neutrons. For optimizing the design of Sci. Fi. detector to measure the triton burn-up neutron profile in the LHD plasma, additional simulation and experiments will be carried out.

[1] Wurden, G. A. et al., Rev. Sci. Instrum. **66** (1) (1995) 901.

[2] Harano, H. : JAERI-Research **97-060** (1997) (in Japanese).

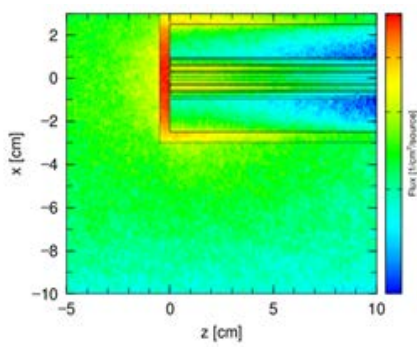


Fig. 1. Distribution of proton flux in the measurement system.

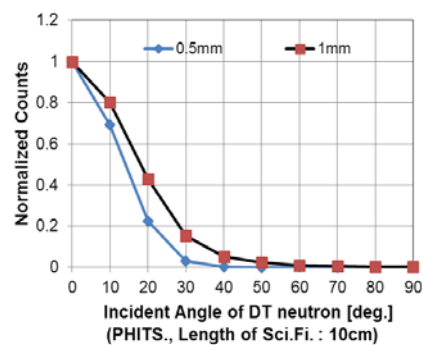


Fig. 2. Comparison of calculated angular distribution.

Observation of termination process of long pulse plasma discharges using stereoscopic fast framing cameras in the Large Helical Device

M. Shoji, H. Kasahara, H. Tanaka, T. Murase, M. Tokitani, S. Morita, M. Goto, T. Oishi, T. Mutoh, E. de la Cal^a, C. Hidalgo^a and the LHD experiment group

National Institute for Fusion Science, 322-6 Oroshi-cho, Toki 509-5292, Japan

^a Centro de Investigaciones Energéticas, Medioambientales y Tecnológicas, 40 Avenida Complutense, Madrid 28040, Spain

The Large Helical Device (LHD) has superconducting helical and poloidal coils by which plasma confinement magnetic configurations can be formed without toroidal plasma current. It is advantageous for sustaining steady state plasma discharges without instabilities induced by the plasma current. In LHD, long pulse plasma discharge experiments have been performed for more than the last ten years using ICH and ECH. As a result, a long pulse discharge with a plasma density of $\sim 1.2 \times 10^{19} \text{ m}^{-3}$, a central electron temperature of $\sim 2 \text{ keV}$ and a plasma heating power of $\sim 1.2 \text{ MW}$ for about 48 minutes was successfully achieved in the experimental campaign in FY2013. The plasma discharge was terminated by abrupt increase in carbon ion emission triggered by the release of large amounts of carbon dusts from a lower divertor region in the inboard side of the torus. Observation with a fast framing camera proved that the carbon-rich mixed material deposition layers accumulated in front of divertor plates in the divertor region were exfoliated just before the termination of the plasma discharge. It was also found that the exfoliated mixed material layers were broken into small fragments (dusts) which penetrated into the main plasma to terminate the long pulse plasma discharge [1].

Before the last experimental campaign in FY2014, the lower divertor configuration was modified so as to suppress the deposition layers in front of the divertor plates, which successfully controlled the termination of long pulse discharges induced by the large amounts of carbon dusts in the last campaign. Nevertheless, the long pulse discharges was often terminated with abrupt increase in iron ion emission. One of the terminations of the plasma discharges was directly observed with a stereoscopic fast framing camera installed in an outer port, which clearly shows the following plasma termination process:

1. in the beginning, a luminescent spot appeared on a gap between the surface of stainless steel tiles for protecting a side wall of a helical coil can in the inboard side of the torus,
2. the spot widely expanded to the entire region of the helical coil can in the inboard side with intensive sparks,
3. after the sparks vanished, large amounts of incandescent dusts were released from near the top of the helical coil can in the inboard side,
4. the released dusts penetrated into the main plasma and induced the radiation collapse to terminate the long pulse plasma discharge.

The stereoscopic analysis of the three-dimensional trajectories of the observed dusts revealed that the dusts locate in the inboard side of the torus. It also proved that the dusts penetrated into the main plasma confinement region to the positions where the normalized minor radius ρ is about 0.8. The analysis clearly indicates that the investigation of the physical mechanism triggering the luminescent spot at the gap between the tiles is essential for controlling the intensive sparks and the release of the dusts. Appropriate measures for suppressing the expansion of the spot can lead to extension of the duration time of the long pulse discharges.

[1] M. Shoji, H. Kasahara, M. Tokitani et al., Nucl. Fusion **55** (2015) 053014.

Identification of helical structure of visible light in Low- A RFP with concave lens array

A. Sanpei, S. Masamune, Y. Aoki, T. Nagano, M. Higuchi, K. Jikuhara, S. Nankanobo,
R. Tsuboi, R. Isomoto, H. Himura, S. Ohdachi^a, N. Mizuguchi^a, T. Akiyama^a

Kyoto Institute of Technology, Kyoto 606-8585, Japan

^a*National Institute for Fusion Science, 322-6 Oroshi-cho, Toki 509-5292, Japan*

sanpei@kit.ac.jp

Three-dimensional (3-D) effects on MHD phenomena in axisymmetric systems such as reversed field pinches (RFPs) have attracted much attention. In the RFP, for example, recent progress has shown the importance of helically deformed RFP configuration where the single helical magnetic axis state is self-organized [1].

In a low-aspect-ratio (low- A) RFP machine RELAX ($R = 0.51 \text{ m}/a = 0.25 \text{ m}$ ($A = 2$)) [2], a quasi-periodic transition to quasi-single helicity (QSH) state has been observed. During the QSH state, the fluctuation power concentrates in the dominant $m = 1/n = 4$ mode, and a (toroidally rotating) 3-D helical structure has been observed with radial array of magnetic probes [3]. We succeeded in identifying the characteristic helical SXR structures which suggest hot or dense helical core in QSH state, using the SXR imaging diagnostic system [4]. A high-speed camera diagnostic has revealed simple helix structure in the visible light image [5,6]. If there is no limitation on observation positions, a 3-D tomographic reconstruction is a powerful method for obtaining 3-D information; however, the observation positions and their available numbers are considerably restricted in plasma experiment devices. It is required that a method for identification of 3-D structure from a single exposure image obtained from one viewing port.

In the present study, we are developing a 3-D recording system where multiple concave lenses and a high-speed camera for the study of time evolution of 3-D structure. As an initial experiment, we have taken vertical visible light images with time resolution of 10 μsec , to identify time evolution of filament-like single helix structure in RELAX plasmas. We will discuss these results to make clear experimental and theoretical requirements for 3-D structural studies.

This work is partly supported by JSPS KAKENHI Grant Number 15K05364.

- [1] R. Lorenzini *et al.*, *Nature Physics* **5** (2009) 570
- [2] S. Masamune *et al.*, 24th IAEA Fusion Energy Conf., EX/P4-24 (2012)
- [3] K. Oki *et al.*, *Plasma Fusion Res.* **7** (2012) 1402028
- [4] A. Sanpei *et al.*, *IEEE Transaction Plasma Science*, **39** (2011) 2410
- [5] T. Onchi *et al.*, *Plasma and Fusion Res.* **3** (2008) 005
- [6] A. Sanpei *et al.*, *Plasma and Fusion Res.* **5** (2010) S2306

Radiation field estimation for the diagnostic and control components by Monte Carlo neutronics calculations with LHD 3-dimensional modeling

T. Nishitani^a, K. Ogawa^{a,b}, M. Isobe^{a,b}

^aNational Institute for Fusion Science, 322-6 Oroshi-cho, Toki 509-5292, Japan

^bSOKENDAI (The Graduate University for Advanced Studies), 322-6 Oroshi-cho, Toki- 509-5292, Japan

LHD has a plan of the deuterium experiment in 2017. Precise estimation of the radiation (neutron and gamma) field should be performed in order to confirm the soundness of the diagnostic and control components for the LHD deuterium experiment. Previously, radiation field in the LHD torus hall was calculated by 2-Dimensional neutron transport DORT. The radiation field around the cryostat must be affected by the structure of the LHD, such as horizontally located outside port (O-port) with large diameter, which could not be estimated by 2-Dimensional neutrons calculations. Here we carried out Monte Carlo neutrons calculation with 3-Dimensional modeling of LHD by using MCNP-6 code with the cross-section library of ENDF B-VI. In MCNP code, all surfaces of cells must be defined by quadratic (or less) equations or torus, however, helical surface could not be treated. In the MACP calculation geometry, the LHD components within the support structure are divided by small toroidal angle, and the components are assumed to be toroidally symmetric in a toroidal pitch angle. The geometry in one toroidal pitch angle is modeled by the CAD drawing with some simplification. As the first step, the toroidal pitch angle is selected to be 6° . Figure 1 shows the poloidal cross sections of the LHD calculation model, where the toroidal angle of $\phi=0$ is defined by the center of the U/L port. A poloidal angle θ of a center of one helical coil is presented by $\theta = \phi (m/l) + \alpha \sin\{\phi (m/l)\}$, where $m=10$, $l=2$ and $\alpha=7.8^\circ$. The LHD plasma is assumed to be a simple torus. Surface equations in each toroidal pitch angle are generated automatically by EXCEL based on this formula. By this calculation, neutron flux is estimated to be 7.50×10^9 n/cm²•s at R=8 m and $\phi = 18^\circ$ on the mid plane (just in front of the 0-port outlet) and 6.50×10^9 n/cm²•s at R=8 m and $\phi = 0^\circ$ for the maximum neutron yield shot with 1.9×10^{16} neutrons/s. In the region of R>10m, the neutron flux is almost symmetric toroidally, and agrees with the result of the 2-Dimensional neutron transport calculation by the DORT code.

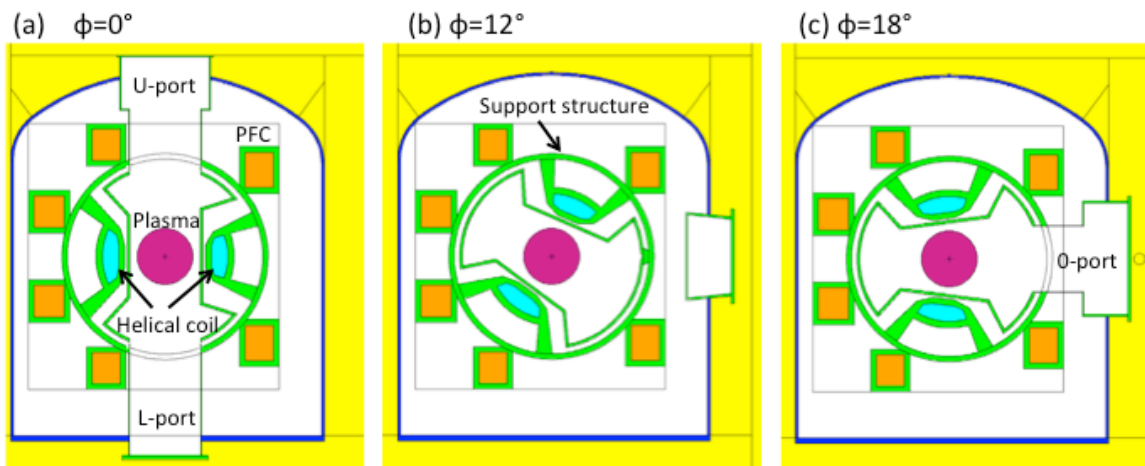


Figure 1 Poloidal cross sections of the LHD calculation model at $\phi = 0^\circ$, 12° and 18° , where the toroidal angle $\phi=0$ is defined by the center of the U/L port.

Integrated heat transport simulation of the helium-hydrogen plasma of LHD by TASK3D

S. Maeta, S. Murakami, H. Yamaguchi, A. Fukuyama, K. Nagaoka^a, H. Takahashi^a,
H. Nakano^a, M. Osakabe^a, K. Tanaka^a, M. Yokoyama^a, and LHD Exp Group^a

Department of Nuclear Engineering, Kyoto University, Kyoto 615-8540, Japan

^aNational Institute for Fusion Science, 322-6 Oroshi-cho, Toki 509-5292, Japan

Various physical phenomena with wide ranges of time and space scales are connected in the fusion plasma. Thus, in order to predict the performance of the fusion plasma, an integrated simulation combining various physics models is required. Many integrated simulation code has been developed for tokamak and helical plasmas. TASK3D is an integrated simulation code for helical plasma and has been applied to the analyses of the plasma transport of LHD plasmas[1, 2].

On the other hand, the deuterium experiment project from 2017 is planned in LHD, where the deuterium NBI heating beams with the power more than 30MW is injected to the deuterium plasma. Main objects of this project are to make clear the isotope effect on the heat and particle transport in the helical plasma, and to study energetic particle confinement in a helical magnetic configuration measuring triton burn-up neutrons.

In the 2014 campaign of LHD we have performed the helium-hydrogen plasma experiment to make clear the ion species dependence on the heat transport, which would be related to the isotope effect on the plasma confinement. We have found that the central ion temperature goes up as the helium fraction increases in the helium-hydrogen plasma.

In this paper, we study the heat transport of the helium-hydrogen experiment plasma to make clear the ion species dependence on the heat transport. We evaluate the NBI heat deposition of multi-ion plasma by GNET code[3, 4] and study the heat transport by TASK3D. It is found that the turbulent transport improvement is necessary to explain the increase of ion temperature in the high fraction helium plasma. We apply the turbulent transport improvement models and obtain relatively good agreements.

- [1] S. Murakami, et al., Plasma Phys. Control. Fusion **57** (2015) 054009.
- [2] A. Sakai, et al., Plasma Fusion Res. **9** (2014) 3403124.
- [3] H. Yamaguchi and S. Murakami, Plasma Fusion Res. **9** (2014) 3403127.
- [4] S. Murakami, et al., Nuclear Fusion **46** (2006) S425.

Full-orbit simulation of fast α -particle in heliac configurations

J. Tachibana, S. Kitajima, H. Takahashi, A. Okamoto^a

Dept. of Quantum Science and Energy Engineering, Tohoku Univ., Sendai 980-8579, Japan

^a*Dept. of Energy Engineering and Science, Nagoya Univ., Nagoya, 464-8603, Japan*

Heliac is one of stellarator configurations, which consists of only simple circular coils. In a heliac a rotational transform of the magnetic field line is produced by helically placed toroidal field coils. The magnetic field geometry of heliac configuration has a deep magnetic well in vacuum configuration, and it is expected that the heliac configuration has good confinement property in a high beta plasma.

In self-heating mechanism of a thermonuclear fusion reactor, it is an important process that fast α -particles produced by D-T reaction are well confined with magnetic field, and are slowing down by collision with particles in a bulk plasma. Therefore it is necessary to examine and evaluate the performance of the fast α -particle confinement in a heliac type reactor. Recently, hybrid guiding-center/full-orbit simulations of fast ion in non-axisymmetric magnetic geometry was reported [1]. It is difficult to calculate accurately the orbit of a particle by the guiding center simulation in the case where the scale length of the gradient of magnetic field is larger than the Larmor radius. Therefore, the full-orbit simulation becomes significant in the orbit calculation of the fast α -particle born in D-T reaction.

In this presentation, we investigate the performance of the α -particle confinement in heliac configuration by computing the full-orbit simulation instead of the guiding center simulation. We also investigate the dependence of the performance of the α -particle confinement on toroidal and helical ripples by changing the ratio of coil currents. And we will discuss candidates for a suitable heliac configuration to confine a fast α -particle. In this simulation, we use the magnetic configuration of Tohoku University Heliac device (TU-Heliac) [2] as one of heliac configuration models.

This work is supported by Grant-in-Aid for Scientific Research (KAKENHI), 24246152.

[1] D. Pfefferlé, *et al.*, Plasma Phys. Control. Fusion **36** (2015) 054017.

[2] S. Kitajima, *et al.*, Nucl. Fusion **46** (2006) 200.

Recent progress of fast-ion loss detector project in magnetic confinement fusion devices in Japan, Korea and China

M. Isobe^{a,b}, Junghee Kim^{c,d}, Yipo Zhang^e, Jiafeng Chang^f,
K. Ogawa^a, Jun-Young Kim^d, and Yi Liu^e

^a National Institute for Fusion Science, 322-6 Oroshi-cho, Toki 509-5292, Japan

^b SOKENDAI(The Graduate University for Advanced Studies), 322-6 Oroshi-cho, Toki 509-5292, Japan

^c National Fusion Research Institute, Daejeon 305-806, Korea

^d Korea University of Science and Technology, Daejeon 305-350, Korea

^e Southwestern Institute of Physics, P.O. Box 432, Chengdu 610041, China

^f Institute of Plasma Physics, Chinese Academy of Science, Hefei 230031, China

isobe@nifs.ac.jp

Good confinement of fast ions in fusion plasmas is crucial to the success of the fusion reactor since fusion-born α particles play an essential role in steady state sustainment of future burning plasma as a primary heating source. Although unfavorable effect on fast-ion orbit caused by axisymmetry breaking of the system is one of the oldest issues in fusion, attention is now being focused on it again because the non-axisymmetric three-dimensional (3D) perturbed field produced by resonant magnetic perturbation (RMP) is often superposed to mitigate ELMs in recent experiments. Fast-ion-driven MHD instabilities such as toroidal Alfvén eigenmodes (TAE) and energetic-particle modes (EPM) are also of great concern since those can potentially lead to fast-ion loss. For reasons above mentioned, tight collaborative activities on fast-ion physics in fusion were initiated in 2012 in Asian three countries in the support of the A3 foresight program on critical physics issues specific to steady state sustainment of high-performance plasmas. Primary purpose of our joint work is to obtain comprehensive understanding of fast-ion transport and/or loss caused by 3D field and fast-ion-driven MHD instabilities in toroidal fusion plasmas. Our immediate goal in the early stage of this program was to set up scintillator-based fast-ion loss detectors (FILDS) onto four major fusion devices in East Asia, i.e., LHD heliotron [1], KSTAR [2], HL-2A [3], and EAST tokamaks, and this task was complete in 2014. In LHD, TAE/EPM-induced fast-ion losses have been intensively studied by using the FILD [4]. The KSTAR FILD is also successfully working. A study on behavior of fast ions due to RMP field is in the center of attention in KSTAR [5]. In HL-2A, fast-ion losses induced by tearing modes, long-lived mode, sawtooth crash and disruption have been observed [6]. A recent big step in our work is that the operation of the FILD on EAST has begun lately. The localized bright spot appears on the screen while neutral beam (NB) is injected and disappears after NB is turned off as expected. In the latter stage of the A3 program, joint experiments will be conducted to reveal common physics issues related to fast ions in tokamak and heliotron/stellarator. In this paper, current status on fast-ion loss detector projects in Japan, Korea and China, and representative results from ongoing activities will be presented.

[1] K. Ogawa *et al.*, J. Plasma Fusion Res. SERIES **8** (2009) 655.

[2] Junghee Kim *et al.*, Rev. Sci. Instrum. **83** (2012) 10D305.

[3] Yipo Zhang *et al.*, Rev. Sci. Instrum. **85** (2014) 053502.

[4] M. Isobe *et al.*, Contrib. Plasma Phys. **50** (2010) 540. ; K. Ogawa *et al.*, Nucl. Fusion **53** (2013) 053012.

[5] Jun-Young Kim *et al.*, 41st EPS Conference on Plasma Physics. Berlin, 23-27 June 2014. **P4.067**.

[6] Yipo Zhang *et al.*, 25th IAEA FEC 13-18 Oct. 2014, St. Petersburg, **EX/P7-24**.

Poster Session 2
Tuesday, 4th November, 2015

Silicon Nitride Film Deposition on Glass Substrates via Plasma Sputter-Type Negative Ion Source

U. Jenica Rozette^a, C. Aren Renz^a, R. Henry^a

^a *Plasma Physics Laboratory, National Institute of Physics, University of the Philippines Diliman, Quezon City, 1101*

Silicon nitride films were successfully deposited on glass substrates using the plasma sputter-type negative ion source. The silicon metal target used was biased with -300V and was sputtered with Ar-N₂ plasma for 2 hours. Total flow rate of the Ar-N₂ gas mixture was fixed to 5.0 sccm while varying the N₂ concentration from 10% to 50%. Filling pressure of the system during deposition is maintained at 2.6×10^{-5} Torr. Visual inspection of the deposited films shows variation in color from grayish black (low N₂) to yellowish gold (high N₂) which suggests variation on film thickness. SEM images actually reveals that films deposited at lower N₂ concentration tends to have higher film thickness. It is because increasing the N₂ concentration decreases the number of available Ar ions for sputtering which then decreases the number of sputtered Si that would react with N₂ plasma. This observation is consistent with the previous studies [1, 2]. However for this study, N₂ concentration seems to have no significant effect on the crystal structure and chemical composition of the deposited silicon nitride films. XRD analysis of all the samples reveals only the same α -Si₃N₄ peaks present in all the samples with increasing intensities as N₂ concentration decreases.

References

- [1] S. K. Habib, A. Rizk, I. A. Mousa, *Vacuum* 49 (1998) 153–160.
- [2] B. S. Yau, J. L. Huang, *Surface and Coatings Technology* 176 (2004) 290–295.

Anti-fog on PMMA by Nitrogen-Argon Atmospheric Plasma Jet Treatment

S.J. Park, K. Penado, M. Jallorina, C. Mahinay, I. Culaba^a

Department of Physics, School of Science and Engineering, Ateneo de Manila University, Katipunan Ave, Quezon City, 1108 MetroManila, Philippines

In this study, 1cm × 1cm × 0.5cm polymethyl-methacrylate (PMMA) samples were treated using Nitrogen-Argon Atmospheric Plasma Jet (APJ). N₂/Ar flow rate ratios of 30:5, 30:10, 30:15, 30:20 to 30:25 SCFH were used. Measurements of the contact angle of different samples were used to determine the best treatment parameters for anti-fog application.

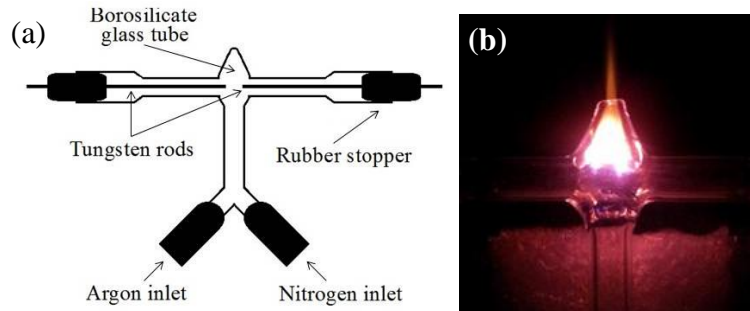


Figure 1. (a) A schematic diagram of the APJ device and (b) an image of nitrogen-argon APJ.

As shown in Figure 1(a), the APJ device was constructed using a borosilicate glass cross tube, pair of tungsten electrodes was secured on each end of the tube and connected to a 15,000V 30mA Neon sign transformer. Rotameters attached to gas tanks were used to regulate the gas flow.



Figure 2. Contact angles of (a) untreated and (b) treated PMMA with nitrogen-argon flow rate ratio of 30:10 SCFH and a (c) photo of the visor after the condensation test.

AFM images revealed an increase in the roughness of the PMMA sample after treatment due to formation of nanograins [1]. Optical emission spectra showed the presence of argon, nitrogen and oxygen ions in the plasma. Both the rough physical, sputtering, and formation of functional groups [2,3] may have contributed to the increase in hydrophilicity of the samples.

The lowest average contact angle of 19.51° was achieved at nitrogen-argon flow rate ratio of 30:10 SCFH. Figure 2(c), condensation test using a helmet visor showed that visibility remained clear on the left side, treated with APJ, because there was no formation of tiny droplets. The aging test showed that the contact angle of the treated samples increased about 8~10° after 3 hours and it remained fairly constant at least up to 7 hours.

1. Masood, S.H., S.A. Mohamed, *J Bagh Coll Dentistry* **24**, (2012)
2. T. Yuji, Y. Suzuki, T. Yamawaki, H. Sakaue, H. Akatsuka, *Japanese Journal of Applied Physics* **46**, pp 795-798, 2007
3. M. Nie, P. Patel, K. Sun, D.D. Meng, *4th IEEE International Conference on Nano/Micro Engineered and Molecular Systems* (Hong Kong, China), pp 1017-1020, 2009

Ion species separated atmospheric pressure plasma source

M. Wada, Y. Fujita, T. Kasuya, M.C.C. Lacdan, J. Matsunaga

Graduate School of Science and Engineering, Doshisha University, Kyotanabe, Kyoto 610-0321, Japan

Atmospheric pressure plasmas can deliver activated molecules and atoms on a surface in an atmospheric environment. They modify surface properties of materials without the usage of wet reactive chemical solution. Highly collisional characteristics of these plasmas allow one to predict their behaviour based on two transport constants: diffusion coefficient and ion mobility. The mobility of an air ion in atmospheric gas depends upon its mass, and several types of ion mobility spectrometers have been developed for trace chemical analyses [1], while a Gerdien condenser has been utilized to measure the ion concentration in the high altitude atmosphere [2]. A Gerdien condenser may realize high throughput of ions with reasonable resolution, and an atmospheric pressure ion source development has been started to realize transport of species separated ion flow.

The mobility separated atmospheric pressure ion source consists of three components: the plasma production part, ion mobility separation part, and the ion flow control part. Figure 1 shows the structure of the current design. The plasma is excited by the high voltage induced needle electrodes. The flow field of ions are created by a couple of DC electric fans attached to a 10 cm wide, 10 cm high, and 25 cm long rectangular flow channel. Inside of the channel, two concentric cylinders form an electric field in the volume between the electrodes to guide ions of proper mobility into an opening. The produced flow of ions are guided to a cylinder to be directed to work piece surface.

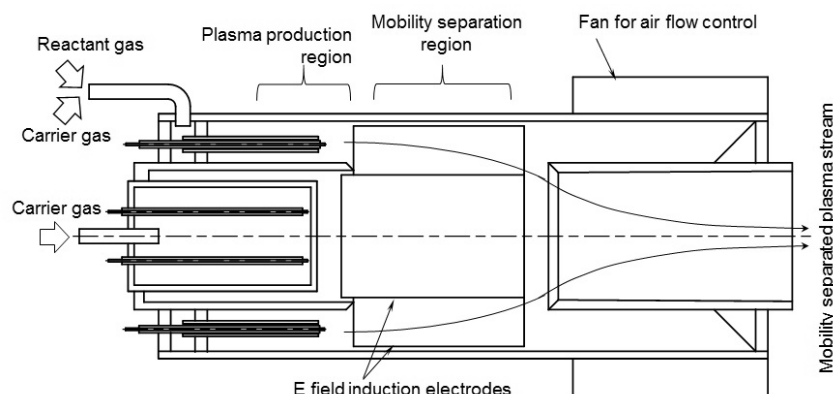


Fig. 1. Atmospheric pressure source with ion mobility selector unit.

The current source employs a modular design, and the plasma production part can be changed to a RF plasma source or a microwave plasma source. The front end that guides the ion flow can be replaced with the component of different dimensions, or different material. Space charge can cause a serious problem to reduce the throughput of the source. The source can contain another tiny inert gas positive ion source at the center of the ion production part to merge reactant negative ions to inert gas positive ions. The effectiveness of merged ion flow to the enhancement of the flux of target ion is being investigated by using a Gerdien condenser for ion species measurement.

- [1] G.A. Eiceman, Z. Karpas, H. H. Hills, Jr. "Ion Mobility Spectrometry," CRC Press, (2013).
 [2] P.E. Raj, P.C.S. A.M. Selvam, A.S.R. Murty, *Advances in Space Research*, **12**, 321 (1992).

Degradation of acetic acid in water using gas-liquid plasma with SPG membrane

Guanyang Tang, Atsushi Komuro, Kazunori Takahashi and Akira Ando

Department of Electrical Engineering, Tohoku University, Sendai 980-8579, Japan

E-mail: tang@ecei.tohoku.ac.jp

Atmospheric-pressure and gas-liquid plasmas have been widely investigated in association with water purification because the plasmas can produce a large amount of active species such as ozone (O_3) and hydroxyl radical ($\cdot OH$), especially the hydroxyl radical which has a very high oxidation potential (2.81V) is well known to play important roles in degradation of persistent organic pollutants (POPs) [1]. Since the hydroxyl radicals are produced at the gas-liquid interface via the discharge process, the energy consumption at the interface rather than that at the gas phase would yield the efficient production of the hydroxyl radicals. Therefore the better production efficiency of the hydroxyl radicals can be obtained for the large surface-to-volume ratio (surface area of the gas liquid interface / volume of the gas phase) [2].

Here a Shirasu porous glass (SPG) membranes tube which has dense micro-pores ($\phi 50\mu m$) is used to introduce a large number of micro gas bubbles into our previous gas-liquid plasma reactor as shown in Figure 1 and to increase the surface-to-volume ratio. Comparing with the previous reactor which has larger holes ($\phi 1mm$) [1], the generation of hydroxyl radical is observed to be enhanced as shown in Figure 2 and the degradation of acetic acid is also predictable to be enhanced. The dependences of acetic acid degradation on the shapes of electrodes and gas flow rate are also discussed with the electric field distribution analyzed by solving two-dimensional Poisson's equation. More details about plasma generation and degradation process of acetic acid will be shown in the presentation.

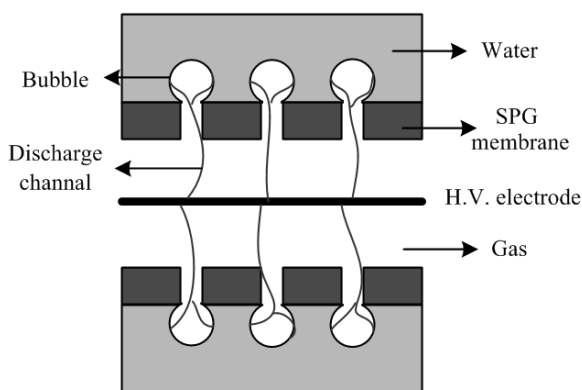


Figure 1. Schematic of discharge reactor with SPG membrane tube.

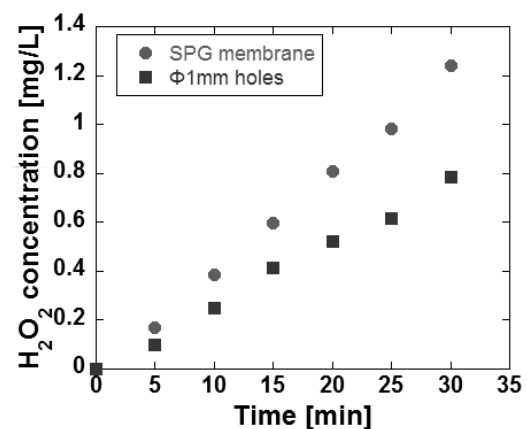


Figure 2. Time variation of H_2O_2 concentration with SPG membrane and previous reactor ($\phi 1mm$).

[1] G. Tang, *et al.* J. Plasma Fusion Res. **10**, 3406022 (2015).

[2] Malik M A, J. Plasma Chemistry and Plasma Processing, **30**, 1 (2010)

Fourier Transform Infrared Spectroscopy of Plasma Polymerized Polyaniline

S. M. Palardonio^a, M. R. Vasquez Jr.^b, H. J. Ramos^a

^a Plasma Physics Laboratory, National Institute of Physics, University of the Philippines, Diliman 1101 Quezon City, Philippines

^b Plasma-Material Interactions Laboratory, Department of Mining, Metallurgical, and Materials Engineering, University of the Philippines, Diliman 1101, Quezon City, Philippines.

This research studied the effect of polymerization time and discharge current to the molecular structure of plasma polymerized polyaniline (PAni). Plasma polymerization of PAni on 1x1 cm glass substrates was performed in a DC plasma-enhanced chemical vapor deposition facility. Prior to polymerization, soluble oils and dusts on the glass substrates were removed by ultra-sonification in 95% ethanol and then air-dried. The glass substrates were lowered in to a 6-cm diameter electrode that serves as a cathode. The anode is 1.5 cm above and has a shower head configuration where precursor gasses can be introduced. The glass substrates were plasma cleaned to further remove adsorbed compounds. Plasma cleaning was done with 5 minutes of argon discharge at <0.4 Pa base pressure, 15 Pa filling pressure, 25 mA current, and 0.40 kV discharge potential. The polymerization was then carried out at a base pressure <0.4 Pa, filling pressure of 80 Pa, discharge potential at 0.48 to 1.00 kV while the discharge current was varied at 1 mA, 2 mA, and 3 mA, and polymerization times of 5 mins, 15 mins, and 30 mins. The plasma polymerized PAni was then analyzed by Fourier Transform Infrared Spectroscopy in Attenuated Total Reflectance mode (ATR-FTIR). ATR-FTIR spectra revealed that all plasma polymerized PAni contains a benzenoid peak at 1600 cm⁻¹ and a secondary amine peak at 3400 cm⁻¹. In addition, peaks at 760 cm⁻¹ and 870 cm⁻¹ suggest a cross-linked polymer in ortho and para position, respectively. Increasing the discharge current was found to introduce quinoid units appearing at 1500 cm⁻¹ and induce aromatic ring opening as suggested by the aliphatic C-H bond peaks at 2900 cm⁻¹. The effect of duration of polymerization was also found to introduce quinoid units but aromatic ring opening was greatly enhanced as polymerization time is increased. It is concluded that introduction of quinoid units and aromatic ring opening is dependent on discharge current and polymerization time.

Effect of electrode shapes and the working gases on production amount of hydroxyl radicals in atmospheric-pressure plasma jets

Y.Okuno^a, H.Matsuura^b, S.Okuda^b, T.Fujiyama^a, M.Furuta^b, Y.Takemura^c, S.Kado^d

^a *Grad. Sch. Eng, Osaka Pref. Univ., 1-1 Gakuen-cho, Naka-ku, Sakai City, Osaka, 599-8531, Japan.*

^b *Osaka Prefecture University, 1-1 Gakuen-cho, Naka-ku, Sakai City, Osaka, 599-8531, Japan*

^c *Kinki University, 3-4-1 Kowakae, Higashiosaka City, Osaka 577-8502, Japan*

^d *Institute of Advanced Energy, Kyoto University, Gokasho, Uji, 611-0011 Japan*

Atmospheric-pressure plasma jets have attracted attentions as a sterilization method in the field of medical applications and biotechnology because of little heat damage and rich reactive oxygen/nitrogen species production. Hydroxyl radicals (OH) have a high sterilization effects in the reactive species due to the strong oxidizing power and the light emission in the vicinity of 309 nm.

Our group has proposed to use plasma degradation of toxic phorbol esters and disinfection procedure of *Escherichia coli* [1]. OH are directly not generated from a working gas of the plasma jets but by involving ambient air and/or water [2]. Thus it is important to improve generation efficiency of OH by optimizing the shape in vicinity of the outlet of the plasma jets. The degradation and the disinfection require a huge amount of expensive helium (He) gas for plasma production. Its running cost is not economical. Argon (Ar) gas, which is cheaper than He, is one possible alternative. Both He and Ar plasma jets are able to eject by one plasma source. In this study, the effect of the electrode shapes and the working gases on the production amount of OH.

Emission spectral analysis are able to measure the production amount of OH. Deferent of light intensity about 309 nm by the each electrode shapes and the working gases is analysed by spectrometer (Maya2000pro, Ocean Optics). The optimal conditions of OH generation will be discussed in the conference.

This work was supported by the "ZE Research Program, IAE (ZE27B-4).

[1] H. Matsuura, Y. Onishi, S. Kongmany, M. Furuta, K. Imamura, Y. Maeda, S. Okuda, *Plasma Medicine*, **4**(1-4), 29 (2014).

[2] Y. Takemura, S. Umeji, K. Ito, S. Furuya, M. Furuta, *Plasma Medicine*, **4**(1-4), 89 (2014).

Effects of a magnetic Laval nozzle to the thrust performance on an MPD thruster

Hiroaki Nabuchi, Kiyotaka Suzuki, Yohei Kobayashi, Atsushi Komuro, Kazunori Takahashi and Akira Ando

Department of Electrical Engineering, Tohoku University, Sendai 980-8579, Japan

e-mail address of submitting author : nabuchi@ecei.tohoku.ac.jp

Recently, various missions of space explorations are proposed and intensive development of space propulsion engines with high thrust and high specific impulse are urgently required. A Magneto Plasma Dynamic (MPD) thruster is one of the candidates for main engines in manned deep space missions because of its high operating electric power above a hundred of kW and the resultant large thrust.

To improve the thrust performance, an applied field MPD thruster has been investigated with various magnetic field configurations and characteristics of the fast-flowing plasma generated in the MPDs have been investigated [1,2]. It has been reported that both the thrust and the plasma flow velocity can be increased by applying a diverging magnetic field [3]. This acceleration seems to be due to the interaction between the discharge current and the applied magnetic field. However, it has been also observed that the fast-flowing plasma is thermalized downstream of the divergent magnetic field.

In this study, the magnetic Laval nozzle shown in Fig. 1 is additionally applied to reaccelerate the plasma via a momentum conversion process in the cross-section-varying plasma flow. The uniform field $B_0 = 0.10$ T, the diverging magnetic nozzle $B_{zc} = 0.28$ T, and the magnetic Laval nozzle B_{zL} corresponding to the magnetic nozzle throat set at $Z = 100$ mm downstream of the MPD thruster are superimposed and helium is chosen as a working gas. Five configurations being tested are labeled as $B_{zL} = 0, 0.10, 0.15, 0.20$ and 0.25 T, respectively.

The maximum thrust of 6.9 N and the maximum plasma flow velocity of 64 km/s at $Z = 200$ mm are obtained for the case of $B_{zL} = 0.15$ T. Assessment of the Lorentz force suggests that the Lorentz force exerted to the plasma flow is mainly in radial direction and does not explain the thrust increase. The detailed results of the thrust, the axial plasma flow velocity, the ion temperature and the ion density of the MPD thruster will be shown and the physics underlying in the magnetic Laval nozzle attached to the MPD thruster will be discussed in the presentation.

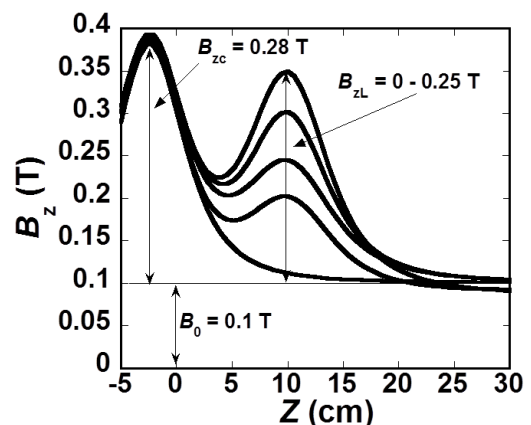


Fig.1 The magnetic field configurations

- [1] A.Sasoh, *et al.*, Journal of Propulsion and Power **11**, 351 (1995)
- [2] M. Inutake, *et al.*, Plasma Phys. Control. Fusion **49** A121 (2007).
- [3] Y. Izawa, *et al.*, JPS Conf. Proc. **1**, 015046 (2014)

Design of electron supplier in a new concept of neutron generator for BNCT

D. Adachi, T. Matsui, M. Yanagi, T. Takahashi, and H. Momota^a

Gunma University, 1-5-1 Tenjin-cho, Kiryu 376-8515, Japan

^a *National Institute for Fusion Science, 322-6 Oroshi-cho, Toki 509-5292, Japan*

Compare to conventional methods of cancer therapy, boron neutron capture therapy (BNCT) is more effective to destroy cancer cells and to lessen damage of healthy cell. Since BNCT needs thermal or epithermal neutrons with the yield of 10^9 particles/sec, an atomic reactor was formerly used as a neutron source [1]. It is not available in Japan after the nuclear power plant accident in 2011. Nowadays, a neutron source with an accelerator has been developed [2,3]. The accelerator neutron sources, however, need large space to install in an urban hospital and its construction cost will be high. Therefore in this study we propose the new concept neutron source which can be installed in hospital room.

The new concept neutron source is electrostatic confinement fusion equipment, which generates neutrons by the D-D reaction [4]. Its size is estimated to be smaller than traditional neutron sources. Deuterium ions sources are installed at both ends of linear neutron generator. Beam ions are accelerated axially in the electrostatic potential gap of 30 kV, and counter beam particles react in the reaction chamber in the central region of the machine. In order to suppress the deleterious two stream instability, the axial magnetic field is applied by the solenoid coil.

The electron supplier controls the electron density in the reaction chamber so that the plasma in the chamber maintains to be in quasi-neutral condition. The electron supplier has two coils that generate the cusp magnetic field, and it separates thermal electrons from beam ions[5]. The electron generator installed in the line cusp region supplies electrons into the reaction chamber, and high-energy beam ions never go into this region. In the present study, we will show calculation results of orbit of beam ions and thermal electrons in the cusp magnetic field, and will design the efficient electron supplier.

[1] T. Yamamoto, A. Matsumura, K. Yamamoto *et al.*, Radiation Research. **160** (2003) 70.

[2] H. Tanaka, Radioisotopes. **64** (2015) 29. (in Japanese)

[3] H. Tanaka, Y. Sakurai, M. Suzuki *et al.*, Appl Radiat Isot. **69** (2011) 1642.

[4] H. Momota and G. H. Miley, J Fusion Energ.. **28** (2009) 191.

[5] A. Taniguchi, N. Sotani, Y. Yasaka *et al.*, J. Plasma Fusion Res. SERIES. **9** (2010) 237.

Beam ion confinement in a new concept of neutron generator for BNCT

T. Matsui, D. Adachi, M. Yanagi, T. Takahashi, and H. Momota^a

Gunma University, 1-5-1, Tenjin-cho, Kiryu 376-8515, Japan

^a *National Institute for Fusion Science, 322-6 Oroshi-cho, Toki 509-5292, Japan*

Boron neutron capture therapy (BNCT) is a new cancer treatment that has been attracting attention in recent years. It is possible to destroy cancer cells selectively and reduce risk of damaging healthy cells [1]. Although BNCT requires a neutron source with the yield of 10^9 particles/sec or more, no sufficient source is available in the present circumstances. Recently, accelerator-based neutron source is further along in development [2].

In this report, we propose a new neutron source using nuclear fusion reaction [3]. It is expected to be more compact than the accelerator. Therefore, this will be easily installed to the hospital. We propose a neutron source consisting of ion source, electronic separator, and reaction chamber. In the present study, we report on beam ion confinement in the reaction chamber. The beam ion is accelerated by the electrostatic potential gap at both ends of linear confinement system. Since counter-beam configuration will cause the deleterious two-stream instability, the suppression effect by the external axial field is studied by 2-dimensional hybrid simulation. Detailed results will be shown in our presentation.

[1] R. F. Barth, A. H. Soloway, R. G. Fairchild, and R. M. Brugger, *Cancer* **70** (1992) 2995.

[2] H. Tanaka, Y. Sakurai, M. Suzuki *et al.*, *Appl Radiat Isot.* **69** (2011) 1642.

[3] H. Momota and G. H. Miley, *J Fusion Energ.* **28** (2009) 191.

Formation Mechanism of Periodic Nano-Grating Structure by Surface Plasma Wave

A. M. Gouda, H. Sakagami,^a M. Hashida,^b and S. Sakabe^b,

Department of Physics, Nagoya University, Nagoya, 464-8602, Japan

^a *National Institute for Fusion Science, Toki, Gifu 509-5292, Japan*

^b *Institute for Chemical Research, Kyoto University, Uji, Kyoto 611-0011, Japan*

E-mail: amany.gouda@nifs.ac.jp

This abstract aims to introduce one of formation mechanisms for the periodic nano-grating structure, which is an emerging multidisciplinary research area at the multifaceted edge at the forefront of the physics of plasmas and gas discharges, nano-science and nanotechnology, astrophysics, materials science and engineering, and structural chemistry [1]. And show the importance of the plasma environments in nano-scale processes spanning from astrophysics to plasma-aided nanofabrication in the laboratory.

The formation mechanism of the periodic nano-grating structure has been investigated and confirmed by 2D PIC code [2] and with irradiating the laser pulses of 500 fs pulse, wavelength 800 nm, incidence angle 0°, p-polarized and intensity of 10^{16} W/cm²-μm². The surface plasma wave plays an expressive role with the oscillating two streams instability in explaining our suggested mechanism. The surface plasma waves are excited by the laser beam and propagate to upper and lower direction composing the standing wave.

In laser plasma interaction, there is a force coupled to the particles in a somewhat subtle way and is called the Ponderomotive force. The Ponderomotive force is a nonlinear force that a charged particle experiences in an inhomogeneous oscillating electromagnetic field. The Ponderomotive force by the standing wave E- field forms perturbations at the boundary, which can be grown by the oscillating two stream instability to form the periodic nano-grating structure. Fig.1 shows the propagation of the electric field component in y-direction by the dashed line, which starts from time $T_{\text{start}}=268.47$ [fs] with time difference $\Delta t=0.27$ [fs]. This is a proof of existence of the surface plasma wave in the upper part of the electric field.

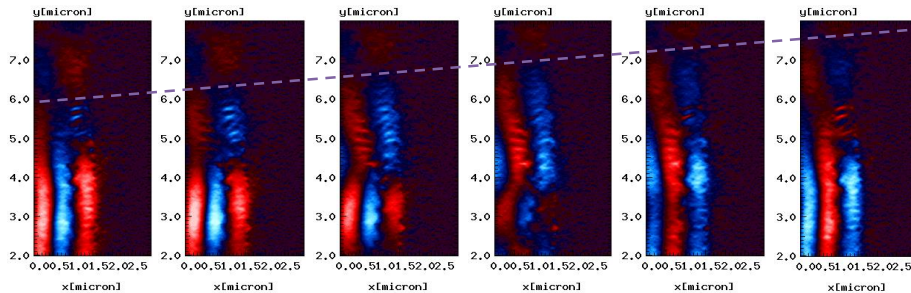


Fig.1. Time evolution of the upper part of the electric field component in y-direction.

[1] K. Ostrikov, “Colloquium: Reactive plasma as a versatile nanofabrication tool,” *Rev. Mod. Phys.*, **77** (2005) 489–511.

[2] H. Sakagami and K. Mima: *Proc. 2nd Int. Conf. Inertial Fusion Sci. Appl.* (2001) 380-383.

Krylov Subspace Method with Communication Avoiding Technique for Linear System Obtained from Electromagnetic Analysis

S. Ikuno^a, G. Chen^a, S. Yamamoto^a, T. Itoh^b, K. Abe^c, and H. Nakamura^{d,e}

^a*School of Computer Science, Tokyo University of Technology, Hachioji, Japan*

^b*College of Industrial Technology, Nihon University, Narashino, Japan*

^c*Faculty of Economics and Information, Gifu Shotoku Gakuen University, Gifu, Japan*

^d*Department of Energy Engineering and Science, Nagoya University, Toki, Japan*

^e*National Institute for Fusion Science, Toki, Japan*

In the present study, Krylov subspace method with a communication avoiding technique is applied for the linear system obtained from electromagnetic analysis. It is well known that the algorithm of Krylov subspace method is very simple, and the most of all the procedure of the method is constituted by addition of vectors, inner products and multiplication of matrices and vectors. These operations are very easy to get a high performance by parallelization. However, the communication between processing units (PUs) must be necessary for parallelized inner products calculation, and the amount of the communication time increases as the size of the system increase. That is to say, the communication time is bottle neck for the effective parallelization.

The communication avoiding technique is one of a settlement for above issue [1, 2]. Although the algorithm of Krylov subspace method with the communication avoiding technique is different from original method, the theoretical methodology is equivalent. In the technique, inner products is rewritten to the recurrence formular using the basis of Krylov subspace, and the inner products are transcribed into scalar calculation. As the results, communications between PUs can be gathered in only one time.

The purpose of the present study is to develop Krylov subspace method with the communication avoiding technique, and to applied for the linear system obtained from electromagnetic analysis. In addition, the parallelized method is implemented on Graphics Processing Unit (GPU) to obtain high performance calculation.

- [1] Mark Hoemmen, "Communication-Avoiding Krylov Subspace Methods", The doctoral dissertation of University of California at Berkeley, Berkeley, CA, USA, 2010.
- [2] J. W. DEMMEL, M. H. and MOHIYUDDIN, M., "Minimizing communication in sparse matrix solvers", in Proceedings of the 2009 ACM/IEEE Conference on Supercomputing (2009).

Magnetic property analysis for spherical shell magnetic substance using Monte Carlo simulation

K. Terashima, K. Yamaguchi, T. Uchimoto^a, T. Takagi^a, H. Nakamura^b

Fukushima University, Kanayagawa 1, Fukushima, 960-1296, Japan

^a *Tohoku University, 2-1-1 Katahira, Aoba-ku, Sendai, 980-8577, Japan*

^b *National Institute for Fusion Science, 322-6 Oroshi-cho, Toki 509-5292, Japan*

In this study, magnetization property of minute spherical shell magnetic substance with hollow inside was analyzed using Monte Carlo (MC) simulation. The spin behavior of spherical shell with different thickness and size was verified. The spherical shell magnetic substance is included to many iron or nickel-based structural materials. For example, in spheroidal graphite cast iron, magnetic layer was deposited around spheroidal graphite. It has been much studied for relationship between mechanical strength of material and shape or composition of magnetic layer [1]. In addition, Ni-base super alloy Alloy600 has ferromagnetism around grain boundary with degradation progress [2]. Here, magnetic layer around grain boundary is considered spherical shell magnetic substance. Thus minute spherical shell magnetic substance has influence for the property of material and knowing the magnetic property is very important from viewpoint of magnetic nondestructive evaluation (NDE).

In this simulation, some clusters were prepared with magnetic site on a lattice point in simple cubic lattice which has different thickness and radius of spherical shell. Following Hamiltonian is set:

$$\begin{aligned}
 H &= H_J + H_D + H_B \\
 &= -\sum_{near} J_{ij} \mathbf{S}_i \cdot \mathbf{S}_j + D \sum_{all} \left(\frac{\mathbf{S}_i \cdot \mathbf{S}_j}{|\mathbf{r}_{ij}|^3} - \frac{3}{|\mathbf{r}_{ij}|^5} (\mathbf{S}_i \cdot \mathbf{r}_{ij})(\mathbf{S}_j \cdot \mathbf{r}_{ij}) \right) + B \sum_i \mathbf{S}_i.
 \end{aligned} \tag{1}$$

Each term of J_{ij} , D and B represents exchange interaction constant for i -th site and j -th site, magnetic dipole interaction constant and external magnetic field, respectively. Here \mathbf{S}_i denotes the magnetic moment of the magnetic site of i -th cell and \mathbf{r}_{ij} represents the vector between i -th site and j -th site.

In the magnetic reversal process, island-shape such as magnetic domain is formed and spin behavior becomes complex. Additionally, reversal process has more complex due to size and thickness of spherical shell.

The behavior of spin in spherical shell magnetic substance was analyzed by MC simulation. Therefore, the relationship between macroscopic and microscopic magnetic property was cleared and shown the possible to estimate the state of microscopic region from macroscopic magnetic measurement for iron or nickel-based structural materials with spherical shell magnetic substance. As a result, the possibility of application was shown for magnetic NDE. Furthermore, the high-precision analysis was expected by comparison for experimental result of local magnetic property using μ -MOKE.

[1] N. Shinohara, N. Suura, N. Hattori and R. Sakuragi, Trans. Jpn. Soc. Mech. Eng. A, 79(797) (2013) 13-22.

[2] R. Oikawa, T. Uchimoto and T. Takagi, Trans. Jpn. Soc. Mech. Eng. A, 75(760) (2009) 1777-1783.

Dissipative particle dynamics simulation of self-assembly in bolaamphiphilic solution

S. Fujiwara, Y. Takahashi, H. Ikebe, T. Mizuguchi, M. Hashimoto, Y. Tamura^a, H. Nakamura^b, R. Horiuchi^b

Kyoto Institute of Technology, Matsugasaki, Sakyo-ku, Kyoto 606-8585, Japan

^a *Konan University, 8-9-1 Okamoto, Higashinada-ku, Kobe 658-8501, Japan*

^b *National Institute for Fusion Science, 322-6 Oroshi-cho, Toki 509-5292, Japan*

The spontaneous formation of structures has recently become the focus of interest in nonequilibrium and nonlinear systems such as plasma systems and soft matter systems. We aim at improving plasma confinement by clarifying the self-organizing properties common to these systems. To this end, we investigate the structure formation in soft matter systems such as the micelle formation and the mesophase formation in amphiphilic solutions. Amphiphilic molecules such as lipids and surfactants are composed of both hydrophilic and hydrophobic groups. In aqueous solvents, such amphiphilic molecules often spontaneously self-assemble into various structures such as micelles, bicontinuous structures and vesicles [1,2]. Although numerous computer simulation studies have so far been done on the structure formation of amphiphilic molecules, each of which consists of a hydrophilic head group and a hydrophobic tail group, there have been few theoretical and simulational studies on the structure formation of bolaamphiphilic molecules, each of which consists of a hydrophobic stalk and two hydrophilic ends. The purpose of this study is to clarify the effect of the interaction difference between the two different hydrophilic ends, Δa , on the self-assembly in bolaamphiphilic solutions. With a view to investigating the self-assembly in bolaamphiphilic solutions at the molecular level, we perform the dissipative particle dynamics simulations of bolaamphiphilic molecules with explicit solvent molecules and analyze the formation processes of micelles and vesicles. Our simulations show that various kinds of self-assembled structures such as worm-like micelles, vesicles and nanotubes are obtained. It is also ascertained that the vesicles formed at small Δa change to the worm-like micelles as the interaction difference, Δa , increases.

[1] J. N. Israelachvili, *Intermolecular and Surface Forces*, 2nd ed. (Academic Press, London, 1992).

[2] I. W. Hamley, *Introduction to Soft Matter*, Rev. ed. (J. Wiley, Chichester, 2007).

Improvement of divertor probe array for heat flux measurement of Heliotron J divertor leg plasma

H. Matsuura, Y. Umeda, D. Oda^a, T. Mizuuchi^a, and Y. Suzuki^b

Osaka Prefecture University, 1-2 Gakuen-chi, Sakai Naka-ku 599-8570, Japan

^a*Kyoto University, Gokasho, Uji 611-0011, Japan*

^b*National Institute for Fusion Science, 322-6 Oroshi-cho, Toki 509-5292, Japan*

matsu@me.osakafu-u.ac.jp

In the design of fusion reactors for high power and long pulse operation, vast heat flux is expected to flow onto divertor target plates. In order to reduce this heat load, the divertor design on stable detached plasma formation must be realized. Compared with Tokamak, helical systems have intrinsic diverted field lines and large variety of divertor configuration such as island divertor. The asymmetry of divertor flux is still an open question and few report on heat flux reduction with detachment has been published yet.

Heliotron J is a medium sized helical axis Heliotron device with a helical winding coil of $L = 1/M = 4$. In the standard configuration, so-called whisker field line structure covers the last closed flux surface, and some of field lines crosses the inner wall of Heliotron J, forming four localized divertor legs in one toroidal period [1]. By adjusting coil current ratio, island divertor configuration is also available. From the beginning of Heliotron J experiment series, multi channel langmuir probe array has been equipped to study particle flux behavior and existence of clear up-down asymmetry was reported [2]. As for heat flux, however, such observation is lacking, since no calorimeters or no thermal probes is prepared in the divertor probe array. According to sheath theory, heat flux through the sheath is the function of the sheath potential drop and also depends on ion parameters such as its temperature or energy reflection coefficient.

In this work, new calorimeter chips is designed to combine with conventional divertor probe array, which is a SUS right-angled parallelepiped with many Molybdenum probe pins on one plasma facing surface. Since magnetic field lines in the divertor leg are almost parallel to this surface. So the calorimeters on this surface may fail to detect the divertor heat flux. calorimeters on the side surface is also necessary. For choice of the calorimeter material, not only thermal diffusion time but also estimated temperature increment must be considered. Copper has fast thermal diffusion necessary for fast heat flux measurement, but its temperature might accumulate during plasma shots and reach the melting point. In the conference, the size and shape of designed calorimeter head will also be presented. This work is partially performed with the support and under the auspices of the NIFS Collaborative Research Program. (NIFS14KUHL061)

- [1] T. Mizuuchi et al., J. Plasma Fusion Res. **3** (2000) 192.
- [2] W. Ang et al., J. Plasma Fusion Res. **5** (2002) 292.
- [3] H. Matsuura et al., 22nd ITC (2002) P1-23.

Study of Heat and Particle flux in the case of Gas Injection in the D-module of GAMMA 10/PDX

M. S. Islam, Y. Nakashima, H. Matsuura^a, K. Ichimura,
M. M. Islam, K. Shimizu, K. Fukui, M. Ohuchi, K. Nojiri, N. Ezumi,
M. Sakamoto and T. Imai

Plasma Research Center, University of Tsukuba, Ibaraki 305-8577, Japan
^aRadiation Research Center, Osaka Prefecture University, Osaka 599-8570, Japan

Influence of gas injection in the D-module of GAMMA 10/PDX has been investigated based on calorimeters and Langmuir probes data in this research. In GAMMA 10/PDX, divertor simulation experiments have been started by using a divertor simulation experimental module (D-module) [1]. In the D-module of GAMMA10/PDX as shows in Fig.1, a V-shaped target made of tungsten has been installed. A set of Langmuir probes and calorimeters has been installed at the upper and lower plates respectively of the V-shaped target for simultaneous measurement of particle and heat flux. Heat flux has been measured by the calorimeter. Electron temperature (T_e), electron density (n_e) and ion saturation current (I_{i-sat}) have been measured by the Langmuir probe. According to the increase amount of gas injection, reduction of T_e , I_{i-sat} , n_e and heat flux have been observed. In the case of gas injection through either gas injection from the port at the front-side (F) or the rear-side (R), the reduction of heat flux, n_e , T_e and I_{i-sat} remained almost same. However, a remarkable reduction of the heat flux, T_e and I_{i-sat} have been observed when gas was injected through both gas injection ports (F) and (R). In the Ar injection experiments, H_2 gas was injected simultaneously to examine the effect of molecular process on detached plasma formation. In this case, both the heat flux and ion saturation current are drastically reduced. The detail of the experimental results will be reported in the presentation.

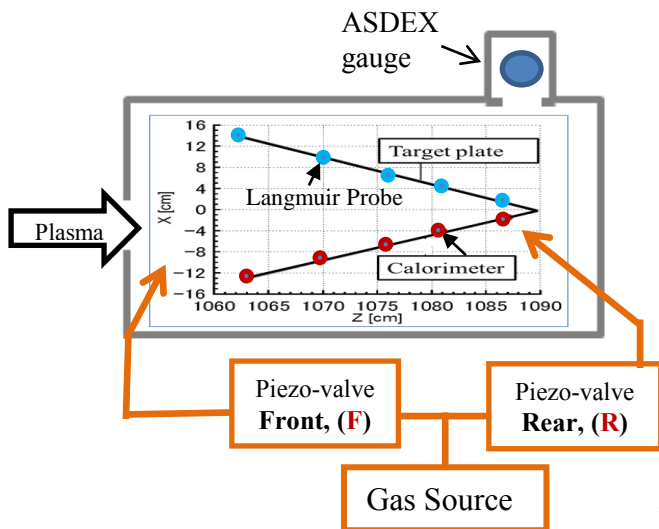


Fig.1 Schematic view of D-module

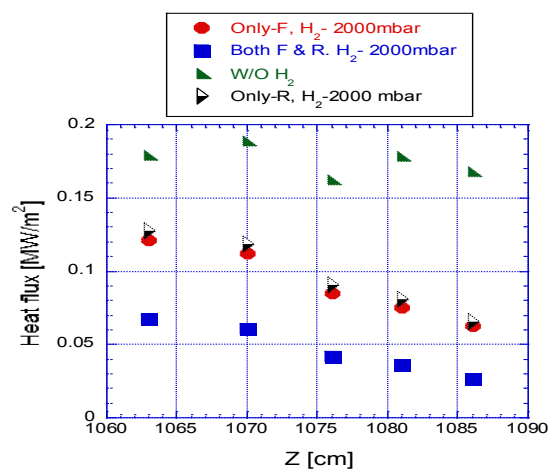


Fig.2 Distribution of heat flux on Z axis in the D-module of GAMMA10/PDX. (Pressure indicates the plenum pressure of the gas source.)

[1] Y. Nakashima et al. J. Nucl. Mater. **438** (2013) S738-S741.

Study of the axial plasma confinement for high particle flux operations in GAMMA 10/PDX

K. Ichimura, Y. Nakashima, M. M. Islam, M. S. Islam, K. Shimizu, K. Fukui,
M. Ohuchi, M. Hirata, R. Ikezoe, M. Yoshikawa, N. Ezumi, M. Sakamoto,
M. Ichimura and T. Imai

Plasma Research Center, University of Tsukuba, Tsukuba, Japan

Enhancing the parameter of the end-loss ion flux is an important issue in the divertor simulation studies in GAMMA 10/PDX [1]. In recent experiments, the end-loss ion flux relevant to the ITER scrape off layer plasma (1.6×10^{23} particles/m²s) was obtained by superimposing the additional ICRF wave heating into minimum-B regions of the tandem mirror. With the ICRF heating, large increase in the electron line-density in the central-cell (NLCC) and the end-loss particle flux were observed [2]. The behavior of the electron line density, plasma temperature and the amount of end-loss ion flux during the experiments suggested that the mechanism of the axial ion loss was changed due to the increase of ion collision frequency. In standard operations of GAMMA 10/PDX, plasma has high ion temperature ($T_{i\perp} = 4000$ eV, $T_{i\parallel} = 400$ eV) and the ratio of mirror length and the axial mean free path of ions is small ($L/\lambda_{i\parallel} \approx 0.01$). In contrast with the standard operations, plasma parameters in high-density operations stays in the range of high collision frequency and the ratio $L/\lambda_{i\parallel}$ is about 0.6. In such collisional plasma, the end-loss ion particle flux show linear dependence on the plasma density instead of the parabolic dependence expected in plasmas of low collision-frequency [3]. Figure 1 shows the experimental and theoretical dependence of the end-loss ion particle flux on NLCC. The dependence in such wide range of NLCC is experimentally observed for the first time. The result is useful to discuss the future prospect of the particle flux enhancement in the tandem mirror machine. In the high collision frequency plasma, it is notable that plasma potential ϕ largely changes the dependence of the particle flux on the plasma density. In the presentation, detailed results of experiments and the discussion on the ion confinement time will be reported.

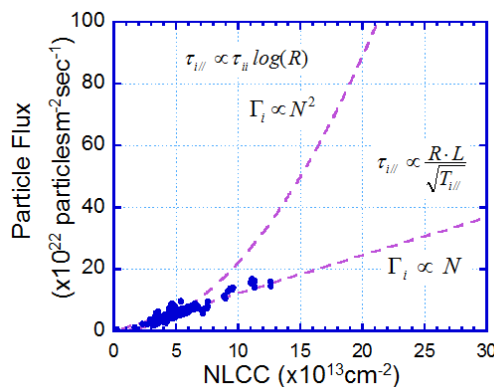


Fig. 1 Dependence of the end-loss ion particle flux on the line density at the central-cell.

- [1] Y. Nakashima et al., J. Nucl. Mater. **438** (2013) S738.
- [2] K. Ichimura et al., Trans. Fusion Sci. Technol. **63** 1T (2013) 209-212.
- [3] R. Minai et al., J. Phys. Soc. Jpn. **66** 7 (1997) 2051-2056.

A study on hydrogen transport in liquid lithium under steady state plasma bombardment

H. Bi^{1,*}, Y. Hirooka^{1,2}, J. Yagi², Y. Xu¹

¹ *The Graduate University for Advanced Studies, 322-6 Oroshi, Toki 509-5292, Gifu, Japan*

² *National Institute for Fusion Science, 322-6 Oroshi, Toki 509-5292, Gifu, Japan*

The application of liquid metals as plasma facing materials draws an increasing interest as a potential means to resolve the technical issues associated with exhaust power and particle handling in magnetic fusion devices. Lithium is one of the promising candidates because of its low atomic number and melting point, and high absorptivity of impinging species. It has been used in fusion devices including NSTX[1] and EAST[2]. In these confinement devices, it is believed that hydrogen transport in liquid lithium plays an important role in determining edge plasma characteristics and hence core confinement performance. Nonetheless, little information is available on hydrogen transport in liquid lithium under steady state plasma bombardment, presumably due to the difficulty of handling liquid metals.

In the present work, an innovative experimental technique holding liquid lithium on a mesh substrate by surface tension has been put together for the plasma-driven permeation (PDP) experiments in a plasma-wall interactions facility: VEHICLE-1[3]. Temperature effects on PDP behaviour have been observed in the temperature range from 313°C to 402°C. It has been found that hydrogen permeation through liquid lithium is recombination limited judged from the breakthrough curve of permeation flux. This shows a similar behaviour to prior PDP experiments on titanium membranes, which are conducted because hydride is formed both in titanium and liquid lithium. As a result, H recombination coefficients are obtained and compared with literature data in **Fig. 1**. [4]. No convection is considered in this work.

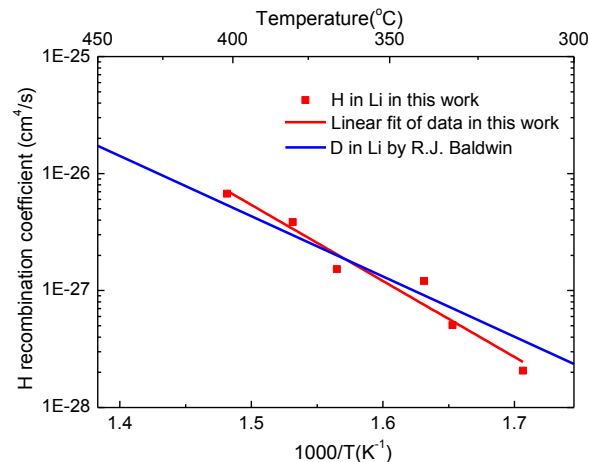


Fig.1. Hydrogen recombination coefficient obtained from PDP experiments.

The thickness of liquid Li membrane is about 2mm. H⁺ incident flux is about 1x10¹⁶ H/cm²s with 100eV.

- [1] H.W. Kugel et al, Fusion Eng. Des.87 (2012) 1724– 1731
- [2] J.S. Hu et al, Fusion Eng. Des.89 (2014) 2875–2885
- [3] H. Zhou et al, Journal of Nuclear Materials 455 (2014) 470–474
- [4] M.J. Baldwin et al, Journal of Nuclear Materials 306 (2002) 15–20

Characterization of detached recombining plasma in Pilot-PSI

Y. Hayashi, K. Ješko^a, H.J. van der Meiden^b, J. Vernimmen^b,
T.W. Morgan^b, N. Ohno, S. Kajita^c

Graduate School of engineering, Nagoya University, Nagoya, Aichi 464-8603, Japan

^a CEA, IRFM, F-13108 Saint-Paul-Lez-Durance, France

^b FOM Institute DIFFER – Dutch Institute for Fundamental Energy Research, partner in the Trilateral Euregio Cluster, Eindhoven, the Netherlands

^c Eco Topia Science Institute, Nagoya University, Nagoya, Aichi 464-8603, Japan

Plasma detachment accompanied by volumetric recombination processes is part of the key physics required for the success of magnetically confined fusion. Linear plasma devices, which simulate the magnetic field geometry from the upstream scrape-off layer (SOL) to the divertor plate in magnetically confined fusion devices, have previously made great contributions to understanding plasma detachment [1, 2]. However, it is necessary to conduct plasma detachment experiments under the high particle flux conditions relevant to detached divertor operations in ITER. The linear plasma device Pilot-PSI is able to generate high density plasma ($> 10^{20} \text{ m}^{-3}$) with high ion flux ($> 10^{24} \text{ ions m}^{-2}\text{s}^{-1}$) [3]. However the essential plasma parameters such as electron temperature, T_e , and electron density, n_e , in detached recombining plasmas have not been sufficiently well characterised. In this study, in order to understand the fundamental properties of detached recombining plasma in Pilot-PSI, the radial profiles of plasma parameters such as T_e and n_e have been measured by reciprocating electrical probes and Thomson scattering (TS) measurement focusing on the neutral pressure, P , dependence. Electrical probes support the TS especially in plasma peripheral region, where the scattering light becomes weak while TS can give an unambiguous determination of the range of probe validity when its signal/noise ratio is high.

The experiments were performed by using the single probe and double probe for T_e and n_e measurements scanned across the plasma column with a reciprocating arm and compared to TS. Figure 1(a) and (b) show, respectively, the P dependence of n_e and T_e at plasma centre. Single and double probe values of n_e monotonically decrease with increasing P , while the n_e from TS has a peak at $P \sim 8 \text{ Pa}$. On the other hand, T_e from the probes is in a good agreement with the TS. The results indicate that a steep gradient of T_e leads to the plasma recombination and the decrease of density as neutral pressure increases.

This work was supported by JSPS KAKENHI Grant Number (25289337). This work is partially supported by NIFS/NINS under the project of Formation of International Network for Scientific Collaborations and NIFS Collaboration Research Program (NIFS14KUGM094).

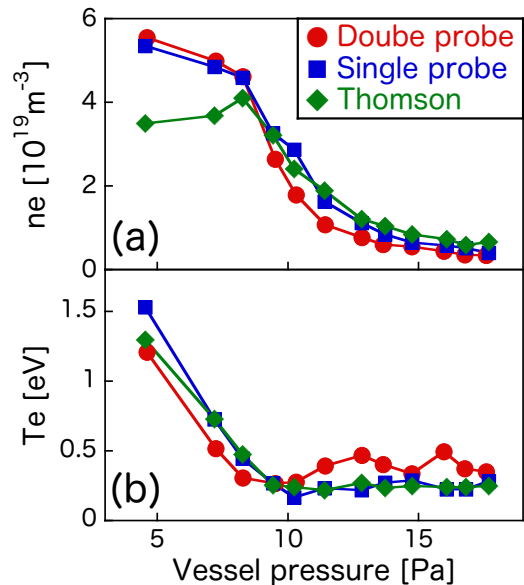


Fig. 1 Neutral pressure dependence of (a) n_e and (b) T_e at plasma center by double probe, single probe and Thomson scattering measurements.

- [1] D. Nishijima, *et al.*, Plasma Phys. Control. Fusion **44** (2002) 597.
- [2] E.M. Hollmann, *et al.*, Phys. Plasmas **20** (2013) 093303.
- [3] G.De Temmerman, *et al.*, Nucl. Fusion **51** (2011) 073008.

Erosion of bubble formed tungsten materials

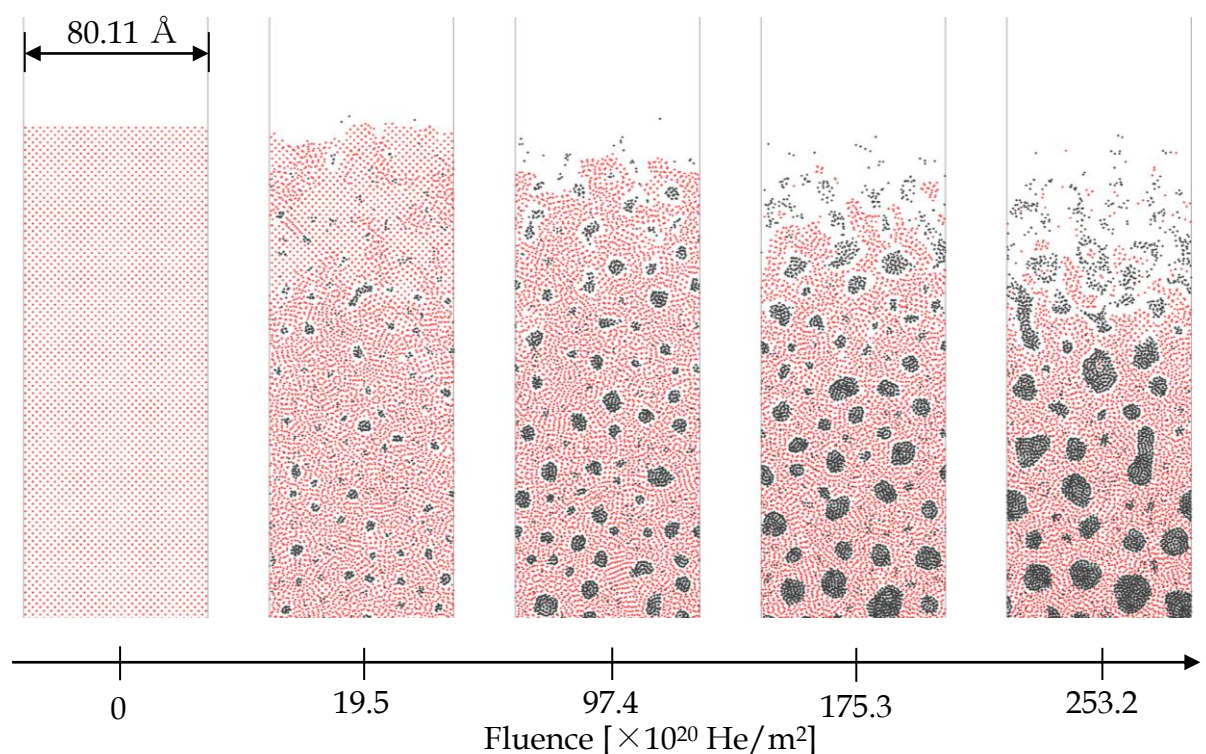
S. Saito, M. Tokitani^a, H. Nakamura^a

Institute of Technology, Kushiro College, 2-32-1 Otanoshikenishi, Kushiro 084-0916, Japan

^a *National Institute for Fusion Science, 322-6 Oroshi-cho, Toki 509-5292, Japan*

When tungsten materials are exposed by helium plasma, bubbles are formed [1] at the surface of tungsten material in wide range of incident energy. The existence of bubbles change the characteristics of tungsten materials as plasma facing material such as sputtering yield, retention, and so on. The depth where bubble forms depends on the incident energy. To reveal the sputtering yield and erosion on bubble formed tungsten materials, binary-collision-approximation-based (BCA-based) simulation is performed in this paper.

Figure 1 shows the simulation results of the time evolution of the surface of a tungsten material irradiated by helium plasma with incident energy of 25 keV. The red and black dots denote the tungsten and helium atoms, respectively. This figure shows the erosion of the tungsten materials. We investigate incident energy dependence of the erosion speed and the sputtering yield by performing the BCA-based simulation (AC ∇ T code) for wide range of incident energy.



- [1] M. Tokitani, N. Yoshida, K. Tokunaga, H. Sakakita, S. Tiyama, H. Koguchi, Y. Hirano, and S. Masuzaki: *Plasma Fusion Res.* volume:5 (2010) 012.
- [2] S. Saito, A. Takayama, A. M. Ito, A. Kenmotsu, and H. Nakamura: *Progress in Nuclear Science and Technology*, volume: 2 (2011) 44.
- [3] S. Saito, A. Takayama, A. M. Ito, and H. Nakamura: *Proc. 30th JSST Annual Conference* (2011) 197.
- [4] S. Saito, M. Tokitani, and H. Nakamura: *Springer CCIS*, volume:474 (2014) 176.

Hydrogen gas-driven permeation through F82H steel coated with vacuum plasma sprayed tungsten

Y. Xu ^{1,*}, Y. Hirooka ^{1,2}, T. Nagasaka ^{1,2}, H. Bi ¹, J. Yagi ^{1,2}

¹ The Graduate University for Advanced Studies, 322-6 Oroshi, Toki 509-5292, Gifu, Japan

² National Institute for Fusion Science, 322-6 Oroshi, Toki 509-5292, Gifu, Japan

Hydrogen isotopes transport behaviour through tungsten coated reduced activation ferritic steels such as F82H has attracted increasing attention in the fusion engineering research community [1]. However, limited amount of literature data is available on the transport parameters related to diffusivity, permeability and solubility of hydrogen isotopes in tungsten coated F82H.

This paper reports on these parameters using a laboratory-scale plasma device: VEHICLE-1 [2] to investigate hydrogen gas-driven permeation behaviour in vacuum plasma sprayed tungsten (VPS-W) coatings on substrate of F82H at a temperature range of 200-500°C. A permeation membrane is prepared. The thicknesses of the tungsten coating and the F82H membrane are 0.09 and 0.5 mm, respectively. It has been found that i) hydrogen permeation through VPS-W coated F82H is diffusion-limited, ii) tungsten coatings have been demonstrated the efficacy to reduce the hydrogen permeability by about one order of magnitude under all the examined temperatures and iii) the values of the effective diffusivity for tungsten coated F82H is between that of the bare F82H and tungsten and the activation energy is increased by ~40% compared to bare F82H (as shown in Fig. 1), which is in agreement with the indication of the multi-layer permeation theory [3].

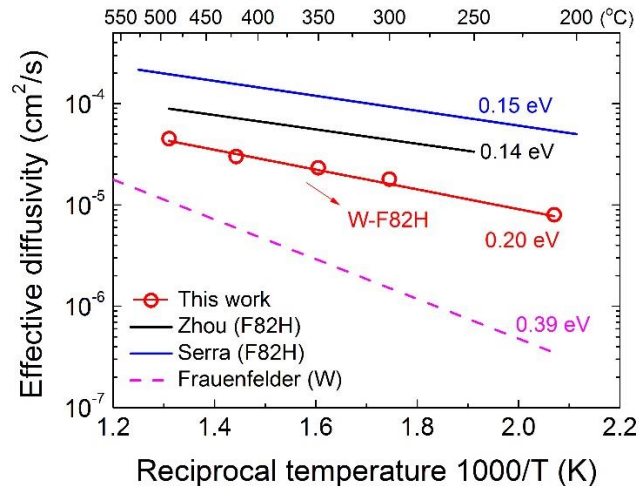


Fig.1 Temperature dependence of hydrogen effective diffusivity for VPS-W coated F82H (W-F82H). The thicknesses of the W coating and the F82H membrane are 0.09 and 0.5 mm, respectively. Literature data [4-6] are shown for comparison.

- [1] R. A. Anderl, D. F. Holland, G. R. Longhurst, *J. Nucl. Mater.* **176–177** (1990) 683-689.
- [2] Y. Hirooka, H. Ohgaki, Y. Ohtsuka, M. Nishikawa, *J. Nucl. Mater.* **337–339** (2005) 585-589.
- [3] J. Crank, *The Mathematics of Diffusion*, 2nd Edition. Clarendon Press Oxford: London, 1975.
- [4] H. Zhou, Y. Hirooka, N. Ashikawa, et al., *J. Nucl. Mater.* **455** (2014) 470-474.
- [5] E. Serra, G. Benamati, *Mater. Sci. Technol.* **14** (1998) 573-578.
- [6] R. Frauenfelder, *J. Vac. Sci. Technol.* **6** (1969) 388-397.

Tritium accumulation on carbon deposition layer and its decontamination by glow discharge

Y. Torikai^{a)}, N. Ashikawa^{b)}, K. Noborio^{a)}, Y. Ueda^{c)}, K. Katayama^{d)}, Y. Nobuta^{e)},
N. Matsuyama^{a)} and K. Nishimura^{b)}

^a Hydrogen Isotope Research Center, University of Toyama, 3190, Gofuku, Toyama 930-8555, Japan

^b National Institute for Fusion Science, 322-6 Oroshi-cho, Toki 509-5292, Japan

^c Graduate School of Engineering, Osaka University, 2-1 Yamadaoka, Suita, Osaka 565-0871, Japan.

^d Department of Advanced Energy Engineering Science, Kyushu University,

6-1, Kasugakoen, Kasuga-shi, Fukuoka 816-8580, Japan

^e Faculty of Engineering, Hokkaido University, Kita-13, Nishi-8, Kita-ku, Sapporo, Hokkaido 060-8628, Japan

E mail address: y2torik@ctg.u-toyama.ac.jp

From a safety point of view, assessment of tritium inventory in plasma-facing materials and selection of methods for tritium decontamination of the materials are important issues due to requirement of the tritium inventory limitation inside fusion machines. In this study, tritium trapping in a carbon layer deposited on the 316L stainless steel (SS316L) was investigated. Besides, methods of tritium decontamination of the carbon deposition layer by thermal release and glow discharge were tested.

Carbon layers were deposited onto SS316L substrates, 15×15×0.5 mm³ in size, by magnetron sputtering. The carbon deposited SS316L specimens were placed in ultra-high vacuum system and was initially pre-heated at 423 K at background pressure of (1.3 - 2.6)×10⁻⁶ Pa. Then the specimens were exposed at 423 K to gaseous deuterium - tritium mixture (7.2 % T) at the total pressure of 1.2 kPa for 3 h. For determination of the tritium content in the near-surface layer of the carbon deposition, the imaging plate (IP) technique (Fujifilm BAS-TR) was employed. The intensity of the photo-stimulated luminescence (PSL) was analyzed with a laser scanner (Fujifilm FLA-7000). The detectable depth range of this technique for tritium in carbon is estimated to be < 1 μm.

Decontamination of the tritiated carbon deposited SS316L specimens were performed by deuterium glow discharge.

Figure shows the results of the tritium decontamination of the carbon deposited SS316L specimen due to D glow discharge. Left photo shows the carbon deposited SS316L specimen. Part 1) shows the IP image of tritium loaded specimen, 2) shows the IP image after exposure to D glow discharge for 30 min and 3) shows the IP image after exposure to D glow discharge additional 60min. After D glow plasma discharges, surface tritium was removed in corresponding with surface carbon deposition layer was removed. Additionally, tritium trapped on the SS316L surface was also removed by the D glow discharge. Therefore, it can be concluded that glow discharge decontamination is a good method to remove tritium from the surface of the plasma-facing wall.

This work was supported by NIFS budget NIFS14KOBEO31.

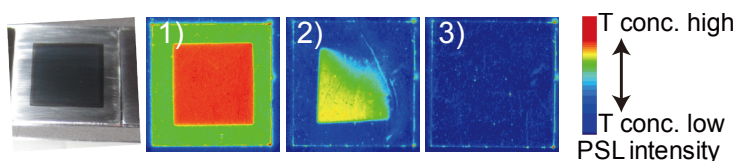


Fig. Picture of a carbon deposited SS316L and IP images of the tritium contaminated SS316L. 1) : before irradiated to D plasma, 2) : after irradiated to D plasma for 30 min, 3) : after irradiated to D plasma for 90 min.

Measurement of tritium sorbed in tungsten deposition layer by imaging plate technique

K. Katayama, Y. Torikai^a, M. Noguchi, N. Ashikawa^b, S. Fukada

*Department of Advanced Energy Engineering Science, Kyushu University,
6-1, Kasugakoen, Kasuga-shi, Fukuoka 816-8580, Japan*

^a *Hydrogen Isotope Research Center, University of Toyama, 3190, Gofuku, Toyama 930-8555, Japan*

^b *National Institute for Fusion Science, 322-6 Oroshi-cho, Toki 509-5292, Japan*

Understanding of tritium (T) behavior in plasma-facing wall of a fusion reactor is an important issue from viewpoints of T economy and safety. The plasma facing surface is changed with plasma operation time by various mass transfer phenomena such as sputtering and deposition. The deposited material has different structure from the original material. Therefore, the investigation of T behavior in not only original materials but also deposited materials is necessary. Tungsten (W) is a candidate material for plasma-facing components because of low solubility and low sputtering yield for hydrogen isotopes. It has been observed that W deposition layer formed by hydrogen plasma sputtering retains a large amount of hydrogen during sputtering-deposition process [1]. However, basic behavior of hydrogen isotopes in W deposition layer is not understood significantly. In this study, W deposition layer formed by hydrogen plasma sputtering was exposed to gaseous T and the reduction of T level by heating under vacuum condition was investigated by the imaging plate (IP) technique.

Samples of W deposition layer were formed on W substrates by hydrogen RF plasma sputtering. Prepared samples were separately put in a reaction tube of the T exposure apparatus installed in University of Toyama, and heated at the preset temperature for 3 hours under the vacuum condition in order to remove adsorbed water on the sample surface. Then, the samples were exposed to the T/D mixture (7.2% T/D) for 3 hours. After the T exposure process, the closed reaction tube in which the samples were contained was transported into a glove box filled with argon. Then, T level of the samples were investigated by IP without air exposure. After that, the samples were put in the reaction tube again and heated under the vacuum condition. IP measurement and heating process were performed repeatedly. For comparison, W substrates without W deposition layer were exposed to T/D mixture at the same conditions.

As an example, IP image from the W deposition layer and the W substrate exposed to T at 573K are shown in Fig.1. The initial intensities of photo-stimulated luminescence (PSL) were 1029 PSL/mm²/h for W deposition layer and 81 PSL/mm²/h for W substrate. T level on W deposition layer was 10 times larger than that on W substrate. A part of retained T was released at a low temperature of 95 °C. These results suggest that the formation of W deposition layer increase T inventory in the vessel and a certain amount of T can be removed at about 100 °C by in-vessel baking.

This work was performed with the support of the NIFS Collaboration Research program (NIFS14KOB031).

[1] K.Katayama et al., Fusion Sci. Technol., 54 (2008) 549-552.

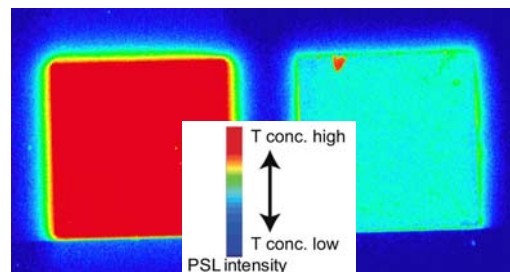


Fig.1 IP image of W deposition layer (left) and W substrate (right) exposed to gaseous T.

Tungsten-surfaces-structure Dependence of Sputtering Yield for Noble GasH. Nakamura^{a, b}, S. Saito^c, A. M. Ito^a and A. Takayama^a^a National Institute for Fusion Science, 322-6 Oroshi-cho, Toki 509-5292, Japan^b Nagoya University, 332-6 Oroshi, Toki 509-5292, Japan^c National Institute of Technology, Kushiro College, 2-32-1 Otanoshike-Nishi, Kushiro, Hokkaido, 084-0916, Japan

hnakamura@nifs.ac.jp

Tungsten nano structure, e.g. a bubble or a fuzz structure, has been studied recently by a lot of plasma-wall interaction researchers [1, 2]. The purpose of these researches is to avoid the decrease of the mechanical property and the heat conductivity of the original tungsten material. To achieve this purpose, it is necessary to reveal the mechanism of the tungsten nano structure formation. We, recently, proposed the scenario of fuzz structure formation using computer simulation [3] which is composed of the binary collision approximation (BCA) [4], density functional theory (DFT) [5], molecular dynamics (MD), and Monte-Carlo (MC) calculations. Especially our MD-MC hybrid code can reproduce the "fuzz"-like structure in the surface of tungsten bulk under the helium irradiation [4]. Thus, we demonstrated that our simulation code is a powerful tool to calculate the interaction between the tungsten and the gases (hydrogen isotopes and noble gases). In this paper, we estimate the sputtering yield and the absorptivity of the noble gas for the tungsten with the nano-structure surface using BCA simulation code AC ∇ T (atomic collision in any structured target) [4,6,7]. Though these physical quantities for the bulk tungsten are already well-known, those of the tungsten with the nano-structure surface are not obtained yet. We, therefore, show the sputtering yield and the absorptivity of the hydrogen isotopes and the noble gases for the tungsten with the nano-structure surface. Moreover, we introduce the tungsten structure dependence of those quantities.

- [1] S. Takamura, N. Ohno, D. Nishijima and S. Kajita, Plasma Fusion Res. Vol. 1, 051 (2006).
- [2] S. Kajita, T. Saeki, Y. Hirohata, M. Yajima, N. Ohno, R. Yoshihara and N. Yoshida: Jpn. J. Appl. Phys. Vol. 50, p. 08JG01 (2011).
- [3] A.M.Ito, et al., J. Nucl. Mat. in press. doi:10.1016/j.jnucmat.2015.01.018.
- [4] S. Saito, A. Takayama, A.M. Ito, H. Nakamura, J. Nucl. Mater. Suppl., Vol. 438 p. S895 (2013).
- [5] A. Takayama, A.M. Ito, S. Saito, N. Ohno, H. Nakamura, Jpn. J. Appl. Phys., Vol.52 p. 01AL03 (2013).
- [6] A. Takayama, S. Saito, A.M. Ito, T. Kenmotsu and H. Nakamura: J. Appl. Phys. Vol. 50, p.01AB03 (2011).
- [7] S. Saito, A. Takayama, A.M. Ito and H. Nakamura: Proc. Int. Conf. Model. Simulation Technol., p.197 (2011).

Color measurements of the first wall toward the systematic evaluation of the thickness distribution of deposition layer in LHD

G. Motojima, N. Yoshida¹⁾, S. Masuzaki, R. Sakamoto, M. Tokitani, H. Tanaka, T. Murase, D. Nagata, K. Matsumoto²⁾, M. Miyamoto³⁾, M. Yajima, M. Sakamoto⁴⁾, H. Yamada, T. Morisaki, and LHD Experiment Group

National Institute for Fusion Science, 322-6 Oroshi-cho, Toki 509-5292, Japan

1) Research Institute for Applied Mechanics, Kyushu Univ., 6-1, Kasuga, Fukuoka 812-8580, Japan

2) Honda R & D Co. Ltd., 4630 Shimotakanazawa, Haga-machi, Tochigi 321-3393, Japan

3) Department of Material Science, Shimane University, Matsue, Shimane 690-8504, Japan

4) Plasma Research Center, University of Tsukuba, 1-1-1 Tennodai, Tsukuba, Ibaraki 305-8577, Japan

An innovative color measurement technique is employed in the Large Helical Device (LHD). This study provides a method for obtaining in broad spatial extent and in great detail the color information of the first wall relating to the thickness of the deposition layer. The RGB (Red, Green, and Blue) value, mainly of the stainless steel plates on the helically twisted coil, is measured by the handy color analyzer.

In the LHD, long-term exposed sample analysis reveals that the deposition layer is primarily composed of carbon formed on the first wall, and may be a contributing factor to wall retention. The total amount of the deposition layer formed in the vacuum vessel influences the wall retention rate. Thus, reliable evaluation of the total amount of the deposition layer is crucial. The color depends on the composition, the structure, and the thickness of the deposition layer. In LHD, the composition of the deposition layer is primarily carbon. Although the surface roughness on the deposition layer presumably affects the reflection coefficient at each RGB, the color is almost certainly related to the thickness of the deposition layer assuming the same surface structure. In this study, a method for obtaining in broad spatial extent and in great detail the color information of the first wall has been provided using an innovative concept for the color measurement [1].

The first wall plates in the vacuum vessel of LHD are stainless steel (SUS316L), while isotropic graphite plates are installed in the divertor section. The former is the main material in LHD (700 m²), while the graphite area (30 m²) constitutes only about 5% of the total plasma facing area. We measure the RGB mainly of the stainless steel plates on the helically twisted coil in one of 10 toroidal sections of the vacuum vessel. The number of measured stainless steel plates totaled 530. On the outer torus side, the colors of almost all stainless steel plates are close to black. On the inner torus side, all plates are close to white, which indicates the reflection coefficient of around 1, except for those neighboring the divertor plates. These results suggest that the outer torus side is deposition-dominant, while the inner torus side is primarily erosion-dominant. Characterization of the deposition layer by this study is qualitatively consistent with the previous results from the direct specimen analysis.

In this presentation, the thickness distribution of deposition layer will be shown from the analysis of samples amounted on the same toroidal section with color measurements as part of the long-term exposed sample analysis, using a focused ion beam system and a transmission electron microscope (TEM) etc.

This work is performed with the support and under the auspices of the NIFS Collaboration Research program (NIFSUMPP003-1).

[1] G. Motojima *et al.*, Plasma Fusion Res. **10**, 1202074 (2015).

Linear stability analysis of Alfvén eigenmodes with arbitrary velocity distribution functions in tokamak plasmas

Taisei Futakuchi, Atsushi Fukuyama, Hideo Nuga

*Graduate School of Engineering, Kyoto University
Kyoto-Daigaku-Katsura, Nishikyo-ku, Kyoto 615-8540, Japan*

futakuchi@p-grp.nucleng.kyoto-u.ac.jp

The excitation of Alfvén eigenmodes (AE) driven by fast ions in tokamak plasmas has been extensively studied theoretically and numerically, since it may cause the loss of fast ions and reduce the heating power to maintain the fusion reaction. Since the heating scheme and absorbed power density strongly affects the velocity distribution function of fast ions, the stability of AE has to be evaluated for arbitrary velocity distribution function. The full wave code TASK/WM has been used to analyze the linear stability of Alfvén eigenmodes driven by fast ions with isotropic Maxwellian and slowing-down distributions. Recently we have developed a module to numerically calculate drift-kinetic electric susceptibility of fast ions with arbitrary radial and velocity distribution function. With this module, complex eigenmode frequencies were obtained by solving Maxwell's equation. Examples of eigenmode frequencies in complex frequency plane are shown in Fig. 1. In the case of isotropic Maxwellian distribution function, TAE and lower-frequency eigenmodes exist and the growth rate of eigenmodes increases with the increase of density or effective temperature of fast ions. Parameter dependence of the eigenmode frequencies and wave structures for arbitrary distribution function will be demonstrated.

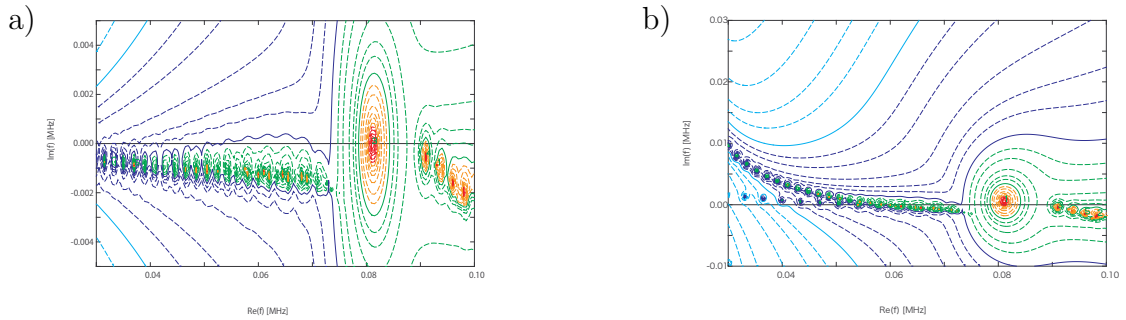


Fig. 1 Eigenmode frequencies without fast ion components (a), and with fast ion components $n_{F0} = 1 \times 10^{17} \text{m}^{-3}$, $T_{F0} = 0.5 \text{MeV}$ (b)

Bifurcation of the interchange mode growth rate and rotation frequency due to the perpendicular heat conductivity in stellarator plasmas

T. Nicolas¹, K. Ichiguchi^{1,2}, M. Sato¹, Y. Todo^{1,2}, Y. Suzuki^{1,2},
 A. Ishizawa^{1,2}, and S. Sakakibara^{1,2}

¹*National Institute for Fusion Science, 322-6 Oroshi-cho, Toki 509-5292, Japan*

²*The Graduate University of Advanced Study, Sokendai, Toki 509-5292, Japan*

The linear stability against interchange modes of heliotrons like the Large Helical Device has not been fully understood yet. The interchange mode is the dominant instability in nearly current-free 3D configurations. Recently, experiments in the so-called inward-shifted configuration have shown the machine can be operated safely up to $\langle\beta\rangle \sim 5\%$ without major MHD event [1]. Here $\langle\beta\rangle$ is the volume averaged ratio between kinetic and magnetic pressure. The rotation of the mode, which seems to play a role in the stability [2], is also not understood. Namely, the modes are observed to rotate in the electron direction [3], whereas extended MHD theory without heat conductivity but including electron and ion diamagnetic effects predicts rotation in the ion direction for Mercier unstable modes and almost no rotation for Mercier stable modes. [4].

In this contribution, we present a new effect on the linear Mercier unstable interchange growth rate caused by the perpendicular heat conductivity χ_{\perp} . When χ_{\perp} is equal to a critical value χ_c , the growth rates of the two most unstable modes become equal. For $\chi_{\perp} > \chi_c$, the two modes have same growth rate and opposite frequency, as shown in Fig. 1. This degeneracy is removed by the diamagnetic effects. In the domain $\chi_{\perp} > \chi_c$, the diamagnetic effects can be destabilizing and the rotation can be in the electron direction. The rotation direction is determined by the value of perpendicular viscosity.

This effect, which sheds a new light on the stability of the interchange mode in stellarators, is found analytically and confirmed both with a 3 field linear eigenvalue solver and with 3D non-linear MHD simulations utilizing the MIPS code [5].

References

- [1] H. Yamada *et al.* Nucl. Fusion **51**(9), 4021 (2011).
- [2] Y. Takemura, *et al.* Nucl. Fusion **52**(10), 102001 (2012).
- [3] Y. Takemura, *et al.* Plasma and Fusion Research **8**(0), 1402123 (2013).
- [4] S. Gupta, *et al.* Phys. Plasmas **9**(8), 3395 (2002).
- [5] Y. Todo, *et al.* Plasma and Fusion Research **5**, S2062 (2010).

Corresponding author: Timothee Nicolas timothee.nicolas@nifs.ac.jp

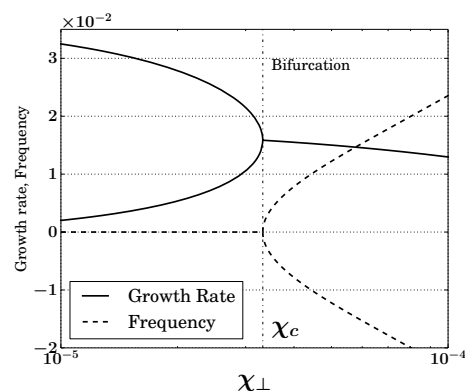


Figure 1: Frequency and growth rate of the first two most unstable modes

Comparison of bootstrap current calculation in helical plasmas among different types of approximations in drift-kinetic equation

B. Huang^a, S. Satake^{a,b}, R. Kanno^{a,b}, S. Matsuoka^c

^a*Sokendai (The Graduate University for Advanced Studies), 322-6 Oroshi-cho, Toki 509-5292, Japan*

^b*National Institute for Fusion Science, 322-6 Oroshi-cho, Toki 509-5292, Japan*

^c*Research Organization for Information Science and Technology, 6F Kimec-Center Build., 1-5-2 Minatojima-minamimachi, Chuo-ku, Kobe, 650-0047 Japan*

In toroidal plasma, neoclassical (NC) theory describes radial NC flux and the bootstrap current. The bootstrap current depends on Magnetohydrodynamics (MHD) equilibrium and collisionality. The bootstrap current is unessential for MHD equilibria of helical plasma. However, in high-beta and high-temperature plasma, the bootstrap current could be large enough to affect equilibrium field. Therefore, a self-consistent method is required to track MHD equilibrium and bootstrap current. For example, Wendelstein 7-X (W7-X) is optimized to have good MHD instabilities and low bootstrap current in order to improve NC confinement.[1] Here W7-X design followed the local NC code.[2] Conventionally, mono-energy and local approximation are employed to reduce computation time and resource. Here, "local" means neglecting the higher order magnetic drift terms in the drift-kinetic equation. The recent NC studies[3][4] indicate that conventional local approximations are deficient for some conditions in radial neoclassical transport. It shows that keeping tangential magnetic drift terms leads to large differences in the radial NC flux where $\mathbf{E} \times \mathbf{B}$ rotation is small. The tangential magnetic drift effect on bootstrap current is still an open question. This work performs the benchmark between conventional and new local code with the tangential magnetic drift and discusses its contribution on bootstrap current in LHD and W7-X.

References

- [1] J. Geiger, C. D. Beidler, Y. Feng, H. Maaberg, N. B. Marushchenko, and Y. Turkin, "Physics in the magnetic configuration space of w7-x," *Plasma Physics and Controlled Fusion*, vol. 57, no. 1, p. 014004, 2015.
- [2] D. I. van Rij and S. P. Hirshman, "Variational bounds for transport coefficients in three-dimensional toroidal plasmas," *Phys Fluids B; (United States)*, vol. 1:3, Mar 1989.
- [3] S. Matsuoka, S. Satake, R. Kanno, and H. Sugama, "Effects of magnetic drift tangential to magnetic surfaces on neoclassical transport in non-axisymmetric plasmas," *Physics of Plasmas*, vol. 22, no. 7, p. 072511, 2015.
- [4] M. Landreman, F. I. Parra, P. J. Catto, D. R. Ernst, and I. Pusztai, "Radially global f computation of neoclassical phenomena in a tokamak pedestal," *Plasma Physics and Controlled Fusion*, vol. 56, no. 4, p. 045005, 2014.

Chaos of nonlinear ion acoustic waves with vorticity

Yuji Ohno and Zensho Yoshida

*Graduate School of Frontier Sciences, The University of Tokyo,
5-1-5 Kashiwanoha, Kashiwa, Chiba 277-8561, Japan*

While there are a lot of works on the ion acoustic waves, especially on the solitons, they have not focused on the *vortex* of the wave fields. For example, the Korteweg–de Vries (KdV) equation considers a spatially one-dimensional system, so the fields do not have a freedom to make a vorticity finite. The two- or three- dimensional generalization of the KdV equation is the Kadomtsev–Petviashvili (KP) equation, which, however, is set to make the vorticity zero.

In this research, we show that the series of KP equations (including higher order series) for ion acoustic waves cannot have vorticities. We also prove that entropy must be homogeneous and baroclinic effects cannot produce any vorticities when we derive the equations. Thus, we can say that the reductive perturbation method, which is used to derive the KP equation, eliminates vortex.

This result motivates us to formulate and analyze a generalized system that has a finite vorticity. We change the expansion of velocity in the reductive perturbation method and derive a new system of equations with a finite vorticity. It consists of the modified three-dimensional KP equation

$$\partial_x \left(\partial_t \phi + \phi \partial_x \phi + \frac{1}{2} \partial_x^3 \phi + [\phi, \psi] \right) + \frac{1}{2} \Delta_{\perp} \phi = 0 \quad (1)$$

and the two-dimensional Euler vorticity equation for $\Delta_{\perp} \psi$.

Painlevé test is widely used to investigate whether a differential equation is integrable. The test shows that KdV equation and 2D-KP equation are integrable, but 3D-KP equation is not integrable [1]. Thus, the equation (1), which is a generalization of 3D-KP equation, is also non-integrable.

We investigate chaotic property by solving the equation (1) with $\psi(y, z) = a \sin(2\pi\kappa y/L) - a \cos(2\pi\kappa z/L)$ (a steady-state solution of the Euler vorticity equation). As the initial condition of ϕ we use a line-soliton $3 \operatorname{sech}^2[(x-2y)/\sqrt{2}]$, the soliton solution of the 2D-KP equation. ϕ is homogeneous in z -direction at $t = 0$, and becomes inhomogeneous at $t > 0$ because of ψ . When ψ is weak ϕ becomes twisted, and when ψ is strong ϕ becomes divided and spread. We evaluated these observation by a calculation of average wave numbers (Fig. 1). We can see that larger ψ makes $\langle k_x \rangle$ larger, even though ψ is independent of x . $\langle k_y \rangle$ and $\langle k_z \rangle$ also grow. The growth of $\langle k \rangle$ means that large scale structures are divided into small scale structures. Thus, we can consider that this result shows the nonintegrability due to vorticity in the new equation (1).

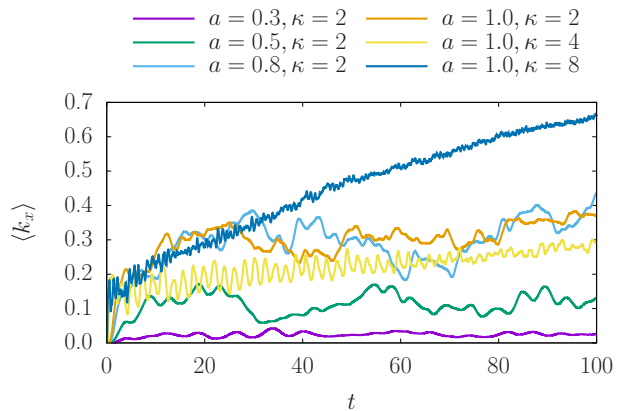


Figure 1: Average wave number $\langle k_x \rangle$.

[1] H.-y. Ruan, S.-y. Lou, and Y.-x. Chen, J. Phys. A: Math. Gen. **32** (1999) 2719.

Electron impact ionization cross sections of the fusion plasma hydrocarbon gas: methane

G. Purohit, P. Singh and V. Patidar

Department of Physics, Sir Padampat Singhania University, Bhatewar, Udaipur-313601, India

e-mail: ghanshyam.purohit@spsu.ac.in

The study of electron impact ionization of atoms, ions and molecules has been of interest since the early days of quantum physics. Particularly, study of electron impact ionization cross section of various targets is important as it gives information about the delicate collision dynamics and wave functions [1]. Electron-impact ionization cross sections of atoms and molecules are important not only for the development of basic collision theory, but also in a wide range of practical applications. For example, the modeling of semiconductor manufacturing by plasma processing requires ionization cross sections of fluorocarbons used as the feed gas, their ions and fragments. Hydrocarbon molecules, such as methane, are found in the vicinity of divertors in a fusion device, making it necessary to include ionization of such molecules to model low-temperature plasmas in tokamaks. Ionization cross sections near the ionization threshold are also used in modeling combustion of flammable gases. Thus, needs for cross section data have been identified in the fields of plasma physics such as astrophysics and fusion plasmas, as well as in the fields of applications: gas discharge lasers, semiconductor manufacturing processes and plasma diagnostics.

We have calculated differential cross sections for the various targets including xenon atoms and water molecule [2, 3]. We report in this communication the electron impact ionization cross section data for methane which has importance in the fusion plasma related processes [4]. We use semi-classical approach to calculate the ionization cross section of methane. We compare our results with the available experimental and theoretical results.

References

- [1] H. Ehrhardt, M. Schulz, T. Tekaas, K. Willmann, *Phys. Rev. Lett.* **22** (1969) 89.
- [2] P. Singh, G. Purohit, V. Patidar, *J. Phys. B: At. Mol. and Opt. Phys.* **46** (2013) 115207.
- [3] P. Singh, G. Purohit, C. Champion, V. Patidar, *Phys. Rev. A* **89** (2014) 032714.
- [4] W. L. Morgan, *Plasma Chem. Plasma Process.* **12** (1992) 477.

Kinetic dynamics simulation of the detached plasmaT. Pianpanit^a, S. Ishiguro^{a,b}, H. Hasegawa^{a,b}^a*Department of Fusion Science, SOKENDAI, 322-6 Oroshi-cho, Toki 509-5292, Japan*^b*National Institute for Fusion Science, 322-6 Oroshi-cho, Toki 509-5292, Japan*

theerasarn.pianpanit@nifs.ac.jp

The detached plasma has been proposed to reduce the heat flux to the divertor. Fluid code has been widely used to investigate the detached plasma [1] but the cooling of plasma, trapped particle effects, and other kinetic dynamics in the detached plasma has not been well understood. Particle-in-Cell (PIC) simulation with the Monte Carlo collisions [2] and the cumulative scattering angle coulomb collision [3] are carried out to study dynamical kinetic behavior of the plasma. The constant pressure and constant temperature of neutral gas box in front of the divertor target model has been used in the simulation. The simulation has been carried out by using the real mass ratio and the self-consistent sheath effect can be observed. The low plasma density and the small system size compare to the real fusion devices have been used, thus by modifying the Coulomb collision frequency, $\nu'_c = 100\nu_c$, the results show the strongly decrease in electron temperature inside the neutral gas box. The electron temperature in front of the divertor target also becomes less than 1 eV, which is one of the conditions for detached plasma.

[1] S. Nakazawa, et al., Plasma Phys. Control. Fusion **43** (2000) 401

[2] V. Vahedi and M. Surendra, Comput. Phys. Commun. **87** (1995) 179

[3] K. Nanbu, Phys. Rev. E **55** (1997) 4642

Local approximation of the drift kinetic equation

H. Sugama,^{1,2} S. Matsuoka,³ S. Satake,^{1,2} and R. Kanno^{1,2}

¹*National Institute for Fusion Science, 322-6 Oroshi-cho, Toki 509-5292, Japan*

²*SOKENDAI (The Graduate University for Advanced Studies), Toki 509-5292, Japan*

³*Research Organization for Information Science and Technology, Kobe 650-0047, Japan*

Conventional calculations of neoclassical transport fluxes are done applying radially local approximation to solving the drift kinetic equation, in which $\mathbf{v}_d \cdot \nabla f_1$ are often neglected as a small term of higher order in the normalized gyroradius parameter $\delta \sim \rho/L$. (Here, \mathbf{v}_d , f_1 , ρ , and L represent the guiding center drift velocity, the deviation of the guiding center distribution function from the local Maxwellian equilibrium distribution, the gyroradius, and the equilibrium scale length, respectively.) However, in stellarator and heliotron plasmas, this $\mathbf{v}_d \cdot \nabla f_1$ term is known to be influential on the resultant neoclassical transport because it significantly change orbits of particles trapped in helical ripples. Therefore, at least, the $\mathbf{E} \times \mathbf{B}$ drift part $\mathbf{v}_E \cdot \nabla f_1$ in $\mathbf{v}_d \cdot \nabla f_1$ has been kept in most studies of neoclassical transport in helical systems. Recently, it was shown by Matsuoka *et al.*[1] that the neoclassical transport is significantly influenced by retaining the magnetic drift tangential to flux surfaces in $\mathbf{v}_d \cdot \nabla f_1$ for the magnetic configuration of LHD especially when the radial electric field is weak. However, as pointed by Landreman *et al.*[2], stationary solutions of the drift kinetic equation with the radially local approximation used require additional artificial sources (or sinks) of particles and energy when the above-mentioned drift terms are retained. In this work, a novel radially local approximation of the drift kinetic equation is presented. The new drift kinetic equation that includes both $\mathbf{E} \times \mathbf{B}$ and tangential magnetic drift terms is written in the conservative form and it has favorable properties for numerical simulation that any additional terms for particle and energy sources are unnecessary for obtaining stationary solutions. Besides, it is shown that the intrinsic ambipolarity condition for neoclassical particle fluxes are satisfied in the presence of quasisymmetry of the magnetic field strength.

[1] S. Matsuoka, S. Satake, R. Kanno, and H. Sugama, *Phys. Plasmas* **22**, 072511 (2015).

[2] M. Landreman, *et al.*, *Phys. Plasmas* **21**, 042503 (2014).

Modification of neutron emission spectra and its effect on determination of fuel ion ratio n_d/n_t in beam injected DT plasma

Y. Kawamoto, H. Matsuura

*Applied Quantum Physics and Nuclear Engineering, Kyushu University,
744 Motoooka, Fukuoka 819-0395, Japan*

To control the DT fusion reactor, it is important to accurately obtain the fuel ion ratio n_d/n_t . In DT plasma, there are neutrons which have 14.1 MeV peak caused by DT reaction and have 2.45 MeV peak caused by DD reaction. The method of obtaining the fuel ion ratio n_d/n_t by measuring peaks of these neutron spectra has been proposed [1]. This method, so far, has been valued for ITER under certain conditions and it has been shown that it is possible to obtain the fuel ion ratio n_d/n_t in reactor core region by the method with sufficient accuracy [2]. However the scattered neutrons caused by DT reaction are detected as noise for DD signals. Hence, use of Neutron Beam Injection (NBI) for neutron spectrometry is considered in order to improve measurement accuracy of DD signals, because DD reactivity is enhanced by NBI. NBI influences not only reactivity but also neutron emission spectra from gauss distribution [3]. In such a case, ratio of DD/DT neutron peak also changes. Therefore it needs to correlate neutron signals measured with the fuel ion ratio n_d/n_t when beam-injection is made. The purpose of this paper is to clarify a correlation between neutron signals measured and the fuel ion ratio n_d/n_t by evaluating the influence of beam-injection. In addition, we evaluated a noise to examine whether the above method can be used for plasma diagnostics in blanket structure such as ITER, Water Cooled Solid Breeder (WCSB), and LiPb blanket.

We assumed the DT plasma with deuteron beam-injection. Deuteron and triton distribution functions are evaluated on the basis of the Boltzmann-Fokker-Planck model and neutron emission spectra are obtained by using the distribution functions. Using the neutron emission spectra obtained, neutron flux in reactor core region is calculated with the continuous-energy Monte Carlo transport code MVP [4]. It is shown that reassessing of correlation between neutron signals measured and the fuel ion ratio n_d/n_t according to plasma conditions is necessary when beam is injected, and NBI is useful for increasing Signal/Noise (S/N).

- [1] K. Källne et al., *Rev. Sci. Instrum* **62** (1991) 2871.
- [2] F. Moro, et al., *Fusion Eng. Des.* **86** (2011) 1277.
- [3] H. Matsuura, et al., *Plasma Fusion Res.* **8** (2013) 2403064.
- [4] Y. Nagaya, et al., *JAERI* (2005) 1348

A verification scenario of knock-on tail formation due to nuclear elastic scattering using γ -ray-generating ${}^6\text{Li}+\text{D}$ reaction in deuterium plasmas

H. Matsuura, S. Sugiyama, Y. Nishimura, Y. Kawamoto
*Applied Quantum Physics and Nuclear Engineering, Kyushu University,
744 Motoooka, Fukuoka 819-0395, Japan*

mat@nucl.kyushu-u.ac.jp

It is well known that in a thermonuclear plasma energetic ions create knock-on tails [1] in fuel-ion velocity distribution functions due to nuclear elastic scattering (NES) [2]. In a thermonuclear plasma 3.52-MeV α -particles are continuously produced and use of beam injection with energy more than 1 MeV is considered. In such a case, NES effects on slowing down of the energetic ions may not be negligible compared with those due to Coulomb collisions. We have evaluated the NES effects on burning plasma properties in beam-injected plasmas [3,4] on the basis of the Boltzmann-Fokker-Planck (BFP) model. It is important to validate the analysis model and ascertain the NES effects previously evaluated via the experimental data.

In this paper, a verification scenario of knock-on tail formation in deuteron velocity distribution function by energetic protons using γ -ray-generating ${}^6\text{Li}+\text{D}$ reaction is examined for proton-beam-injected deuterium plasmas. Previously we roughly evaluated the ${}^6\text{Li}+\text{D}$ reaction rate coefficient assuming a uniform plasma [5]. In this paper we re-evaluate the rate coefficient using more precise model supposing the future experiment. We take into account behaviours of beam-injected protons in a magnetic confinement device. Using volume-averaged 2D velocity distribution function of beam-injected protons, which is obtained by means of the ion trajectory analysis, knock-on tail formation in deuteron velocity distribution function due to NES is examined in 2D velocity space using 2D Boltzmann collision term. From the 2D deuteron velocity distribution function obtained enhancement of the emission rate of 0.48-MeV γ -rays by ${}^6\text{Li}(d,p){}^7\text{Li}^*$, ${}^7\text{Li}^*\rightarrow{}^7\text{Li}+\gamma$ reaction [6,7] due to NES is evaluated. To grasp the potential diagnostic capabilities, ratio of 0.48-MeV γ -rays to background noise component is also evaluated on the basis of Monte-Carlo simulation for neutron transport equation. A possible scenario to verify the BFP numerical model and NES effects including knock-on tail formation is studied on the basis of a newly-developed model, and discussion is made for the implementability of the scenario.

- [1] L. Ballabio, et al., Phys. Rev. E, **55** (1997) 3358.
- [2] J. J. Devaney and M.L.Stein, Nucl. Sci. Eng. **46** (1971) 323.
- [3] H. Matsuura, Y. Nakao, Phys. Plasmas, **13** (2006) 062507.
- [4] H. Matsuura, Y. Nakao, Phys. Plasmas, **14** (2007) 054504.
- [5] H. Matsuura, et al., Plasma Fusion Research, **2** (2007) S1078.
- [6] V. T. Voronchev, et al., Phys. Rev. E, **63** (2001) 26413-1.
- [7] V. T. Voronchev, et al., Mem, Fac. Eng. Kyushu Univ., **51** (1991) 63.

Transmission Mode Analysis in Polarizer Miter Bend

Y. Fujita^a, S. Ikuno^b, S. Saito^c, T. I. Tsujimura^d, S. Kubo^{a,d}, and H. Nakamura^{a,d}

^a*Nagoya University, 322-6 Oroshi-cho, Toki 509-5292, Japan*

^b*Tokyo University of Technology, 1404-1 Katakura, Hachioji 192-0982, Japan*

^c*Kushiro National College of Technology, 2-31-1 Otanoshike Nishi, Kushiro 084-0916, Japan*

^d*National Institute for Fusion Science, 322-6 Oroshi-cho, Toki 509-5292, Japan*

In the electron cyclotron resonance heating (ECRH), the corrugated waveguide is employed to reduce the deterioration of the transmission efficiency due to induced current density. The miter bend (MB) is also employed in ECRH for changing the wave propagation direction. Moreover, the millimeter waves injected into the plasma should be polarized to accurately resonance with electrons in the plasma. The polarizer miter bend (PMB) is implemented by carving grooves in MB mirror. The polarization can be controlled by rotating the reflector of PMB [1, 2]. The structure of the PMB is very complex because of grooves on the surface. In addition, other modes than the input mode are generated due to the reflection at MB/PMB reflector [3, 4]. However, the electromagnetic wave propagation phenomena in the MB/PMB have not been sufficiently verified [5, 6]. It is necessary to investigate the influence of the groove shape of PMB reflector on the polarization. Besides, the ratio of other modes that generated by MB/PMB to the transmission mode should be confirmed for the efficient heating.

The purpose of the present study is to develop the numerical code for analyzing the electromagnetic wave propagation phenomena using the finite-difference time-domain (FDTD) method [7, 8, 9]. Furthermore, the existing modes that generated by MB/PMB are numerically investigated by using the results [3, 10].

- [1] J. L. Doane, *Int. J. Infrared Millimeter Waves* **13** (1992) 1727
- [2] K. Nagasaki *et al.*, *Rev. Sci. Instrum.* **66** (1995) 3432
- [3] K. Ohkubo *et al.*, *Fusion Sci. Technol.* **62** (2012) 389
- [4] Y. Fujita *et al.*, *Proc. of the Compumag 2015, Montreal, Canada*
- [5] T. Ii *et al.*, *Rev. Sci. Instrum.* **86** (2015) 023502
- [6] B. Plaum *et al.*, *J. Infrared Milli. Terahz. Waves* **32** (2010) 482
- [7] Y. Tamura *et al.*, *J. Phys.: Conf. Ser.*, **410** 012029
- [8] H. Nakamura *et al.*, *J. Phys.: Conf. Ser.*, **410** 012046
- [9] H. Nakamura *et al.*, *ITC24 (poster)*, Gifu, Japan, Nov. 4-7
- [10] J. L. Doane, in *Infrared and millimeter waves* (Academic Press, Orlando, 1985) Vol. 13, Chap. 5, p. 123.

Kinetic full wave analysis of electron cyclotron wave mode conversion in tokamak plasmas

S. A. Khan¹, A. Fukuyama¹, H. Igami², H. Idei³

¹ *Department of Nuclear Engineering, Kyoto University, Kyoto, Japan*

² *National Institute for Fusion Science, Toki, Japan*

³ *Research Institute for Applied Mathematics, Kyushu University, Kasuga, Japan*

shabbir.khan.36m@st.kyoto-u.ac.jp

For heating and current drive in high-density core plasmas of tokamaks, electromagnetic waves with electron cyclotron (EC) range of frequencies have been extensively studied theoretically and experimentally. The propagation and absorption of EC waves are usually analyzed by the ray tracing method based on geometrical optics for waves with short wave length. In a plasma with high density or low magnetic field, however, the presence of cutoff layer may prevent the waves from penetrating into the central part from the low field side. In this case, the full wave analysis of EC waves is required for evaluating the absorption profile and optimizing the wave launching conditions. In the present analysis, two schemes of the full wave analysis in which the boundary value problem of Maxwell's equation is solved are presented. The first one is a one-dimensional kinetic analysis of the X-O-B mode conversion using the TASK/W1D code. The finite gyroradius effects are represented by an integral form of the dielectric tensor derived by integrating along particle orbits and introducing variable transformation from velocities to spatial coordinates. The mode conversion to the electron Bernstein waves and the absorption near the cyclotron harmonic resonance are successfully described. Parameter dependence of the absorption rate and the deposition profile is discussed. The second one is a two-dimensional analysis near the cutoff-resonance layer using the TASK/WF2D code. Using the integral formulation of the dielectric tensor, the mode conversion to the electron Bernstein wave near the upper hybrid layer is demonstrated in addition to the reflection and tunneling near the cutoff-resonance layer. Comparison with the analysis using a cold plasma model will be presented.

Benchmark of electromagnetic gyrokinetic codes in high performance fusion plasma

S. Maeyama, T.-H. Watanabe, H. Doerk^a, M. Nakata^b, A. Ishizawa^b

Nagoya University, Furo-cho, Nagoya 464-8602, Japan

^a *Max-Planck-Institut für Plasmaphysik, Boltzmannstraße 2, D-85748 Garching, Germany*

^b *National Institute for Fusion Science, 322-6 Oroshi-cho, Toki 509-5292, Japan*

Since the high plasma β value is desirable to make a fusion reactor efficiently and economically, JT-60SA is being developed to demonstrate and study high- β discharge for DEMO reactor. At the same time, to examine the finite β effects and improve the achievable β value, high- β experiments have been conducted in various fusion devices.

Electromagnetic gyrokinetics simulation is regarded as a fundamental tool to investigate the finite β effects on micro-turbulence. As the β value increase, typically, electrostatic ion temperature gradient modes (ITGs) are stabilized, while electromagnetic modes are destabilized such as kinetic ballooning modes (KBMs) and micro-tearing modes (MTMs). The dominant instability and their nonlinear dynamics depend not only on the β value or density/temperature gradients but also on the equilibrium magnetic configuration and Coulomb collision. Thus, in order to understand the experimentally-relevant turbulence, comprehensive gyrokinetic simulations including the realistic magnetic geometry and the multiple-species collision operator are required. For this purpose, a verification study based on a code-code benchmark is helpful.

We have carried out a benchmark between the electromagnetic gyrokinetic codes GKV [1] and GENE [2]. By using the ASDEX Upgrade H-mode discharge data [3], both codes are used to analyze micro-instabilities in a local flux-tube model. It is confirmed that constructed field-aligned coordinates and dispersion relation show good agreements. MTMs and ITGs coexist in the examined parameter, where MTM is significantly driven by the collisionality. In the presentation, more detailed and extended comparison will be reported.

[1] T.-H. Watanabe, and H. Sugama, Nucl. Fusion 46, 24 (2006).

[2] F. Jenko, W. Dorland, M. Kotschenreuther, and B. N. Rogers, Phys. Plasmas 7, 1904 (2000).

[3] H. Doerk, M. Dunne, F. Jenko, F. Ryter, P. A. Schneider, E. Wolfrum, and The ASDEX Upgrade Team, Phys. Plasmas 22, 042503 (2015).

Moment extracted formulation for describing kinetic Alfvén waves

T.-H. Watanabe, S. Maeyama, and Y. Watanabe

Department of Physics, Nagoya University, Nagoya 464-8602

Electromagnetic gyrokinetic equations have been widely used for describing drift waves, kinetic ballooning modes, and kinetic Alfvén waves in fusion, space, and astrophysical plasmas, where kinetic models of ions and electrons are dealt with. In describing the electromagnetic perturbations with frequencies much lower than the ion gyrofrequency, however, separation of space and time scales for the two species leads to numerical difficulties (such as a severe restriction on the time step size and a demand of high phase-space resolution). In order to develop an efficient numerical scheme for the electromagnetic gyrokinetic equations, we discuss a formulation of the kinetic Alfvén waves convenient to numerical simulations.

In the gyrokinetic simulations with ions and electrons, the fast parallel motion of electrons often restricts the time-step size. The semi-Lagrangian (SL) method may be useful to relax the numerical restriction [1, 2]. However, in case with electromagnetic perturbations, characteristics of the shear Alfvén waves need to be decoupled from the parallel electron motion. Otherwise, the SL method may suffer from numerical instability.

Before application of the SL scheme to the electromagnetic gyrokinetic equations, we consider a simple drift kinetic system of electrons with the ion polarization effect. This is the minimal set for describing the kinetic Alfvén waves. Then, we rewrite the governing equations so that the low-order moment equations are extracted from the drift kinetic equations. The electron distribution function is modified to satisfy constraints given by the low-order moments. Numerical properties in regard to the new formulation will also be discussed at the conference.

[1] S. Maeyama, et al., *Plasma Fusion Res.* **6**, 2401028 (2011).

[2] S. Maeyama, et al., *Comput. Phys. Comm.* **183**, 1986-1992 (2012).

Equilibrium reconstruction of plasma discharges in the Aditya tokamak

Deepti Sharma, Santanu Banerjee, A. K. Singh, R. Srinivasan, D. Raju, R. L. Tanna, J. Ghosh, Y. Shankara Joisa, P. K. Atrey, S. K. Pathak and the Aditya team

Institute for Plasma Research, Bhat, Gandhinagar 382428, Gujarat, India

External magnetic measurements with flux loops and magnetic pick-up coils in tokamaks have provided vital information on the shape of the plasma column and also global current profile parameters, such as the sum of the poloidal beta (β_p) and the internal inductance (ℓ_i) [1]. Such a reconstruction needs to be fast and sufficiently accurate such that it can be used routinely as a complementary input with other experimentally measured parameters for any sort of physics analysis of the plasma discharges.

Here we present a method which can be used to proficiently reconstruct the current profile parameters, the plasma shapes, and a current density profile satisfying the MHD equilibrium constraint, reasonably conserving the external magnetic measurements. A Grad-Shafranov (GS) equation solver, named as IPREQ [2], has been developed in IPR to search for the best-fit current density profile. GS equation is a nonlinear elliptical differential equation describing axisymmetric toroidal equilibria. Ohmic transformer current (OT), vertical field coil current (BV) along with the plasma pressure (p) and current (I_p) profiles are used as inputs to the IPREQ code to reconstruct the equilibrium and the poloidal flux, plasma shape, β_p and the safety factor (q) are inferred.

At the four corners of the square cross-section vacuum vessel of Aditya, there are four magnetic pick-up coils aligned to measure the poloidal magnetic field (B_θ) during a plasma discharge. Further, there are two toroidal flux loops at the shadow of the limiter on the high field side to measure the loop voltage inside the vacuum vessel. Vacuum shots with OT and BV and no fill gas are used to calibrate these coils and loops. Measurement from these coils and flux loops are used to reconstruct the equilibrium consistently with the peak density and temperature measurements. Finally, the reconstructed equilibria are validated against the visible images from the fast visible imaging diagnostic on Aditya.

- [1]. L. L. Lao *et al.*, "Reconstruction of current profile parameters and plasma shapes in tokamaks," *Nucl. Fusion*, **25**, 1611 (1985).
- [2]. Tokamak equilibrium code-IPREQ, R. Srinivasan and S. P. Deshpande IPR/RR-393/2007 (August, 2007)

Two dimensional hybrid simulation of a translated field-reversed configuration

M. Yanagi, D. Adachi and T. Takahashi

Gunma University, 1-5-1 Tenjin-cho, Kiryu 376-8515, Japan

The field-reversed configuration (FRC) is a compact torus with extremely high β [1], and its magnetic field structure is simply connected. This feature lets a FRC move in an axial direction; the motion is called translation. Translation provides FRC experiments with advantages. One of them is that the formation region and the confinement region can be separated by using translation technology, which is still used by recent experiments or projects like C-2 [2] and FRC-HX [3].

However, there are many unclear phenomena observed in FRC translation experiments. So we have developed a simulation code for the FRC translation research. The simulation uses 2D hybrid simulation method and we modeled the temporal change of external field in order to reproduce the axial acceleration control in FRC translation experiments. In our presentation, we will present our simulation results for several types of external field time-variation.

[1] M. Tuszewski, Nucl. Fusion **28** (1988) 2033.

[2] H. Y. Guo *et al.*, Phys. Plasmas **18** (2011) 056110.

[3] C. Grabowski *et al.*, IEEE Trans. Plasma Sci. **42** (2014) 1179.

Influences of Hall effect on MHD behavior of two axially colliding FRCs

K. Matsuzaki, S. Koike, M. Yanagi, N. Mizuguchi¹, and T. Takahashi

Division of Electronics and Informatics, Gunma University, Kiryu, Gunma 376-8515, Japan

¹*National Institute for Fusion Science, Toki, Gifu 509-5292, Japan*

As one of the effective ways to improve lifetime of Field-Reversed Configurations (FRCs), there is a merging formation technique that is introduced in the C-2 experiment. By colliding two accelerated FRCs, the merged FRC plasma exhibited a better confinement performance [1, 2]. In the report from merging experiments, the structure and profiles of the merged FRC plasma after completion of the merging process were presented intensively. However, detailed study for a transient process which involves magnetic reconnection phenomena is needed to improve the refueling efficiency for application to a nuclear reactor design.

We report here the simulation results of colliding two accelerated FRCs. In our simulation code, we modeled to separate the external magnetic field and the field generated by plasma. By using time-variable external magnetic field, we reproduced the translation of FRCs. Meanwhile, the Hall effect is to play an important role in the magnetic reconnection research. For this reason, we employed both the 2-D resistive MHD model and the 2-D resistive Hall-MHD model. We compare the simulation results and report on the changes in the property of the plasma. Detailed results will be reported in our presentation.

[1] M. W. Binderbauer *et al.*, Phys. Rev. Lett. **105** (2010) 045003.

[2] H. Y. Guo, M. W. Binderbauer, D. Barnes *et al.*, Phys. Plasmas **18** (2011) 056110.

Flux supply by Neutral Beam Injection into Field-Reversed Configuration plasma with resistive decay

R. Sekiguchi, S. Koike, and T. Takahashi

Gunma University, 1-5-1 Tenjin-cho, Kiryu 376-8515, Japan

Sustainment of Field-Reversed Configuration (FRC) plasma by NBI is most effective, because the motion of injected beam ions is compatible with kinetic characteristics of FRC [1]. Although several numerical works showed current drive [2] and power deposition [3] by NBI, target FRC plasmas were supposed to be in a stationary or equilibrium state. In the present study, we consider NBI into an FRC plasma with resistive decay; it is reproduced by 2-dimensional resistive MHD simulation. Neutral Beam (NB) particles are injected tangentially to the toroidal plasma current, and their ionization processes are reproduced by a Monte-Carlo method. From the particle-tracking calculation of beam ions, we obtain the density and current for beam ions. Since the magnetic field generated by the beam current affects the MHD behavior of FRC plasma, the MHD calculation and particle-tracking calculation are done alternately.

In our presentation, we will show the shine-through ratio of NB particles, augmentation of the poloidal flux, and the orbit loss ratio of beam ions.

[1] T. Asai, Y. Suzuki, T. Yoneda *et al.*, Phys. Plasmas **7** (2000) 2294.

[2] A. F. Lifschitz, R. Farengo, and N. R. Arista, Nucl. Fusion **42** (2002) 863.

[3] T. Takahashi, Y. Kondoh, Y. Hirano *et al.*, J. Plasma Fusion Res. **82** (2006) 775.

Estimations of Beam-Beam Fusion Reaction Rates in the Deuterium Experiment Plasma on LHD

M. Homma, S. Murakami and H. Yamaguchi

Department of Nuclear Engineering, Kyoto University, Kyoto 615-8540, Japan

Email: homma@p-grp.nucleng.kyoto-u.ac.jp

Deuterium plasma experiment campaign from 2017 is planned in the Large Helical Device (LHD). During deuterium discharges, 1 MeV tritons are produced by D-D fusion reactions, and then 14 MeV neutrons are generated by triton burn-up. The D-D fusion reaction rates in the LHD deuterium plasma have been calculated by the FIT3D-DD code[1], which is an extension version of FIT3D. In the FIT3D-DD code, we have evaluated the fraction of tritons which are produced only through the reactions between deuterium beams from the Neutral Beam Injection (NBI) heating and deuterium thermal ions (beam-thermal reactions). In the deuterium experiment plasma, however, beam-beam reactions in which both reacting ions are injected NBI deuterons would also occur. Therefore, it is necessary to estimate the contribution of the beam-beam fusion reactions for more precise prediction of triton burn-up ratios and neutron production rates.

In this study, we estimate beam-beam fusion reaction rates between the NBI deuteron beams in the deuterium experiment plasma of LHD. We obtain the deuterium beam distribution functions by the GNET (Global NEoclassical Transport) code[2,3], in which the drift kinetic equation of energetic particles is solved in five-dimensional phase space, and the beam-beam fusion reaction rates are calculated. The radial profiles of triton and neutron production rates are evaluated and are compared with that of the beam-thermal reaction rates. We also investigate their dependences on plasma parameters.

- [1] M. Homma *et al.*, Plasma Fusion Res. **10**, 3403050 (2015)
- [2] S. Murakami *et al.*, Nucl. Fusion **40**, 693 (2000)
- [3] Y. Masaoka *et al.*, Nucl. Fusion **53**, 093030 (2013)

Simulations of Energetic Particle Driven Geodesic Acoustic Mode in 3-dimensional LHD Equilibrium

H. Wang^a, Y. Todo^{a,b}, and Y. Suzuki^{a,b}

^aNational Institute for Fusion Science, 322-6 Oroshi-cho, Toki 509-5292, Japan

^bThe Graduate University for Advanced Studies, 322-6 Oroshi-cho, Toki 509-5292, Japan

wanghao@nifs.ac.jp

The first simulation results of energetic particle driven geodesic acoustic mode (EGAM) in 3-dimensional LHD equilibrium are presented. MEGA, which is a hybrid code for energetic particles interacting with a magnetohydrodynamic fluid, is used for the simulations. The equilibrium data is based on LHD shot #109031 and generated by HINT2 code. The simulation parameters are also based on the same shot. The energetic particle velocity distribution is slowing-down type with charge exchange, and pitch angle distribution is Gaussian type. The simulated EGAM frequency is $61kHz$, which is the same as the experimental observation[1]. The mode time evolution is shown in Fig. 1(a). The mode amplitude v_θ increases with $\gamma/\omega_{EGAM} = 19\%$. At $t = 0.15ms$, the mode amplitude reaches the maximum value and starts to be saturated. The mode is located near the magnetic axis, and the poloidal mode number is 0 for v_θ , as shown in Fig. 1(b). The velocity is high in the low field side and low in the high field side. In the linear growth phase, the mode propagates outward, but in the saturated phase, the propagation direction changes with time. In addition, the poloidal mode number is 1 for density and pressure, and 2 for perturbed magnetic field strength. The simulated mode numbers are consistent with theoretical prediction and experimental observation.

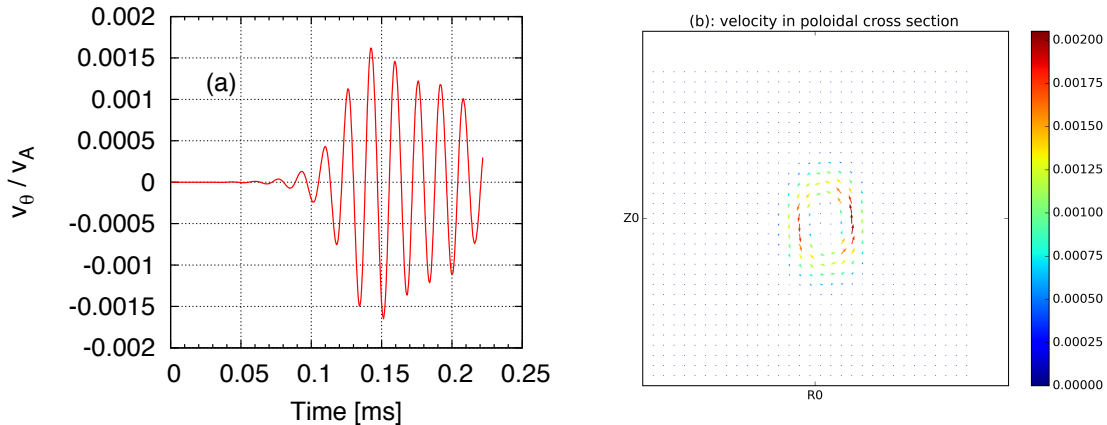


Figure 1: (a) Time evolution of mode amplitude v_θ . (b) Velocity in poloidal cross section at $t = 0.15ms$.

[1] M. Osakabe, T. Ido, K. Ogawa *et al*, 25th IAEA Fusion Energy Conference, St. Petersburg, Russia.

Advances in applying the gyrokinetic heat diffusivity model to transport simulations for helical plasmas

S. Toda¹, M. Nunami¹, A. Ishizawa¹, S. Murakami², T. -H. Watanabe³ and H. Sugama¹

¹*National Institute for Fusion Science, Oroshi-cho 322-6, Toki, Gifu, 509-5292, Japan*

²*Department of Nuclear Engineering, Kyoto University, Nishikyo, Kyoto, 615-8540, Japan*

³*Department of Physics, Nagoya University, Furo-cho, Nagoya, Aichi, 464-8602, Japan*

A reduced transport model for the turbulent ion heat diffusivity due to the ion temperature gradient (ITG) mode was obtained from the gyrokinetic simulation using the GKV-X code for the high- T_i Large Helical Device (LHD) plasmas [1]. This model is given by the function of the normalized zonal flow decay time $\tilde{\tau}_{ZF}$ and the mixing length estimate $\tilde{\gamma}_{\tilde{k}_y}/\tilde{k}_y^2$ integrated over the poloidal wavenumber space, where $\tilde{\gamma}_{\tilde{k}_y}$ is the normalized linear growth rate of the ITG mode. The nonlinear gyrokinetic transport simulation results are quantitatively reproduced by the reduced model, which we call the gyrokinetic heat diffusivity model. However, it is costly to carry out linear calculations of the growth rate by the gyrokinetic simulation at each time step of the transport simulation. How to apply the turbulent heat diffusivity model derived from the gyrokinetic simulations to the dynamic transport simulation with a low computational cost was shown [2]. This additional modeling for the turbulent ion heat diffusivity has been applied to the integrated code, TASK3D. The TASK3D simulation of the high T_i plasmas with the carbon pellet injection in LHD was performed [3] using the gyro-Bohm+ ∇T_i model for the turbulent ion transport. In this study, the method to apply the reduced model to the transport simulation is used for the LHD shots different from that in [2]. Dependence of the density scale length on the turbulent heat diffusivity is examined in a case of the pure hydrogen plasma. We examine the ion temperature profiles before and after the C pellet injection for applying the gyrokinetic heat diffusivity model to TASK3D. The neoclassical transport is numerically estimated in the TASK3D simulation. Introduction of the carbon impurity density remains to be improved in the turbulent transport studies of the LHD high T_i plasmas. The simulation results without the effects of the carbon density on the turbulent heat diffusivity are compared with the experimental results. The effect of the multi-ion species plasma on the heat diffusivity after the C pellet injection is investigated.

[1] M. Nunami, *et al.*, 2013 *Phys. Plasmas* **20** 092307

[2] S. Toda, *et al.*, 2014 *J. Phys.: Conf. Ser.* **561** 012020

[3] S. Murakami, *et al.*, 2015 *Plasma Phys. Control. Fusion* **57** 054009

Development of TASK3D/WM module for evaluation the ICRF wave propagation and absorption in LHD

R. Seki, A. Fukuyama^{al}, T. Seki, K. Saito, H. Kasahara, S. Kamio,
M. Yokoyama, K. Y. Watanabe and T. Mutoh

National Institute for Fusion Science, 322-6 Oroshi-cho, Toki 509-5292, Japan

^a *Graduate School of Engineering Kyoto University, Kyoto 606-8501, Japan*

In the ICRF (ion cyclotron range of frequencies) in the LHD, the maximum value of input power reached about 4 MW and the helium plasma of the relatively high density with a center electron density $\sim 6 \times 10^{19} \text{ m}^{-3}$ can be maintained by using the hydrogen minority heating. To investigate the transport characteristic or to optimize the heating condition of ICRF, it is important to evaluate the heating power profile of ICRF properly. In particular, since the ray-tracing cannot be used because of long wave length of ICRF wave, to calculate the wave propagation from the Maxwell's equation is required.

The TASK3D/WM [1] has been developed as the wave propagation and absorption evaluation code of ICRF in the non-axially symmetric 3-dimensional magnetic configuration such as LHD. In the TASK3D/WM, the Fourier expansion is used in the poloidal and toroidal directions, and the Maxwell's equation where finite difference method is used in the minor radius is solved for electric field as a boundary value problem. Each electric field components (Erho, Etheta, Ephi) are expressed in the torus magnetic coordinates.

In calculations of the wave absorption of ICRF heating using the TASK3D/WM in LHD, the cold plasma approximation is assumed in the dielectric constant tensor [2]. In the cold plasma approximation, since the thermal motion of plasma is not included, the wave propagation can be calculated only in the region where a phase velocity of the wave is much larger than a thermal velocity of plasma, i.e. the region except for near the resonance layer. The plasma heating from the wave near resonance layer cannot be evaluated properly. Therefore, in the TASK3D/WM, the wave collisional dumping model is introduced so that the heating power from the wave to plasma near the resonance layer can be evaluated. In this case, only the locations where particles resonate with the wave can be calculated but the evaluation of heating power is not properly. In addition, the wave propagation near the resonance layer can be calculated properly because the cold plasma approximate is assumed. Thus, in order to evaluate the wave propagate and absorption properly, to introduce the dielectric constant tensor including the thermal motion of plasma is required

However, in the case assumed the dielectric constant tensor including the thermal motion of plasma, non-physical minus heating is calculated. Its minus heating is thought to be caused a numerical error when the electric field components are transformed to the Stix frame defined in the basis of the field line direction.

In order to reduce the numerical error, we change the electric field components from the torus magnetic coordinates to the coordinates like the Stix frame, Erho, Eperp, Epara in the TASK3D/WM. In addition, the TASK3D/WM where finite element method is used in the minor radius has been developed too. In the conference, the modeling and algorithm of TASK3D/WM will be explained in detail. The primary results of two codes will be shown.

[1] A. Fukuyama and T. Tohnai, in *5th IAEA Technical Committee Meeting on Alpha Particles in Fusion Research*, IAEA, Vienna, 1997.

[2] R. Seki, et al., Proc. of plasma conference 2012, 23P095-P.

Analysis of High Energy Electron Tail and Its Effect on the H⁻ Production in the Linac4 H⁻ Source

S. Mochizuki¹, S. Mattei², K. Nishida¹, A. Hatayama¹ and Jacques Lettry²

¹Faculty of Science and Technology, Keio University, 3-14-1 Hiyoshi, Kohoku-ku, Yokohama 223-8522, Japan

²CERN, 1211 Geneva 23, Switzerland

A numerical simulation code based on the Electromagnetic Particle in Cell (EM-PIC) Model with Monte Carlo method for Collision processes (MCC) has been developed to understand the Radio Frequency Inductively Coupled Plasmas (RF-ICP) [1]. The code has already been applied to the simulation of the Linac4 H⁻ source plasma. The code is able to obtain the Electron Energy Distribution Function (EEDF) and Ion Energy Distribution Function (IEDF) in RF-ICP. This is the most distinct feature of the code compared with the conventional fluid model. The code has been improved step by step by including various effects, such as i) capacitive component of the electric field[2], ii) Coulomb collision[3] and iii) coupling to the Collisional Radiative (CR) model[4,5] for the calculation of Balmer emission lines from the source plasmas. Most of these studies, however, were focused on the macroscopic property of RF plasmas and detailed discussion of the EEDF in RF plasmas has not been given so far.

The purpose of this study is to clarify the characteristic features of EEDFs in RF H⁻ Sources. We have performed the analysis of EEDF with simple theoretical approach [6] based on the Boltzmann equation. Comparison between the EEDFs derived from analysis mentioned above and those obtained by numerical simulation shows that the low energy parts of EEDFs become Maxwellian distribution. In addition, the temperature calculated by the simulation agrees well with theoretically calculated one. On the other hand, it has not been clarified the relationship between the high energy part of EEDF and plasma source parameters (RF driven frequency, RF-coil current, etc.). High energy part of EEDF plays a key role to enhance the dissociation of molecules. The resultant enhancement of the atomic flux onto the PG leads to the increase in the surface H⁻ production. The parameter survey for the dependence of the high energy part of EEDF on these parameters is now underway and the results will be presented.

- [1] S. Yoshinari, T. Hayami, R. Terasaki, A. Hatayama and A. Fukano, *Rev. Sci. Instrum.* **81**, 02A728 (2010)
- [2] S. Mattei, M. Ohta, M. Yasumoto, A. Hatayama, J. Lettry and A. Grudiev, *Rev. Sci. Instrum.* **85**, 02B115 (2014)
- [3] S. Mochizuki, S. Mattei, T. Shibata, K. Nishida, A. Hatayama and J. Lettry, *AIP Conf. Proc.* **1655**, 020016 (2015)
- [4] T. Yamamoto, T. Shibata, M. Ohta, M. Yasumoto, K. Nishida, A. Hatayama, S. Mattei, J. Lettry, K. Sawada and U. Fantz, *Rev. Sci. Instrum.* **85**, 02B118 (2014)
- [5] T. Shibata, S. Mattei, K. Nishida, A. Hatayama and J. Lettry, *AIP Conf. Proc.* **1655**, 020008 (2015)
- [6] V. E. Golant, A. Zhilinskii, S. A. Sakhavov, *Fundamentals of Plasma Physics*, (Wiley, New York, 1977)

Effect of Coulomb Collision on the Negative Ion Extraction Mechanism in Negative Ion Sources

I. Goto^a, K. Miyamoto^b, S. Nishioka^a, S. Abe^a, A. Hatayama^a

^a Faculty of Science and Technology, Keio University, 3-14-1 Hiyoshi, Kohoku-ku, Yokohama 223-8522, Japan

^b Naruto University of Education, 748 Nakashima, Takashima, Naruto-cho, Naruto-shi, Tokushima 772-8502, Japan

Negative hydrogen ion (H^-) beam has a wide range of applications, such as fusion plasma heating, accelerators for medical use and high energy particle physics. However, the extraction mechanism of negative ions from the ion sources has not been fully understood yet. To clarify the extraction mechanism of H^- ions from H^- negative ion sources is an important subject for optimizing the negative ion beam extraction. In our previous study, numerical simulations using the 2D3V-PIC (two dimension in real space and three dimension in velocity space)·(Particle In Cell), and 3D3V-PIC model, aiming to understand the H^- extraction mechanisms[1-3].

In this study, Coulomb collisions such as electron- H^- , H^-H^+ have been taken into account to our 2D3V-PIC to (a) clarify the energy relaxation of the surface produced H^- ions and (b) to estimate the detailed effect of electron transport across the filter magnetic field.

Initial energy of the surface produced H^- ions is set to be $T_{H-SP0} = 1.0$ eV for the energy of the surface produced negative ion because the energy of H^- ions produced on the PG surface is estimated to be ~ 1 eV from the theoretical formula[4]. The energy relaxation process is important because the energy of surface produced H^- ions strongly affect the beam emittance. The preliminary result of the simulation including the Coulomb collision process shows that the energy of H^- ions in the region 8 mm far from the inner surface of the PG has been reduced $T_{H-} = 0.66$ eV due to the Coulomb collision with the lower energy particles.

Electron diffusion across the magnetic field was introduced by a simple model derived from diffusion equation with some approximations in the previous PIC model of the extraction region[6]. In the present model, electron diffusion across the filter magnetic field can be taken into account naturally without such a simple model, because we include the full effect of Coulomb collision. Comparison of the results by the previous simple diffusion model with the present model including the full effect of Coulomb collision will be presented. The effect of electron diffusion across the magnetic field on the potential structure near the PG and the resultant H^- extraction will be also discussed in this paper.

- [1] K. Miyamoto, S. Okuda, and A. Hatayama, Appl. Phys. Lett., 100, 233507(2012).
- [2] K. Miyamoto, S. Okuda, S. Nishioka, and A. Hatayama, J. Appl. Phys., 114, 103302/1-7(2013).
- [3] S. Nishoka, K. Miyamoto, S. Okuda, I.Goto, A. Hatayama and A. Fukano, Rev. Sci. Instrum. 85, 02A737/1- 3(2014).
- [4] R. McAdams, A. J. T. Holmes, D. B. King, and E. Surrey, Plasma Sources Sci. Technol. **20**, 035023-1 (2011).
- [5] S. Nishoka, K. Miyamoto, S. Okuda, I.Goto, A. Hatayama and A. Fukano, Rev. Sci. Instrum. **85**, 02A737/1- 3(2014).

Saturation mechanism of ion temperature gradient driven trapped electron mode turbulence

Y. Idomura

Japan Atomic Energy Agency, Wakashiba 178-4, Kashiwa, Chiba 277-0871, Japan

Full-f gyrokinetic simulations are important tools in studying stiff temperature profiles imposed by non-local transport, non-diffusive momentum transport leading to intrinsic rotation, interplay between neoclassical and turbulent transport, and plasma size scaling of turbulent transport [Idomura, NF09, CSD12, POP14a, POP14b, PFR14]. However, most of existing full-f gyrokinetic simulations are limited within electrostatic ion temperature gradient driven (ITG) turbulence simulations with adiabatic electrons, and electron transport problems have been still open in full-f approaches. In this work, we develop a kinetic electron model for electrostatic ITG and trapped electron mode (TEM) turbulence simulations in the Gyrokinetic Toroidal 5D full-f Eulerian code, GT5D. In the model, a full kinetic electron model including both trapped and passing electrons is solved for collisional processes and radial electric fields. In the axisymmetric limit, this model imposes a neoclassical equilibrium with an ambipolar condition. The neoclassical transport is computed using a multi-species linear Fokker-Planck collision operator [Sugama, POP09], and the particle transport, the ion and electron heat transport, the bootstrap current, and the radial force balance condition are verified against the standard moment approach [Hirshman, NF87]. On the other hand, turbulent fluctuations are computed by kinetic (adiabatic) response of trapped (passing) electrons in order to avoid a high frequency mode, which appears as the electrostatic limit of kinetic Alfvén waves. It is noted that unlike a bounce-averaged trapped electron model [Idomura, JPFR04], this model involves collisional and turbulent trapping and de-trapping processes, which are essential as physically relevant source and sink models for the trapped electron distribution. The linear ITG-TEM stability is verified against former benchmark results [Rewoldt, CPC04], and linear critical gradient parameters of the ITG mode are confirmed. In this work, we address saturation mechanisms in decaying ITG (adiabatic electrons) and ITG-TEM (kinetic electrons with $m_i/m_e=100$) turbulence simulations using the same Cyclone parameters [Dimitis, POP00] with a small plasma size parameter $1/\rho^* \sim 150$. In both simulations, density and temperature profiles evolve during nonlinear saturation processes, and turbulent transport is quenched after the nonlinear saturation phase. What is important here is that in the nonlinear quasi-steady phase, the temperature profiles are sustained above linear critical temperature gradient parameters of the ITG mode. This kind of nonlinear critical gradient is often explained by stabilizing effects of turbulence driven zonal flows. In fact, in the ITG turbulence, a radial electric field E_r contains turbulence driven zonal flows, and its shearing rate $\omega_E \sim 0.1 v_{ti}/L_n$ is comparable to the linear growth rate of the ITG mode. However, it is found that this mechanism is not the case for the ITG-TEM turbulence. A remarkable feature of the full-f ITG-TEM turbulence simulation is that a corrugated density profile is generated in the saturation process, and E_r is determined by a radial force balance relation, where a density gradient term is dominant. The resulting E_r also shows a fine corrugation, and its shearing rate is quite high $\omega_E \sim v_{ti}/L_n$. In the simulation, it is found that the density profile structure is related to passing electrons transport near low order mode rational surfaces, where non-adiabatic response of passing electrons may become important [Dominsky, POP15].

Kinetic equilibrium of a non-adiabatic trapT. Takahashi, H. Momota^a*Division of Electronics and Informatics, Gunma University, 1-5-1 Tenjin-cho, Kiryu 376-8515, Japan**^a National Institute for Fusion Science, 322-6 Oroshi-cho, Toki 509-5292, Japan*

Quest for an economically-competitive nuclear reactor concept is necessary for post-ITER phase. A non-adiabatic has attractive properties to be a candidate of a next-generation compact reactor. It consists of the solenoid and mirror coils, and a field-canceling coil (the Helmholtz coil). The magnetic field of the trap vanishes widely near its center region. As a result, a confined plasma is in a high-beta state. Moreover, the confined plasma is expected to be stable against interchange modes because the field lines surrounding the core plasma have good curvature. Since plasma ions move stochastically in the zero-field region, the mirror confinement concept breaks and the probabilistic nature dominates an end-loss process in the non-adiabatic traps. One of the authors has proposed a new concept of the multi-linked non-adiabatic traps [1], where plasma particles escaping a trap are re-trapped in neighboring traps. The resultant overall particle confinement time can be extended in proportion to the square of the number of traps; it offers drastic improvement of confinement.

We study here kinetic equilibrium state of the plasma confined in a non-adiabatic trap by 2-dimensional (2-d) hybrid simulation in order to find the 2-d profiles of the diamagnetic current and the magnetic field structure. Detailed results will be reported at our presentation.

[1] H. Momota, G. H. Miley, and O. Motojima, *J. Fusion Energ.* **27**(2008) 77.

Kinetic behavior of electron magnetohydrodynamic structures

M. Hata, H. Sakagami^a, A. Das^b

Institute of Laser Engineering, Osaka University, 2-6 Yamadaoka, Suita 565-0871, Japan

^a *National Institute for Fusion Science, 322-6 Oroshi-cho, Toki 509-5292, Japan*

^b *Institute for Plasma Research, Bhat, Gandhinagar 328428, India*

The Electron Magnetohydrodynamic (EMHD) fluid model (simplified fluid depiction of fast electron time scale phenomena for plasmas) supports exact nonlinear solutions in the form of electron vortex currents with associated induced magnetic field in two-dimensional uniform plasma [1,2]. The consideration of immobile ion and zero temperature employed in the EMHD formalism, however, is pretty restrictive. Recent simulation studies have shown that such structures can be created as a result of laser-plasma interaction and these structures play important roles in the beam electron energy dissipation [3,4]. Understanding the kinetic behavior of EMHD structures become more important, but these properties have not been clarified yet. Therefore kinetic behavior of EMHD structures has been explored in the present study. According to recent research, kinetic effects on robustness of EMHD monopole solution have been studied and its robust condition was investigated [5]. In this study, kinetic effects on propagation of EMHD dipole structures in homogeneous and inhomogeneous plasma are investigated.

For this purpose, Particle-In-Cell (PIC) simulations that include kinetic effects are conducted. The exact dipole solution derived in EMHD model, which approximately consists of a combination of two counter-rotating electron vortex currents and their induced magnetic fields, is used as initial conditions. This solution has traveling property and it can travel to higher density region depending on the situation. Electron velocities are given to satisfy Maxwell velocity distribution with the given electron temperature and then the current-derived drift velocity is added to each electron. Changing the electron temperature, we perform PIC simulations to investigate finite temperature effects. Furthermore we also investigate effects of density inhomogeneity on dipole behavior.

[1] M. B. Isichenko and A. M. Marnachev, *Sov. Phys. JETP* **66** (1987) 702.

[2] A. Das, *Plasma Phys. Controlled Fusion* **41** (1999) A531.

[3] T. Nakamura, S. V. Bulanov, T. Z. Esirkepov, and M. Kando, *Phys. Rev. Lett.*, **105** (2010) 135002.

[4] Q. Jia, K. Mima, H. B. Cai, T. Taguchi, H. Nagatomo, and X. T. He, *Phys. Rev. E*, **91.2** (2015) 023107.

[5] M. Hata, H. Sakagami, and A. Das, *Phys. Plasmas*, **20.4** (2013) 042303.

Simulation study on helium in the vicinity of tungsten grain boundaryA. Takayama^a, A. M. Ito^{a,b}, H. Nakamura^{a,c}^a *National Institute for Fusion Science, 322-6 Oroshi-cho, Toki 509-5292, Japan*^b *Sokendai, 322-6 Oroshi-cho, Toki 509-5292, Japan*^c *Nagoya University, 322-6 Oroshi-cho, Toki 509-5292, Japan*

Tungsten is one of plasma facing materials in magnetic confinement nuclear fusion reactors. In the surface region of plasma facing materials, high concentrations of hydrogen isotopes and helium as a nuclear fusion product can build up and interact with the materials. These interactions will induce changes in the surface morphology and the bulk microstructure and thus in the mechanical properties. Therefore, the mechanical properties and the structural strength of tungsten under exposure to plasma irradiation have been intensively investigated both experimentally and theoretically.

In our previous work [1], the binding energies of helium and hydrogen clusters interstitially trapped in bcc tungsten are evaluated by first-principles calculations based on density functional theories (DFT). It is shown that helium-rich interstitially-trapped clusters have the positive binding energies and the low electron-density region expands as the number of helium in the cluster increases. These results indicate that the helium-rich interstitially trapped clusters can act as a trapping site for hydrogen, and interstitially trapped helium interrupts or disturbs the hydrogen diffusion in tungsten.

Tungsten material is polycrystal in reality, containing grain boundary. In the present study, helium atom(s) in the vicinity of tungsten grain boundary is investigated by use of DFT calculation. Difference between helium behavior in bcc tungsten and one in the vicinity of tungsten grain boundary will be discussed.

[1] A. Takayama, A. M. Ito, Y. Oda, H. Nakamura, *J. Nucl. Mater.* **463** (2015) 355.

Three-dimensional numerical analysis of shear flow effects on MHD stability in LHD plasmas

K. Ichiguchi^{a,b}, Y. Suzuki^{a,b}, Y. Todo^{a,b}, M. Sato^a, T. Nicolas^a, B. A. Carreras^c, S. Sakakibara^{a,b}, Y. Takemura^a, S. Ohdachi^{a,b}, Y. Narushima^{a,b}

^aNational Institute for Fusion Science, 322-6 Oroshi-cho, Toki 509-5292, Japan

^bSOKENDAI, The Graduate University for Advanced Studies, Toki, 509-5292, Japan

^cUniversidad Carlos III, 28911 Leganes, Madrid, Spain

In the Large Helical Device (LHD), experiments for high beta achievement has been extensively conducted. The highest value of $\langle\beta\rangle = 5.1\%$ was obtained in the configuration with $R_{ax} = 3.6\text{m}$ and $\gamma_c = 1.20$ [1]. Here, R_{ax} and γ_c are the horizontal position of the vacuum magnetic axis and the parameter of the aspect ratio of the helical coils, respectively. On the other hand, the plasma in this configuration is predicted to be unstable with respect to the Mercier criterion. It follows that some stabilizing effects work on the LHD plasma for the achievement of the high beta. In order to design the coil configuration in the heliotron DEMO accurately, it is crucial to identify the stabilizing mechanism in the viewpoint of the magnetohydrodynamic (MHD) stability. In the recent experiments, the phenomenon like a locked mode was observed [2,3]. In this case, the mode grows rapidly just after the mode rotation stops, and brings a partial collapse of the profile in the electron temperature. This phenomenon indicates that the shear flow of the plasma may be a candidate which can suppress the growth of the mode. Thus, we numerically study the effects of the shear flow on the stability against the pressure driven modes in the LHD plasmas. For this purpose, we utilize three-dimensional (3D) numerical codes. It has not been established how to obtain a 3D equilibrium consistent with finite flows. Hence, we utilize a static equilibrium, and then, we set a finite flow in the stability examination, as the first step of the flow analysis. In the equilibrium and the stability calculations, the HINT2 code [4] and the MIPS code [5] are utilized, respectively. In both codes, rectangular grids are employed in the coordinates (R, ϕ, Z) . The MIPS code examines the stability by following the time evolution of the plasma. We set the shear flow \mathbf{v} satisfying $\mathbf{v} \cdot \nabla\Psi = 0$ as the initial condition of the MIPS code. Here, Ψ denotes the label of the equilibrium flux surface. The profile of the flow close to the experimental data is assumed. It is reported how the shear flow affects the linear growth rate and the nonlinear dynamics of the pressure driven modes.

- [1] H. Yamada, *et al.*, 2011 *Nucl. Fusion* **51** pp.094021.
- [2] Y. Takemura, *et al.*, 2012 *Nucl. Fusion* **52** pp.102001.
- [3] S. Sakakibara, *et al.*, 2013 *Plasma Phys. Control. Fusion* **55** pp.014014.
- [4] Y. Suzuki, *et al.*, 2006 *Nucl. Fusion* **46** pp.L19.
- [5] Y. Todo, *et al.*, 2010 *Plasma and Fusion Res.* **5** pp.S2062.

Pressure anisotropy analyses based on MHD equilibrium calculations and magnetic diagnostics in LHD

R. Ueda^a, Y. Suzuki^{a,b}, K.Y. Watanabe^a and W. A. Cooper^c

^a*National Institute for Fusion Science, 322-6 Oroshi-cho, Toki 509-5292, Japan*

^b*SOKENDAI, The Graduate University for Advanced Studies, 322-6 Oroshi-cho, Toki 509-5292, Japan*

^c*Ecole Polytechnique Federale de Lausanne (EPFL), Centre de Recherches en Physique des Plasmas, Association Euratom-Confederation Suisse, CH1015 Lausanne, Switzerland*

Large Helical Device (LHD) is a heliotron-type plasma confinement experiment device which has achieved the volume averaged β that exceeds 5% [1]. The high- β plasmas are produced by the tangential Neutral Beam Injection (NBI) in the low density and the low magnetic field. For the conditions, the beam pressure enhances the parallel component to the magnetic field line, which leads to the pressure anisotropy. The pressure anisotropy is expected to affect on the characteristics of transport and stability. Additionally, for the anisotropic pressure, the shape of the magnetic flux surface does not coincide with the pressure isosurface.

However, the plasma pressure of the future reactor device is predicted to be isotropic because the α -heating, which is a major heating system in a fusion reactor, produces the isotropic velocities. To extrapolate the knowledge obtained by LHD high- β discharges to future device designs, we should investigate the pressure anisotropy of the LHD experiment plasmas.

In previous works, an identification method for the pressure anisotropy has been proposed [2], which has been studied using ANIMEC code [3]. The code is an extended version of VMEC, and can treat the anisotropic pressure. The study shows the anisotropy can be predicted tolerably even if we use VMEC code. The equally weighted averaging β of the perpendicular and parallel component, β_{eq} , and the perpendicular component, β_{\perp} , are obtained by the saddle loop flux and the diamagnetic flux, respectively. Then, the parallel component, β_{\parallel} , is calculated by $\beta_{\parallel} = 2\beta_{\text{eq}} - \beta_{\perp}$. The identification of the pressure profile is carried out by investigating the relationships between the saddle loop flux and the location of the magnetic axis. However, the application to the actual LHD experiment plasma has not been studied in detail. In this study, we apply the method to a number of LHD discharges and show the characteristics of the equilibrium focusing on the anisotropy and the pressure profile.

[1] A. Komori *et al.*, Nucl. Fusion **49** (2009) 104015.

[2] Y. Asahi *et al.*, Phys. Plasmas **20** (2013) 022503.

[3] W. A. Cooper *et al.*, Comput. Phys. Commun. **180** (2009) 1524.

Benchmark of multi-ion-species collision operator for δf Monte-Carlo neoclassical simulation

S. Satake^{a,b}, M. Nakata^{a,b}, T. Pianpanit^b, S. Matsuoka^c, M. Nunami^{a,b}, H. Sugama^{a,b}

^aNational Institute for Fusion Science, 322-6 Oroshi-cho, Toki 509-5292, Japan

^bSokendai, 322-6 Oroshi-cho, Toki 509-5292, Japan

^cResearch Organization for Information Science and Technology (RIST), 1-5-2 Minatojima-Minamimachi, Chuo-ku, Kobe 650-0047, Japan

satake@nifs.ac.jp

To study and evaluate the neoclassical transport process in burning plasma in nuclear fusion reactor, it is required to develop a neoclassical transport simulation code for multiple ion species plasmas which treats the Coulomb collisions between unlike ion species. We plan to extend the neoclassical simulation code FORTEC-3D[1,2] by implementing the unlike-species collision operator which keeps the self-adjointness nature even if the temperature of two ion species are different[3]. In δf neoclassical transport simulation, the linearized collision operator for the perturbation part of the distribution function of particle species a , $\delta f_a = f_a - f_{Ma}$, should satisfy the following properties.

$$\int d^3v C_{ab}^T(\delta f_a) = \int d^3v C_{ab}^F(\delta f_b) = 0, \quad (1)$$

$$m_a \int d^3v \{v_{\parallel}, v^2\} C_{ab}^T(\delta f_a) = -m_b \int d^3v \{v_{\parallel}, v^2\} C_{ba}^F(\delta f_a), \quad (2)$$

$$\int d^3v \frac{\delta f_a}{f_{aM}} C_{ab}^T(\delta g) = \int d^3v \frac{\delta g}{f_{aM}} C_{ab}^T(\delta f_a), \quad (3)$$

$$T_a \int d^3v \frac{\delta f_a}{f_{aM}} C_{ab}^F(\delta g_b) = T_b \int d^3v \frac{\delta g_b}{f_{bM}} C_{ba}^F(\delta f_a), \quad (4)$$

where Eqs. (1)-(3) represent the conservation property and the last two are the adjointness of the operator. In this presentation, a numerical method to implement the collision operator in the δf Monte-Carlo particle code is explained. Benchmark of the new collision operator with the same one implemented in a gyrokinetic continuum code[4] and the other one in a full-f PIC code, based on Nanbu-method[5] are to be reported. Dependence of the numerical accuracy of the operator on the mass-ratio is studied.

To accelerate the collision calculation among many particle species, we test the implementation of the simulation code on the Intel Phi accelerator. Optimization method of the code for the Phi architecture is explained.

[1] S. Satake, R. Kanno, and H. Sugama, Plasma Fusion Res. **3** (2008) S1062

[2] S. Matsuoka et al., Phys. Plasmas **22** (2015) 072511

[3] Sugama et al., Phys. Plasmas **16** (2009) 112503

[4] M. Nakata, et al., "Improved collision operator for plasma kinetic simulations with multi-species ions and electrons" Comput. Phys. Comm. (2015) in press

[5] K. Nanbu, Phys. Rev. E **55** 4642 (1997)

Improvement of a Multi-Hierarchy Simulation Model for Magnetic Reconnection Studies

S. Usami^a, H. Miura^{ab}, H. Ohtani^{ab}, R. Horiuchi^{ab}, M. Den^c

^a National Institute for Fusion Science, 322-6 Oroshi-cho, Toki 509-5292, Japan

^b The Graduate University for Advanced Studies (SOKENDAI), 322-6 Oroshi-cho, Toki 509-5292, Japan

^c National Institute of Information and Communications Technology, 4-2-1 Nukui-Kitamachi, Koganei, 184-8795, Japan

A fusion plasma consists of multiple hierarchies. It is characterized by the wide range of spatiotemporal scales from macroscopic transports and instabilities covering the entire system to microscopic processes relating to the dynamics of each electrons and ions. Furthermore, a fusion plasma is composed of not only multiple hierarchies but also multiple sciences, such as plasma physics, material science, and nuclear physics. In fusion plasma studies with computer simulations, different hierarchies or physics are treated independently by different models. Studies on each hierarchy or physics are advancing remarkably [1]. On the other hand, it is poorly understood that how and where multiple hierarchies or physics couple each other. For the complete comprehension of fusion plasmas, simulation models which deal with multiple hierarchies or physics self-consistently and simultaneously are required.

We have developed a multi-hierarchy simulation model which couples an MHD code and a PIC code [2]. Using our model, we have studied on collisionless magnetic reconnection, since magnetic reconnection is one of typical multi-hierarchy phenomena and is believed to be strongly involved with sawtooth oscillations, which cause tokamak disruption. Our multi-hierarchy model employs the domain decomposition method, namely real space in a simulation domain is divided into the following three parts: an MHD domain to deal with global plasma dynamics away from reconnection points, a PIC domain to solve kinetic physics in the vicinity of the neutral sheet, and an interface domain to commute the MHD and PIC information and interlock the MHD and PIC domains. In 2014, by means of our multi-hierarchy simulations we have investigated on the influence of macroscopic dynamics on microscopic physics of magnetic reconnection and reported the first results [3].

In the near future, we have a plan to apply our model to sawtooth oscillations. In fusion devices such as tokamak, the finite Larmor radius and Hall effects play important role in the entire region of a device. As ongoing activities, we improve our multi-hierarchy model as follows. An extended MHD code [4] including non-ideal terms such as the finite Larmor radius and Hall effects, and a PIC code are interlocked (In the current model, an ideal MHD code and a PIC code are coupled). In our presentation, we would like to introduce the development plan of our multi-hierarchy model and demonstrate simulation results performed with the improved model as the first step.

[1] R. Horiuchi and NSRP members, Plasma Fusion Res. **6** (2011) 2101055.

[2] S. Usami, R. Horiuchi, H. Ohtani, and M. Den, Phys. Plasmas **20** (2013) 061208.

[3] S. Usami, R. Horiuchi, H. Ohtani, and M. Den, Journal of Physics: Conference Series **561** (2014) 012021.

[4] R. Goto, H. Miura, A. Ito, M. Sato, and T. Hatori, Phys. Plasmas **22** (2015) 032115.

Neutron incident angle and energy distribution to vacuum vessel in beam-injected LHD deuterium plasmas

S. Sugiyama, H. Matsuura, T. Goto^a

*Department of Applied Quantum Physics and Nuclear Engineering,
Kyushu University, 744 Motoooka, Fukuoka 819-0395, Japan*

^a*National Institute for Fusion Science, 322-6 Oroshi-cho, Toki 509-5292, Japan*

In toroidal devices, it is known that neutron wall loading and incident flux to first wall depend on poloidal angular wall position because of the torus wall shape [1, 2]. As the vacuum vessel of helical devices has a dumbbell-shaped poloidal cross section, the shape of the first wall would cause additional nonuniformity of the neutron incident flux. The neutron flux has been evaluated for neutron measurement, e.g. *in situ* calibration for neutron monitor [3], using Monte Carlo simulation code in the Large Helical Device (LHD) approximately incorporating the complex shape of the vacuum vessel. Neutron emission profile can be taken into account for these calculations [4]. However, analysis of the neutron flux for effects on structural materials has not been studied. From this point of view, it is important that the dependence of the neutron energy spectra on incident angle at all wall positions is clarified. In addition to the geometrical effects of the first wall, anisotropic high-energy ion tail formation in fuel ion velocity distribution function [5, 6] also affects the neutron flux distribution, energy spectra, and incident angle distribution.

In this study, the neutron incident angle distribution and energy spectra at all wall positions are evaluated assuming deuterium-beam-injected deuterium plasmas confined in the LHD considering exact shape of the vacuum vessel and the fuel ion velocity distribution function. It is presented that the neutron spectra significantly differ by the wall position and incident direction.

- [1] P. P. H. Wilson, et al., *Fusion Eng. Des.* **83** (2008) 824.
- [2] J. C. Rivas, et al., *Fusion Sci. Technol.* **64** (2013) 687.
- [3] Y. Nakano, et al., *Rev. Sci. Instrum.* **85** (2014) 11E116.
- [4] M. Homma, et al., *Plasma Fusion Res.* **10** (2015) 3403050.
- [5] H. Matsuura, Y. Nakao, *Phys. Plasmas* **16** (2009) 042507.
- [6] H. Matsuura, et al., *Plasma Phys. Control. Fusion* **53** (2011) 035023.

Particle-in-cell simulations of a kink instability in a pinched current filament

T. Haruki

*Graduate School of Science and Engineering, University of Toyama,
3190 Gofuku, Toyama, Toyama 939-8555, Japan*

haruki@eng.u-toyama.ac.jp

Current filaments are often observed in astrophysical and laboratory plasmas. It is well known that a filament pinches [1] and/or becomes unstable against magnetohydrodynamic (MHD) instabilities. Understanding the physics of the current filaments is important to a variety of applications, including electric discharge, solar flares and a pinch device.

Haruki *et al.* already reported the dynamics of a current filament in three dimensional, relativistic, fully electromagnetic particle-in-cell (PIC) simulations [2]. The plasma column located at the center of system is initially accelerated by an externally applied electric field to produce a current filament. The filament then starts to pinch, due to the Lorentz force, and becomes unstable initially against a sausage instability and then a kink instability. High-energy particles are produced by these two types of instabilities.

However, further analysis showed that out-going electromagnetic waves were reflected from the numerical boundaries of the system and affect the current filament at the center. These reflected waves enhanced the current filament instabilities.

In this study, more accurate simulations of a pinched current filament were performed with absorbing boundary conditions applied perpendicular to the axial direction. As a result, the enhancement of instabilities are suppressed and the current filament pinches only weakly. For the strong current filament, it starts to pinch while oscillating and becomes unstable against a kink instability (a sausage instability is not observed here). The positive and negative isosurface levels of the axial component of an electric field and current density showed double helical structures. After the kink instability, the current filament diffuses and the ions are heated.

These results are important to understanding not only the basic plasma physics but also to the newly proposed concept of *focus fusion* [3], which uses a dense plasma focus device, improved upon from a pinch device, to produce a p-¹¹B reaction without neutrons (aneutronic).

- [1] W. Bennett, Phys. Rev. **45**, 890 (1934)
- [2] T. Haruki *et al.*, Phys. Plasmas **13**, 082106 (2006)
- [3] E.J. Lerner *et al.*, Phys. Plasmas **19**, 032704 (2012)

Basic Comparison of the Numerical Method to Solve Fluid Equations for SOL/Divertor Plasmas

Ryoko Tatsumi¹, Yuki Homma², Shohei Yamoto¹, Kazuhiro Ishibashi¹,
and Akiyoshi Hatayama¹

¹Graduate School of Science and Technology, Keio University, 3-14-1, Hiyoshi, Kohoku-ku, Yokohama 223-8522, Japan

²Japan Atomic Energy Agency, Rokkasho, Aomori 039-3212, Japan

Understanding plasma transport in the SOL/Divertor region is one of the most important issues in order to reduce heat and particle loads to the divertor plate in future fusion reactors. For this purpose, several numerical codes based on the fluid plasma equations have been developed so far. Among them, there are mainly two types of method, finite difference method like B2-EIRENE(SOLPS)[1], and Monte Carlo method like EMC3[2]. The former seems to be harder for 3D (three dimensional) large scale simulations, while the latter seems to have difficulty on setting boundary conditions. Therefore, the objective of our study is to solve the benchmark problem with both methods and compare them.

The plasma transports can be described as the following convection-diffusion equation[3]:

$$\nabla_{\parallel} \cdot [\alpha_{\parallel} f - \nabla_{\parallel}(\beta_{\parallel} f)] + \nabla_{\perp} \cdot [\alpha_{\perp} f - \nabla_{\perp}(\beta_{\perp} f)] = S \quad (1)$$

where f stands for density, momentum, and temperature of the plasma. (Other notations are given in the Ref. [3]) In one-dimensional case where $\beta = 0, S = 0$ for density, $\beta = 0, S = -\nabla p$ for momentum, and $S = 0$ for temperature, the analytic solution can be obtained as:

$$v(x) = \frac{mv_0^2 + T_0 + \sqrt{(mv_0^2 + T_0)^2 - 4mv_0^2 T(x)}}{2mv_0}, \quad n(x) = n_0 v_0 / v(x) \quad (2)$$

where x is the distance along the magnetic field, n, v , and T correspond to the density, velocity, and temperature, respectively.

As the first step, we have developed a simple 1D simulation model using the Monte Carlo method and conducted the calculation in the case mentioned above with the boundary conditions, $v_0 = (T_0/m)^{1/2}$ and $q = -\kappa \partial T / \partial x(0) = 10 \text{ MW/m}^2$. The results agree with the analytic solutions (see Fig. 1). The comparison between the Monte Carlo method and finite difference method will be presented at the conference as the next step.

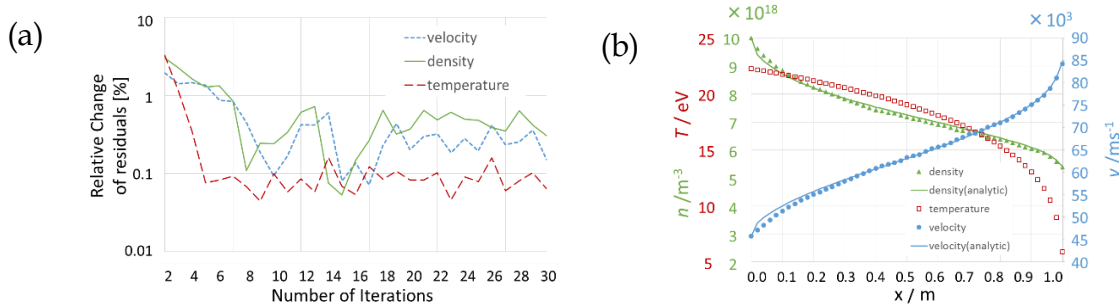


Fig. 1. (a) Convergence property of the iteration [Relative change of the residuals for each equation of (1)] (b) Numerical solution of f (n , v , and T) at the iteration number $N=15$ for 1D simulation along the field line.

[1] R. Schneider et al., J. Nucl. Mater. **196-198**, 810 (1992).

[2] Y. Feng, et al: Contrib. Plasma Phys. **54** (2014) 426-.

[3] Y. Feng, et al: J. Nucl. Mater. **266-269** (1999) 812-818.

Multi-scale simulation of magnetic reconnection using particle-in-cell with magnetohydrodynamics on adaptively refined mesh

T. Ogawa, S. Usami^a, R. Horiuchi^a, M. Den^b, K. Yamashita^c

Kitasato University, 1-15-1 Kitasato, Sagami-hara 252-0373, Japan

^a *National Institute for Fusion Science, 322-6 Oroshi-cho, Toki 509-5292, Japan*

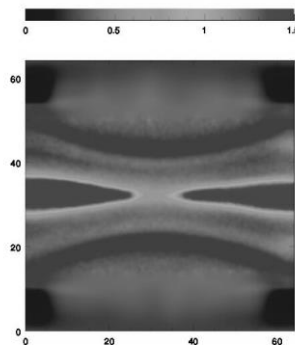
^b *National Institute of Information and Communications Technology, 4-2-1 Nukui-kitamachi, Koganei 184-8795, Japan*

^c *University of Yamanashi, 4-4-37 Takeda, Kofu 400-8510, Japan*

Magnetic reconnection is a phenomenon during which magnetic field topology changes and magnetic energy is transformed into plasma kinetic or thermal energy. Both macroscopic plasma dynamics and microscopic particle kinetics play important roles there. In numerical study, magnetohydrodynamics (MHD) is an efficient method to deal with macroscopic plasma dynamics, but it needs some artificial resistivity or non-MHD effects to model the phenomenon [1, 2]. While particle methods can bring microscopic kinetics, they need higher computational cost. Usami et al. developed an efficient multi-scale simulation model of magnetic reconnection. They used particle-in-cell (PIC) method near a magnetic neutral sheet and MHD distance from the sheet [3, 4, 5]. In our previous study, we extended their MHD part to a hierarchical mesh controlled by adaptive mesh refinement (AMR) technique and calculated Alfvén wave propagation to test the code [6].

We apply the code to a magnetic reconnection in this study (Figure). PIC is localized near the neutral sheet while a hierarchical mesh for MHD spreads outer region. In addition, we import external physical quantities onto outer boundary. It enables to decide outer boundary conditions by a global structure of another simulation. We aim to link a global MHD model, such as a model of Earth's magnetosphere, and a PIC calculation smoothly by the AMR-controlled hierarchical mesh sandwiched as a bridge.

This work was supported by JSPS Grant-in-Aid for Scientific Research (B) 23340182.



Resulting density distribution of the magnetic reconnection model.

- [1] M. Ugai, *Phys. Fluids* **4** (1992) 2953.
- [2] M. Yamada, *Phys. Plasmas* **14** (2007) 058102.
- [3] S. Usami, H. Ohtani, R. Horiuchi, and M. Den, *Commun. in Comput. Phys.* **11** (2012) 1006.
- [4] S. Usami, R. Horiuchi, H. Ohtani, and M. Den, *Phys. Plasmas* **20** (2013) 061208.
- [5] S. Usami, R. Horiuchi, H. Ohtani, and M. Den, *J.Phys.: Conf. Ser.* **561** (2014) 012021.
- [6] T. Ogawa, S. Usami, R. Horiuchi, M. Den, K. Yamashita, *JPS Conf. Proc.* **1** (2014) 016013.

Three dimensional magnetic reconnection of stressed X-point collapse

N. Tsujine, T. Haruki^a

Graduate School of Science and Engineering for Education, University of Toyama, 3190 Gofuku, Toyama 930-0885, Japan

^a*Graduate School of Science and Engineering for Research, University of Toyama, 3190 Gofuku, Toyama 930-0885, Japan*

m1571113@ems.u-toyama.ac.jp

Magnetic reconnection in plasmas is an important mechanism for converting magnetic field energy into thermal plasma heating and non-thermal particle acceleration. In particular, a stressed X-point collapse is a well know mechanism for explaining solar flares [1]. The magnetic field configuration for an X-point is

$$B_x = y, B_y = \alpha^2 x, B_z = 0,$$

where α is the stress parameter, and the x-point is located at the origin.

This model has been numerically simulated using a two dimensional, relativistic, fully electromagnetic, particle-in-cell (PIC) code [2]. The stress (plasma pressure) causes magnetic reconnection in the vicinity of the X-point, via the formation of a current sheet. Magnetic field energy is dissipated (about 20% in the strongly stressed case), followed by the production of high energy plasmas generated by the magnetic reconnection process. However, three dimensional simulations of the stressed X-point collapse model have not yet been studied. Including three dimensional effects into the numerical simulation is necessary to understand realistic magnetic reconnection.

In this study, three dimensional stressed X-point collapse was investigated by using a three dimensional PIC code. The X-point starts to collapse as in the two dimensional PIC simulations. A similar current sheet is also produced in the vicinity of the X-point. However, magnetic field lines are distorted in the z -axis direction - an effect not seem in the two dimensional case. These results are useful for understanding the physics in three-dimensional magnetic reconnection.

[1] E. Priest, T. Forbes, *Magnetic Reconnection: MHD Theory and Applications* (Cambridge University Press, Cambridge, 2000)

[2] D. Tsiklauri, T. Haruki, *Physics of Plasma*. **14**, 112905 (2007)

Simulation study on resistive instabilities in a small aspect ratio reversed field pinch

Yasuo Nagamine and Masamitsu Aizawa

*Institute of Quantum Science, Nihon University
1-8-14 Kanda-Surugadai, Chiyoda-ku, Tokyo 101-8308, Japan*

A reversed-field pinch (RFP) plasma is the result of a self-organization process, which is produced by a dynamo effect due to magnetohydrodynamic (MHD) instabilities. In the recent progress of the RFP study, improvement of the confinement properties by the transition to a single-helical-axis state is observed in the large experimental device. Also recent numerical simulations show the possibility of reproducing such single-helical-axis states [1]. As for a low aspect ratio RFP with $A \approx 2$, formation and rotation of the helical structure such as quasi-single-helicity states have been observed in experiments [2]. Towards the understanding of this structure formation mechanism, analysis using the detailed three-dimensional MHD simulation through the comparison with the experiment has been conducted [3].

In this study, from an analogy with the spherical tokamak (ST), we focus our attention on the RFP configuration having an elongated cross section with a small aspect ratio $A < 2$, in other words, spherical RFP. The basic characteristics of the equilibrium configuration and dynamical behavior of resistive instabilities are examined by using the MHD simulation model. Regarding the spherical RFP concept, its characteristic already has been introduced briefly in the first theoretical study on the spherical tokamak [4].

Since a stabilizing shell located near the plasma surface is necessary to sustain the RFP configuration, it is considered that it is not easy to develop spherical RFP device with a non-circular cross section like the ST. In addition, as the reactor, the extreme lowering of the aspect ratio becomes disadvantageous from the viewpoint of neutron irradiation of the torus center region. However, considerably high beta plasmas were attained in the ST than the conventional standard tokamak. With respect to the RFP, it is considered that the theoretical prediction of plasma properties such as the resistive instabilities and the search for the beta limit condition in this small aspect ratio regime are much important.

- [1] Onofri M, *Nuclear Fusion* **51**, 112003 (2011).
- [2] Oki K, *et al.*, *J. Phys. Soc. Jpn.* **77**, 075005 (2008).
- [3] Mizuguchi N, *et al.*, *Plasmas Fusion Res.* **7**, 2403117 (2012).
- [4] Peng Y-K M and Strickler D J, *Nuclear Fusion* **26**, 769 (1986).

Large-scale simulation of contactless crack detection in HTS films: application of \mathcal{H} -matrix method to fast matrix-vector multiplication

T. Takayama, A. Saitoh, A. Kamitani, H. Nakamura^a

Yamagata University, 4-3-16 Johnan, Yonezawa, Yamagata 992-8510, Japan

^aNational Institute for Fusion Science, 322-6 Oroshi-cho, Toki 509-5292, Japan

takayama@yz.yamagata-u.ac.jp

The practical applications of the high-temperature superconductors (HTSs) require the measurement of a critical current density j_C . Recently, Hattori et al. proposed a contactless and a high-speed measuring method of j_C in an HTS film [1]. In the following, this is called a scanning permanent magnet method. In the method, a permanent magnet is moved along the HTS surface. As a result, they found that a spatial distribution of j_C can be estimated from the distribution of an electromagnetic force acting on the film. However, note that the scanning permanent magnet method has been not yet applied to the crack detection.

In order to reproduce a scanning permanent magnet method numerically, a numerical code was developed for analyzing the time evolution of a shielding current density in an HTS film with multiple cracks. After an initial-boundary-value problem of the shielding current density is spatially discretized with the finite element method (FEM), the resulting ordinary differential system is solved by using the backward Euler method and the Runge-Kutta (R-K) method with an adaptive step-size algorithm. Consequently, it is found that the R-K method is a useful tool with increasing the number of nodes for the FEM. However, it is necessary to consider the further high-speed of the shielding current analysis for a large-scale problem.

The purpose of the present study is to develop a numerical code analyzing the time evolution of the shielding current density in an HTS film with cracks by using the \mathcal{H} -matrix method [2]. Also, by using the code, we simulate the scanning permanent magnet method for measuring j_C and detecting cracks by FEM with using large number of nodes.

[1] K. Hattori, A. Saito, Y. Takano, H. Yamada, T. Takayama, A. Kamitani, S. Ohshima, *Physica C*, **471** (2011) 1033

[2] M. Bebendorf, Springer-Verlag (2008)

Performance Improvement of Extended Boundary Node Method for Solving Elliptic Boundary-Value Problems

A. Saitoh, T. Takayama, A. Kamitani and H. Nakamura^a

Yamagata University, 4-3-16, Jōnan, Yonezawa, Yamagata 992-8510, Japan

^aNational Institute for Fusion Science, 322-6 Oroshi-cho, Toki, Gifu 509-5292, Japan

saitoh@yz.yamagata-u.ac.jp

Recently, the boundary node method (BNM) [1] which is one of boundary-type meshless methods has been proposed. As the feature of the BNM, a boundary does not need to be divided into a set of elements before executing the BNM code. However, integration cells must be used for calculating matrix elements.

In order to resolve the above demerit, the BNM has been reformulated without using integration cells. Throughout the present study, the method is called the extended BNM (X-BNM) [2]. The results of computations have shown that the accuracy of the X-BNM is much higher than that of the dual reciprocity boundary element method [3, 4].

In spite of a high usefulness of the X-BNM, the calculation speed for obtaining the numerical solution is extremely slow. This is because the coefficient matrix of the resulting linear system becomes non-symmetric and dense. In effect, this means that the X-BNM is difficult to be applied to a large-scale simulation.

The purpose of the present study is to develop the fast numerical code for solving the elliptic boundary value problems on the basis of the X-BNM and to numerically investigate its performance. The numerical results will be shown in the conference.

- [1] Y.X. Mukherjee, S. Mukherjee, *Int. J. Numer. Methods Eng.* **40(6)** (1997) 797.
- [2] A. Saitoh, S. Nakata, S. Tanaka and A. Kamitani, *Information* **12(5)** (2009) 973 [in Japanese].
- [3] A. Saitoh, N. Matsui, T. Itoh, A. Kamitani, *IEEE Trans. Magn.* **47(5)** (2011) 1222.
- [4] A. Saitoh, K. Miyashita, T. Itoh, A. Kamitani, T. Isokawa, N. Kamiura, N. Matsui, *IEEE Trans. Magn.* **49(5)** (2013) 1601.

Stability analysis on node arrangement in Meshless Time-Domain Method

Y. Ohi and S. Ikuno^a

RIKEN Advanced Institute for Computational Science, Kobe, Hyogo 650-0047, Japan

^a*School of Computer Science, Tokyo University of Technology, Hachioji, Tokyo 192-0982, Japan*

yoshiharu.ohi@riken.jp

The meshless time-domain method (MTDM) based on the radial point interpolation method is employed for electromagnetic wave propagation simulations [1]. In the MTDM, since meshes of a geometrical structure does not require, nodes of electric and magnetic fields only are scattered in an analysis domain. However, appropriate arrangement of nodes is not clear. In this paper, influence of node arrangement on stability is numerically investigated in order to find appropriate arrangement of nodes.

Four types of node arrangement are proposed, and schematic views of each node distribution are shown in Fig. 1, (a): the standard arrangement based on an orthogonal mesh, (b): nodes for H_x move to positions of nodes for H_y , (c): nodes for H_y move to positions of nodes for H_x , (d): nodes for H_x and H_y move to furthest positions from nodes for E_z . Numerical simulations of electromagnetic wave propagation by using these node arrangement are performed. Contour lines of $E_x = 0$ are shown in Fig. 2. We can see from these results that anisotropy of propagation direction is observed in case of (b) and (c). In addition, since contour lines crowd, solutions includes vibration except case of (a). If nodes of H_x and H_y are located at the same position, a numerical simulation may be unstable. It is indispensable that numerical experiments are performed with various parameters. Details of numerical results will be shown in ITC25.

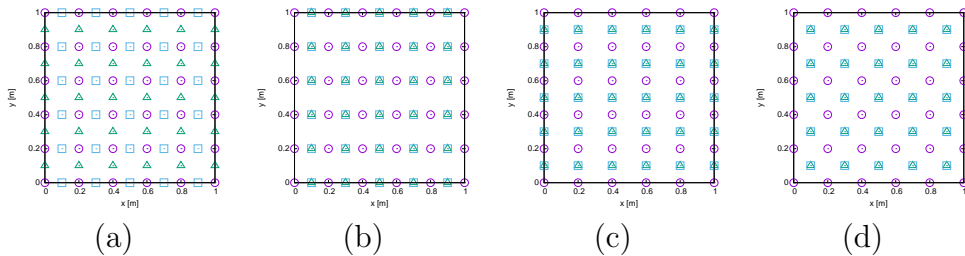


Figure 1: Schematic four types of node arrangements (\circ : E_z , \triangle : H_x , \square : H_y).

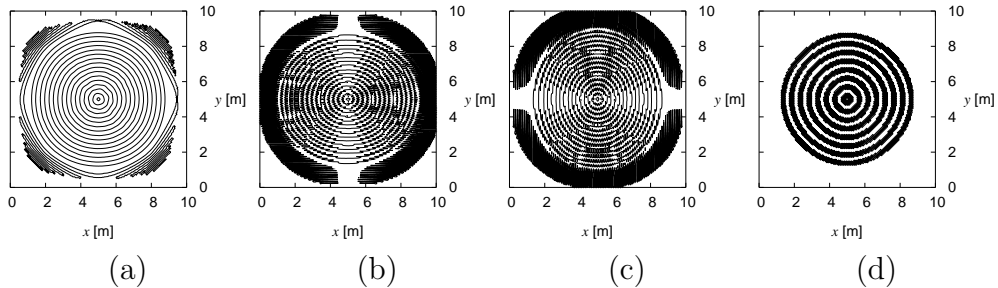


Figure 2: Contour lines of $E_x = 0$.

[1] Y. Ohi, Y. Fujita, T. Itoh, H. Nanamura, S. Ikuno, Plasma Fusion Res., **9:3401144** (2014).

Structure transition in forced magnetohydrodynamic turbulence with uniform background magnetic field

H. Miura, K. Araki^a

National Institute for Fusion Science, 322-6 Oroshi-cho, Toki 509-5292, Japan

^a*Okayama University of Science, 1-1 Ridaicho, Kita-ku, Okayama, Okayama 700-0005, Japan*

Direct numerical simulations (DNS) of forced magnetohydrodynamic (MHD) turbulence with uniform background magnetic field are carried out to elucidate small-scale natures in magnetized MHD turbulence and provide basic information to construct sub-grid-scale (SGS) model for a Large Eddy Simulation (LES). DNSes are carried out for the two cases, (1) with the Hall term and (2) without the Hall term. The Hall term is a part of the two-fluid effect in the generalized Ohm's law in the extended MHD equations, which have been widely used to study instabilities including torus plasmas[1-4]. The Hall term restricts the time step width in a numerical simulation severely and excite high-wave-number coefficients significantly[4]. Consequently, the introduction of the Hall term brings about very small step width and increases a demand for a very high resolution in a simulation. While the former difficulty can be managed by the use of an implicit time-marching technique, the latter remains as a controversial problem. Because of the nonlinearity of the equations, artificial truncation of the short-wave-length components (insufficient grid width) often deteriorates numerical convergence in a simulation. In order to overcome the difficulty, an LES (See [5], for example) can be a reasonable compromise between the correctness of a simulation and a computational cost. Numerical simulations presented here provide basic database to construct numerical models required for LESes.

In our study, DNSes of the magnetized MHD turbulence with the uniform background magnetic field B_0 are carried out. Number of grid points N^3 is 1024^3 . It is shown that the introduction of the Hall term brings about an essential change in the small-scales of turbulent field. While an intense vorticity region is sheet-like (so-called vortex-sheets) in MHD turbulence, it is tubular in Hall-MHD turbulence, showing that the dominant fluid motion is changed from the shearing motions to the swirling motions associated with the introduction of the Hall term. While the transition of the vortex structure has been reported in Refs.[3,4], we find that some of current sheets at large scales also become tubular due to the Hall effect. Mechanism of the structure transitions are discussed. We will also estimate the applicability of the Smagorinsky-type SGS model proposed in Ref.[6] and discuss further development of the model to a torus plasma instability.

- [1] W. Park et al., Phys. Plasmas **6** (1999) 1796.
- [2] C.R. Sovinec et al., J. Comput. Phys. **195** (2004) 355.
- [3] H. Miura, R. Goto, et al., 25th IAEA FEC, TH/P5-17 (Oct. 13-18 2014, St. Petersburg, Russia).
- [4] R. Goto, H. Miura et al., Phys. Plasmas **22** (2015) 032115.
- [5] F. Hamba and M. Tsuchiya, Phys. Plasmas **17** (2010) 012301. [6] H. Miura and K. Araki, Phys. Plasmas **21** (2014) 072313.

Extension of integrated transport analysis suite, TASK3D-a, to be capable for analysis of fast ion particles and plasma flows in LHD

M. Sato, R. Seki, M. Yokoyama, M. Osakabe,
Numerical Simulation Reactor Research Project, and LHD Experiment Group

National Institute for Fusion Science, 322-6 Oroshi-cho, Toki 509-5292, Japan

The integrated transport analysis suite, TASK3D-a has been developed and applied mainly to NBI-heated LHD plasmas [1]. Recently, extension has been conducted such as including ECH ray-tracing codes and the module for creating ascii files to be registered on to the International Stellarator-Heliotron Confinement Database [2]. In this paper, further extension of the TASK3D-a to make possible the analyses of fast ion particles and plasma flows in LHD is described. For analysis of the fast ion particles, FIFPC code [3], which solves Fokker-Planck equation, has been linked to VMEC, NEWBOZ, HFREYA and MCNBI codes (see eg., [4]) as shown in Fig.1(a). This calculation flow can evaluate the time evolution of the distribution function of the fast ion particles in velocity space (v, θ) for NBI-heated plasmas as shown in Fig.2, where θ is the angle between the velocity vector and the magnetic field line. For analysis of plasma flows, DKES [5] and PENTA [6] codes have been integrated to TASK3D-a as shown in Fig.1(b). From this calculation flow, the neoclassical plasma flows on flux surfaces can be evaluated in addition to such as the neoclassical radial diffusion and neoclassical ambipolar electric field. The application examples for LHD plasmas with this further extended TASK3D-a will also be reported in the conference.

Extensive cooperation by Dr. D. A. Spong (Oak Ridge National Laboratory) for providing PENTA and assisting its implementation into TASK3D-a has been highly acknowledged.

- [1] M. Yokoyama et al., Plasma and Fusion Research, **9** (2014) 3402017.
 [2] M. Yokoyama et al., to be presented at the 20th International Stellarator-Heliotron Workshop (Greifswald, Germany, 5-9 October 2015).
 [3] R. H. Fowler et al., Comput. Phys. Comm. **13** (1973) 323.
 [4] M. Yokoyama for task3d users and developers, NIFS-MEMO-61 (Nov.2012).
 [5] W. I. Van Rij and S. P. Hirshman, Phys. Fluids **B1** (1989) 563.
 [6] D. A. Spong, Phys. Plasmas **12** (2005) 056114.

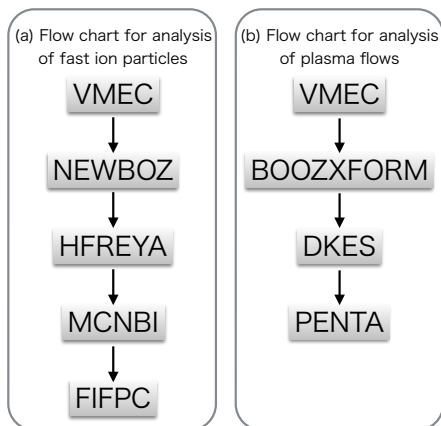


Fig.1. Flow chart for analysis of (a) fast ion particles and (b) plasma flows.

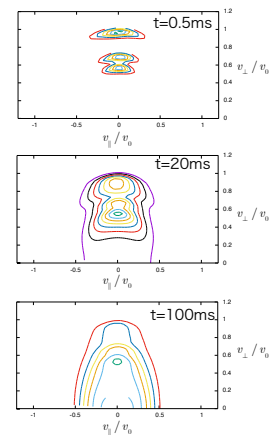


Fig.2. Time evolution of a distribution function of fast ion particles for a test simulation obtained by FIFPC code.

Validation of Tungsten Transport Model in JT-60U Plasmas

Y.Shimizu^a, T.Fujita^a, A.Okamoto^a, H.Arimoto^a,
T.Nakano^b, K.Hoshino^c, N.Hayashi^b, M.Honda^b

^aNagoya University, Furo-cho, Chikusa-ku, Nagoya 464-8603, Japan

^bJapan Atomic Energy Agency, 801-1, Mukoyama, Naka 311-0193, Japan

^cJapan Atomic Energy Agency, 2-166, Omotedate, Obuchi, Rokkasho 039-3212, Japan

shimizu-yuusuke14@ees.nagoya-u.ac.jp

Tungsten (W) is planned to be used as plasma-facing material in ITER divertor, but accumulation of tungsten in the core plasma is concerned because of its large radiation loss due to its high atomic number (high Z). In JT-60U H-mode plasma, tungsten accumulation was observed to be enhanced as the toroidal rotation opposite to the plasma current (CTR rotation) increased [1]. This phenomenon cannot be explained by the conventional neoclassical transport. From theoretical considerations, three effects related to the toroidal rotation (i.e., PHZ pinch, Er pinch, and centrifugal force) are proposed. Hoshino et al. have proposed PHZ pinch and Er pinch [2]. The PHZ pinch is caused by changes in the ion charge state along its drift orbit. The Er pinch is caused by the effect of the radial electric field through Coulomb collisions. The centrifugal force makes poloidal asymmetry in heavy impurity ion density, which effects the neoclassical transport. In this study, we introduce these three pinch models into transport code TOTAL [3] and study dependence of the tungsten accumulation on the toroidal rotation. We simulate the experimental data of the 5 cases in JT-60U H-mode plasmas [1].

The tungsten transport is solved with the following fluxes

$$\Gamma_k = \Gamma_k^{NC} - D_k^{AN} \partial n_k / \partial \rho + V_k^{\text{pinch}} n_k, \quad \Gamma_k^{NC} = -D_k^{NC} \partial n_k / \partial \rho + V_k^{NC} n_k \quad (1)$$

where Γ_k is particle flux of impurities in the charge state k, n_k is density of impurities in the charge state k. The subscript NC and AN represent neoclassical and anomalous transports, respectively. PHZ pinch and Er pinch models are introduced in the V_k^{pinch} term. Centrifugal force effects are introduced in the D_k^{NC} and the V_k^{NC} terms. The tungsten accumulation c_w ($c_w = (n_w/n_e)$) is evaluated when the steady state is reached in the simulation.

In previous research [4], we introduced the PHZ pinch and the Er pinch, but investigated the effect of the PHZ pinch only because the Er pinch model equation was not valid in the experimental conditions. By introducing the PHZ pinch, the larger accumulation observed experimentally at higher toroidal rotation was reproduced in the simulation. However, the dependence on toroidal rotation was weaker in the simulations than in the experiments. In this study, we develop a new Er pinch model equation that is valid in the experimental conditions, and also newly introduce the centrifugal force model ([5] for instance). By combining the three effects (PHZ pinch, Er pinch and centrifugal force), we will study if the dependence of the tungsten accumulation on the toroidal rotation observed in the experiments is quantitatively reproduced in the simulation.

[1] T. Nakano, J. Nucl. Mater. **415**, S327-S333 (2011)

[2] K. Hoshino, et al., Nucl. Fusion **51**, 083027 (2011)

[3] K. Yamazaki and T. Amano, Nucl. Fusion **32**, 633 (1992)

[4] Y. Shimizu, et al., Plasma and Fusion Res. **10**, 3403062 (2015)

[5] K.G. McClements, and R. J. McKay, Plasma Phys. Control. Fusion **51**, 115009 (2009)

Study of Plasma Coherent Structure Transport Dynamics with Particle-in-Cell Simulation

Hiroki Hasegawa^{a,b} and Seiji Ishiguro^{a,b}

^a*National Institute for Fusion Science, 322-6 Oroshi-cho, Toki 509-5292 Japan*

^b*Department of Fusion Science, SOKENDAI, 322-6 Oroshi-cho, Toki 509-5292 Japan*

hasegawa.hiroki@nifs.ac.jp

Recent experiments of magnetic confinement fusion devices have shown the evidence of non-diffusive radial transport in the scrape-off layer (SOL) by intermittent filamentary plasma coherent structures along the magnetic field line (such structures are called “plasma blob”). Motivated by the experiments, many theoretical and computational studies about the blob dynamics have been made [1, 2]. However, most of those studies are based on two-dimensional reduced fluid models and such kinds of macroscopic models treat kinetic effects (e.g. sheath formation between plasma and divertor plates, velocity difference between ions and electrons, etc.) as some adjustable parameters under some empirical assumptions. Thus, we have investigated kinetic dynamics on blob transport with a three dimensional electrostatic plasma particle simulation [3, 4]. In our previous study, we studied kinetic effects on plasma blob dynamics in the system where the periodic boundary condition is applied in the direction parallel to the magnetic field line and found that the symmetry breaking in a blob profile occurs by the kinetic effect [5]. In this study, we have applied the particle absorbing boundaries to the ends in the direction parallel to the magnetic field line and studied such kinetic effects with the plasma sheath. In the simulation, not only the symmetry breaking shown in the previous study but also other properties which were not found in the periodic boundary case have been observed. Furthermore, we will report results of simulation of the “hole” (which is a filamentary structure with lower density than that of surrounding plasma) propagation.

[1] S. I. Krasheninnikov, D. A. D’Ippolito, and J. R. Myra, *J. Plasma Phys.* **74** (2008) 679 and references therein.

[2] D. A. D’Ippolito, J. R. Myra, and S. J. Zweben, *Phys. Plasmas* **18** (2011) 060501 and references therein.

[3] S. Ishiguro and H. Hasegawa, *J. Plasma Phys.* **72** (2006) 1233.

[4] H. Hasegawa and S. Ishiguro, *Plasma Fusion Res.* **7** (2012) 2401060.

[5] H. Hasegawa and S. Ishiguro, 23rd International Toki Conference (2013) P1-28.

Intuitive interface for visualizing numerical data using gesture recognition

Y. Tamura , H. Nakamura^a and S. Fujiwara^b

Konan University, Kobe 658-8501, Japan

^a*National Institute for Fusion Science, 322-6 Oroshi-cho, Toki 509-5292, Japan*

^b*Kyoto Institute of Technology, Kyoto, 616-8354, Japan*

Our purpose of this study is to propose an intuitive and natural interface for visualizing numerical data, for example, numerical simulation result and experimental result. Scientific visualization is indispensable technique for recognizing complex numerical data. In nuclear fusion research, large scale visualization systems using virtual reality technology have been used [1], and developed visualization interface [2].

On the other hand, an inexpensive virtual reality system, for example, head mounted display (HMD) widely comes to be used to watch 3-dimensional scene. The HMD is useful for scientific visualization in that the user can look around the scene in 360 degrees and other users don't disturb scene; however the user cannot see his/her own hand. Therefore, we introduce an intuitive gesture recognition system to a visualization system. Automatic extraction of human intuitive movement from natural behavior is difficult task and it is difficult to detect gesture correctly. We introduced singular spectrum transformation for extracting gesture [3]. This method has disadvantage in that computational speed is slow, but can stably detect human behavior. At first, a key frame from time series of human behavior is extracted using singular spectrum transformation method. After that, the recognition engine specifies which part of the body moves intentionally. Finally, a function assigned to a gesture is executed. By using this system, the user can naturally control numerical data in 3-dimensional scene.

[1] A. Kageyama, Y. Tamura and T. Sato, Trans. Virtual Reality Societ of Japan **4**, 4 (1999)

[2] A. Kageyama, Y. Tamura and T. Sato, Progress of Theoretical Physics Supplement **138** (2000)

[3] J. B. Elsner and A. A. Tsonis, Plenum Press (1996)

Applications of the virtual-reality technology to Plasma Physics and Fusion Plasmas

H. Ohtani^{a,b} and S. Ishiguro^{a,b}

^a*National Institute for Fusion Science, 322-6 Oroshi-cho, Toki 509-5292, Japan*

^b*The Graduate University for Advanced Studies, 322-6 Oroshi-cho, Toki 509-5292, Japan*

In 1997, the National Institute for Fusion Science (NIFS), Japan, installed the CompleXcope virtual-reality (VR) System based on CAVE system [1] as an instrument for scientifically analyzing simulation results. We report the recent two developments in visualization researches at NIFS in this paper.

We have developed the visualization system which displayed in the VR world the three-dimensional trajectories of dust particles observed by the stereoscopic fast framing cameras in Large Helical Device (LHD). The trajectories, equilibrium plasma simulation data and device data were displayed integrally in the one VR space [2]. Their three-dimensional relative positions can be investigated. This system will promote viewer's understanding.

It is important to consider how to assemble and remove parts in the reactor design. Especially it is difficult to remove the part through the small hole with rotating it, since the information of depth is lost. However, by using the VR system, a viewer can watch and move the parts three-dimensionally. We constructed the system which displayed CAD data by the desktop-VR system (Fig.1, right figure). By using this system, the viewer can grasp and move the parts, and can perform collision detection when assembling.

VR technology is powerful equipment for analyzing simulation and experimental data, and designing the reactor. We believe that the buildup in this paper will boost up the research of the plasma physics and fusion plasmas.

This work is supported by the NIFS Collaboration Research program (NIFS15KNTS037) and the NIFS/NINS under the project of Formation of International Scientific Base and Network. The authors thank Prof. Ohno, Prof. Kageyama and Prof. Tamura for useful discussions. The HINT2 data, the dust data and CAD data were provided by Dr. Suzuki, Dr. Shoji and Dr. Tamura of NIFS, respectively.

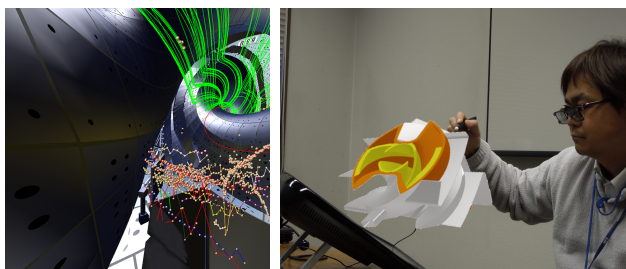


Figure 1: Left: Integrated VR visualization of dust trajectory data, equilibrium plasma simulation result and the inner surface of the LHD vacuum vessel. Right: The viewer using the desktop-VR system. This picture is a composite photograph and only the viewer can watch the CAD data in the VR world.

[1] C. Cruz-Neira, et al. ACM SIGGRAPH 93 (1993) 135

[2] H. Miyachi, et al. IEEE Comp. Soc., (2005) 530

Direct observation of electron heating by electron Landau damping of Alfvén ion cyclotron waves with Thomson scattering system in the tandem mirror GAMMA 10/PDX

M. Yoshikawa, R. Ikezoe, K. Ohta, X. Wang, J. Kohagura, Y. Shima, M. Chikatsu, K. Ichimura, M. Sakamoto, M. Ichimura, T. Imai, R. Minami, and Y. Nakashima

Plasma Research Center, University of Tsukuba, Tsukuba, Ibaraki 305-8577, Japan

In GAMMA 10/PDX tandem mirror, the ion cyclotron range of frequency (ICRF) waves have been used for plasma production, heating and sustaining MHD stability. Maximum ion temperature has reached 10 keV and the temperature anisotropy (which is defined as the temperature ratio of perpendicular, T_{\perp} , to parallel, T_{\parallel} , to the magnetic field line) becomes more than 10. In such a strong temperature anisotropy condition, a slow Alfvén ion cyclotron (AIC) wave was spontaneously excited in the central cell of GAMMA 10/PDX. When the power of heating ICRF is increased, the diamagnetism increases and the anisotropy becomes strong. In the experiments, saturation of the diamagnetism is sometimes observed. The excitation of the AIC modes, which can scatter the hot ions confined in the magnetic mirror field into loss cone of the velocity space in the central cell, is one of the possible mechanisms of confinement degradation. On the other hand, the parametric decay of the heating ICRF waves is discussed for the saturation mechanism of the diamagnetism. Low-frequency (LF) magnetic fluctuations with beat frequencies between the heating ICRF waves and discrete peaks of the AIC modes are clearly detected in GAMMA 10/PDX. The AIC modes have several discrete peaks in the frequency spectrum just below the ion cyclotron frequency. There is no resonance with ions, and resonant interaction with electrons can be extracted. The electron acceleration by using waves of ICRF caused by the electron Landau damping. We directly detect the accelerated electrons at a machine end by making use of the open field configuration of GAMMA 10/PDX and examining the effects of the AIC mode on electrons. The AIC mode is normally observed with reflectometers and magnetic probes. The AIC mode makes an electron temperature heating, and end loss electron flux and temperature increases, which is measured by the loss electron energy analyzer (LEE).

In this presentation, the direct observation of electron heating by the interaction of AIC wave is reported. The electron temperatures were directly measured by using a Thomson scattering system with changing the laser injection time every 10 ms shot-by-shot. In the former study, the electron temperatures were estimated indirectly by using LEE signals. The electron temperature increase along with the increase of diamagnetism. However, the peak electron temperature reached faster than that of diamagnetism. At that time of the electron temperature peak, the AIC wave spontaneously occurred and scattered the electrons to the parallel directions. From the analysis of the transient feature of the electron temperature, electron Landau damping is attributed to this interaction.

New Proposal on Development of Machine Protection Function in Conventional Control System Using Information Technologies

T. Yamamoto, E. Yatsuka, T. Hatae, K. Ota^a, Y. Hashimoto^a, K. Nakamura^a,
T. Sugie, M. Takeuchi, S. Kitazawa, H. Ogawa, Y. Kawano, K. Itami

Japan Atomic Energy Agency, 801-1, Mukouyama, Naka-shi, Ibaraki 311-0193, Japan

^a *Japan Expert Clone Corp., 2-8-6, Shinjuku, Shinjuku-ku, Tokyo 160-0022, Japan*

Machine protection is an important function to ensure high reliability and safe operation in a large experimental facility [1]. ITER edge Thomson scattering system (ETS) is being developed in Japan. ETS measures electron density and temperature profiles using high energy laser more than 5 J [2]. Therefore, ETS has to contain interlock system to protect optical components from damage caused by laser malfunctions. As same as interlock system, conventional control also should sustain components good conditions. We proposed new method that templates for program codes of conventional control were generated from interlock logics using information technologies such as semantic web technique. Information of plant system described in digital data allows plant characteristic data to generate other information by transformation and inference.

The software library EPICS (experimental physics and industrial control system) [3] is recommended to develop instrumentation and control systems in ITER project. Input / output controller (IOC) of EPICS manages signal values and provides programming interface to signals. We proposed a template generator from interlock logics to IOC source codes (that is database file). The generator describes program codes, which inhibit or permit output to signal, automatically. This template avoids missing actions for machine protection in the conventional control.

In addition, we applied the plant description data to risk analysis. HAZOP (hazard and operability study) is a useful method to indentify hazards and problems in a system [4]. In HAZOP, guide words are used for investigating risks. To describe plant functionalities and behaviors using ontology for functional knowledge [5], list of possible risks are extracted from the description by applying substitution and/or inference rules.

The views and opinions expressed herein do not necessarily reflect those of the ITER Organization.

- [1] G. Raupp, et al., "Real-time exception handling – Use cases and response requirements", *Fusion Engineering and Design* **87** (2012) 1891-1894.
- [2] E. Yatsuka, et al., "Progresses in development of the ITER edge Thomson scattering system", *Journal of Instrumentation* **8** (2013) C12001.
- [3] EPICS: <http://www.aps.anl.gov/epics/>.
- [4] T. Kletz, "Hazop & Hazan: Identifying and Assessing Process Industry Hazards" 4th edition, Philadelphia, Taylor & Francis (1999).
- [5] Y. Kitamura, et al., "A Framework for Systematization of Functional Knowledge based on Ontological Engineering", *Transactions of the Japanese Society for Artificial Intelligence* **17** (2002) 61-72.

Studies of AM He Atomic Magnetometer for Application in Fusion Plasmas

H. Kiyonaga, Y. Yamada, T. Fukuda

Graduated School of Engineering, Osaka Univ., A1-214, 2-1Yamadaoka, Suita 565-0871, Japan

1. Introduction

The detailed measurement of magnetic field is above all fundamental in fusion research, and various approaches, as represented by the Faraday rotation and motional stark spectroscopy techniques, have hitherto been extensively developed.

An atomic magnetometer [1] allows spatially resolved magnetic field measurements and He atom suggested as a probing target in this work is produced as a result of the D-T fusion reaction. Neither heating beam nor impurity species are necessary. This study aims at investigating the proposed AM-AOM i.e. amplitude modulated atomic magnetometer.

2. Design of Amplitude Modulated He atomic magnetometer

Fig.1 shows a schematic of the AM-AOM system. The pump and probe beams of which wavelength is 1083nm (He D1 line), are injected into a He discharge cell. The former is amplitude modulated at frequency f_{pump} and circularly polarized for the spin-polarization of the He atom, whilst the latter is only circularly polarized. When f_{pump} equals the Larmor frequency $f_L(=\gamma B)$, the resonant property is detected in the transmission rate, and magnitude of the magnetic field at the cell is evaluated. Here, γ is the gyromagnetic ratio; 28[GHz/T] for He.

3. Development of the light source

In order to produce the 1083nm emission efficiently, a hollow-cathode type He discharge lamp shown in Fig.2 has been manufactured in the lab. The power supply of the discharge lamp has also been designed and built. This power supply can produce high frequency AC voltage with DC voltage offset which is enough high to discharge the lamp. The frequency range of this power supply includes the aimed frequency 1.4[MHz]. This frequency is equivalent to the geomagnetic field (50[μ T]) measurement, anticipated in the rudimentary experiment. The AM He D1 emission was thereby successfully obtained.

4. Status of the experiment

With the developed light source, we have performed an exploratory experiment of geomagnetic field measurement. The magnetic field measured by a Gaussmeter (475DSP) was about 30-60[μ T]. Fig.3 shows the transmitted light intensity and the transmission rate between 0.6-1.6 [MHz]. The transmission rate seems to have its peak around 0.85 [MHz] which corresponds to 30.4[μ T]. Accordingly, it is deduced that the result of preliminary experiment indicates the possible sign of magnetic field. However, quality of the measurement has yet to be improved. We believe that (1) elimination of stray magnetic field produced by the surrounding electronics and (2) calibration of the source power would increase the signal integrity.

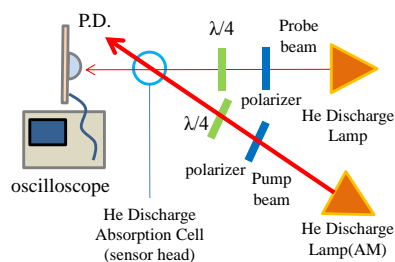


Fig.1 Schematic of AM-AOM.

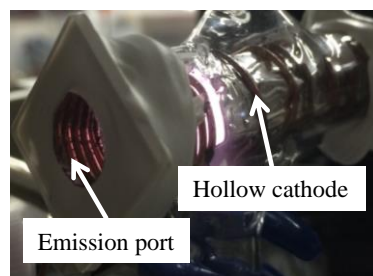


Fig.2 He discharged lamp.

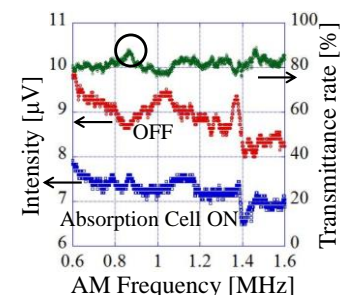


Fig.3 Transmitted light property.

[1] W.E.Bell and H.L.Bloom, *Phy.Rev.Lett.*6, 280.

P2-74 Digital Signal Processing on FPGA for Plasma Diagnostics

Rachana Rajpal, Hitesh Mandaliya, Pramila Gautam

Institute for Plasma Research, Gandhinagar, Gujarat- 382428

rachana@ipr.res.in

Abstract

The overall goal of this experiment is to establish a technology for real time processing of the signals coming from various sensors via signal conditioning electronics. One such requirement is for interferometer diagnostics of Aditya and SST-1 Tokamak. The two signals (Reference and Probe) are phase shifted to each other and for feedback application the phase shift between these two needs to be measured in real time. The existing system of the interferometer system provides two analog signals in form of sin and cosine trigonometry functions (IQ modulated). One of the method to calculate phase difference is to find inverse of tan of these two signals. No Von Neumann Architecture processor provides the trigonometry functions in hardware. Some high-end 32 bit processors provide these function but they use ANSI-C library to perform calculations in software defined manner, which can not assure real time performance. For feedback application real time response must be deterministic. FPGA can solve this problem by using CORDIC algorithm. The IP (Intellectual Property VHDL Code) is used to find arc tan of these two signals. The hardware is design which mainly consists of ADC, DAC, FPGA and single board computer.

The two signals from I and Q interferometer diagnostic is first digitized through high speed pipeline ADC and then processed in FPGA for implementation of algorithm. The processed phase data is fed to DAC in real time as well as acquired by host PC. The output of DAC can be used for real time control. All the commands required by FPGA is issued through PC 104 bus of onboard single board computer. The control signals for interfacing various components are generated by FPGA. Ethernet is used as communication medium between host PC and board.

The paper will high light the details of CORDIC algorithm in FPGA, hardware architecture, results of real time response and software architecture of system.

Progress of KSTAR Thomson Scattering Diagnostic System in 2015

J.H. Lee^a, S.H. Lee^a, W.R. Lee^a, K.P.Kim^a, I.Yamada^b, K. Narihara^b

^a*National Fusion Research Institute (NFRI), Korea*

^b*National Institute for Fusion Science (NIFS), Japan*

jhlee@nfri.re.kr

In KSTAR tokamak, Nd:YAG Thomson scattering diagnostic system was installed five years ago. Until last year, KSTAR Thomson scattering system used proto-type ITER edge Thomson YAG laser system by rent from JAEA, but proto-type ITER laser was returned to JAEA in this year. For this reason, a commercial Nd:YAG laser system newly setup for the KSTAR Thomson system. This laser's specification was specially ordered to the Continuum Laser Co., that was 2.5J, 20Hz. In this year, to suppress the stray light and electrical noise, we installed a long baffle and UPS (Uninterruptible Power Supply: battery) system. The length of long baffle is ~505mm, and inside of the baffle 25 carbon rings were installed. In case of UPS, an electric power switched to the UPS before the plasma shot then all of DAQ system was operated under the UPS system. The electric power supply switch returned to the normal position when plasma was turned off. In case of upgrade of optical fiber bundle, three optical fiber bundles were increased at core Thomson thus we have 12 for core and 15 for edge in 2015. To measure the electron temperature and density, we calibrated Thomson system by using Rayleigh calibration and relative calibration by tungsten lamp. During the Rayleigh calibration experiment, we could measure the Raman signal also. For the alignment, we used the vertical alignment system in the optical fiber block both core and edge.

This year is transition point for the KSTAR Thomson scattering system because of the great changes of the laser system and electric power system. In my poster, I will present the change of Thomson system moreover we will compare the data with other diagnostic system in KSTAR.

P2-76

withdrawal

Behavior of non-thermal electrons during ECR pre-ionization at Aditya tokamak

S. Purohit, Y. S. Joisa, J. V. Raval, M. B. Chowdhuri, J. Ghosh, B. K. Shukla, R. Manchanda, N. Ramaiya, R. Tanna, K.A Jadeja, S.B Bhatt, C. N. Gupta, A. Kumar and Aditya team

Institute for Plasma Research, Bhat, Gandhinagar, 382 428, India

E-mail: pshishir@ipr.res.in

The non-thermal electrons (NTE) in tokamak plasma have a strong effect over the plasma properties and on the plasma facing components. This establishes an importance of NTE to be studied in both flux and energy space. The NTE were studied for Aditya tokamak, by Silicon Drift Detector (SDD) based X-ray spectroscopic diagnostic for the ECR pre-ionization experiments. The calibrated spectrometer, which is having energy resolution of 134 eV at 5.89 keV, is mounted on the radial mid plane of Aditya tokamak with a 15 μm thickness beryllium window. The X-ray spectra were acquired in energy range of 1.5 keV – 26.0 keV. The spectra for ECR pre-ionization shows X-ray line radiation band on top of the bremsstrahlung. It is primarily the combination of multiple characteristics lines existed between 5 keV to 7 keV and mostly associated with multiple ionized states of iron, tokamak wall material. This is likely due to the interaction between the non-thermal electrons, generated from ECR, with the stainless steel vessel wall of the Aditya Tokamak. The behaviour of NTE was studied as a function of vertical field and pre-filled pressure. With the increasing vertical field the interaction weakens which is most likely due to the reduction of particle drift at higher vertical field. It was also found that the X-ray line radiation strength reduces dramatically with higher pre-filled pressure at fixed vertical field. This indicates the reduction of NTE with increasing pre-filled pressure.

Fast ion loss associated with RMP in KSTAR

Jun Young Kim^a, Junghee Kim^{a,b}, T. N. Rhee^b, Won-Ha Ko^{a,b},
S. W. Yoon^b, Y. M. Jeon^b, and M. Isobe^c

^a*Korea University of Science and Technology, Daejeon, Korea*

^b*National Fusion Research Institute, Daejeon, Korea*

^c*National Institute for Fusion Science, Toki-shi, Japan*

Recent numerical simulations and experimental results have shown that the beam-ion loss in the presence of non-axisymmetric magnetic perturbation (or resonant magnetic perturbation), aiming at mitigation or suppression of the ELMs, is enhanced at the toroidally localized positions [1-5] depending on the configuration of the perturbation field.

Fast ion losses measured through 2011 to 2014 KSTAR campaigns with the application of the RMP have shown the enhanced or suppressed signals exhibited on the FILD (fast-ion loss detector). It implies that fast ion loss during RMP is non-axisymmetric and sensitive to the radial perturbation direction. In addition, fast ion loss level is elevated at least one order of magnitude higher than that in case of conventional L-mode plasma when the RMP-induced mode-locking, which shows a big drop of toroidal rotation level, is occurred. Recent study shows the screening effect on the magnetically perturbed plasmas by the toroidal plasma rotations. [6]. In this sense, it is necessary to investigate the influence of the toroidal rotation velocity on the fast ion loss level during RMP application in order to understand the relation between the toroidal rotation screening the perturbation field and the local fast-ion loss intensity. Electron heating [7] is used to change plasma rotation speed during n=2 RMP (middle-coil only). As a result, both in L- and H-modes, toroidal rotation dependency on the fast-ion loss is observed clearly. As rotation level increases, fast-ion loss decreases. In cases of low rotation or locking-plasmas, fast-ion loss level is enhanced significantly.

Additional fast ion loss detectors at I-port (FILD-2, scintillator type, fixed) and D-port (FILD-3, Faraday-cup, radially movable) are ready to observe the asymmetric and localized loss according to various RMP spectra during 2015 KSTAR experimental campaign.

- [1] K. Tani et al., Nucl.Fusion **52**, 013012 (2012).
- [2] K. Shinohara et al., Nucl. Fusion **52**, 094008 (2012).
- [3] J. Kim et al., Rev. Sci. Instrum. **83**, 10D305 (2012).
- [4] M. Garcia-Munoz et al., Nucl. Fusion **53**, 123008 (2013).
- [5] J.-Y. Kim et al., 41st EPS Conference on Plasma Physics. P4.067.
- [6] Y. Q. Liu et al., Plasma Phys. Control. Fusion **54** (2012) 124013
- [7] Y.J. Shi et al., Nucl. Fusion **53** (2013) 113031

The temperature calibration for IR camera of the IRVB system including periscope system for KSTAR

Dongcheol Seo^{a,b} and B. J. Peterson^c

^a National Fusion Research Institute, 169-148 Gwahak-ro, Daejeon 34133, Korea

^b University of Science and Technology (UST), Daejeon, Korea

^c National Institute for Fusion Science, 322-6 Oroshi-cho, Toki 509-5292, Japan

An infrared imaging video bolometer (IRVB)[1] provides a 2-dimensional measurement of the total radiation power loss from the plasma. The IRVBs have installed in the Korea Superconducting Tokamak Advanced Research (KSTAR)[2,3] and LHD and JT60-U. The IRVB diagnostic consists of periscope optics, Phoenix IR camera (Indigo) and a platinum (Pt) foil for KSTAR. For accurate measurement, temperature calibration technique of the IR camera has been developed. This new temperature calibration technique was applied to IR camera of IRVB which is installed on KSTAR. In this conference, it will show the details of the new temperature calibration method and results of the measurement on KSTAR.

[1] B.J. Peterson, *et al.*, Rev. Sci. Instrum., **70** (2000) 3696

[2] M. Kwon, *et al.*, Nucl. Fusion **51** (2011) 094006

[3] G. S. Lee, *et al.*, Nucl. Fusion **41** (2001) 1515

The effect of thermal history on microstructure of Er₂O₃ coating layer prepared by MOCVD process

Masaki Tanaka¹, Takayuki Shinkawa¹, Yoshimitsu Hishinuma²,
Teruya Tanaka², Takeo Muroga², Susumu Ikeno³, Kenji Matsuda⁴
and Seungwon Lee⁴

¹ Graduate School of Science and Engineering for Education, University of Toyama,

² National Institute for Fusion Science

³ Hokuriku Polytechnic College

⁴ Graduate School of Science and Engineering for Research, University of Toyama

E-mail: ikenolab@eng.u-toyama.ac.jp

Erbium oxide (Er₂O₃) was shown to be a high potential candidate for tritium permeation barrier and electrical insulator coating for advanced breeding blanket systems with liquid metal or molten-salt types. Recently, Hishinuma *et al.* succeeded to form homogeneous Er₂O₃ coating layer on large interior surface area of metal pipe using Metal Organic Chemical Vapor Deposition (MOCVD) process. In this work, evaluating the influence of thermal history on microstructure of Er₂O₃ coating layer on stainless steel 316 (SUS 316) substrate via MOCVD process was investigated using SEM and TEM observation and XRD analysis. The selected-area electron diffraction (SAED) diffraction pattern and the ring-shaped diffraction pattern of Er₂O₃ coating are obtained to each SUS substrates, so it revealed that homogeneous Er₂O₃ coating had been formed easily on SUS substrate from these diffraction patterns.

The typical SEM images of the surface area on the Er₂O₃ coating before and after thermal cycling up to 700°C in Ar atmosphere. We confirmed that the columnar-like Er₂O₃ grains were changed to granular structure by thermal history. the columnar-like Er₂O₃ grains were promoted to change to granular structure by thermal history. From the cross-sectional image of TEM observations, furthermore, the formation of interlayer between Er₂O₃ coating and SUS substrate was also confirmed. In this study, comparisons of microstructure on the Er₂O₃ coating layer between with and without thermal history were investigated in detail.

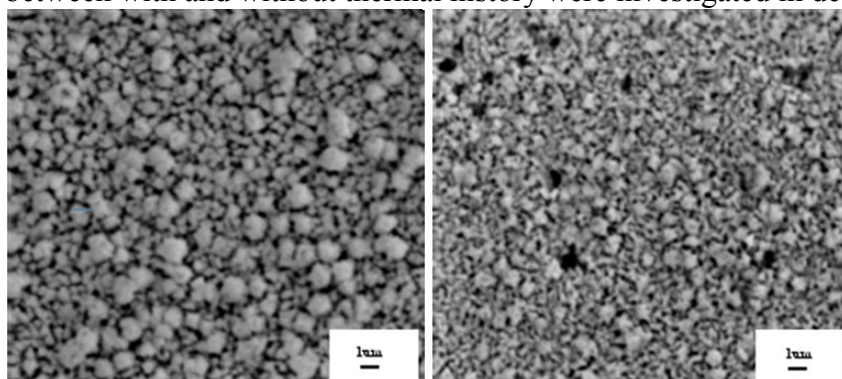


Fig. 1 Typical SEM images of the surface area on the Er₂O₃ coating before and after thermal cycling up to 700°C in Ar atmosphere.

1) Y. Hishinuma, T. Tanaka, T. Tanaka, T. Nagasaka, Y. Tasaki, A. Sagara, T. Muroga: Fusion Eng. Des., 86, (2011), 2530-2533.

Development of the In-vessel Components of ITER Microfission Chamber System for Fusion Power Measurements in ITER

M. Ishikawa, K. Takeda, K. Itami

Japan Atomic Energy Agency, 801-1, Mukoyama, Naka 311-0193, Japan

A neutron flux monitor is one of the most important systems in ITER because it provides total neutron source strength and fusion power of ITER. The in-vessel neutron flux monitor equipped with Microfission Chambers (MFC) [1] is designed by Japan Domestic Agency. Since the MFC can measure neutrons without attenuation by a thick vacuum vessel (VV), it has advantages for accurate measurements compared with the other ex-vessel flux monitors. On the other hand, in-vessel components of the MFC are exposed to the extreme ITER environment, such as high temperature, high radiation and high electromagnetic (EM) forces. Therefore, the in-vessel components need to withstand such ITER environment. In this study, the in-vessel components of the MFC have been developed in order to apply ITER conditions.

ITER will experience about 500 times of baking of the VV during its lifetime of 20 years. Since the in-vessel components of the MFC cannot be replaced during ITER operation, those components must withstand for a lot of thermal cycles. In order to demonstrate that the in-vessel components of the MFC would be able to sufficiently withstand the ITER environment, the thermal cycle tests which simulate baking of the VV of the ITER were performed. In the thermal cycle tests, severer thermal stresses (+45 °C /h during warm-up, and -35 °C /h during cool-down) than the ITER regulation (+5 °C /h during warm-up, and -7 °C /h during cool-down) were exposed to the in-vessel components. After the thermal cycle tests, soundness of the in-vessel components was investigated through the helium leak test (bombing method), and the measurements of the insulation resistance, the withstand voltage, and the impedance. As a result, it was verified there were no problems in the performance of the in-vessel components as a signal transmission system.

The in-vessel components are further exposed to high radiation condition due to high performance of the D-T plasma. Such high radiation generates negative influence on materials of the in-vessel components, for example, crack of the insulation material of the signal cable due to swelling. In order to apply to the extreme ITER environment, proven tri-axial mineral insulated (MI) cables in several fission reactors have been adopted as in-vessel cables. It was reported that any problem has not been observed in MI cables even if integrated neutron flux to the MI cable exceeded $\sim 10^{22}$ nvt in fission reactors. On the other hand, in the case of ITER, integrated neutron flux to the MI cable has been estimated $\sim 10^{20}$ nvt for ITER life. However, radiation conditions such as neutron spectrum in ITER is much difference from those of fission reactors. Then, in order to show that the MI cable of the MFC system has radiation hardness during the ITER life, neutronic analysis has been conducted. In the neutronic analysis, absorbed dose of the MI cable in ITER was calculated and compared with that in fission reactor. As a results, absorbed dose of the MI cable in the ITER condition was calculated 4.5×10^{10} Gy. On the other hand, that in fission reactors has been evaluated $> 10^{11}$ Gy if integrated neutron flux is $\sim 10^{22}$ nvt. This result indicates that MI cable of the MFC can maintain the radiation hardness for the ITER lifetime.

In this study, it was verified that the in-vessel components of the MFC can be used in the extreme ITER environments for 20 years without any replacements. Detail conditions, methods and results of the test and analysis as well as detail structure of the in-vessel components are described together with other tests and analysis in this paper.

[1] M. Ishikawa et. al., Rev. Sci. Instrum. **79** (2008) 10E507.

Clarification of arcing mechanism on filament-driven high-current arc discharge in Cs-seeded negative ion source

M. Ichikawa, M. Yoshida, A. Kojima, M. Hanada, M. Kashiwagi, K. Watanabe, N. Umeda, H. Tobari, R. Nishikiori, J. Hiratsuka and NB Heating Technology Group.

Japan Atomic Energy Agency, 801-1, Mukoyama, Naka 311-0193, Japan

Reliable long pulse injections of 500keV 10 MW D^0 beam are required on the negative-ion-based neutral beam injector for JT-60SA. For this purpose, a large negative ion source has been developed to achieve negative ion current of 22A for 100s. As a result of R&D efforts, 100 s productions have been achieved with a negative ion current of 15 A. The available current for the 100 s production is limited by arcing in the cesium-seeded filament-driven plasma generator. The arcing that is an abnormal localized discharge damages tungsten filaments during high-power long-pulse arc discharge over 150 kW with cesium seeded. In order to realize the JT-60SA negative ion source, the suppression of the arcing based on physics understandings is one of the critical issues. Therefore, the physical mechanism of the arcing in the negative ion source has been investigated by employing JT-60 negative ion source shown in Fig. 1.

Arcing is supposed to be driven by secondary particles produced by injection of accelerated ions to filaments via plasma sheath. It is expected that the impurities in plasma affect arcing. Therefore, the analysis focusing on relation between arcing rate and amount of impurities was performed. The arcing rate defined by the number of the arcing in one pulse duration was plotted as a function of total operation time in Fig. 2. At first, large intensity of OI emission and high arcing rate were measured. After 1500 s of sufficient conditioning time of arc discharges, the arcing rate was maintained to low level even for the high power arc discharge of > 150 kW. However, after 13000 s from the beginning of the cesium (Cs) injection for the enhancement of the negative ion production, by when Cs of about 5 g was seeded, the arcing rate increased again with Cs amount, although the arc power was kept almost same. This result means amount of Oxygen and Cs correlated to arcing rate.

From these results, it was seemed that one of the possibility of arcing might be the interaction between the filament and the plasma with impurity ions because the arcing increased with amount of the impurities.

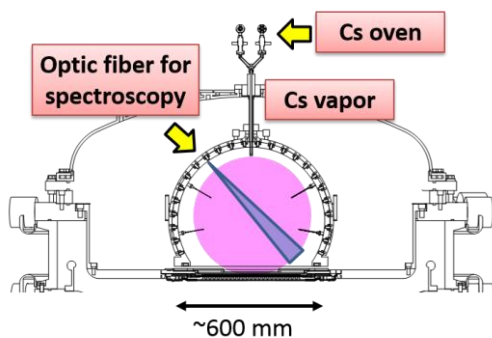


Figure 1: Layout of experimental setup.

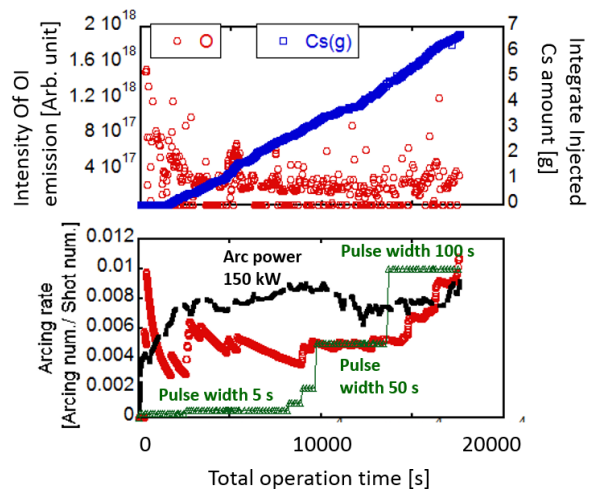


Figure 2: Arcing rate, integral injected amount of Cs and luminescence intensity of oxygen ion in operational time.

Fokker-Planck Simulation for Runaway Electron Generation in ITER Disruptions

H. Nuga, A. Matsuyama^a, M. Yagi^a, A. Fukuyama

Kyoto University, Kyoto-Daigaku-Katsura, Nisikyo-Ward, Kyoto 615-8540, Japan

^a*Japan Atomic Energy Agency, 2-166, Omotedate-Obuchi, Rokkasho 039-3212, Japan*

It is known that the disruptive plasma termination causes severe problems for tokamaks. One of the problems in disruptions is the generation of runaway electrons (REs). The high energy REs may damage the the plasma facing components on impact. Moreover, there is a possibility that the number of REs increases exponentially with plasma current by avalanche effect. Therefore, the RE generation should be suppressed especially in large scale tokamaks. In this reason, the accurate estimation of the number of REs generated in disruptions is required for the the large scale tokamak design and operation scenario developments.

In large scale tokamaks like ITER, the RE generation process seems to be different to that in present tokamaks. Since the thermal quench started from the higher plasma temperature encourages the formation of the hot-tail of the electron velocity distribution because of the low collisionality, the seed REs are easy to generate. The RE multiplication by the avalanche effect becomes remarkable due to the higher plasma current. The impurity gas injection which is proposed for the heat load suppression to ITER disruptions makes the current quench faster. The faster current quench may induce the higher toroidal electric field.

The purpose of this study is the development of the three-dimensional (two-dimension in momentum space and one in radial direction) Fokker-Planck code, TASK/FP[1], for RE generation and the simulation for ITER parameters. Since the non-Maxwell effect like a hot-tail effect will be remarkable in ITER disruptions as noted above, the kinetic simulations are required. Moreover, two-dimensionality in momentum space is required because the information of the pitch angle distribution of REs is important for the RE mitigation operation. In our simulations, the RE generation and the evolution of the electric field are calculated self-consistently.

It will be reported that the RE generation simulation in ITER disruptions, especially the contribution of the hot-tail effect.

[1] H. Nuga, A. Matsuyama, M. Yagi, and A. Fukuyama, Plasma Fusion Res. **10**, 1203006 (2015).

Effect of UHR location on non-inductive formation of overdense spherical tokamak by electron Bernstein wave heating and current drive on LATE

M. Uchida, Y. Nozawa, A. Yoshida, K. Kuroda, H. Tanaka, T. Maekawa

*Graduate School of Energy Science, Kyoto University,
Kitashirakawa Oiwakecho, Sakyo-ku, Kyoto 606-8502, Japan*

Non-inductive startup of spherical tokamak (ST) without the use of central solenoid is a key issue for realizing compact, economical fusion ST devices since there is only a restricted space in the center column of ST [1]. In the Low aspect ratio Torus Experiment (LATE) device, non-inductive formation of ST by electron Bernstein (EB) waves has been explored. It has been shown that EB wave heating and current drive is quite effective for formation of initial closed flux surfaces [2] and rapid plasma current ramp-up [3]. Moreover, recent results shows that an extremely overdense ST plasma can be also started-up with EB wave heating and current drive, where a plasma current reaches ~ 12 kA and a line-averaged density reaches more than seven times the plasma cutoff density [4].

To study and improve the mode conversion rate from incident electromagnetic waves to EB waves in such extremely overdense plasmas, a multi-chord 70 GHz interferometer system with five vertical and two horizontal chords has been developed. In this paper we report the density profiles and their influences on mode conversion to EB waves in such plasmas.

Microwaves at 2.45 GHz from four 20kW magnetrons are used for EB heating and current drive, which are injected from four midplane launchers. When a microwave power of $P_{inj} = 10$ kW is injected under a weak vertical field of $B_v = 20$ G, a plasma current is initiated and increases up to ~ 2 kA, resulting in the formation of closed flux surfaces under the steady external field [2]. The plasma current ramps up with ramps of the microwave power and B_v , and finally reaches $I_p \sim 10.5$ kA. The line-averaged electron density at the final steady phase reaches $n_e = 5.5 \times 10^{17} \text{ m}^{-3}$, which is more than 7 times the plasma cutoff density. In this plasma, midplane density measurements along a tangency radius of $R_t = 35.5$ cm shows that the UHR layer is well inside of the 2nd ECR layer. This indicates that the EB waves are mode-converted at their first propagation band (between the fundamental and 2nd ECR layer), after which the EB waves propagate towards the fundamental ECR layer and heat the bulk electrons as well as current carrying tail electrons.

On the other hand, if we set the ECR layer at a slightly higher field side, the electron density becomes much lower. In this case the density does not increase significantly as the current increases, and the line averaged density at the final steady phase is only one third of the higher density discharge. In this lower density discharge, the UHR layer is estimated to be just outside the 2nd ECR layer. This suggests that a large portion of the incident wave power is mode-converted to EB waves at their 2nd propagation band and they are absorbed before the 2nd ECR layer. This may significantly reduce the power coupled to EB waves at the first propagation band, resulting in decreases in the density and the current at the plasma center.

[1] Y.-K. M. Peng et al, *Proc. 23rd Int. Conf. on Fusion Energy* (Daejeon, Korea, 2010)

[2] T. Yoshinaga et al., *Phys. Rev. Lett.*, 96 (2006) 125005.

[3] M. Uchida et al., *Phys. Rev. Lett.*, 104 (2010) 065001.

[4] M. Uchida et al., *Proc. 24th Int. Conf. on Fusion Energy 2012* (San Diego, USA, 2012)

Inter-strand conductance measurement of ITER TF coil under epoxy impregnation

H.Kudoh, T.Yagai, T.Matsuda, H.Shoji, H.Kajitani^a, T.Obana^b, S.Hamaguchi^b

Sophia University, 7-1, Kioi-cho, Chiyoda-ku, Tokyo, 102-0094, Japan

^a *Japan Atomic Energy Agency, 801-1, Mukoyama, Naka-shi, Ibaraki, 311-0193, Japan*

^b *National Institute for Fusion Science, 322-6 Oroshi-cho, Toki-shi, Gifu, 509-5292, Japan*

The toroidal field (TF) coils for ITER are developed by Japan Atomic Energy Agency (JAEA). TF coils are made of Cable in conduit conductor (CICC). Local current distribution in CICC is unknown and epoxy impregnation is needed in order to fix strands and measure inter-strand conductance in CICC. We decomposed CICC by each bundles and measured inter-strand conductance comparing epoxy impregnated with unimpregnated one. We are also fabricating devices which can specific strand location and measure local contact resistance in liquid helium temperature.

Preliminary thermal analysis for ITER Lower Port #02 Integration Engineering in JADA

T. Maruyama, S. Kitazawa, H. Ogawa, K. Itami

Japan Atomic Energy Agency, 801-1, Mukoyama, Naka 311-0193, Japan

maruyama.toshiyuki@jaea.go.jp

Many diagnostic systems will be installed in the ITER through the diagnostic ports. The diagnostic lower ports will be used to exchange the diverter cassettes and install diagnostic systems. Therefore the diagnostic systems in the lower ports have to be designed to be removed and re-installed. In-vessel components of the lower ports will be mounted on a support structure, so-called a diagnostic rack, to be removed and re-installed with this rack. The diagnostic rack is a critical component in the lower port since the rack will be exposed the harshest environment and has to withstand those environment such as nuclear heating, electromagnetic force and seismic load. The rack should be designed to withstand these environments.

Japan Domestic Agency (JADA) has responsibility to integrate the diagnostic Lower Port #02 (LP#02) engineering, and JADA will also provide the diagnostic rack. The conceptual design of the diagnostic rack is already finished with some issues which still have been left, and then we performed the structural assessments to clear some issues for future work. In our previous work [1], we found that the diagnostic rack needs water cooling to withstand nuclear heating load. Especially the plasma facing front end of the rack which receives the highest heat load needs to be intensively cooled. A fabrication method of the water cooling in the rack is very important for the whole structure and manufacturability.

In this paper, we focused upon a water cooling structure and assessed its fabrication method for the most effective manufacturability of the rack. A drilling fabrication method and a joining pipe method have been expected as realistic fabrication methods, and we assessed the cooling performance of each method by finite element method (FEM) analysis, ANSYS 15.0. We used a simplified analysis model of the front end of the rack. The model is the simple plate structure and has the same size and shape as the rack, and it provides the cooling path by each fabrication method. Environmental conditions which have been estimated in the lower ports were used. The thermal load is in range of 0.1 to 0.2 MW/m³. Obtained results indicate that the drilling fabrication method needed only a simple and short layout of cooling path, on the other hand the joining pipe method needed a longer layout than the drilling because the thermal contact of the joining pipe method is lower (about 15 % of the drilling method). By changing the layout of the joining pipe a little bit, the joining pipe method gives enough cooling performance. In terms of feasibility, the joining pipe method has major advantages because this method is easier to fabricate and it is possible to greatly reduce the welding areas of vacuum boundary which are required the non-destructive inspection in ITER. In conclusion, the joining pipe method is preferred to the diagnostic rack of LP#02.

[1] S. Kitazawa, T. Maruyama, H. Ogawa, K. Itami and N. Casal, Plasma Fusion Res. **10**, 3402044 (2015).

Reduction Rate of MHD potential energy by toroidal plasma current drive at tokamak plasma formation with stationary direct current of central solenoidal coil

Osamu Watanabe

Research Institute for Applied Mechanics, 6-1 Kasuga Koen, Kasuga, Hukuoka, 816-8850, Japan

A sufficient stationary direct current applying in a central solenoidal coil (DC_{CS}) can decrease the MHD potential energy W_M of the tokamak plasma to below a vacuum magnetic field energy W_{VCB} before a tokamak plasma formation[1]. A vertical magnetic field in inner region of a magnetic axis of the tokamak plasma is reversed by the toroidal plasma current drive at the tokamak plasma formation. In a case of without the DC_{CS}, the vertical magnetic field in inner region of the central solenoidal coil (CS region) is also reversed. However, the sufficient DC_{CS} increases the vertical magnetic field only in the CS region. In this case, the vertical magnetic field energy in the CS region is decreased in proportion to the toroidal plasma current, and the magnetic field energy in the CS region is reduced approximately in proportion to the DC_{CS}. As the result, if the reduced magnetic field energy exceeds a thermal stored energy of the tokamak plasma, the MHD potential energy is decreased by increase of the toroidal plasma current. In the case of the tokamak plasma with sufficient DC_{CS}, the magnetic field energy in the CS region must be regain by get of any energy from somewhere in order to decrease the toroidal plasma current. Therefore, the decrease of the toroidal plasma current is inhibited energetically, and a stability of the tokamak plasma is improved.

At a sustainment of the tokamak plasma by microwave heating[2], law of conservation of energy is satisfied by the MHD potential energy including a radiation from the tokamak plasma and injection of heating powers which is mainly microwave power injection. However, there is a time evolution of the magnetic field energy in the CS region caused by the toroidal plasma current perturbation, which is same as Joule heating. The magnetic field energy transition by the toroidal plasma current perturbation is distributed into the toroidal plasma current drive, an eddy current generation and current modify of poloidal field coils, temporarily. Then, its energy state shifts easily to a local minimum again, with change of the radiation. Therefore, to return to same energy state after the perturbation, an energy minimization shape is better for tokamak plasmas in same thermal stored energy.

Characteristics of an energy reduction rate δW_M by the toroidal plasma current drive at the tokamak plasma formation is investigated numerically. In one instance, Figure 1 shows a dependence of the energy reduction rate based on a current distribution, which is defined by a pressure function P of a magnetic surface function Ψ as follows.

$$P(\Psi) = 2T_0 \left[n_1 \exp \left\{ \frac{1}{\sigma_1} \left(\frac{\Psi - \Psi_{ax}}{\Psi_{ax} - \Psi_{sep}} \right) \right\} + n_2 \exp \left\{ \frac{1}{\sigma_2} \left(\frac{\Psi - \Psi_{ax}}{\Psi_{ax} - \Psi_{sep}} \right)^2 \right\} \right] \quad (1)$$

When the current distribution has a hole current component 20 %, the energy reduction rate at the tokamak plasma formation is maximized in this parameter set.

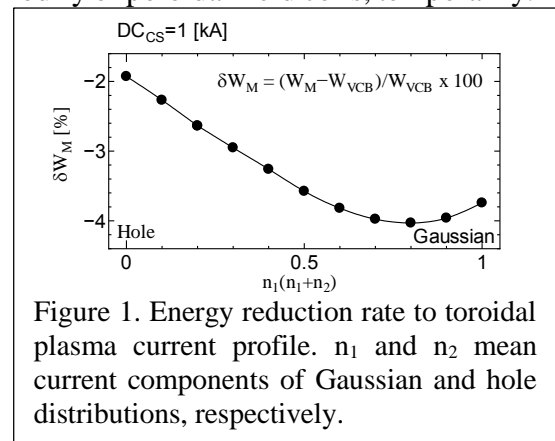


Figure 1. Energy reduction rate to toroidal plasma current profile. n_1 and n_2 mean current components of Gaussian and hole distributions, respectively.

[1] Watanabe, Osamu. Plasma and Fusion Research **8** (2013): 2401026-2401026.

[2] Takase, Y., et al., Nuclear Fusion **53.6** (2013): 063006.

Investigation of pressure profile controllability during plasma current ramp-up with reduced magnetic flux consumption in JT-60SA

T. Wakatsuki, T. Suzuki, N. Hayashi, J. Shiraishi, S. Ide, H. Kubo and Y. Takase^a

Japan Atomic Energy Agency, 801-1, Mukoyama, Naka 311-0193, Japan

^a *The University of Tokyo, 5-1-5, Kashiwanoha, Kashiwa 277-8561, Japan*

Investigation of the plasma current ramp-up with reduced magnetic flux consumption of the central solenoid (CS) is important to relax a strong constraint on the required CS size in the tokamak reactor design. Feasibility of plasma current ramp-up in JT-60SA without additional CS flux consumption after initial plasma formation has been investigated using an integrated modeling code suite (TOPICS). In our previous study, we developed a scenario in which the plasma current is ramped-up from 0.6 MA to 2.1 MA without additional CS flux consumption by overdriving the plasma current using neutral beams (NB) and electron cyclotron (EC) waves [1]. The investigation of the ramp-up scenarios with several prescribed density profiles revealed that a pressure profile with an H-mode pedestal and a wide internal transport barrier (ITB) whose foot is located at a large minor radius is required in order to obtain a large bootstrap current within the MHD stability limit. Although time evolution of the temperature profile was calculated using CDBM model [2,3], time evolution of the density profile was prescribed. Therefore, the controllability of the pressure profile by changing the heating and current drive method might be underestimated.

In this study, we introduce a particle transport model according to experimental results of JT-60U. In reversed shear plasmas on JT-60U, the effective particle diffusivity in the ITB region was estimated to be 0.04-0.2 times the ion thermal diffusivity when particle pinch effect was ignored [4]. Thus, we assume an effective anomalous particle diffusivity $D_{\text{ano}} = 0.2 \times \chi_{\text{ano},i}$, where $\chi_{\text{ano},i}$ is an anomalous thermal diffusivity of ions calculated using CDBM model. Particle transport is calculated by assuming that the particle diffusivity is a sum of neoclassical and anomalous diffusivities with zero particle pinch velocity. The neoclassical diffusivity is needed for including a strong neoclassical diffusion inside the reversed shear region. On the other hand, the neoclassical diffusivity is negligibly small compared to the anomalous diffusivity in the positive shear region. Particle sources are NBI and the edge gas puff. The volume averaged density is feedback controlled by the edge gas puff.

As a result, it is shown that the location and strength of the ITB can be modified by changing the heating, current drive and fueling method using NB and EC. An ITB which is strong enough to overdrive the plasma current can be obtained within the proposed NB and EC capability at JT-60SA. Ideal MHD instabilities are investigated using a linear ideal MHD stability analysis code (MARG2D). We will show controllability of the pressure profile considering the ideal MHD stability.

This work is supported by JSPS Grant-in-Aid for Research Activity Start-up 26889069.

[1] T. Wakatsuki, et al., Plasma Phys. Control. Fusion **57** (2015) 065005.

[2] M. Honda, et al., Nucl. Fusion **46** (2006) 580.

[3] A. Fukuyama, et al., Plasma Phys. Control. Fusion **37** (1995) 611.

[4] H. Takenaga, et al., Nucl. Fusion **43** (2003) 1235.

The effects of current density profiles on core toroidal rotation in EAST plasmas

Fudi Wang¹, Bo Lyu¹, Ruiji Hu^{1,2}, Jun Chen^{1,2}, Xianghui Yin^{1,2}, Jia Fu¹, Manfred Bitter³, Kenneth Hill³, John Rice⁴, Patrick Diamond⁵, Shigeru Morita⁶, Yi Yu², Minyou Ye², Baonian Wan¹, Yuejiang Shi^{7,2}, and EAST team

¹*Institute of Plasma Physics, Chinese Academy of Sciences, Hefei 230031, China*

²*School of Nuclear Science and Technology, University of Science and Technology of China, Hefei 230026, China*

³*Princeton Plasma Physics Laboratory, MS37-B332, Princeton, NJ 08543-0451, USA*

⁴*Plasma Science and Fusion Center, Massachusetts Institute of Technology, Cambridge, MA, 02139, USA*

⁵*CMTFO and CASS, University of California, San Diego, CA 92904, USA*

⁶*National Institute for Fusion Science, Toki 509-5292, Gifu, Japan*

⁷*Department of Nuclear Engineering, Seoul National University, Seoul, 151-742, Korea*

fdwang@ipp.ac.cn

The strong correlation between toroidal rotation (u_ϕ) and q (safety factor), l_i (internal inductance) has been observed in SOC plasmas, in LHCD at 4.6 GHz plasmas, in combination of LHCD at 2.45GHz and LHCD at 4.6GHz plasmas, in conjunction of LHCD at 4.6GHz and ICRF at 35 MHz plasmas, in synergism between LHCD at 2.45GHz, LHCD at 4.6GHz and ICRF at 35 MHz plasmas, and in association between co-NBI, LHCD at 4.6GHz and RMP plasmas on EAST. In detail, when toroidal rotation (u_ϕ) is increasing in co-current direction during above plasmas, the q is also augmenting, but l_i is decreasing. On the contrary, when u_ϕ is descending, q is also diminishing, but l_i is enhancing. The u_ϕ is incremental with l_i reducing and with q increasing. The above experimental result is consistent with the prediction of entropy balance theory, for turbulent plasma, associating with residual stress by comparing rates of entropy production (destruction) due to thermal relaxation (flow) generation.

Agenda

25th International Toki Conference (ITC-25)

Creating the Future — Innovative Science of Plasma and Fusion —

03-06 November, 2015, Toki

3. Nov Tuesday	Opening Group Photo	Chair: S. Kubo	N.J. Fisch	10:55 coffee break	Chair: S. Kubo	M. Osakabe K. Itoh	12:15 Lunch	Poster 1	P1-1~118 (exc.72) P2-69	Chair: M. Osakabe	M. Shiratani K. Kitano H. Saitoh M. Sato	16:15 16:35 18:15	
4. Nov Wednesday	Chair: N. J. Fisch	M. Ono H. Meyer	10:15 coffee break	Chair: A. Sagara	H. Tamura M. Sakamoto Y. Ueda	12:05 Lunch	Chair: C. Z. Cheng	B. Unterberg Y. Ueki A. Kimura	14:45 coffee break	Chair: B. Unterberg	A. Kasugai H. Shishido H. Etoh Poster2	P2-1~89 (exc.69) P1-72	18:15
5. Nov Thursday	Chair: H.P. Laqua	J-M. Noterdaeme S. Murakami	10:15 coffee break	Chair: H. Meyer	G. Serianni K. Ikeda N.C. Luhman, Jr. B.D. Blackwell	12:25 Lunch	Social Program Excursion	19:00 Banquet	15:40	Chair: J.-M. Noterdaeme K. Nishiyama M. Tendler Summary T. Mutoh Closing Closing	15:25	15:40	21:00
6. Nov Friday	Chair: B.D. Blackwell	H.P. Laqua M. Nunami	10:15 coffee break	Chair: N.C. Luhmann, Jr.	C.Z. Cheng Y. Miyoshi T. Minea N. Sato	12:25 Lunch	Chair: J.-M. Noterdaeme K. Nishiyama M. Tendler Summary T. Mutoh Closing Closing	15:40	15:40	15:40	21:00		